Investigating the role of TCR signalling during T cell development

Grandjean, Capucine L-A

For additional information about this publication click this link.
http://qmro.qmul.ac.uk/xmlui/handle/123456789/12819

Investigating the role of TCR signalling during T cell development

Capucine L-A Grandjean

Submitted in partial fulfillment of the requirements of

the Degree of Doctor of Philosophy

August 2015

Centre for Immunology and Infectious Diseases

The Blizard Institute

Barts and The London School of Medicine and Dentistry

Queen Mary University

4 Newark Street

London E1 2AT

To Eric & Odette

"Science is an activity that suits people who question, test ideas and then embrace the intellectual and philosophical consequences of their findings."

Peter Doherty
Nobel laureate

Statement of originality

I, Capucine Laure-Antoinette Grandjean, confirm that the research included within this thesis is my own work or that where it has been carried out in collaboration with, or supported by others, that this is duly acknowledged below and my contribution indicated. Previously published material is also acknowledged below.

I attest that I have exercised reasonable care to ensure that the work is original, and does not to the best of my knowledge break any UK law, infringe any third party's copyright or other Intellectual Property Right, or contain any confidential material.
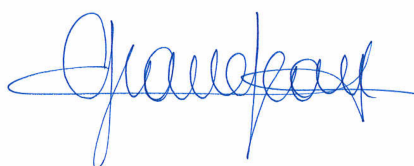
I accept that the College has the right to use plagiarism detection software to check the electronic version of the thesis.

I confirm that this thesis has not been previously submitted for the award of a degree by this or any other university.

The copyright of this thesis rests with the author and no quotation from it or information derived from it may be published without the prior written consent of the author.

Date: 20th August 2015

Signature:

Abstract

The thymus generates multiple T cell populations from an early common CD4$^{(-)}$ CD8$^{(-)}$ double negative (DN) progenitor. Conventional $\alpha\beta$ T cells, such as CD4$^{(+)}$ and CD8$^{(+)}$ T cells undergo thymic positive selection on partial agonist interactions with self-peptide/MHC, whereas unconventional TCR$\alpha\beta^{(+)}$CD8$\alpha\alpha^{(+)}$ intraepithelial lymphocytes (IELs) and regulatory T cells (Tregs), are thought to require full agonist interactions. By contrast, very little is known about how $\gamma\delta$ T cells undergo selection. While it has been suggested that IL-17A-secreting $\gamma\delta$ T cells rely on strong TCR signals resulting from potential interactions with a ligand, several studies have led to opposite conclusions. This thesis investigates the role of TCR signal strength during the early stages of thymocyte development, and how this dictates subsequent T cell fate.

We show that FVB/n mice have relatively few unconventional TCR$\alpha\beta^{(+)}$CD8$\alpha\alpha^{(+)}$ IELs in comparison to C57Bl/6 animals. This depleted IEL compartment correlated with reduced thymic IEL progenitors, an inefficient preTCR-driven DN-to-DP transition, and a relatively increased expression of full length pTα^{a} transcripts in CD44$^{(-)}$CD25$^{(+)}$ DN3 cells. Transgenic over-expression of pTα^{a} in the absence of pTα^{b} transcripts mimicked the phenotype of FVB/n animals. CD5 levels on DN3 cells from pTα^{a} transgenic mice indicate that preTCR signalling was weaker than in C57Bl/6 mice, suggesting that signal strength at the β-selection checkpoint may influence subsequent selection of mature T cell populations. Consistent with this, we show that OT-II mice, which express a transgenic TCR$\alpha\beta$ from an early DN stage of thymocyte

development, and which have high levels of CD5 on DN3 cells, have a relatively increased unconventional TCR$\alpha\beta^{(+)}$CD8$\alpha\alpha^{(+)}$IEL compartment. For $\gamma\delta$ T cell development, we also show that weakening signal strength impairs the development of IL-17A-secreting $\gamma\delta$ T cells. However, increasing signal strength, through the use of a cross-linking antibody, does not favour their development as predicted. These seemingly paradoxical observations are explored further.

Taken together, these data suggest that the quality or quantity of TCR-mediated signals early in T cell development have fundamental consequences for subsequent T cell selection events that differentially generate distinct T cell subsets.

Contributions

The BAC pTα^a transgenic animals used throughout this thesis were generated by Dr. Juliet Mahtani-Patching.

Figure 3.1 entitled "pTα^a and pTα^b are differentially expressed in the thymus" was taken from Dr. Juliet Mahtani-Patching thesis.

Figure 3.30 entitled "preTCR^a is expressed at lower surface levels than preTCR^b." was taken from Dr. Juliet Mahtani-Patching thesis.

Acknowledgements

First and foremost, I would like to thank my supervisor Prof. D. Pennington for giving me the opportunity to join his team and for his guidance throughout this incredible adventure. Thank you for your patience during these past five years, for coping with my insecurities and my doubts, but most importantly for always encouraging me to aim for the best, think independently and embrace fully challenging experiences. For everything you have done for me, Dan, I thank you deeply.

I am extremely indebted to Nital, who has been of extraordinary help during these years. Not only did she teach me most of the techniques I know today, but provided incredible help during this thesis write-up. Thank you for sharing your unique OCDs so that I could worsen mine and for all the good laughs and gossips that marked my years and significantly brightened my days.

I would also like to thank all of the past and current members of the DJP team, particularly, John, Joana, Claudio (adopted DJP), Claire, Juliet and Kosta for their support, numerous scientific advices and also their enthusiasm towards not only science but beers and Tayyabs treats too! Thank you to Paul for his daily goodmood, and his willingness to share his own thesis corrections, which undoubtedly allowed me to survive mine... A special thank you to Stef for being such a good student and for all the good laughs we shared during our hour-long gut experiments. I hope your PhD will strengthen your interest in science as much as it did for me.

I am taking this opportunity to thank everyone from CIID and the Blizard Institute for their technical advices, and coffee-time chats throughout my time at QMUL and for sharing food from all around the world. Thank you also to Philippe

Table of content

List of figures

List of tables

List of abbreviations

AIDS   Acquired Immune Deficient Syndrome
AIRE   Autoimmune Regulator
AP1   Activator Protein 1
APCs   Antigen Presenting Cells
APC   Allophycocyanine
APECED   Autoimmune polyendocrinopathy-candidiasis-ectodermal dystrophy
BAC   Bacterial Artificial Chromosome
BCR   B Cell Receptor
bHLH   Basic Helix-Loop-Helix
BM   Bone Marrow
bp   Base Pair
$Ca^{(2+)}$ Calcium
CCL21   Chemokine Ligand 21
CCR7   Chemokine Receptor 7
CD   Cluster of Differentiation
CDR   Complementary Determining Regions
CELF2   CUGBP, Elav-Like Family Member 2
CLIP   Class II-associated Invariant Chain Peptide
CRAC   Calcium Release Activated Channel
CSK   C-terminal SRC kinase
cTEC   Cortical Thymic Epithelial Cells
CTLs   Cytotoxic T cells
CXCR4   Chemokine Receptor 4
DAG   Diacylglycerol
DC   Dendritic Cells
DETC   Dendritic Epithelial T cell
DLL   Delta Like Ligand
DN   Double Negative ($CD4^{(-)}CD8^{(-)}$ T cell)
DNA   Deoxyribonucleic Acid
DNA-PK   DNA dependent Protein Kinase
DP   Double Positive ($CD4^{(+)}CD8^{(+)}$ T cell)
E11   Embryonic day 11
EDTA   ethylenediaminetetraacetic acid
eGFP   Enhanced Green Fluorescent Protein
Egr   Early growth response
EMSA   Electrophoretic Mobility Shift Assay
ER   Endoplasmic Reticulum
ERK   Extracellular-signal-regulated kinase
FACS   Fluorescent-activated Cell Sorting

FCεRIγ	High-affinity IgE receptor
FGL2	Fibronogen like 2
FITC	Fluorescein Isothiocyanate
Foxp3	Forkhead box P3
FSC	Forward Scatter
FTOC	Foetal Thymic Organ Culture
GALK	Galactokinase
GAPDH	Glyceraldehyde 3-phosphate Dehydrogenase
HIV	Human Immunodeficiency Virus
IEL	Intra-Epithelial Lymphocytes
IkB	Inhibitor of kappa B
IL-17A	Interleukin 17A
IL-7R	Interleukin 7 Receptor
IPEX	Immune Dysregulation Polyendocrinopathy Enteropathy X-linked
ISP	Immature Single Positive
ITAM	Immunoreceptor Tyrosine-based Activation Motif
ITK	IL-2-Inducible T cell Kinase
iTregs	Inducible T regulatory cells
JNK	c-Jun N-terminal kinases
Kb	Kilo Base
KO	Knock out
LAG3	Lymphocyte activation gene 3
LAT	Linker of Activation of T cell
Lck	Lymphocyte-specific protein tyrosine Kinase
LN	Lymph Node
LPS	Lipopolysaccharide
LTβ	Lymphotoxin β
MALT-1	Mucosa-Associated-Lymphoid-Tissue (MALT) lymphoma-translocation gene-1
MAPK	Mitogen activated protein kinase
MFI	Mean Fluorescent Intensity
MHC-I	Major Histocompatibility Complex class I
MHC-II	Major Histocompatibility Complex class II
MMTV	Mouse Mammary Tumour Virus
mTEC	Medullary Thymic Epithelial Cell
NFAT	Nuclear Factor of Activated T cell
NFκB	Nuclear Factor Kappa B
NHR	NFAT-Homology Region
NK	Natural Killer
NKG2D	Natural-Killer Group 2, member D
NKT	Natural Killer T cell
NTC	No Template Control
nTregs	Naturally occurring T regulatory cells
OVA	Ovalbumin

PAMPS	Pathogen Associated Molecular Pattern
PBS	Phosphate Buffered Saline
PCR	Polymerase chain reaction
PE	Phycoerythrin
PH	Pleckstrin Homology
PI3K	Phosphoinositide 3-kinase
PIP2	Phosphatidylinositol (4,5)-bisphosphate
PIP3	Phosphatidylinositol (3,4,5)-trisphosphate
pITAM	Phosphorylated Immunoreceptor Tyrosine-based Activation Motif
pMHC	Peptide MHC complex
Pre TCR	Pre T Cell Receptor
pTα	Pre T cell receptor α
RAG	Recombination Activating Genes
Ras-GRP	RAS-Guanyl-Nucleotide-Releasing Protein
RNA	Ribonucleic Acid
RORγt	RAR-related orphan receptor γt
RSS	Recombination Signal Sequence
S1P	Sphingosine-1-Phosphate
S1P1	Sphingosine-1-Phosphate Receptor 1
SCID	Severe Combined Immune Deficiency
SD	Standard Deviation
SH2	Src-Homology 2 domain
SLC	Stem cell Leukemia
SLP-76	SH2-domain-containing Leukocytes protein of 76kDa
SOS	Son of Sevenless
SP	Single Positive (CD4$^{(+)}$ or CD8$^{(+)}$ T cell)
SSC	Side Scatter
STAT	Signal Transducer and Activation of Transcription.
SYK	Spleen Tyrosine Kinase
TAP	Transporter Associated with Antigen Processing
TCR	T Cell Receptor
TDC	Thymic Dendritic Cells
Tdt	Terminal Deoxynucleotidyl Transferase
TEC	Thymic Epithelial Cells
TGF-β	Transforming Growth Factor β
T$_H$	T helper cells
TLR	Toll-Like Receptor
TNF	Tumour Necrosis Factor
TNFR	Tumor Necrosis Factor Receptor
TRAF6	TNF receptor associated factor 6
Tregs	Regulatory T cells
TRIM	T Cell Receptor - Interacting Molecule
VCAM	Vascular Cell Adhesion Molecule

WT	Wild Type
Zap-70	ζ-chain-Associated Protein Kinase of 70 KDa
β_2-m	Beta 2 Micro-globulin
CFSE	Carboxyfluorescein Succinimidyl Ester
PMA	Phorbol Myristate Acetate

Chapter 1

Introduction

1.1 The immune system

All living organisms have an immune system capable of identifying and killing potentially harmful foreign pathogens that may cause disease. The immune system is conventionally divided into two branches; the innate and adaptive immune systems, which communicate tightly with each other via cell/cell contact and the secretion of mediators (cytokines, chemokines) (Cooper and Alder, 2006).

1.1.1 The innate immune system

The innate (from the latin "innasci" meaning "to be born in") immune system constitutes the first line of defence against an infectious pathogen and is shared by both simple and complex organisms. The identification of infectious agents and the initiation of a fast (minutes to hours) immune response occurs following the recognition of pathogen-conserved structures - also known as pathogen-associated-molecular patterns (PAMPS); such as flagellin or lipopolysaccharide (LPS) (Table 1.1). Granulocytes (Neutrophils, Eosinophils, Basophils), dendritic cells (DC) and macrophages are the principal cellular components of the innate immune system and all share a common myeloid progenitor. The main purpose

of the innate immune system is to control the early phase of infection while recruiting a more specific and robust branch of the immune system that can fully eradicate the infection; the adaptive immune system.

	Innate Immunity	Adaptive Immunity
Timeframe in which an immune response is initiated	Immediate response (few hours)	Delayed response (few days)
Specificity	A very broad response with limited specificity for distinguishing between different pathogen products	A highly focused response mounted towards specific pathogens and individual antigens
Diversity of the receptors	Limited diversity Recognition of the pathogen occurs through receptors that recognise pathogen-associated patterns	Extensive diversity. Enables highly specific recognition of individual antigens
Immunological memory	Absent	Present Subsequent infection by the same pathogen will trigger a more robust response

Table 1.1 Representative characteristics of the innate and adaptive immune system.

1.1.2 The adaptive immune system

In contrast to the innate immune system, the adaptive immune system appeared with the jawed vertebrates and is thus not found in all organisms. The adaptive immune system has the ability to recognize numerous and diverse pathogen-derived antigens with great specificity. It can also acquire an immunological memory enabling a faster and more robust response in subsequent infections by the same pathogen. Lymphocytes are the central component of the adaptive immune response and are divided into two main families; the T and B lymphocytes, which share a common lymphoid progenitor.

T cells are so called because of their thymic origin, whereas B lymphocytes were named after the bursa of fabricius of birds from where they were first discovered in 1956 (Miller, 1994). While T cells provide the bulk of the cell-mediated arm of the adaptive immune response, B cells are a key mediator of the humoral immune response through the secretion of antibodies.

The work presented subsequently in this thesis focuses on one component of the adaptive immune system; T cells. Thus, this introduction concentrates on reviewing T cell function, development and signalling.

1.2 T cells are the central components of the adaptive immune system

T cells are an indispensable component of a healthy body. Indeed, a lack of T cells leads to severe combined immunodeficiencies (SCID), which may result in death in the first year of life unless appropriate treatment is given. The importance of T cells can also be illustrated in human immunodeficiency virus (HIV) infection; as viral load increases, the numbers of a particular subset of T cells (helper T cells also known as CD4$^{(+)}$ T cells; introduced subsequently) decrease over time to eventually fall below 200 cells/mm^3 of blood (normal range is: 500 to 1200 cells/mm^3 for adults) resulting in a dramatically weakened adaptive immune response. This corresponds to the establishment of acquired immune deficiency syndrome (AIDS) where common infections, usually of no

threat for healthy individuals, are no longer controlled, leading to the death of the patient (Figure 1.1) (Klatzmann et al., 1984).
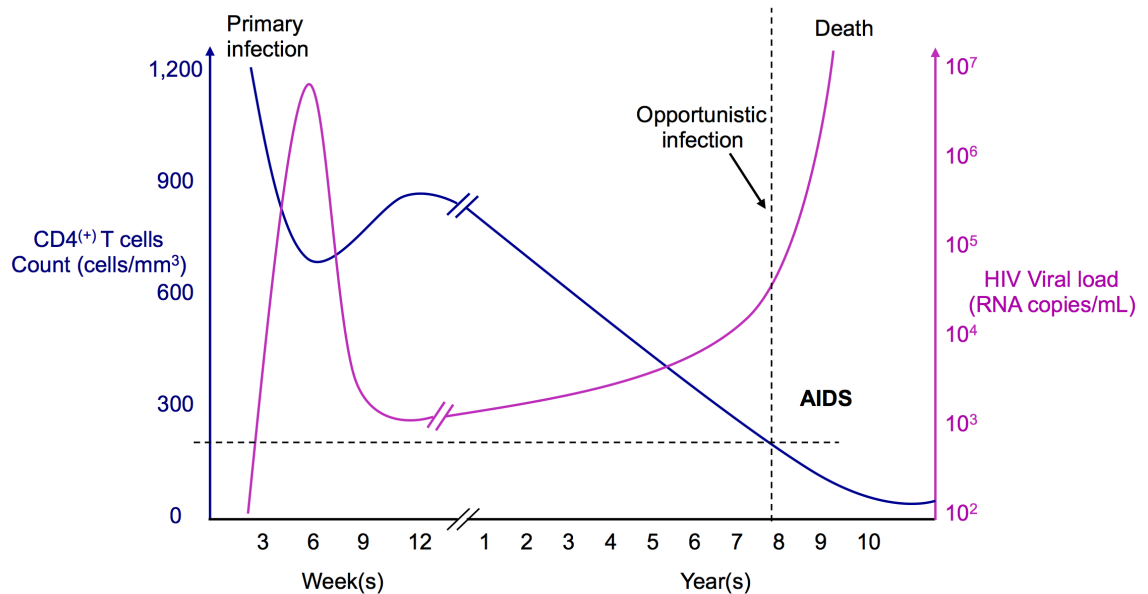
Figure 1.1 Helper T cell depletion after HIV infection. During an HIV infection, numbers of CD4$^{(+)}$ T cells drop gradually over time reaching a point where the T cell compartment cannot deal with opportunistic infections leading eventually to the death of the patient. Adapted from (Simon and Ho, 2003)

1.2.1 $\alpha\beta$ and $\gamma\delta$ T cells

T cells are characterised by the expression of a membrane-bound T cell receptor (TCR) and can be broadly divided into two subsets according to the type of TCR they express. $\alpha\beta$ T cells display a TCR$\alpha\beta$ consisting of a TCRβ chain bound to a TCRα chain, and are mainly found in blood, lymphoid organs and tissues. They represent the largest subset of T cells being more than 90-95% of peripheral blood T cells. By contrast, $\gamma\delta$ T cells express a TCR$\gamma\delta$ composed of a TCRγ and a TCRδ chain, and represent only about 1 to 5% of peripheral blood T cells, being predominantly found in the body's tissues

30

(Carding and Egan, 2002). γδ T cells can be further segregated by usage of certain variable domains ("V" regions) of either TCRγ or TCRδ. For example, in mouse, γδ T cells are often sub-divided based on the use of one of seven Vγ regions, which correlates with a specific tissue tropism (Carding and Egan, 2002; Krecko and Tonegawa, 1989). Vγ5[(+)] cells, also known as dendritic epithelial T cells (DETC) are found in the mouse skin while Vγ6[(+)] cells are principally found in the lining of the genital tract, peritoneal cavity and the tongue. The Vγ7[(+)] subset is principally found in the gut. Vγ4[(+)] and Vγ1[(+)] T cell are found in blood, spleen and lymph nodes (Table 1.2) (Carding and Egan, 2002).

Type of γδ T cells					
	Vγ5	Vγ6	Vγ7	Vγ4	Vγ1
Sites of migration	Skin	Genital Tract Tongue Peritoneal cavity	Gut	Blood Spleen Lymph nodes	

Table 1.2 γδ T cells can be characterised by the variable region of their TCRγ chain (Vγ). Vγ5 migrate exclusively to the skin while Vγ6 T cells preferentially go to the lining of the genital tract, the peritoneal cavity and the tongue. Vγ7 T cells preferentially populate the gut while Vγ4 and Vγ1 T cells are found in the spleen, lymph nodes and blood.

1.2.2 Structure of the TCR complex

The TCR is a disulfide-linked heterodimer, and member of the immunoglobulin super-family. Encoded by three loci, four different TCR chains can be generated; TCRα, TCRβ, TCRγ and TCRδ. Each TCR chain shares some

structural features; an extracellular portion composed of two Ig-loop structures forming the variable (V) and the constant (C) regions; a cysteine residue essential for the establishment of a disulphide bond between the two chains; a hydrophobic transmembrane domain; and a short intracellular tail (Figure 1.2) (Wood and Tonegawa, 1983). The ligand-binding region of the TCR, encoded by the V region, contains three hyper-variable regions (or complementarity determining regions (CDR1-3)) with CDR3 largely dictating the binding affinity of the TCR to the antigen (Davis and Bjorkman, 1988).

A fully signalling-competent TCR complex is composed of four CD3 (CD3δ, CD3γ or CD3ϵ) and two TCRζ (TCRζ or Fcϵ Receptor I γ (FCϵRIγ)) signalling molecules (Letourneur and Klausner, 1992). The various pairs of CD3 subunits (CD3$\epsilon\gamma$, CD3$\zeta\delta$) lack autonomous kinase activity but instead contain immunoreceptor tyrosine-based activation motifs (ITAMs) involved in signal transduction, which share a consensus sequence of two pairs of leucine and tyrosine residues, such as (D/E)xxYxxL(x)$_{6-8}$YxxL (Letourneur and Klausner, 1992; Reth, 1989). CD3γ, δ, and ϵ contain a single ITAM while CD3ζ has three providing altogether ten ITAMs through which signal transduction can be initiated.

TCRαβ
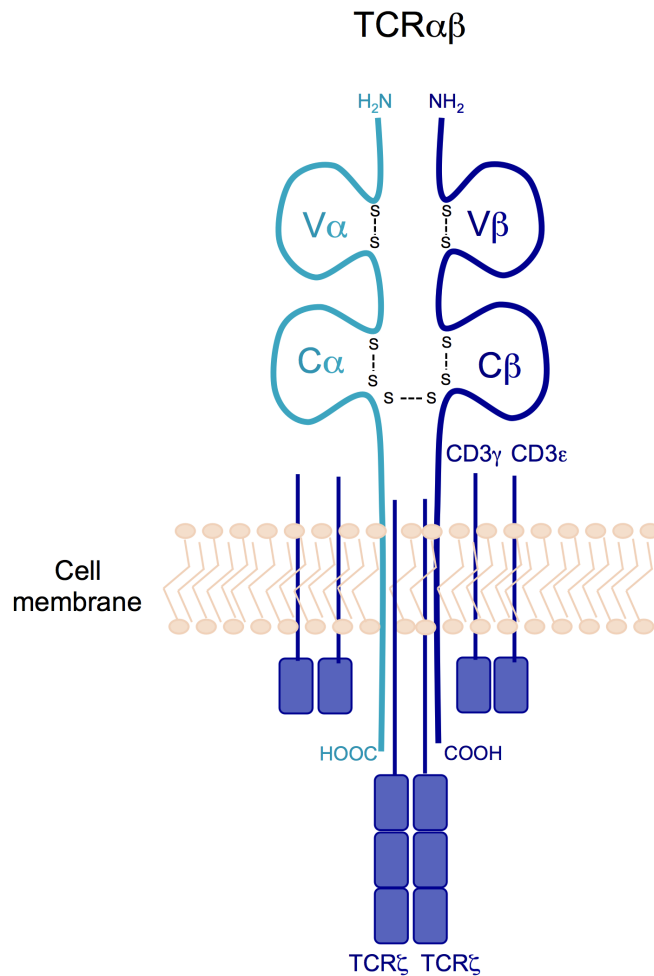
Figure 1.2 Schematic representation of the structure of a T cell receptor αβ. TCRαβ is composed of a TCRα chain interacting with a TCRβ chain by disulphide bonds generated by cysteine residues. Each TCR chain is composed of two Ig-loop structures stabilised by interactions between cysteine residues and represents the variable domain (V) and constant domain (C). The V region encodes the binding region involved in the recognition of MHC-presented peptides. Interaction between the TCR chains occurs through the transmembrane domain.

1.2.3 TCR gene-rearrangement; the source of great TCR diversity

The adaptive immune system generates millions of T cells that each has a unique TCR specificity that is capable of recognising a distinct antigen. Clearly, such diversity in TCR recognition cannot be inherently encoded in our genome of 20-25,000 genes. Instead, TCR diversity is generated by a process of

somatic recombination. This mechanism involves the random selection of certain DNA segments from the TCR loci that are cut and pasted together, while unwanted intervening segments are removed from the genome. It has been estimated that about 10^{12} different TCRs can be produced throughout our lifespan. This process takes place mainly in the thymus and is known as "TCR gene rearrangement" (Arstila et al., 1999).

1.2.4 Organisation of the TCR loci

Analysis of genomic organisation revealed that all TCR loci are composed of at least three families of gene segments; variable (V), joining (J) and constant (C) regions with TCRβ and TCRγ containing an extra set; the diversity (D) regions (Figure 1.3) (Wood and Tonegawa, 1983).
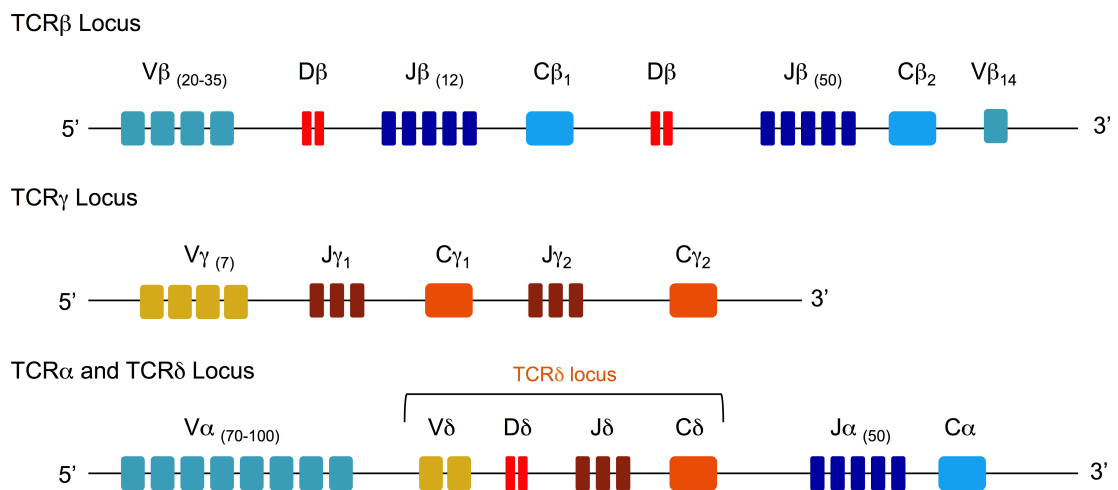
Figure 1.3 Organisation of the murine TCRβ, TCRγ, TCRα and TCRδ loci. Each TCR locus is composed of at least three types of gene segments; the variable (V), the junction (J), the constant (C) segments and the diversity (D) segments are an extra set found in the TCRβ and TCRγ loci.

Interestingly, the TCRδ locus is entirely contained within the TCRα locus resulting in its deletion during TCRα rearrangement (Figure 1.3). The TCRβ locus is composed (in mouse) of thirty-one V-regions, followed by two clusters containing a D-region, twelve J-regions, and a C-region (Giudicelli et al., 2005). Generation of a TCRβ chain occurs first by juxtaposition of one Dβ and Jβ region and then of one Vβ to the DJβ (Alt et al., 1984). Following transcription, the intron between the Cβ region and the rearranged VβDβJβ segment is spliced out from the RNA molecule, giving rise to a unique type of TCRβ mRNA and TCRβ protein (following translation). By contrast, the TCRα locus has far more V-regions than TCRβ (between 75 and 100 Vα segments) but lacks diversity regions. During rearrangement, Vα and Jα regions are first assembled before transcription takes place and RNA splicing leads to the fusion of the Cα region with VαJα resulting in a TCRα protein after translation (Figure 1.4).

Specific rearrangement and correct orientation between two types of segments are ensured by the presence of 28bp or 39bp long Recombination Signal Sequences (RSS). These are composed of palindromic heptamers found adjacent to a V, D or J segment, and are separated from a nonamer by a spacer of 12bp or 23bp. Gene rearrangement is said to follow the "12/23bp" rule where a RSS containing a spacer of 12bp will only associate with one that has a spacer of 23bp (Figure 1.5) (Krangel et al., 2004). This event is orchestrated by two lymphocyte-specific genes: Recombination Activating Genes (RAG) 1 and RAG-2 (Lacomini et al., 1992).
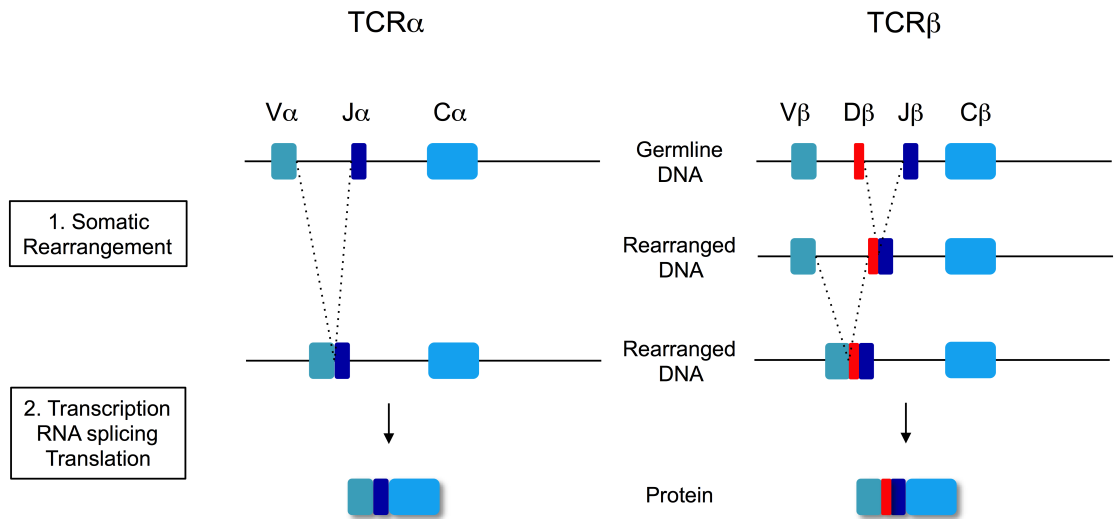
Figure 1.4 Schematic representation of TCRα and TCRβ rearrangement. During TCRβ rearrangement, the D and J regions are fused first before the addition of a V region. The rearranged DNA molecule is transcribed and RNA splicing allows the C region to be juxtaposed to the VDJ segment. Due to the lack of D regions in the TCRα locus, fusion of V and J happens first. Once the genes have been rearranged, transcription will take place and translation will follow to give rise to the TCRα or TCRβ protein.
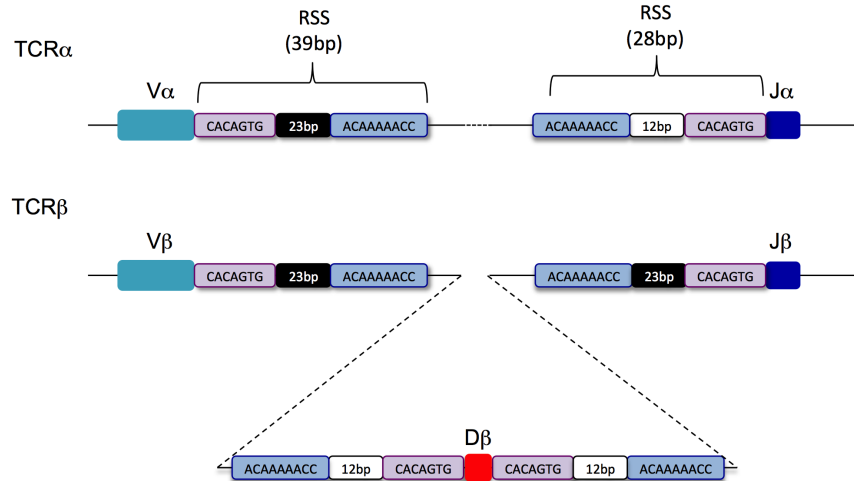
Figure 1.5 TCR rearrangement follows the 12/23bp rule. V, D, J regions are juxtaposed to a recombination signal sequence (RSS) composed of either 39bp or 28bp. Each RSS is composed of a heptamer (in pink) and a nonamer (in blue) palindromic sequences separated by a spacer of 12bp or 23bp. Juxtaposition of two gene segments results from the association of a RSS containing a 12bp spacer with another RSS containing the 23bp spacer ensuring the correct orientation of the gene segment.

RAG proteins recognise and associate with the RSS allowing two segments (e.g. Vα and Jα) to be brought into proximity. Cleavage of the DNA occurs through hydrolysis of the DNA strand separating the coding segment from the RSS. Once cleaved, the two DNA strands associate leading to the formation of a hairpin intermediate structure (Oettinger et al., 1990). Binding of Ku proteins (Ku70, Ku80) and DNA dependent protein kinase (DNA-PK) to the DNA triggers phosphorylation and activation of Artemis, the terminal deoxynucleotidyl transferase (Tdt), the DNA repair protein XRCC4 and the ligase IV. Artemis is thought to be responsible for opening up the hairpin structure creating "sticky ends" (or DNA overhang), which once repaired, produce palindromic sequence (also known as P-nucleotides) (Figure 1.6) (Ma et al., 2002). Finally, Tdt adds random nucleotides (N-nucleotides) at the joins, which together with the P-nucleotides further extend the sequence diversity of the VDJ or VJ regions and essentially makes the theoretical number of rearrangement possibilities infinite (Mansilla-Soto and Cortes, 2003; Villartay et al., 2003).

Although TCRγ and TCRδ loci contain fewer V-segments than the TCRα or TCRβ loci with only seven Vγ and six Vδ segments (in mouse), the TCR$\gamma\delta$ still possesses a great potential for diversity as the TCRδ chain can incorporate two D regions as opposed to TCRβ which only uses a single D region. This extra D creates an extra join, hence a further opportunity for the inclusion of P and N nucleotides (Michael, 2006).
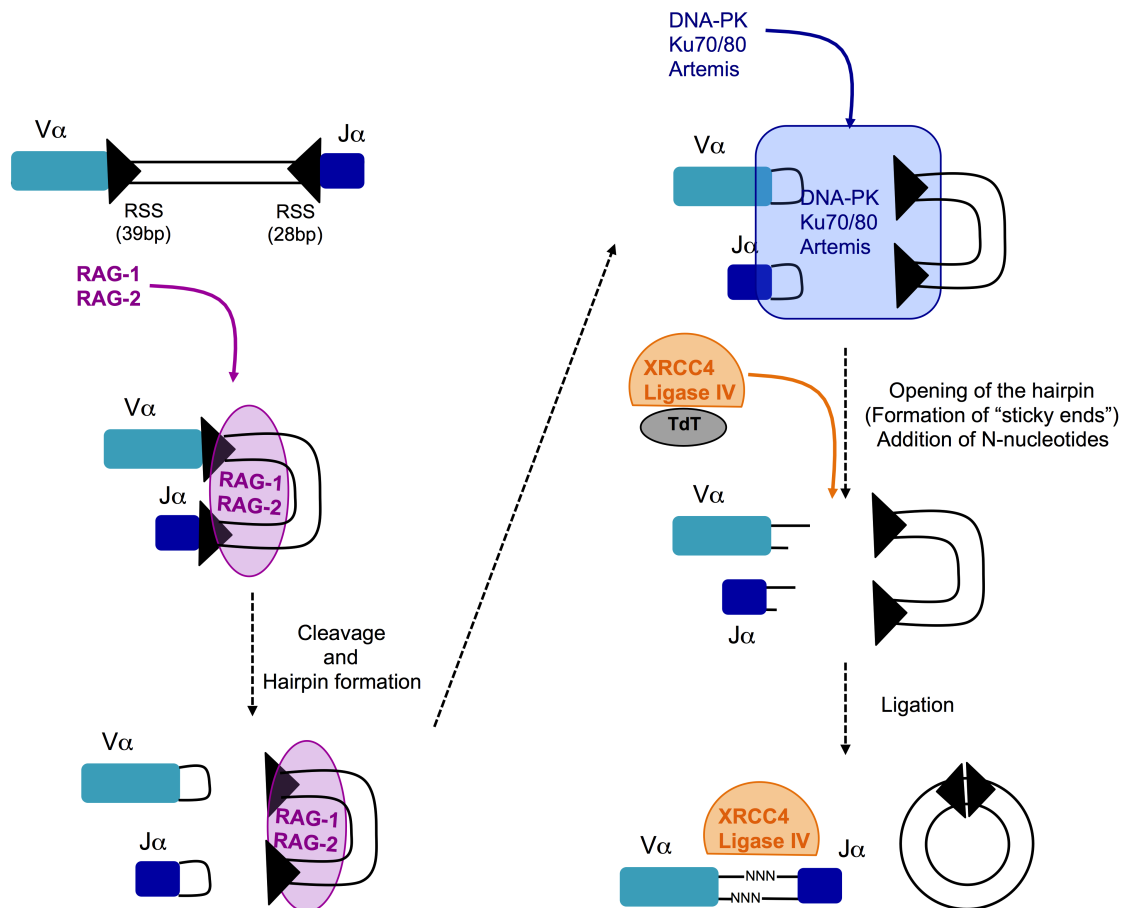
Figure 1.6 TCR gene rearrangement is initiated by RAG1 and RAG2. RAG1/2 associate with the RSSs bringing into proximity two segments (here Vα and Jα) to cleave the DNA. The DNA-PK/Ku70/80 complex is subsequently recruited where Artemis gets activated and is responsible for opening up the hairpin structure creating "sticky ends". XRCC4 and ligase IV subsequently mediate the repair and ligation of the sticky ends creating palindromic sequences while Tdt is responsible for the addition of N nucleotide. RAG, Recombination Activating Gene; Tdt, Terminal deoxynucleotidyl transferase; RSS, Recombination Signal Sequences;

1.2.4 Major pathways in T cell receptor signalling

The TCR translates extracellular stimuli into cytoplasmic and nuclear signals via a highly complex network of proteins that is critical for cell survival, proliferation and of particular interest to this thesis, differentiation. For simplicity, only the major T cell receptor signalling pathways are reviewed in this section.

1.2.4.1 Proximal TCR signalling

a. Lck signalling

The lymphocyte-specific protein tyrosine kinase (Lck) belongs to the src-family kinase and contains two phosphorylation sites, Y394 and Y505, which when phosphorylated, dictate the activity of the kinase (active and inactive respectively) (D'Oro et al., 1996). Lck activity represents the initial step of TCR signalling and is critical for signal transduction through the TCR (van Oers et al., 1996). Lck is negatively regulated by the phosphatase CD45 and the C-terminal src-kinase (CSK) (Autero et al., 1994). There has been some debate regarding how Lck triggers TCR signalling. It was shown that Lck can be found in a constitutively active state in the cytoplasm at steady state, as shown by a high proportion of phosphorylated Y394 Lck in jurkat and CD4[(+)] human T cells (Nika et al., 2010). However, this did not trigger T cell activation, and CD3-dependent stimulation of T cells did not increase the proportion of phosphorylated Y394 Lck (Nika et al., 2010). By contrast, inhibition of active Lck through the use of an inhibitor of the Lck chaperon protein Hsp90, severely impaired phosphorylation of the CD3ζ chains, suggesting that basal amounts of active Lck are required for successful TCR signalling (Nika et al., 2010). Thus it is thought that Lck can be found in a constant active state and that it is its recruitment to the membrane, as a result of TCR engagement, probably through remodelling of the cytoskeleton, that triggers signal transduction (Acuto et al., 2008; Nika et al., 2010; Tan et al., 2014). Alternatively, the kinetic segregation model of TCR triggering suggests that interactions between the TCR and the peptide-MHC complex creates a zone of close contact where large phosphatases like CD45 are excluded, allowing Lck to adopt an activated state and phosphorylate

downstream signalling molecules (Davis and van der Merwe, 2006). However, this model is not fully compatible with a ligand-independent signalling mechanism (Figure 1.7).

b. Zap-70 signalling

Phosphorylation of the CD3 ITAMs by Lck creates docking sites for SH2-domain-containing-proteins such as the ζ-chain-associated protein kinase of 70 KDa (Zap-70) (Straus and Weiss, 1993; Wang et al., 2010; Wange et al., 1993). Zap-70 is composed of two SH2-domains, two inter-domains (A and B), a carboxy-terminal kinase domain and five phosphorylation sites (Y292, Y315, Y319, Y492, Y493) (Kong et al., 1996). Binding of Zap-70 to phosphorylated ITAMs results in its phosphorylation by Lck at site Y493 followed by autophosphorylation of site Y492 both located in its kinase domain (Chan et al., 1995; Kong et al., 1996). This enhances its kinase activity that results in Zap-70 phosphorylating linker of activation of T cells (LAT) and SH2-domain-containing leukocytes protein of 76kDa (SLP76) (Figure 1.7) (Mege et al., 1996). This establishes an important foundation for the activation of numerous downstream signalling pathways.
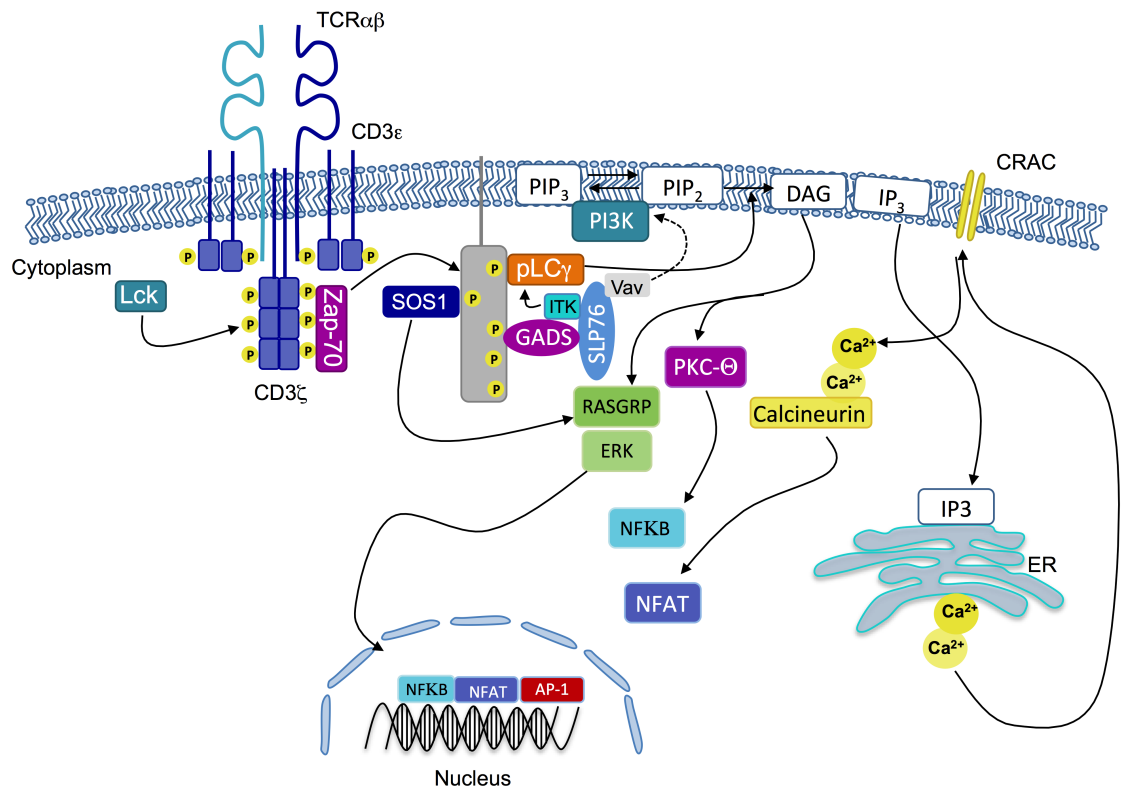
Figure 1.7 The signalosome. Signal initiation is thought to start with the phosphorylation of Lck, which phosphorylates in turn the ITAMs located on the CD3 signalling molecules creating a docking site for Zap-70. Zap-70 subsequently phosphorylates LAT, which represents a "hub" for TCR signalling. PLCγ-1 associates to LAT and cleaves PIP_2 into IP_3 and DAG. DAG stimulates the RASGRP pathway leading to the activation of the ERK pathway (Ras-Raf-Mek-ERK cascade) and activation of nuclear transcription factors. DAG also activates PKC-Ө resulting in NFκB activation. IP_3 binds to IP_3R on the ER and triggers release of $Ca^{(2+)}$ which is sensed by CRAC, which in turn allows an influx of $Ca^{(2+)}$ resulting in the activation of calcineurin. Calcineurin dephosphorylates NFAT allowing it to translocate into the nucleus. All these pathways are critical for cell proliferation, differentiation and survival. Lck, lymphocyte-specific protein tyrosine kinase; Zap-70, Zeta-chain-associated protein kinase 70; LAT, linker for activation of T cells; PLC, phospholipase Cγ1; PI3K, phosphoinositide 3-kinase; PIP3, Phosphatidylinositol-3,4,5-triphosphate; IP3, Inositol 1,4,5-triphosphate; DAG, diacylglycerol; PIP2, Phosphatidylinositol 4,5-bisphosphate; ER, endoplasmic reticulum; ERK, Extracellular signal-regulated kinases; NFAT, nuclear factor of activated T cells; NFκB, nuclear factorκB;

c. LAT signalling

LAT represents a central hub for the propagation of TCR signals and plays a critical role in the activation of several downstream signalling pathways (Zhang et al., 1998). Deficiency in LAT severely impairs T cell receptor signalling (Zhang et al., 1999). Structurally, LAT is a transmembrane protein with nine tyrosine sites conserved between human and mice, five of which can undergo phosphorylation (Y127, Y132, Y171, Y191, and Y226) (Paz et al., 2001). Once phosphorylated, they constitute major docking sites for multi-protein complexes regulating transcription, cytoskeletal reorganization, and cell adhesion (Sommers et al., 2001). Experimental mutation of these tyrosine residues to phenylalanine revealed that phosphorylation of Y132 recruits phospholipase-C-γ (PLC-γ), which can subsequently mediate the $Ca^{(2+)}$-dependent activation of the nuclear factor of activated T cells (NFAT), and the activation of the extracellular-signal-regulated kinase (ERK)/MAPK pathway through Ras-guanyl nucleotide-releasing protein (RasGRP) (Lin and Weiss, 2001; Paz et al., 2001). Y171, Y191, and Y226 are recognised by growth factor receptor-bound protein 2 (Grb2)-family members (Grb2, Gads, and Grap) and are critical for recruiting SLP76 and son of sevenless 1 (SOS1) (Zhang et al., 1998). Finally, distal signalling pathways are recruited with, for instance, activation of the nuclear factor-kappa B (NFκB) cascade through a SLP76-PKC-θ axis or the phosphoinositide 3-kinase (PI3K)- activator protein 1 (AP1) pathways, which are further reviewed below (Paz et al., 2001; Zhang et al., 2000).

1.2.4.2 Distal signalling and signal diversification

a. Calcium/NFAT signalling

Recruitment of lipase PLC-γ1 to LAT and SLP-76, followed by its activation via interleukin-2-inducible T cell kinase (ITK) permits PLC-γ1 to hydrolyse phosphatidylinositol-4,5-bisphosphate (PIP$_2$) to diacylglycerol (DAG) and inositol-1,4,5-trisphosphate (IP$_3$)(Min et al., 2009). IP$_3$ binds to its receptor (IP$_3$R) on the ER membrane allowing the release of Ca$^{(2+)}$. The decrease of Ca$^{(2+)}$ within the ER is sensed by stromal interaction molecule 1 (STIM 1), which has been hypothesised to translocate to the plasma membrane to activate calcium-release-activated calcium (CRAC) channels, which triggers a further influx of Ca$^{(2+)}$ (Bootman, 2012; Zhang et al., 2005). This increased intracellular Ca$^{(2+)}$ binds to calmodulin which in turn activates the calmodulin-dependent enzyme, calcineurin. The latter promotes the translocation of NFAT into the nucleus by dephosphorylating its regulatory domain (or NFAT-homology region; NHR) (Bootman, 2012). Indeed The NHR contains several serine residues, which are phosphorylated under steady state (Macián, 2005; Macián et al., 2001). Once in the nucleus, NFAT acts in synergy with other partners to regulate the transcription of target genes and one of its principal partners is the activating protein 1 (AP1) complex composed of FOS and JUN (Macián, 2005). This pathway is also regulated by the RAS/MAPK pathway (reviewed below).

b. ERK/MAPK signalling

The PLC-γ1-mediated hydrolysis of PIP$_2$ also generates DAG that can activate RAS-guanyl-nucleotide-releasing protein (RasGRP), which regulates Ras activity. It has been postulated that TCR signal strength would

compartimentalise Ras within the cell (Harding et al., 2005). TCR signalling triggers $Ca^{(2+)}$ and DAG release which are responsible for activating RasGRP and the golgi-associated form of Ras through guanine exchange (GDP to GTP), while at the same time negatively regulating membrane-associated Ras (Bivona et al., 2003). Work *in vitro* undertaken on Jurkat cells have shown that low-grade signals preferentially activate golgi-associated ERK while strong TCR signals target membrane-associated ERK (Chiu et al., 2002; Daniels et al., 2006; Perez de Castro et al., 2004). Ras subsequently activates the MAPK/ERK pathway via Raf and MEK. Once activated, ERK has several targets including the AP1 complex (Minden et al., 1994).

b. PI3K signalling

The PI3K family of kinases phosphorylate the D3 position of phosphoinositides resulting in the generation of lipid second messengers (Okkenhaug and Vanhaesebroeck, 2003). The PI3K family can be divided into three subclasses (Class I, Class II, Class III) according to structural similarities (Okkenhaug and Vanhaesebroeck, 2003). Class I PI3Ks have been largely implicated in lymphocyte signalling and therefore will be the only class reviewed in this introduction (Okkenhaug and Vanhaesebroeck, 2003). Class I PI3Ks are divided into two groups: Class IA PI3Ks are found downstream of tyrosine-kinase-associated receptors such as the TCR. They consist of a heterodimeric complex composed of a regulatory subunit (p85α, p85β or p55γ) and a catalytic subunit with kinase activity (p110α, p110β or p110δ) (Okkenhaug and Vanhaesebroeck, 2003). There is a single known member of the class IB PI3K family; PI3Kγ that is found downstream of G-coupled protein receptors such as chemokine receptors. PI3Kγ is a heterodimeric protein composed of a

regulatory subunit p101 and a catalytic subunit p110γ. Importantly, while p110α and p110β are expressed in a variety of cell types, p110δ and p110γ are restricted to leukocytes (Okkenhaug et al., 2002; Okkenhaug and Vanhaesebroeck, 2003). Class I PI3Ks phosphorylate PIP$_2$ to produce phosphatidylinositol-(3,4,5)-trisphosphate (PIP$_3$) at the inner part of the membrane which in turn constitutes the binding site for various Pleckstrin-Homology (PH) domain-containing proteins such as AKT that has been shown to be critical for cell proliferation, growth, and survival (Harriague and Bismuth, 2002; Hemmings and Restuccia, 2012). Although PI3K has been shown to be essential for signalling in lymphocytes, it remains uncertain how it is linked to the TCR. The p85 isoform contains two SH2-domains and one SH3-domain allowing interactions with other signalling molecules. It has been shown that SLP-76 and LAT were required for the activation of PI3K probably through the interaction with VAV1 (Reynolds et al., 2002; Shim et al., 2011). Alternatively, the TCR-interacting molecule (TRIM), which gets phosphorylated following activation (probably by Zap-70), has been proposed to activate PI3K (Bruyns et al., 1998). Finally, the CD28 co-stimulatory protein has been shown to associate with p85 and can activate PI3K signalling (Okkenhaug and Vanhaesebroeck, 2003; Pages et al., 1994; Prasad et al., 1994).

c. NFκB signalling

The NFκB family consist of five transcription factors; RelA (p65), Relb , c-Rel, p50 (NFκB1) and p52 (NFκB2), which are found as inactive dimeric complexes (p50/p65, Relb/p50 or p52/Relb) in the cytoplasm where they are sequestered by inhibitors IκB (p100 or p105) (reviewed in (Bonizzi and Karin, 2004).

Activation of NFκB signalling occurs through a wide range of stimuli delivered by various types of receptor such as the tumour necrosis factor receptor (TNFR), Toll-like receptor (TLR) or the antigen receptor (BCR or TCR). NFκB signalling is commonly divided into canonical and non-canonical pathways. TCR signalling was shown to activate the canonical signalling pathway through protein Kinase C (PKCΘ) and the CMB complex (including CARD11, Bcl10, Carma1 and MALT-1) as deletion of any of the CMB proteins led to a major block in T cell activation following TCR stimulation by cross-linking of CD3 molecules (Paul and Schaefer, 2013; Pomerantz et al., 2002; Sommer et al., 2005; Sun, 2010; Wang et al., 2002). Signalling through the TCR or cytokine receptors induces phosphorylation and activation of an IKKα:IKKβ complex that also includes the regulatory subunit NEMO (also known as IKKγ) possibly in a TNF receptor-associated factor 6 (TRAF6) dependent manner (Paul and Schaefer, 2013). This activated IKK complex then phosphorylates IκB targeting it for destruction via ubiquitination. This enables the NFκB hetero-dimer (p50/p65) to translocate to the nucleus where it can alter gene expression. By contrast, certain receptors such as the lymphotoxin-β receptor (LTβ-R) trigger both the canonical and non-canonical NFκB branches. Signalling through LTβ-R results in NIK and IKKα phosphorylation, which in turn phosphorylate the p100-Relb dimer resulting in the partial degradation of p100 into p52 (Heusch et al., 1999). The p52-Relb dimer then translocates to the nucleus to again regulate a set of target genes (Figure 1.8) (Gerondakis et al., 2006).
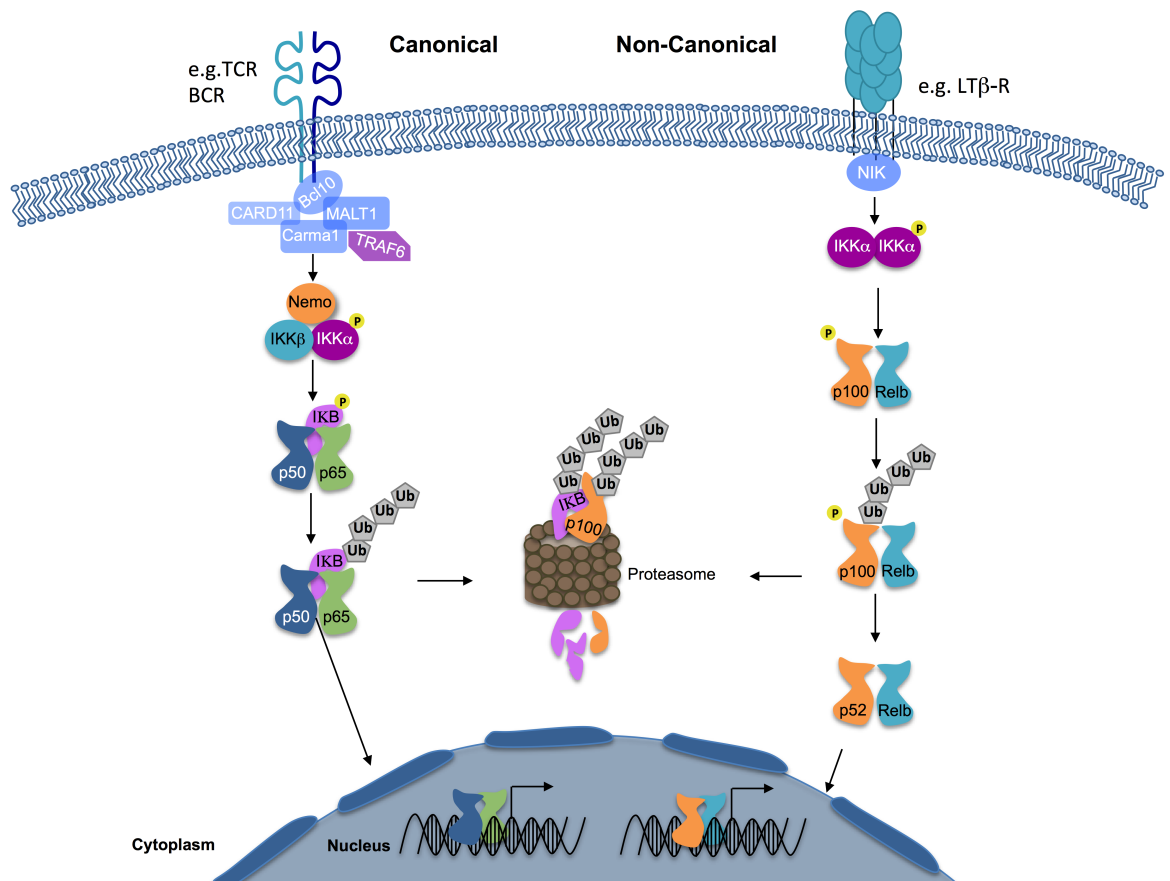
Figure 1.8 The canonical and non-canonical NFκB pathways. Signalling through the TCR triggers the NFκB canonical pathway. IKKα, which is part of a complex containing Nemo and IKKβ, gets phosphorylated and in turn phosphorylates IκB. Phosphorylated IκB is targeted for degradation freeing up the p50-p65 heterodimer to translocate to the nucleus. Activation of the non-canonical pathway phosphorylation of an IKKα dimer result in the phosphorylation, ubiquitination and degradation of the p100 to p52. The p52/Relb heterodimer is then translocated to the nucleus where it can modulate gene transcription (Oeckinghaus et al., 2011).

1.2.5 Conventional and unconventional T cells

T cells can also be broadly divided into conventional or unconventional subsets according to; their capacity to recognise and respond in a non-detrimental manner to self-antigen; their location in the body (secondary lymphoid organs

versus tissues); and their development; all of which will be introduced subsequently in this thesis.

1.2.5.1 Conventional T cells

Conventional T cells mainly include cytotoxic T cells (CTLs) and helper T cells (T_H cells), which express along with TCR$\alpha\beta$, a heterodimeric CD8$\alpha\beta$ co-receptor, or the monomeric CD4 co-receptor, respectively. CTLs constitute a fairly homogeneous subset of T cells and exhibit cytotoxic activity allowing them to directly induce apoptosis in target cells. T_H cells are mainly implicated in the recruitment and direction of the humoral and cell-mediated branches of the immune system through the production of cytokines. They can be divided into several further subsets depending on the cytokine environment in which they are generated, the effector function they exhibit, and the type of pathogens against which they are most effective. For simplicity, only three T_H subsets will be discussed here.

a. T helper cell subsets

Upon infection, antigen-presenting cells (APCs) such as dentritic cells (DC) migrate from the site of infection to lymphoid organs and present pathogen-derived products to naïve CD4$^{(+)}$ T cells through MHC-II, which represents the initial step of T cell activation (referred as signal 1). In order to become fully activated, naïve T cells require two additional signals; interaction between CD28 and CD80/CD86 co-stimulatory molecules present on T and DC respectively (signal 2), and cytokines produced by DCs (signal 3). T cells activation triggers cell division and differentiation of naïve CD4$^{(+)}$ T cell into

effector T_H subsets. Differentiation into a T_H1 phenotype is dependent on interleukin 12 (IL-12) while polarisation into a T_H2 or T_H17 phenotype is driven by IL-4 or a combination of transforming growth factor β (TGF-β) and IL-6, respectively (Figure 1.9) (Hsieh et al., 1993; Mosmann et al., 1986). Each T_H subset is also characterised by the expression of certain "master" transcription factors and the major cytokines they produce. T_H1 cells produce interferon γ (IFN-γ) and express the transcription factor T-bet. T_H2 cells are producers of IL-4 and express GATA3. Finally, differentiation into IL-17-secreting T_H17 cells is dependent on the transcription factor RORγt. Each T_H subset performs a specific function in the adaptive immune response. T_H1 cells promote the cell-mediated branch of the adaptive immune system and are involved for instance in the clearance of intracellular pathogens. By contrast, T_H2 cells promote the humoral immune response that is important for controlling parasitic infections. Finally, T_H17 cells have a pro-inflammatory role and are implicated in clearing extra-cellular pathogens, particularly extracellular bacteria. T_H17 cells are also often implicated in autoimmune conditions.
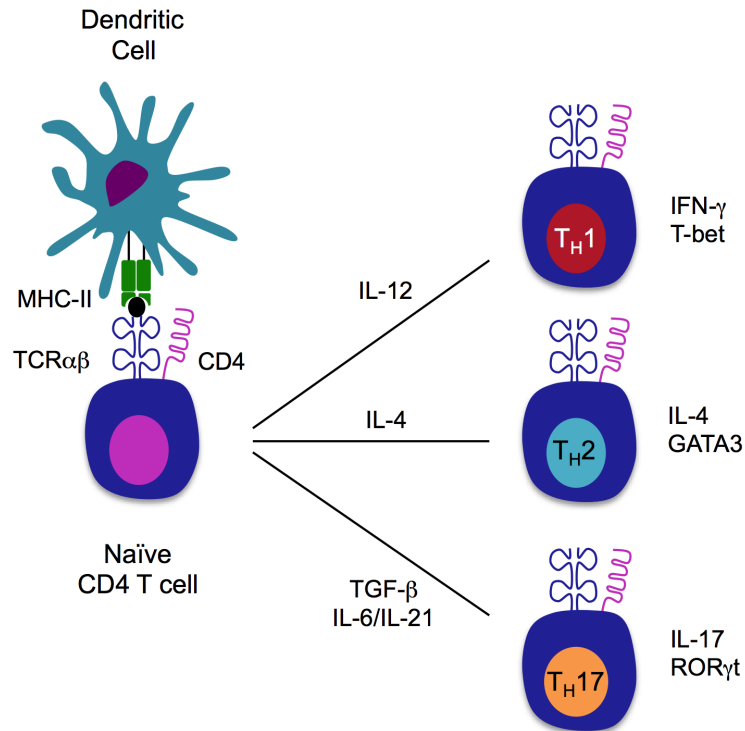
Figure 1.9 CD4$^{(+)}$ T cells can be polarised into at least three T$_H$ subsets. Differentiation of naïve CD4$^{(+)}$ T cells into an effector T$_H$ subset is dependent on the cytokine milieu in which activation takes place. It occurs in lymph nodes following interaction with pathogen-derived antigens presented by antigen presenting cells (APCs) such as dendritic cells (DC). Each T$_H$ subset can be characterised by a "master" transcription factor and a secreted cytokine signature. T$_H$1 cells express Tbet and produde IFN-γ. T$_H$2 cells express GATA3 and secerete cytokine IL-4. T$_H$17 cells express RORγt and secrete IL-17.

b. CD8$^{(+)}$ T cells

Conventional CD8$^{(+)}$ T cells have a central role in eradicating intracellular infections and tumours. During an immune response, intra-cellular pathogens or tumour-associated antigens undergo proteosomal degradation within the infected/transformed cell. The resulting antigens are transported to the endoplasmic reticulum (ER) by ABC transporters antigen processing (TAP) 1 and TAP2, which mediate the loading of the antigen onto the major

histocompatibility complex class I (MHC-I) peptide-binding groove with the help of the chaperon molecule Tapasin. The peptide/MHC complex is then transported to the surface of the cell to allow interaction between TCR$\alpha\beta$ and peptide/MHC-I complex resulting in the activation of the CD8$^{(+)}$ T cell and the acquisition of a cytotoxic phenotype (Williams et al., 2002). Two additional models have been proposed to describe the mechanism by which CD8$^{(+)}$ T cells get activated and they both involve CD4$^{(+)}$ T cells which would cooperate to provide "extra" help during activation. In one model, CD4$^{(+)}$ and CD8$^{(+)}$ T cells interact simultaneously with the same DC (Bennett et al., 1997). Activation of the CD4$^{(+)}$ T cell results in the secretion of interleukin 2 (IL-2) thought to be responsible for driving the expansion of CD8$^{(+)}$ T cells (Bennett et al., 1997). Alternatively, CD4$^{(+)}$ T cells can interact and trigger activation of DCs through the CD40/CD40L axis endowing them with increased ability to activate CD8$^{(+)}$ T cells (Ridge et al., 1998). In all models, activation of the CD8$^{(+)}$ T cell results in clonal expansion and subsequent secretion of granzymes and perforins which induce lysis of infected/transformed cells. Moreover, CD8$^{(+)}$ T cells can release inflammatory cytokines (IFN-γ and TNF) responsible for recruiting additional immune cells and driving disease clearance (Barth et al., 1991).

1.2.5.2 Unconventional T cells

Unlike conventional T cells, unconventional T cells reside mainly in peripheral tissues, have a relatively high affinity for self-antigens, and have a poorly understood developmental pathway. They often, but not always, express a TCR with limited diversity and display innate-like functions. These unconventional T

cells mainly consist of $\gamma\delta$ T cells, intra-epithelial lymphocytes (IELs), natural

killer T cells (NKT) and arguably include regulatory T cells (Tregs) (Figure 1.).
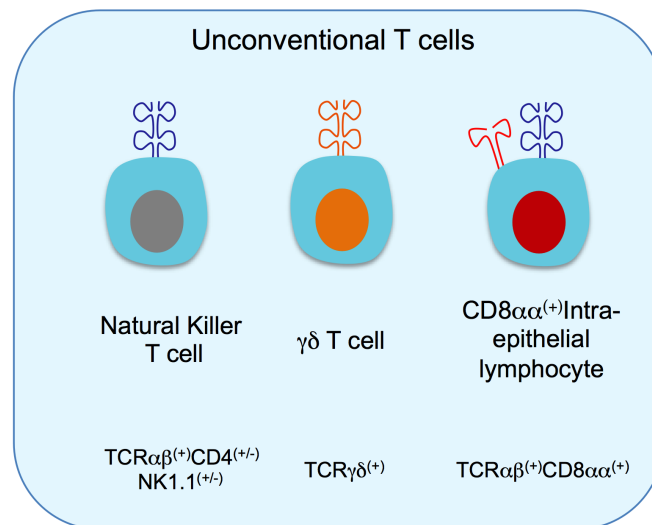
Figure 1.10 The unconventional T cell family. Unconventional T cells undergo a different mechanism of selection, are often found in tissues, and display innate-like features. The prototypic unconventional T cell is the $\gamma\delta$ T cell, but also includes natural killer T cells, and TCR$\alpha\beta^{(+)}$CD8$\alpha\alpha^{(+)}$IELs.

a. $\gamma\delta$ T cells

$\gamma\delta$ T cells are prototypic unconventional T cells that are thought to straddle the

innate and adaptive immune systems. They display innate-like functions such

as rapid effector function to infections, a preferential tropism to epithelial

tissues, the expression of innate-like receptors such as natural killer group 2D

(NKG2D) and the expression of a TCR$\gamma\delta$ with reduced diversity. $\gamma\delta$ T cells

mediate immunity against pathogens and are potent mediators of tumor

immunosurveillance (Street et al., 2004). Indeed, $\gamma\delta$ T cell recognition of

tumours occurs through TCR$\gamma\delta$ and NKG2D receptors, triggering a potent

cytotoxic phenotype and the production of high levels of cytokines such as

tumour necrosis factor (TNF) and IFNγ (Gao et al., 2003). In agreement with this, mice deficient for $\gamma\delta$ T cells (TCRδ-deficient animals) are significantly more susceptible to chemically-induced, transplantable and spontaneous tumours (Girardi et al., 2001).

$\gamma\delta$ T cells can be segregated into two functionally distinct subsets depending on expression of the TNF-superfamily receptor CD27 (Ribot et al., 2009). IFN-γ-producing $\gamma\delta$ T cells express CD27 ($\gamma\delta^{(27+)}$) whereas absence of CD27 describes an IL-17A-producing $\gamma\delta$ T cell subset ($\gamma\delta^{(27-)}$), which mainly consists of Vγ4$^{(+)}$ and the Vγ6$^{(+)}$ cells (Cai et al., 2011; Hamada et al., 2008; Ribot et al., 2009; Sumaria et al., 2011).

b. Unconventional intraepithelial lymphocytes (IELs)

Intraepithelial lymphocytes (IELs) are a large heterogeneous population of T cells that can be members of either the $\gamma\delta$ or $\alpha\beta$ lineage. They display anti-inflammatory and anti-microbial responses, while tolerating commensal bacteria and controlling epithelial homeostasis. This thesis focuses on IELs located in the epithelial layer of the ileum that along with TCR$\alpha\beta$ express the homodimeric form of CD8α (Gangadharan and Cheroutre, 2004). Unconventional TCR$\alpha\beta^{(+)}$CD8$\alpha\alpha^{(+)}$ IELs display abundant cytotoxic function through the expression of granzymes, perforins and FAS-ligands but produce low amounts of IFN-γ despite an activated phenotype (as demonstrated by high levels of CD69) (Shires et al., 2001). Their precise role in the gut has yet to be fully described but expression of NK-like activatory markers DAP12, 2B4, or inhibitory Ly49, implicate them as a stress-sensing population essential for epithelial immune surveillance (Denning et al., 2007; Shires et al., 2001).

Finally, they have been implicated in immune regulation due to expression of immune regulators such as lymphocyte activation gene 3 (LAG3), TGF-β and fibrinogen-like 2 (FGL2) (Cheroutre et al., 2011). Indeed, transfer of TCRαβ$^{(+)}$CD8αα$^{(+)}$ IELs to a colitis model prevented induced-intestinal inflammation (Poussier et al., 2002).

c. NKT cells

NKT cells represent only 0.5% of all blood T cells but constitute a major component of tumour immunity. They are found in blood, spleen, liver, and lymph nodes and express a TCRαβ. They can be divided into two main categories in mouse according to the co-receptors they express, their TCRαβ specificity, the diversity of their TCR and the presenting molecules they recognise. Type I NKT cells express NK1.1 and a TCRαβ repertoire composed of a TCRα chain using Vα14–Jα18 and a TCRβ chain using Vβ8.2/7/2, which has been shown to have high affinity for α-galactosylceramide (α-GalCer) presented in the context of CD1d. The second category of NKT cells express CD4 or none of the co-receptors and a semi-variable TCRαβ, characterised by frequent pairing of Vα3.2–Jα9 TCRα chains with Vβ8 TCRβ chains and their reactivity is unclear (Kronenberg and Gapin, 2002).

d. Regulatory T cells

Regulatory T cells (Tregs), are not involved in the clearance of infections but instead suppress unwanted immune responses. In addition to expressing TCRαβ and the co-receptor CD4, the major population of Tregs express the α-chain of the IL-2 receptor, CD25, the transcription factor forkhead box P3

(foxp3), and mediate their suppressive functions through a variety of mechanisms that include cell-contact-dependent mechanism and the production of IL-10 or TGF-β. Foxp3$^{(+)}$ Tregs can be divided into naturally-occurring Tregs (nTregs) arising from the thymus and inducible Tregs (iTregs) that develop in the periphery from naïve CD4$^{(+)}$ T cells in the specific cytokine milieu of TGF-β. Inducible Tregs are often divided into two additional subsets with Tr1 Tregs secreting large amounts of IL-10 and Th3 Tregs preferentially producing TGF-β. Their suppressive functions were first described in a seminal study in which transfer of CD4$^{(+)}$ T cells depleted of CD4$^{(+)}$CD25$^{(+)}$ T cells into athymic mice triggered the development of auto-immunity. Transfer of CD4$^{(+)}$CD25$^{(+)}$ T cells successfully prevented the appearance of the symptoms in a dose-dependent manner (Sakaguchi et al., 1995). Thus, Tregs represent an important subset for controlling unwanted immune responses and maintaining peripheral tolerance.

Collectively, this section describes the significant heterogeneity of the T cell family. Nonetheless, despite displaying diverse effector functions, sites of action and method of activation, all T cells develop from a common thymic progenitor and are indispensable for a healthy immune system. One of the central questions of the lab focuses on understanding how this heterogeneity in T cell phenotype is achieved in development.

1.3 T cell development

T cell development principally takes place in the thymus, an organ located in the upper part of the chest above the heart. Despite being identified as the

lymphocyte-producing organ by Sir Peter Medawar and Sir James Learmonth Gowans, its pillar immunological role was only demonstrated by Jacques Miller in 1962 through the use of thymectomised mice (Miller, 1961). It has been suggested that some unconventional T cells develop extra-thymically. Indeed, the presence of TCR$\alpha\beta^{(+)}$CD8$\alpha\alpha^{(+)}$ IELs or NKT cells in athymic mice supports the idea that these cells could develop in localized structures found in the periphery (Guy-Grand et al., 2003; Kikly and Dennert 1992; Makino et al., 1993). However, numbers and proportions of these cells were highly reduced in athymic mice highlighting the importance of the thymus for a full T cell compartment. Thus, this thesis concentrates on thymic T cell development.

1.3.1 Structure of the thymus

The thymus is composed of two lobes and is divided into a cortex, corresponding to the outer layer of the organ, and a medulla that constitutes the core. The cortex is itself divided into four regions with region one being more proximal to the medulla and region four found in the sub-capsular region or outer cortex (Blackburn and Manley, 2004). The thymus involutes with age as a result of stromal atrophy, mainly consisting of fat by the time an individual reaches adulthood (Figure 1.11) (Dorshkind and Montecino-Rodriguez, 2009).
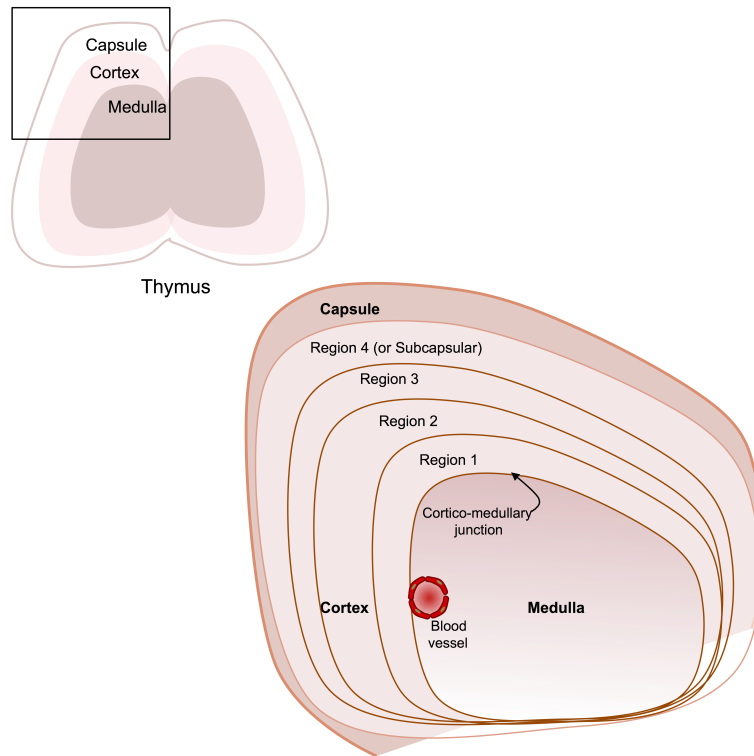
Figure 1.11 A schematic representation of the structure of the thymus. The thymus is conventionally divided into the cortex, constituting the outer layer of the organ and the medulla constituting the core. The cortex is further divided into four regions with region 1 being more centrally localised, near the cortico-medullary junction than region 4, that is found near the capsule.

1.3.2 An overview of $\alpha\beta$ T cell development

T cell development is commonly divided into two main phases based on the expression of the CD4 and CD8 co-receptor molecules; the Double Negative (DN) phase in which immature thymocytes lack surface expression of both co-receptors and the Double Positive (DP) phase where both CD4 and CD8 are expressed (Germain, 2002). The DN phase is further divided into four stages (DN1-DN4) based on cell surface expression of CD44, CD25 (α chain of the IL2 receptor) and c-Kit. T cells develop sequentially through the DN1 (CD44$^{(+)}$CD25$^{(-)}$c-Kit$^{(+)}$), DN2 (CD44$^{(+)}$CD25$^{(+)}$c-Kit$^{(+)}$), DN3 (CD44$^{(-)}$ CD25$^{(+)}$c-

Kit$^{(-)}$), and DN4 (CD44$^{(-)}$CD25$^{(-)}$c-Kit$^{(-)}$) stages (Figure 1.12) (Godfrey et al., 1993).

The DN1 subset is very heterogeneous and is believed to retain the potential to give rise to T cells, B cells or NK cells (Porritt et al., 2004). Full commitment of DN1 cells to the T cell lineage is dependent on signalling through the transmembrane glycoprotein Notch-1. Indeed, Radtke and co-workers showed that conditional ablation of Notch-1 in mice caused DN1 cells to acquire a B cell phenotype (Radtke et al., 2000).

A high proportion of DN2 cells proliferate and display some features indicative of T cell lineage commitment. Indeed, CD3, TCRζ, the invariant protein pTα and Lck can be detected (Wilson and MacDonald, 1995). Moreover, the expression of RAG-1 and RAG-2 is initiated in DN2 cells, which drives TCR rearrangement. However, foetal thymic cultures (FTOC) revealed that DN2 thymocytes still retain potential to adopt alternative non-T cell lineage fates such as B, NK or macrophages lineages when cultured in different conditions (Balciunaite et al., 2005; Yui, 2010).

DN3 thymocytes are fully committed to the T cell lineage and mark the first major T cell developmental checkpoint; the β-selection checkpoint. This stage also correlates to when thymocytes adopt either a γδ or αβ fate (this is discussed subsequently). Expression of the pre-T cell receptor (preTCR; the invariant pTα chain paired to TCRβ) allows DN3 cells to survive, proliferate and differentiate to the subsequent DN4 stage. Two populations within the DN3

subset can be identified, which correspond to pre-β-selected thymocytes (DN3S also known as DN3a), and post-β-selected thymocytes (DN3L, DN3b) that are fully committed to an αβ T cell fate. DN3S thymocytes are not yet proliferating as shown by their arrest in the G1 phase of the cell cycle, and are considerably smaller than DN3L cells (hence their nomenclature) (Hoffman et al., 1996). Although DN3S cells express high levels of RAG proteins, suggesting that rearrangement of TCRβ has been initiated, only 33% of TCRβ chains are found to be rearranged in-frame. This is because only one of the possible reading frame of TCRβ makes functional protein, and the rearrangement process essentially produces equal numbers of rearranged TCRβ chains in each of the three frames (Alt et al., 1984). By contrast, most DN3L thymocytes express in-frame TCRβ chains as only TCRβ[(+)] cells (or γδ cells) can traverse the β-selection checkpoint. DN4 cells are also enriched in cyclin A and CDK2 indicative of entry into the cell cycle (Hoffman et al., 1996).

DN4 thymocytes represent an intermediate subset from which thymocytes transit to an "Immature Single Positive" (ISP) phenotype, expressing low levels of the co-receptor CD8 but no CD4 (Miyazaki, 1997). CD4 up-regulation rapidly follows allowing cells to reach the DP stage. DP cells start to rearrange their TCRα locus in an attempt to generate a mature TCRαβ (Mombaerts et al., 1992). Interactions between MHC/self-peptide molecules and TCRαβ triggers cell surface expression of CD5, CD69 and termination of TCRα gene rearrangement, allowing DP cells to develop as either naïve TCRαβ[(+)]CD4[(+)] or TCRαβ[(+)]CD8[(+)] single positive cells (SP) (Azzam et al., 1998; Yamashita et al., 1993).
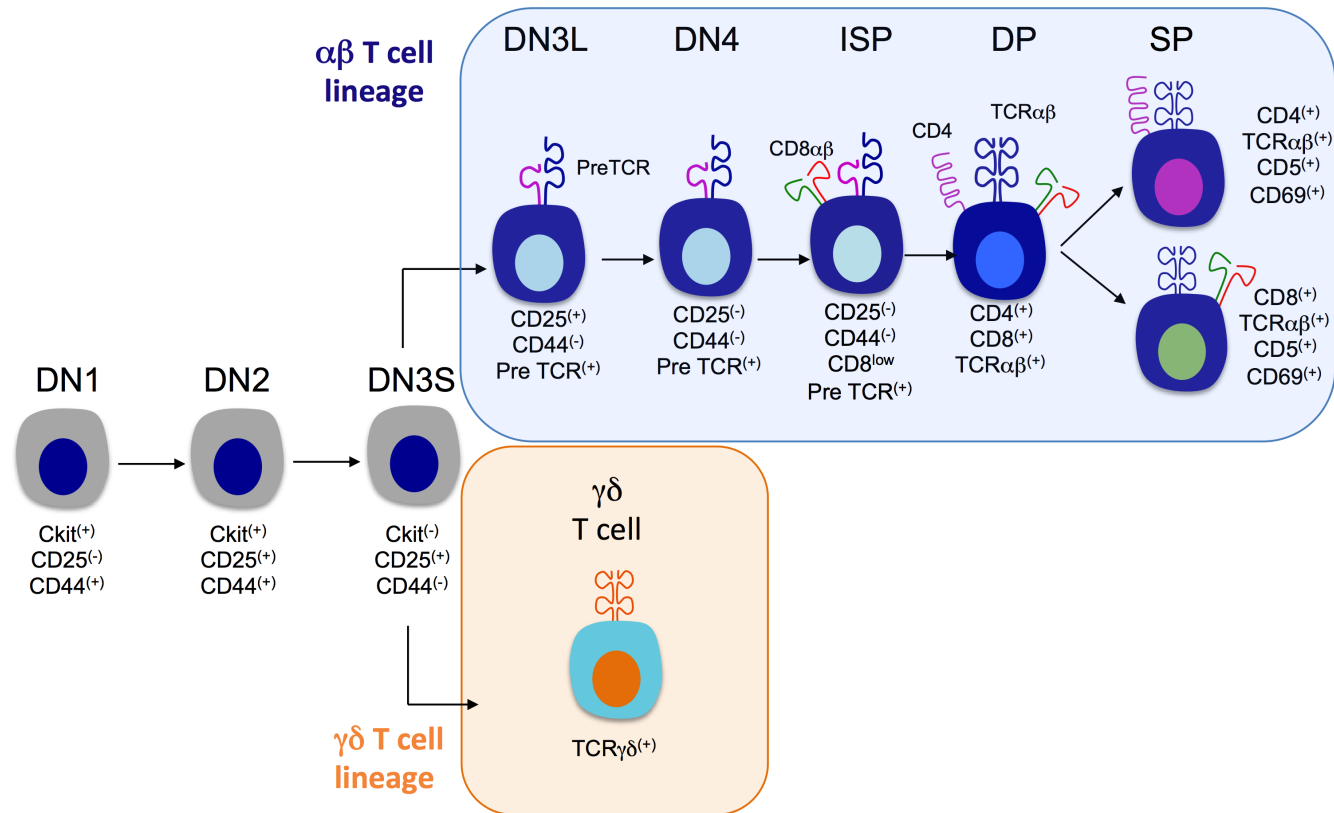
Figure 1.12 An overview of thymic T cell development. A progenitor enters the thymus with a double negative (DN) phenotype due to lack of CD4 and CD8 expression. The DN stage is conventionally divided into five DN steps: DN1 (CD44$^{(+)}$CD25$^{(-)}$cKit$^{(+)}$), DN2 (CD44$^{(+)}$CD25$^{(+)}$cKit$^{(+)}$), DN3s (CD44$^{(-)}$CD25$^{(+)}$cKit$^{(-)}$), DN3L (CD44$^{(-)}$CD25$^{(+)}$cKit$^{(-)}$pre TCR$^{(+)}$), and DN4 (CD44$^{(-)}$CD25$^{(-)}$cKit$^{(-)}$pre TCR$^{(+)}$). At the DN3s stage, expression of preTCR will drive the cell towards an $\alpha\beta$ fate whereas expression of TCR$\gamma\delta$ will drive commitment towards the $\gamma\delta$ T cell lineage. Progression from the DN4 stage leads to the immature single positive (ISP) stage followed by the double positive (DP) stage, from which single positive (SP) TCR$\alpha\beta^{(+)}$CD4$^{(+)}$ and TCR$\alpha\beta^{(+)}$CD8$^{(+)}$ thymocytes are generated.

1.3.3 Intra-thymic migration

Thymic T cell development involves maturation of cells as they migrate within the thymus, a journey that relies on expression of integrins and chemokine receptors, and their respective ligands on thymic epithelial cells (TEC) of the thymic stroma (Petrie, 2003). TEC can be subdivided into cortical thymic epithelial cells (cTEC) and medullary thymic epithelial cells (mTEC) (Lucas et al., 2003; Takahama, 2006). Hematopoietic progenitors enter the thymus at the cortico-medulla junction and subsequently migrate to the sub-capsular region. From there they move inwards towards the medulla to finally egress the thymus via blood vessels found in the medulla. Importantly, colonization of the thymus is said to be a "gated" phenomenon, in which T cell precursors are recruited periodically and populate the thymus in waves (Foss et al., 2001).

Seeding of the thymus by hematopoietic progenitors starts at embryonic day 11.5 (E11.5) in mice, and at week 8 of gestation in humans. It is thought that this can occur in a vasculature-independent manner through the combined action of chemokine ligand 21 (CCL21) and CCL25 on progenitor-expressed chemokine receptors 7 (CCR7) and CCR9 respectively (Liu et al., 2006; Liu et al., 2005; Misslitz et al., 2004). T cell progenitors are recruited to the outer cortex by CCR7, CCR9 and C-X-C chemokine receptor type 4 (CXCR4). However, although, CCR9-deficient animals show aberrant distribution of DN3 thymocytes within the cortex it did not result in a defect in T cell development (Figure 1.13) (Benz et al., 2004). Progression through the β-selection

checkpoint is dependent on CXCR4, which acts as a co-stimulatory signal (Ara et al., 2003; Plotkin et al., 2003; Trampont et al., 2009).
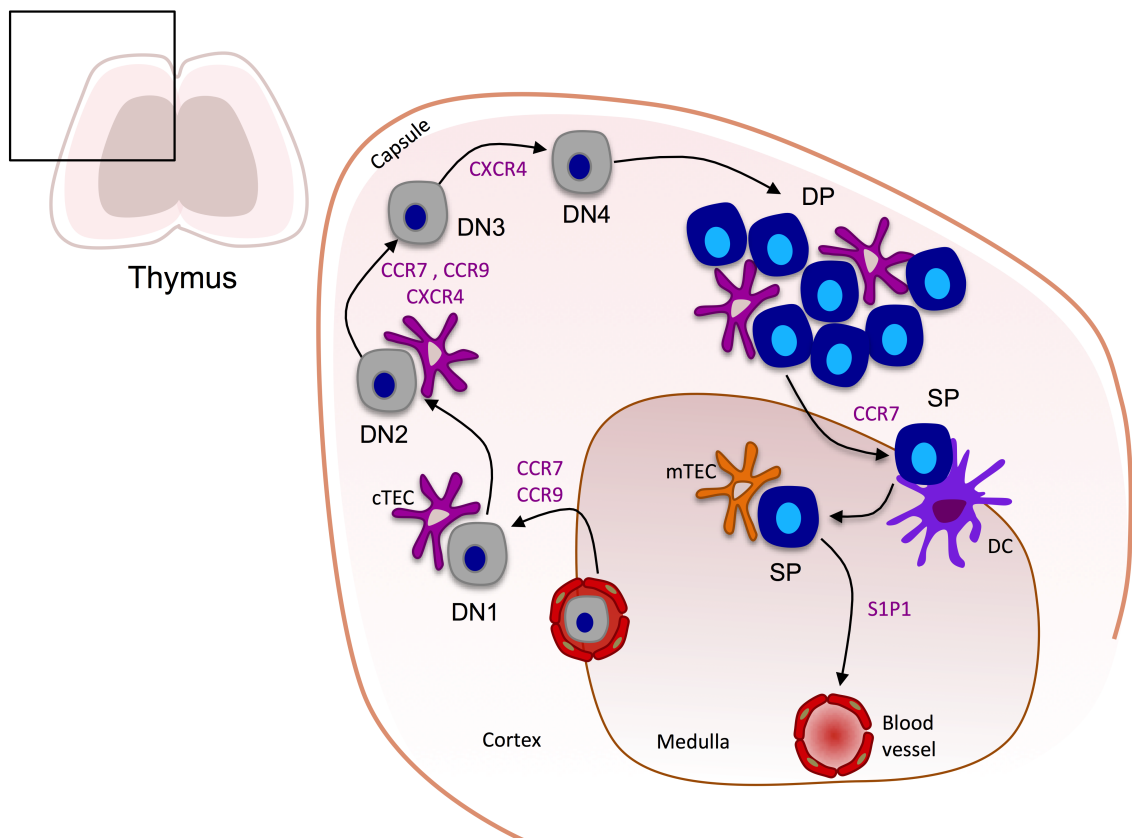
Figure 1.13 Schematic representation of intra-thymic migration. A hematopoietic progenitor enters the thymus at the corti-medulla junction via blood vessels. Migration of DN progenitors to the cortex is dependent on CCR7, CCR9 and CXCR4. Positive selection of DP thymocytes takes place in the cortex as peptides are presented by cTEC. CCR7 expression allows them to progress to the medulla once positively selected where their TCR$\alpha\beta$ will be further tested for self-reactivity by mTEC. Egress of the thymocytes relies on the expression of S1P1. DN, CD4$^{(-)}$CD8$^{(-)}$; CXC4 CX-chemokine receptor 4; CCR7, CC-chemokine receptor 7; CCR9,CC-chemokine receptor 9; DP, CD4$^{(+)}$CD8$^{(+)}$; DC, Dendritic cells; cTEC, cortical thymic epithelial cells; mTEC, medullary thymic epithelial cells; sphingosine-1-phosphate receptor 1 (S1P1). Adapted from (Takahama, 2006)

Finally, positively selected double positive (DP) thymocytes progress towards the medulla following a CCL19/21 gradient (CCR7 ligands) and up-regulate the G-coupled protein Sphingosine-1-Phosphate Receptor 1 (S1P1) (Kurobe et al.,

2006; Ueno et al., 2004). Because concentrations of Sphingosine-1-Phosphate (S1P) are low in the perivasculature cells but high in blood vessels connected to the thymus, thymocytes are attracted to follow this gradient and egress the thymus (Matloubian et al., 2004; Reinhardt et al., 2014; Schwab et al., 2005; Spiegel and Milstien, 2011)

1.3.4 Thymic T cell selection – a fundamental checkpoint for $\alpha\beta$ T cell development

1.3.4.1 Positive and negative selection of conventional T cells

The DP stage is the first point at which developing $\alpha\beta$ T cells express a newly generated TCR$\alpha\beta$ complex. Importantly, releasing self-reactive T cells in the periphery represents an obvious threat to health due to their ability to trigger autoimmune diseases. Thus, during a filtering process, known as T cell selection, TCR$\alpha\beta$ self-reactivity to self- antigens is assessed ensuring that only DP thymocytes with low self-reactivity develop into naïve conventional CD4$^{(+)}$ and CD8$^{(+)}$ T cells and egress the thymus. As highly motile DP thymocytes (3 to 8μm.min^{-1}) migrate throughout the thymic medulla, they halt to interact with self-peptides presented by mTECs (Bousso et al., 2002). Indeed, mTECs have the ability to display tissue-specific self-antigens due to the expression of the transcriptional factor autoimmune regulator (AIRE) (McCaughtry et al., 2008; Ramsey, 2002). The strength of TCR$\alpha\beta$ signal received by DP progenitors instructs the developmental outcome of (death or survival) and is proportional to the affinity between TCR$\alpha\beta$ and self-peptide/MHC. High affinity interactions (i.e.

full agonist) result in negative selection via induction of apoptosis. This prevents the maturation of self-reactive T cells and is often termed "central tolerance". Alternatively, a medium affinity interaction (i.e. a partial agonist) generates a positively selecting signal resulting in the survival and differentiation of DP cells (about 5% of all DPs) into CD4$^{(+)}$ or CD8$^{(+)}$ T cells. Finally, failure of a TCR$\alpha\beta$ to recognise self-peptide/MHC leads to a process known as "death by neglect" in which "useless" TCR$\alpha\beta$ are purged from the T cell repertoire (Figure 1.14) (Palmer, 2003; Stefanová et al., 2002). It has been estimated that as many as 75% of DP thymocytes that have initiated selection fail to mature and complete this process (Sinclair et al., 2013; Yates, 2014).

Number of thymocytes

TCR affinity to self-peptide MHC

TCRs not selected
TCRs positively selected
TCRs negatively selected
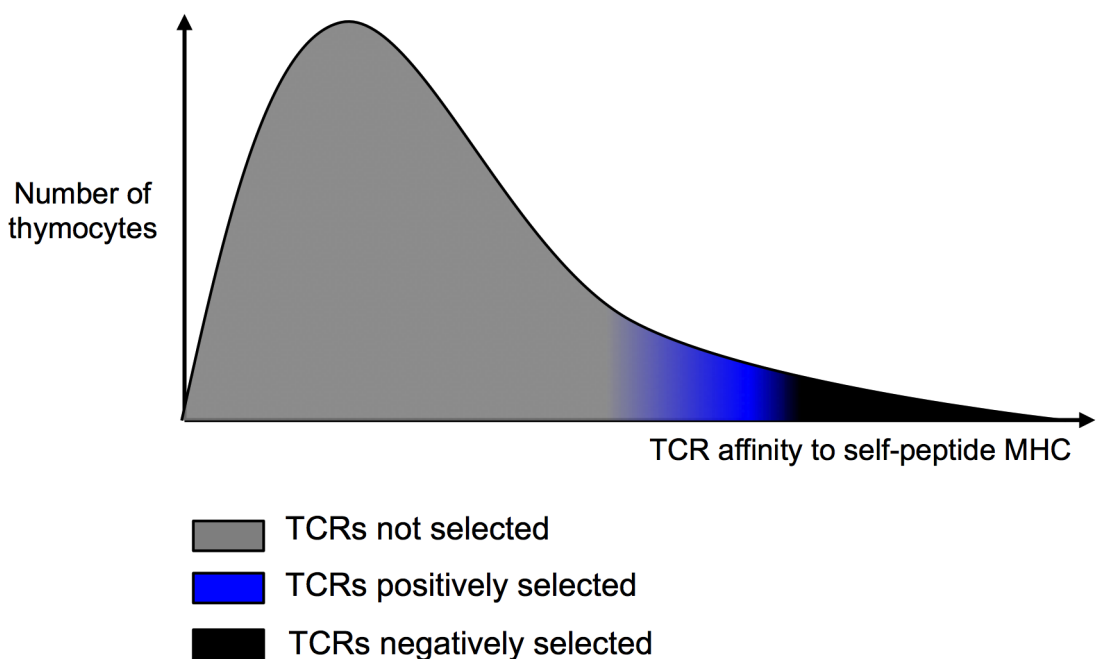
Figure 1.14 Central tolerance. DP thymocytes expressing a TCR$\alpha\beta$ which recognises self-peptide MHC with medium affinity undergo positive selection and are allowed to differentiate into TCR$\alpha\beta^{(+)}$CD4$^{(+)}$ and TCR$\alpha\beta^{(+)}$CD8$^{(+)}$ T cells. TCRs with high affinity towards peptide/MHC will be negatively selected resulting in their apoptosis. Finally, TCRs unable to recognise peptide/MHC will undergo death by neglect.

1.3.4.2 Agonist selection of unconventional αβ T cells

Unconventional αβ T cells follow an alternative method of selection in that they appear to undergo agonist-driven positive selection in which strong affinity between TCRαβ and self-peptide-MHC is required for DP cells to acquire an unconventional phenotype (Figure 1.15) (Jordan et al., 2001; Leishman et al., 2002).
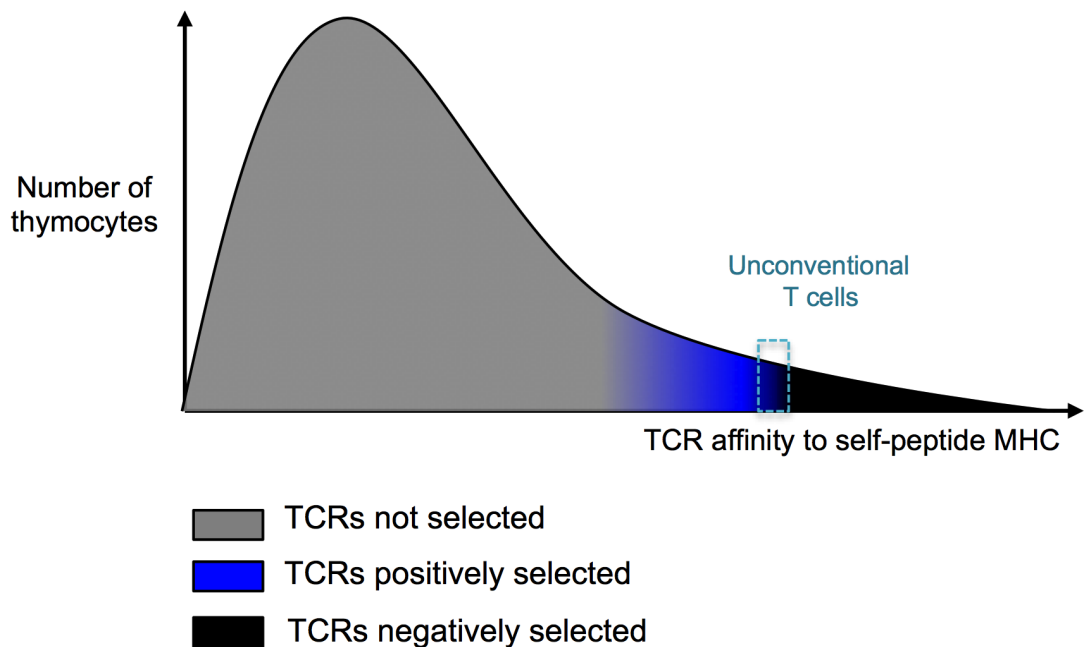
Figure 1.15 Agonist selection for unconventional αβ T cells. Conventional αβ T cells develop following interactions with weak affinity self-peptide MHC. By contrast, unconventional T cells are thought to be selected on stronger affinity interactions with self-peptide/MHC. Failure to recognise self-peptide or strong affinity binding with self-peptide result in death by neglect or negative selection respectively.

- Agonist selection of regulatory T cells

Agonist selection of regulatory T cells was demonstrated in a landmark study, which used the MHC-II-restricted TCR$\alpha\beta$ transgenic 6.5 system (also known as TSI TCR) recognising hemagglutinin of the influenza (HA) virus (Jordan et al., 2001). Crossing of these mice with a HA-expressing transgenic animal resulted in a striking increase of CD4[(+)] CD25[(+)] T cells, indicative of regulatory T cells, amongst CD4[(+)] thymocytes (Jordan et al., 2001). When the TSI transgenic TCR was mutated to bind HA with weaker affinity, regulatory T cell development was no longer favoured (Jordan et al., 2001).

- TCR$\alpha\beta$[(+)]CD8$\alpha\alpha$[(+)] IELs

Data suggests that TCR$\alpha\beta$[(+)]CD8$\alpha\alpha$[(+)] IELs also undergo agonist selection driven by self-peptide. Indeed, male mice transgenic for a TCR$\alpha\beta$ recognising the male specific antigen HY (that is presented on MHC-I) were shown to have a greater proportion of HY-specific TCR$\alpha\beta$[(+)]CD8$\alpha\alpha$[(+)] IELs compared to conventional HY-specific $\alpha\beta$ T cells. The authors concluded that TCR$\alpha\beta$[(+)]CD8$\alpha\alpha$[(+)] IELs must be developing via agonist selection in the thymus (Cruz et al., 1998). In another study, co-culture of HY-TCR-bearing thymocytes with stromal cells from female thymuses (i.e. that lack the H-Y antigen) and supplemented with increasing concentrations of agonist HY peptide, showed an increased generation of CD8[(+)] T cells with a TCR$\alpha\beta$[(+)]CD8$\alpha\alpha$[(+)] phenotype when compared to conventional cytotoxic T cell progenitors (Yamagata et al., 2004). Similar results were obtained when OT-I transgenic T cells, recognising an ovalbumin peptide presented by MHC-I, were supplemented with increasing dose of peptide or when the MHC-II restricted 5CC7 TCR transgenic cells

recognising cytochrome c preferentially adopted a $TCR\alpha\beta^{(+)}CD8\alpha\alpha^{(+)}$ phenotype in the presence of high dose of cytochrome c (Leishman et al., 2002). Thus, supplementation of agonist peptide in three different TCR transgenic models correlated with gradual disappearance of conventional $TCR\alpha\beta^{(+)}CD8\alpha\beta^{(+)}$ cells and appearance of $TCR\alpha\beta^{(+)}CD8\alpha\alpha^{(+)}$ cells (Yamagata et al., 2004).

It remains unclear why some DP thymocytes undergo conventional selection based on medium affinity $TCR\alpha\beta$/self-peptide/MHC interactions to become conventional naïve $CD4^{(+)}$ and $CD8^{(+)}$ T cells, while other DP cells that receive an agonist signal develop as unconventional T cells. It may suggest that the DP stage consists of a heterogeneous subset of cells, which do not have equal potential to become conventional or unconventional T cells. This leads to some interesting questions; How is this heterogeneity achieved? And why do some DP cells survive strong signals and develop into unconventional T cells while others undergo apoptosis? These questions form a basis for the work presented in this thesis.

1.3.4.3 Major signalling pathways implicated in T cell selection

Differing affinities of interaction of $TCR\alpha\beta$ with self-peptide/MHC during T cell selection trigger qualitatively different intracellular signals that result in DP cell survival or death. This raises the question of how signalling through a single receptor (here $TCR\alpha\beta$) leads to opposing developmental outcomes. This can be principally explained by engagement of qualitatively different signalling pathways. Indeed, the affinity and length of interaction between $TCR\alpha\beta$ and

self-peptide/MHC during positive selection dictates the frequency of $Ca^{(2+)}$ oscilliations and likely influences downstream MAPK pathways including those that engage ERK, JNK and p38; weak affinity interactions have been associated with an oscillatory $Ca^{(2+)}$ signal, medium affinity interactions with a sustained $Ca^{(2+)}$ signal, while high affinity interactions (with full agonist) with a transient $Ca^{(2+)}$ signal (Kupzig et al., 2005). The role of ERK in the positive selection of T cells was initially demonstrated in a study where transgenic expression of a dominant negative MEK1 transgene, that is the up-stream activator of ERK, was shown to reduce positive selection of DP thymocytes as shown by a reduction in DP CD69[(+)] cells (Alberola-Ila et al., 1995). However, HY-TCR transgenic mice expressing the dominant negative transgene did not show a difference in the degree of negative selection, supporting initially a role for the MEK1/ERK1 pathway only in the positive selection of T cells (Alberola-Ila et al., 1995). Subsequent studies analysing the kinetics of ERK signalling showed that negatively-selecting peptides triggered a short but strong ERK signal while positively-selecting peptides resulted in a sustained long-lived ERK signal (Mariathasan et al., 2001; Starr and Hogquist, 2005; Werlen et al., 2000). It was subsequently shown by Crabtree's lab that negatively-selecting ligands (high affinity ligands) activated ERK as well as the Bim-expressing apoptotic pathway, resulting in cell death. By contrast, positively-selecting ligands triggered the calcineurin-NFAT signalling pathway and turned ERK in what the authors described a "high competence state" preventing activation of Bim and allowing positive selection and further differentiation of DP thymocytes (Gallo et al., 2007). However, negative selection is not solely mediated by Bim and ERK but is also dependent on JNK and p38, which are mainly activated by the

kinases MAKK4/7 and MAKK3,4,6 respectively (Enslen et al., 1998; Remy et al., 2010; Sabapathy et al., 2001; Tournier et al., 1997). Indeed, DN cells from transgenic mice expressing a dominant-negative JNK1 transgene under the control of the Lck promoter were less able to undergo apoptosis following intravenous injection of anti-CD3 that is believed to mimic a strong signal through TCR$\alpha\beta$ (Rincón et al., 1998). Moreover, JNK1 or JNK2-deficient thymocytes did not undergo negative selection following CD3 cross-linking thus implicating JNK2 as a mediator of negative selection (Sabapathy, 2001; Sabapathy et al., 1999). Preliminary data supporting a role for p38 in negative selection came from the observation that FTOC of E17 C57Bl/6 thymuses supplemented with the p38 inhibitor SB203580, harboured a greater proportion of TCR$\alpha\beta^{high}$ SP thymocytes than in controls suggesting that DP cells had survived strong (possibly negatively-selecting) signals (Sugawara et al., 1998). Moreover, addition of SB203580 to E17 FTOC of HY-TCR transgenic thymuses rescued negative selection in male mice and did not alter positive selection in female. Finally, inhibiting p38 prevented the apoptosis of DP thymocytes following CD3-crosslinking (Sugawara et al., 1998). Altogether, these studies indicate a model where the strength of signal through TCR$\alpha\beta$ recruits different signalling pathways responsible for inducing death versus survival of DP thymocytes.

1.3.5 The β-selection checkpoint – An early checkpoint in T cell development

Commitment to the $\gamma\delta$ or $\alpha\beta$ T cell lineages occurs during a window of development that straddles the DN2, DN3 and DN4 stages. It is now widely

accepted to be dictated by the strength of signal delivered by one of the competing TCRs expressed at the β-selection checkpoint; TCRγδ or preTCR.

1.3.5.1 The pre T cell receptor (PreTCR)

a. The structure of the preTCR

The preTCR consists of a rearranged TCRβ chain and an invariant pTα protein (Figure 1.16). pTα was first identified in the early 1990s following the observation that TCRα-deficient animals showed normal TCRβ expression and T cell development at the DN stage. Instead, T cell development was impaired at the DP stage where TCRα replaces pTα to form TCRαβ (Saint-Ruf et al., 1994). It was subsequently discovered that TCRβ was associated, in addition to CD3 signalling molecules, with an unknown [^{3}H]-leucine-labeled-33kD glycoprotein later named pTα (Fehling et al., 1995; Groettrup et al., 1993)

The *ptcra* gene is located on mouse chromosome 17 (Chr 17) and on the short arm of human chromosome 6 (Chr 6), and is approximately 8kb long. Its structure is highly conserved across species, with nearly 77% homology between mice and humans, most of which arises from the extracellular and transmembrane portions (Del Porto et al., 1995; Saint-Ruf et al., 1998).

b. There are two isoforms of pTα

Two isoforms of pTα exist, as a result of alternative splicing (Figure 1.17). Full-length pTα (referred to as pTα[a]) is composed of all four exons while the truncated isoform (referred to as pTα[b]) lacks the Ig-loop structure encoded by exon 2, and has been widely ignored (Barber et al., 1998). pTα[b] was first

discovered in H4β cells originally derived from splenocytes obtained from TCRα-deficient mice (Barber et al., 1998).
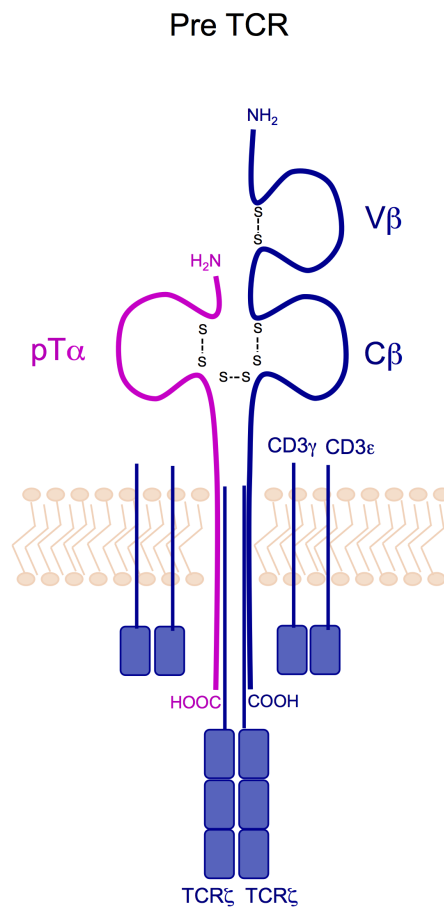
Pre TCR

Figure 1.16 The preTCR complex. The preTCR complex is composed of a TCRβ chain and an invariant pTα protein together with CD3 signalling molecules.

Indeed, it was found that despite the lack of TCRα, these mice possessed a population of peripheral TCRβ$^{(+)}$-only cells. Importantly, H4β cells expressed similar levels of TCRβ, CD69, CD3 and Zap-70 as peripheral T cells from wild-type animals. Using PCR, it was revealed that these cells expressed a pTα mRNA lacking approximately 300bp, which is roughly the size of exon 2. Thus, it was hypothesised that pTα may be undergoing alternative splicing in the thymus. Thymic expression of both RNA isoforms in DN cells undergoing β-

selection was subsequently confirmed both by PCR and northern blot (Barber et al., 1998).

c. The role of pTα

The role of pTα was initially demonstrated in pTα-deficient animals in which exon 3 and the beginning of exon 4 were disrupted by the insertion of a neomycin cassette. Importantly, pTα-deficient mice cannot give rise to either of the two pTα isoforms (Barber et al., 1998). These animals showed a profound block at the DN3 stage (with only 10% of the thymus represented by DP cells), illustrating the important role of pTα at the β-selection checkpoint.
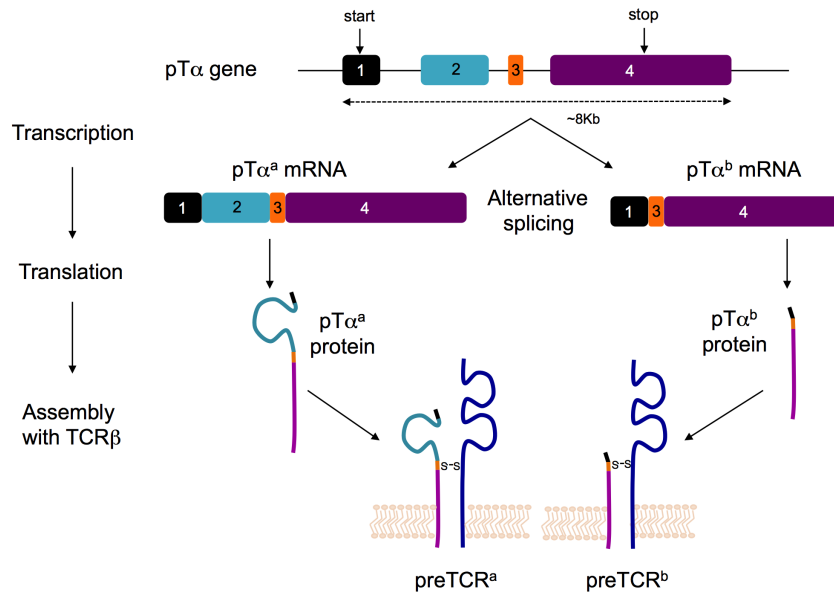
Figure 1.17 pTα can undergo alternative splicing to give rise to two isoforms. The pTα gene is composed of 4 exons. Exon 1 encodes the leader peptide (black), exon 2 the Ig-loop structure (blue), exon 3 (orange) the cysteine residues necessary for disuphilde bonds, and exon 4 (purple) the transmembrane domain and the cytoplasmic tail. Following transcription, alternative splicing of the pTα primary mRNA transcript can give rise to two mRNA; pTα[a] mRNA is encoded by exons 1, 2, 3 and 4 while pTα[b] lacks exon 2 and is composed of only three exons. Translation of the mRNA gives rise to two different proteins which, once paired with TCRβ chain, give rise to two different preTCRs; preTCR[a] and preTCR[b]

Conversely, the γδ T cell compartment was increased by nearly 3-fold illustrating that, in normal circumstances, the preTCR competes with TCRγδ to divert DN progenitors to an αβ fate (this is reviewed below). The 10% of DP thymocytes observed in pTα-deficient mice appear to result from the use of TCRγδ. These DP cells can then undergo TCRα rearrangement to generate a TCRαβ that permits subsequent T cell development (Buer et al., 1997; Fehling et al., 1995). Expression of the preTCR triggers survival and proliferation of DN3 cells, and differentiation to the DN4 stage. Importantly, the preTCR also

promotes allelic exclusion at the TCRβ locus that prevents a second TCRβ chain from being rearranged once a successful TCRβ chain has formed the preTCR. Indeed, whereas most mature TCRαβ[(+)]CD8[(+)]T cells were found to contain only one productive TCRβ chain in BALB/c mice, two productive TCRα rearrangements were detected in nearly 30% of them (Casanova et al., 1991). This led to the hypothesis of an "ordered rearrangement process" where the first rearranged TCRβ chain would feedback and prevent the rearrangement of the second allele (Alt et al., 1984). Importantly Single cell PCR analysis of CD4[(-)]CD8[(-)]CD25[(+)]thymocytes expressing intracellular TCRβ chains subsequently showed an increased frequency of in-frame TCRβ in WT cells (30%) compared to pTα-deficient cells, implicating the preTCR as a key regulator of TCRβ allelic exclusion (Aifantis et al., 1997). PreTCR-induced proliferation of DN3 thymocytes was recently shown to be important for subsequent αβ differentiation. In this study, sorted DN3s cells that had not undergone at least four rounds of proliferation were unable to differentiate when cultured on OP9-Delta-like 1 (OP9-DL1) cells, widely accepted to support T cell development (Kreslavsky et al., 2012). Thus, preTCR signalling may also be important for subsequent stages of T cell development.

There have been only a few studies that have investigated the role of the truncated isoform of pTα (pTα[b]) in T cell development (Barber et al., 1998; Gibbons et al., 2001). Barber *et al.* showed that co-transfection of a TCRβ construct with either pTα[a] or pTα[b] in TCR-deficient H4β cells resulted in a lowered surface expression of TCRβ in the presence of pTα[a] but not pTα[b] (Barber et al., 1998). Interestingly, co-transfection of TCRβ with either one of

the pTα isoforms in a panel of twelve different cell lines revealed that cells co-expressing pTα^b and TCRβ were the highest IL-2 producers following CD3 cross-linking (that is β/300.2, T6 and T10 cell lines) in comparison to cell lines expressing only TCRβ, only pTα^a, or both TCRβ and pTα^a (Barber et al., 1998). Thus, these preliminary results were the first to reveal a potential different biological role for each pTα isoform at the β-selection checkpoint. Subsequently, Gibbons *et al.,* generated transgenic mice on a pTα-deficient background expressing either full-length pTα^b or a truncated pTα^b lacking the proline rich region of its cytoplasmic tail. These animals both showed a rescued DP compartment, a decreased proportion of $\gamma\delta$ T cells and allelic exclusion of the TCRβ locus when compared to pTα-deficient animals (Gibbons et al., 2001). However, both strains displayed reduced thymic cellularity compared to WT animals (i.e. with normal preTCR function). This suggested that although a preTCR consisting of pTα^b was able to delivery most of the signals required to traverse the β-selection checkpoint, both pTα isoforms were needed to fully rescue T cell development. Importantly, expression of the pTα transgene in these animals was under the control of the proximal Lck promoter, which is constitutively expressed from the DN3 stage of T cell development onwards (Molina et al., 1992; van Oers et al., 1996). Thus, expression of the pTα transgene did not reproduce endogenous pTα expression. Nonetheless, these two studies suggest that pTα^b is biologically active and capable of transmitting signals at the β-selection checkpoint. Thus, in conclusion the two preTCRs (that is preTCR^a and preTCR^b resulting from the association of pTα^a or pTα^b with TCRβ respectively) may have non-redundant roles at the DN to DP transition

that may reflect either qualitative or quantitative differences in the engagement of downstream signal transduction pathways.

d. Regulation of the pTα gene - c-Myb, E-proteins and Notch

Preliminary studies investigating pTα expression were hampered by its low cell-surface expression and its high rate of endocytosis preventing the use of pTα-specific antibodies. To circumvent this issue, reporter mice expressing human CD25 protein under the control of the pTα promoter (hCD25Tg) were generated and used to investigate pTα expression (Gounari et al., 2002). pTα mRNAs were detected in small gut-associated lymphoid structures called cryopatches and CD19$^{(-)}$ bone marrow cells in WT-C57Bl/6 mice using PCR (Bruno et al., 1995). These bone marrow progenitors were subsequently further characterised in hCD25 mice and were c-Kit^{low}Sca-1^{low}IL-7Rα$^{(+)}$, a phenotype corresponding to the common lymphoid progenitors (Gounari et al., 2002; Kondo et al., 1997; Reizis and Leder, 2001). However, pTα expression is mainly restricted to the thymus (Bruno et al., 1995). Its expression is initiated at the DN2 stage of T cell development, reaches a peak at the DN3 stage, and subsequently ceases at the DP stage (Reizis and Leder, 1999). Characterisation of the upstream portion of the pTα gene revealed the presence of a proximal promoter (Reizis and Leder, 1999). In addition, a highly conserved region of both the human and mouse pTα gene (with up to 60% homology) located 4Kb upstream of the 5' end of the pTα gene was suspected to contain an enhancer (Reizis and Leder, 1999). Its presence was confirmed using two strains of BAC transgenic mice both containing an enhanced green fluorescent protein (eGFP) sequence

adjacent to exon 1 of the pTα gene, and either a functional or disrupted enhancer due to the insertion of a zeocin cassette. Flow cytometry analysis of DN3 thymocytes in four different transgenic founders revealed a lack of GFP expression in transgenic mice lacking the enhancer. The authors concluded that the presence of the enhancer was required for pTα expression (Reizis and Leder, 2001; Tremblay et al., 2003). Moreover, analysis of the nucleotide sequence of the enhancer identified the presence of a consensus binding site for the transcription factor c-Myb. An electrophoretic mobility shift assay (EMSA) confirmed the interaction of c-Myb with the DNA sequence and showed that its mutation abolished interaction (Reizis and Leder, 2001). Finally, mutating the c-Myb site in BAC eGFP pTα transgenic mice significantly decreased levels of pTα expression.

E12, E47, E2-2 and HEB are all members of the basic helix-loop-helix (bHLH) family of E protein transcription factors. They bind DNA in a homodimeric or heterodimeric manner at enhancer box sites (E-box site) that contain the palindromic sequence CACGTG (Osborne, 2000). An E-box site was identified in the enhancer region of the pTα gene and initial work showed that overexpression of the stem cell leukemia (SCL) member of the bHLH family, resulted in a block at the DN to DP transition that correlated with a significant decrease in pTα mRNA transcripts in DN3 and DN4 thymocytes. Interestingly, SCL and E2A or HEB transcription factors have an inverse expression through T cell development, which prompted the authors to investigate the role of E2A and HEB in regulating pTα transcription. Genetic deletion of HEB resulted in

decreased expression of pTα mRNA suggesting that it is also a regulator of pTα expression (Herblot et al., 2000; Tremblay et al., 2003).

It was also demonstrated that the pTα enhancer contained a binding region (CCTGGGAA) recognised by the Notch 1-activated transcription factor CSL (CBF1, Suppressor of Hairless, Lag-1) suggesting that notch signalling had an important role at the β-selection checkpoint (Reizis and Leder, 2002). This was further confirmed with the use of reporter mice. Insertion of an eGFP reporter under the influence of a CSL binding site, revealed GFP expression at the DN2 and DN3 stages, matching the pattern of pTα expression (Reizis and Leder, 2002). Moreover, mutation of the CLS binding site resulted in a delay in pTα up-regulation (Reizis and Leder, 2002).

Thus, expression of the pTα gene is regulated by c-Myb, E-proteins and the Notch 1-induced transcription factor CSL (Reizis and Leder, 1999; Reizis and Leder, 2001).

e. Interleukin-7 (IL-7) signalling at the β-selection checkpoint

IL-7 has a central role in T cell development as demonstrated by the profound block observed at the DN2/DN3 stage of T cell development in IL-7Rα-deficient mice (Peschon et al., 1994; Sudo et al., 1993). Administration of anti-CD3 *in vivo* into RAG-deficient animals is often used to mimic progression through the β-selection checkpoint. It was shown that IL-7R mRNAs could be detected within 1.5hrs of anti-CD3 injection and was followed by the cell-surface expression of IL-7Rα within 6hrs suggesting that preTCR signalling was implicated in IL-7R expression (Trigueros et al., 2003). In agreement with this,

DN4 cells from pTα$^{-/-}$ and TCRβ$^{-/-}$ mice expressed significantly lowered levels of IL-7Rα than DN4 cells from WT, and TCRα$^{-/-}$ mice (Trigueros et al., 2003). Finally, DN4 cells from IL-7Rα$^{-/-}$ mice showed normal proliferation but increased cell death suggesting that the IL-7/IL-7Rα axis is implicated in transmitting survival signals at the DN4 stage. IL-7 is thought to convey survival signals through the activation of the pro-survival factor Bcl2. Indeed, expression of a Bcl2 transgene in IL-7Rα-deficient mice rescued T cell development past the DN stage with numbers of peripheral CD4$^{(+)}$ and CD8$^{(+)}$ T cells similar to those found in IL-7Rα sufficient mice (Maraskovsky et al., 1997).

1.3.5.2 γδ or αβ lineage commitment

Several models have been postulated to explain why DN3 thymocytes adopt either a γδ or αβ T cell fate. These are; the instructional model, the stochastic or selective model and the signal strength model.

The instructional model proposes that commitment to one lineage is solely dependent on the expression of a specific TCR. Thus, DN cells expressing TCRγδ will commit to the γδ T cell lineage whereas DN cells expressing preTCR will enter the αβ T cell lineage. This model led from observations made in the late 1980s that TCRδ transcripts could be detected two days earlier than TCRβ transcripts. It was therefore suggested that T cell progenitors would first attempt

to rearrange TCRγ and TCRδ to form a TCRγδ. If that failed the cells would then attempt to rearrange TCRβ to commit to the αβ T cell lineage (Pardoll et al., 1987; Snodgrass et al., 1985). This idea then developed into a model in which TCRγδ and preTCR competed to instruct fate. In this version of the instructional model, DN cells would attempt TCRγ, TCRδ, and TCRβ rearrangements simultaneously, with the cell adopting a γδ cell fate if TCRγδ rearranged first, and an αβ T cell fate if TCRβ rearranged first. Despite its obvious merits, more recent work from mice deficient for TCRβ or pTα suggested that TCRγδ is also able to drive commitment to the αβ T cell lineage (Buer et al., 1997; Fehling et al., 1995). Indeed, thymuses from pTα-deficient animals, which cannot form a preTCR, harboured a significant number of DP thymocytes and some SP thymocytes (Fehling et al., 1995). In these animals, the DN to DP transition is partially driven by TCRγδ as pTα$^{-/-}$.TCRδ$^{-/-}$ mice have a much smaller DP pool than pTα-deficient mice (Buer et al., 1997). Moreover, early expression of TCRαβ complexes at the DN stage in transgenic animals (e.g. in HY Tg mice) allows development of T cells with a γδ-like phenotype, as suggested by the presence of the TCRδ locus that is usually absent from conventional αβ T cells due to rearrangement of the TCRα locus (Bruno et al., 1996). This suggests that lineage commitment is not instructed by the type of TCR *per se,* although TCRγδ expression and signalling is clearly important for γδ T cell development.

The stochastic or selective model, suggests that early DN thymocytes do not possess equal potential to adopt an αβ or γδ lineage fate and that pre-existing factors within the cell predispose it to one lineage or the other. In this model,

expression of a particular TCR is thought to only reinforce pre-commitment to a specific lineage. Initial observations by the Raulet group revealed that while all DN1 cells expressed similar levels of the IL-7 receptor α (IL-7Rα) chain, DN2 cells had heterogenous expression. More importantly, IL-7Rα$^{(-)}$ DN2 thymocytes appeared to be skewed towards the αβ lineage, whereas IL-7Rα$^{(+)}$ DN2 cells preferentially developed as γδ T cells (Kang et al., 2001). Of note, IL-7 signalling is essential for TCRγ rearrangement, which would be in agreement with the idea that IL7Rα$^{(+)}$ DN2 preferentially adopt the γδ lineage (Schlissel et al., 2000). However, the same group demonstrated that TCRγ rearrangement was independent of the IL-7Rα-mediated skewing of lineage commitment. The transcription factor SOX13, has also been suggested to be required for γδ but not αβ lineage commitment (Melichar et al., 2007). SOX13 was found to be expressed in only 45% of DN2 thymocytes, and correlated with expression of IL-7Rα (Melichar et al., 2007). While mice deficient in SOX13 showed normal αβ T cell development, numbers of γδ T cells were reduced by more than 50% (Melichar et al., 2007). Furthermore, over-expression of SOX13 compromised development of αβ T cells when compared with γδ T cells, suggesting that expression of both IL-7Rα and SOX13 within DN2 cells pre-commits progenitors to the γδ T cell lineage (Melichar et al., 2007). Although these two reports favour a pre-commitment model, further studies showed that immature TCRγδ-expressing DN3 thymocytes cultured on OP9-DL1 stromal cells, could give rise to both γδ T cells and *bona fide* αβ T cells (Kreslavsky et al., 2008). However, increasing signal strength through cross-linking of CD3 molecules impaired progression to the DP stage, instead favouring a γδ T cell fate

(Kreslavsky et al., 2008). This illustrates that DN3 cells still possess some plasticity to divert to the $\gamma\delta$ or $\alpha\beta$ lineage under instruction from TCR signalling.

The most recent suggested model, the signal strength model, tries to unite the observations described above. This model proposes that it is signal strength, delivered by a particular TCR complex (TCR$\gamma\delta$ or preTCR) that dictates lineage commitment. Specifically, the model states that "weak" signals drive DN progenitors into the $\alpha\beta$ T cell lineage, whereas "strong" signals instruct DN cells to become $\gamma\delta$ T cells. Thus, the preTCR, that undergoes high levels of endocytosis resulting in a low cell-surface expression, generally signals weakly to drive cells to the DP stage, while TCR$\gamma\delta$ that is expressed at higher surface levels generally signals strongly to instruct adoption of a $\gamma\delta$ cell fate (2005; Ciofani and Zuniga-Pflucker, 2010; Hayes et al., 2005). The "signal strength" model is best illustrated by two landmark studies. Hayes and co-workers showed that modulating TCR signal strength could affect lineage commitment of DN3 cells regardless of the type of TCR being expressed. Specifically, mice expressing a specific transgenic TCR$\gamma\delta$ (Vγ6Vδ6Tg or Vγ6/Jγ1Cγ1-Vδ6/Dδ6/Jδ2/Cδ) during early T cell development, before TCRβ is rearranged, could generate both $\gamma\delta$ T cells and DP thymocytes (Hayes et al., 2005). However, weakening of the TCR$\gamma\delta$ transgene signal by crossing these mice onto a TCR$\zeta^{+/-}$ background, in which signal transduction through the TCR is likely to be weakened due to a reduction of 50% in cell-surface expression of the TCR$\gamma\delta$, resulted in a significant reduction in $\gamma\delta$ T cells and a development skewed towards the $\alpha\beta$ lineage with a 1.5 fold increase in DP thymocytes (both in proportions and cell numbers) (Hayes et al., 2005). Conversely, increasing

signal strength by over expression of a TCRζ transgene in Vγ6Vδ6Tg TCRζ$^{+/+}$ mice resulted in higher TCRγδ surface expression and increased generation of γδ T cells over DP thymocytes, illustrating that quantitative signalling differences could dictate T cell lineage commitment (Hayes et al., 2005). Finally, analysis of DN thymocytes *ex vivo* from TCRα-deficient animals, which can express only either a TCRγδ or the preTCR, showed that γδ T cells had higher levels of both phosphorylated Zap-70 and ERK1/2 when compared to αβ-lineage cells (DN3, DN4, ISP and DP cells) (Hayes et al., 2005). γδ T cells also had a higher cell surface expression of CD5, widely accepted to translate the strength of signal received by the cell, compared to TCRβ$^{(+)}$ DN3 thymocytes (Hayes et al., 2005).

In the second study, Haks and co-workers manipulated the strength of signal delivered by a TCR on the basis of Lck availability. They used the KN6 transgenic TCRγδ on a RAG-deficient background. The KN6 TCRγδ recognises the β$_2$m-dependent non-classical MHC class Ib molecules, T10 and T22. Importantly, ligand engagement of the KN6 transgenic TCRγδ with T22 was assumed to generate a "strong" signal. In one experiment, KN6 transgenic animals on a RAG-deficient background (KN6$^{(+)}$RAG$^{-/-}$) were crossed with a Lck-deficient animal to prevent transduction of a "strong" signal, while other KN6$^{(+)}$RAG$^{-/-}$ transgenic animals were crossed with a β$_2$m-deficient animal, in which the KN6 TCRγδ could no longer interact with T22. KN6 transgenic animals on a RAG$^{-/-}$ background have only ~1% of DP cells, but attenuation of signal strength, by Lck deficiency or the absence of T22, as demonstrated by lowered CD5 expression, led to a 126-fold and 188-fold increase in DP thymocytes respectively (Haks et al., 2005). Strong signalling through TCRζγδ

has been shown to trigger increased phosphorylation of ERK, which in turn can activate the early growth response (Egr)-Id3 pathway that is thought to initiate commitment to the $\gamma\delta$ lineage (Lauritsen et al., 2009). In agreement with this, the absence of Lck in the KN6 model resulted in reduced ERK phosphorylation as well as reduced expression of the transcription factors Egr1 and Egr3 (Haks et al., 2005; Hayes et al., 2005).

A more recent study that presented data consistent with the signal strength model demonstrated co-operation between preTCR and TCR$\gamma\delta$ to increase signal strength to drive cells toward the $\gamma\delta$ T lineage (Zarin et al., 2014). Indeed, simultaneous expression of TCRβ and the KN6 TCR$\gamma\delta$ in RAG2-deficient DN3 cells led to the development of mainly mature $\gamma\delta$ T cells. This illustrates that TCR$\gamma\delta$ signals "override" the weakly-signalling preTCR, presumably on the basis of signal strength (Zarin et al., 2014).

Collectively, these studies strongly suggest that quantitative differences in TCR signal strength in DN thymocytes can influence commitment towards the $\gamma\delta$ or $\alpha\beta$ lineage by modulating qualitatively different signalling pathways (e.g. ERK and Egr3).

1.4 Initiation of TCR signalling: Autonomous or ligand-driven?

1.4.1 Autonomous signalling capacity of the preTCR

Evidence that the preTCR may not require ligand engagement to initiate signal transduction first came from the observation that thymocytes could successfully traverse the β-selection checkpoint in MHC-I and MHC-II deficient animals (Koller et al., 1990). A subsequent study then demonstrated that Lck-driven expression of a TCRβ transgene lacking its variable domain in a RAG-1-deficient animal rescued development of DP cells (Irving et al., 1998). By contrast, expression of a fully truncated TCRβ, lacking both the variable and constant regions, was inefficiently expressed as demonstrated by a low CD3 cell-surface expression and did not restore T cell development in RAG-1 deficient mice suggesting that association with endogenous pTα chain was somehow unstable (Irving et al., 1998). Surprisingly, transgenic expression of a truncated preTCR, lacking all pTα and TCRβ Ig-loop structures (both V and C regions), and therefore presumably unable to engage ligand, rescued T cell development in RAG-1-deficient animals (with CD3 cell surface expression) suggesting that a fully truncated preTCR might be more stable than an assymetrical heterodimer (Irving et al., 1998). To assess the signalling capacity of the fully truncated preTCR, the latter was transfected into TCRβ-deficient Jurkat T cells along with a luciferase reporter plasmid regulated by NFAT activity. Transfection of truncated TCRβ alone, did not alter NFAT activity and did not restore CD3 cell surface expression (Irving et al., 1998). By contrast, transduction of the fully truncated preTCR or full-length TCRβ resulted in a

transient peak of luciferase activity within 15 hours indicative of NFAT-dependent signalling. Thus, it was concluded that cell-surface expression of the preTCR was sufficient for signal initiation (Irving et al., 1998). Surface localization by confocal microscopy showed that the preTCR was found in "patchy" distribution on the cell surface reminiscent of TCRαβ cell surface distribution following ligand binding and raft co-localisation (Saint-Ruf et al., 2000). Transduction into SCID thymocyte-derived cell line SCIET.27 of a vector containing a TCRβ (Vβ8.2Dβ1Jβ2.6Cβ2) chain and an eGFP fusion protein revealed clustering of the GFP signal, which was not observed when a vector containing GFP alone or a TCRγδ (Vγ1Jγ1Cγ4 and Vδ7.1Jδ1Cδ) gene was expressed, suggesting that preTCR complexes oligomerise (Saint-Ruf et al., 2000). Lck was also shown to co-localize with more than 80% of the pTα chains at the cell surface (Saint-Ruf et al., 2000). Importantly, targeting of the preTCR complex to the cell membrane is critical for T cell development, as retention in the ER impairs the DN to DP transition (O'Shea et al., 1997). A subsequent study showed that expression of the preTCR induces rapid endocytosis that mimics that of TCRαβ following ligand engagement (Yamasaki et al., 2006; Yamasaki and Saito, 2007). Indeed, expression analysis by fluorescence microscopy of either a pTα-eGFP or TCRα-eGFP fusion protein into TCRα-deficient hybridoma cell lines (TG40β) revealed that a significant portion of the pTα-eGFP protein was found within intracellular vesicles compared to TCRα-eGFP. Incubation of the cells with PE-labelled anti-TCRβ antibody for 30 mins showed a greater proportion of PE signal within the cells transfected with pTα than TCRα (Yamasaki et al., 2006). Thus, the consensus opinion is that cell-surface expression of the preTCR is sufficient to drive signal

transduction at the β-selection checkpoint in a ligand-independent manner (Panigada et al., 2002; Saint-Ruf et al., 2000).

Whether oligomerization of the preTCR is important for signal transduction is still a matter of debate. It was thought that the cysteine residues in the cytoplasmic tail of pTα played a role in recruiting pTα to lipid rafts that in turn facilitates ligand-independent signalling, but mutation of these cysteine residues (to alanine) did not abrogate preTCR signalling (Aifantis et al., 2002; Gibbons et al., 2001). Subsequently, four charged amino acids (D22 R24 R102 R117) contained in the Ig-loop of pTα, conserved between humans and mice, were implicated in the initiation of oligomerisation and subsequent preTCR triggering. Indeed, substitution of these residues to alanine was shown to impair preTCR function (Yamasaki et al., 2006). However, by contrast, evidence also exists to suggest that oligomerization mediated by the extracellular domains of pTα does not initiate signal transduction. This study used retroviral transduction of truncated pTα chains in foetal thymic organ cultures to show that pTα^b (that lacks three of the four charged residues mentioned above) could induce preTCR signal in a very similar manner to that seen with "wild-type" pTα^a (Ishikawa et al., 2010; Mahtani-Patching et al., 2011; Yamasaki et al., 2006). Crystallographic data also suggested that preTCR signalling was a consequence of the dimerization of two preTCR complexes through their extracellular Ig-loop domains resulting in a "sandwich-like" structure (Pang et al., 2010).

1.4.2 TCR$\gamma\delta$ signalling in DN thymocytes

As mentioned, commitment to the $\gamma\delta$ T cell lineage at the DN stage of thymocyte development is currently thought to result from a strong signal emanating from TCR$\gamma\delta$. Although a strong signal could be explained by greater surface expression of TCR$\gamma\delta$ compared to the lowly-expressed preTCR, strong signalling is generally considered to result from ligand-engagement as illustrated by the activation of mature $\alpha\beta$ T cells. However, the paucity of identified TCR$\gamma\delta$ ligands has made this very difficult to study, especially in mice. To complicate matters further, $\gamma\delta$ cells also acquire effector functions, in the shape of commitment to cytokine production, in the thymus. These developmental steps have also been postulated to depend on signal strength through TCR$\gamma\delta$. Thus, strong vs weak TCR$\gamma\delta$ signals, that may (or may not) correlate with ligand-dependent versus ligand-independent signal initiation, may well not only influence $\alpha\beta$ versus $\gamma\delta$ lineage commitment, but also affect subsequent effector function of developing $\gamma\delta$ cells.

Ligand independent signalling through TCR$\gamma\delta$ was first suggested by demonstration of oligomerisation of TCRδ chains *in vitro* mediated by the extracellular Ig-like variable regions of TCRδ (Jensen et al., 2008). However, expression in RAG-deficient cells of a truncated TCR$\gamma\delta$ lacking either both variable domains or all four Ig-like extracellular domains (and thus in both cases lacking the CDR regions implicated in ligand binding) successfully restored $\gamma\delta$ T cell development in foetal thymic organ culture suggesting that ligand-

independent signalling was compatible with $\gamma\delta$ T cell development (Mahtani-Patching et al., 2011).

Ligand-dependent signalling from TCR$\gamma\delta$ has been largely studied in the context of T10 and T22 binding that are non-classical or unconventional MHC class-Ib molecules, which are known to interact with the G8 and KN6 TCR$\gamma\delta$. T10 and T22 are encoded by the TL locus and share more than 94% sequence identity. Both T10 and T22 associate with β2-microglobulin (β_2m) but they are not involved in antigen presentation (Schild et al., 1994). While T10 is expressed by all mouse strains, T22 is absent from the BALB/c strain making them a useful strain in which to study $\gamma\delta$ T cell selection and development (Ito et al., 1990). Thus, development of $\gamma\delta$ T cells has been investigated in mice transgenic for the G8 or KN6 TCR$\gamma\delta$s crossed onto a C57Bl/6, BALB/c or β_2m-deficient background to modulate the presence or absence of the selecting ligands T10 and T22 (see below) (Crowley et al., 1997; Houlden et al., 1989). These sorts of studies were further helped by the generation of T22-tetramers that were used to identify $\gamma\delta$ T cells with T22-specific TCRs. T22-specific $\gamma\delta$ T cells in the β_2m-deficient animals had a phenotype characteristic of naïve T cells (CD44^{low}CD122^{low}) and with $\gamma\delta$ T cells known to secrete IL-17-A (Jensen et al., 2008). By contrast, T22-specific $\gamma\delta$ T cells from C57Bl/6 mice, where both T10 and T22 are present, expressed a typical "ligand-engagement" phenotype (CD44^{hi}CD122^{hi}) and could produce IFN-γ (Jensen et al., 2008). Thus, it was concluded that ligand engagement by TCR$\gamma\delta$ drives cells to adopt IFN-γ-secreting potential. However, it was unclear from the study whether

development of T22-specific IL-17A-secreting γδ T cells was the result of ligand-independent signalling or occurred following interactions with ligands unrelated to T10 and T22.

Further data pertaining to the involvement of ligands in γδ T cell development have been obtained from the study of dendritic epidermal γδ T cells (DETC). DETC development was shown to be dependent on the expression of the surface-associated B7-like Ig superfamily member Skint-1, which is expressed both by keratinocytes and mTECs (Barbee et al., 2011). These findings stemmed from observations by Lewis and co-workers that FVB/n mice from the supplier Taconic farms (FVB-Tac) were devoid of DETC when compared to FVB/n mice from Jackson Laboratories (FVB-Jax). Development of DETC was restored when thymocytes from FVB-Tac animals were transferred to FVB-Jax thymic stroma, suggesting that the missing determinant was expressed in non-haematopoeitic cells (Barbee et al., 2011). Genetic comparison between the two strains revealed a mutation in the *Skint-1* gene leading to a premature termination of transcription. Although direct engagement of Skint-1 by γδ T cells remains to be shown, further work from the lab showed that in the presence of Skint-1, developing DETC up-regulate the transcription factors Egr3 and Tbx21 (T-bet) in a NFAT/NFκB dependent manner that ultimately correlates with an IFN-γ-producing phenotype. In agreement with ligand-dependent development, cross-linking of the TCR with GL3, an anti-TCRδ antibody widely used to mimic ligand engagement, also led to the up-regulation of Egr3. By contrast, absence of Skint-1 led to the up-regulation of the transcription factors Sox13 and RORγt,

and led to the adoption of an IL-17A-secreting phenotype (Turchinovich and Hayday, 2011). Thus, these studies collectively suggest that ligand-engagement favours an IFN-γ-secreting $\gamma\delta$ T cell fate while ligand-independent signalling drives development of IL-17A-producing $\gamma\delta$ T cells.

Finally, a recent study published again by the same group seems to contradict their previous findings. This work investigated the role of signal strength in the development of IFN-γ versus IL-17A-secreting $\gamma\delta$ T cells using the SKG mouse model, which carries a mutation in Zap-70 resulting in a 90% loss in kinase activity (Sakaguchi et al., 2003). Flow-cytometry analysis of lymph nodes from these mice revealed a severely reduced complement of IL-17-producing $\gamma\delta$ T cells but a largely unchanged compartment of IFN-γ-producing $\gamma\delta$ T cells, when compared to WT mice (Wencker et al., 2014). This phenotype was tracked to a developmental defect in the thymus. From this, it was concluded that IL-17A-producing $\gamma\delta$ T cells require strong TCR$\gamma\delta$-mediated signals (through Zap-70) for their development, and that possibly this is likely to result from ligand interactions (Wencker et al., 2014).

Despite significant work over the past few years, the studies reviewed in this section provide opposing conclusions as to the requirement of a ligand for $\gamma\delta$ T cell development or the type of $\gamma\delta$ T cell subsets generated following ligand engagement/strong signalling (Figure 1.18). This illustrates the general lack of consensus regarding the mechanism by which strong TCR$\gamma\delta$ signals are generated and the role of signal strength in $\gamma\delta$ T cell development. These areas represent a main interest of our lab, and thus will also feature significantly in this thesis.
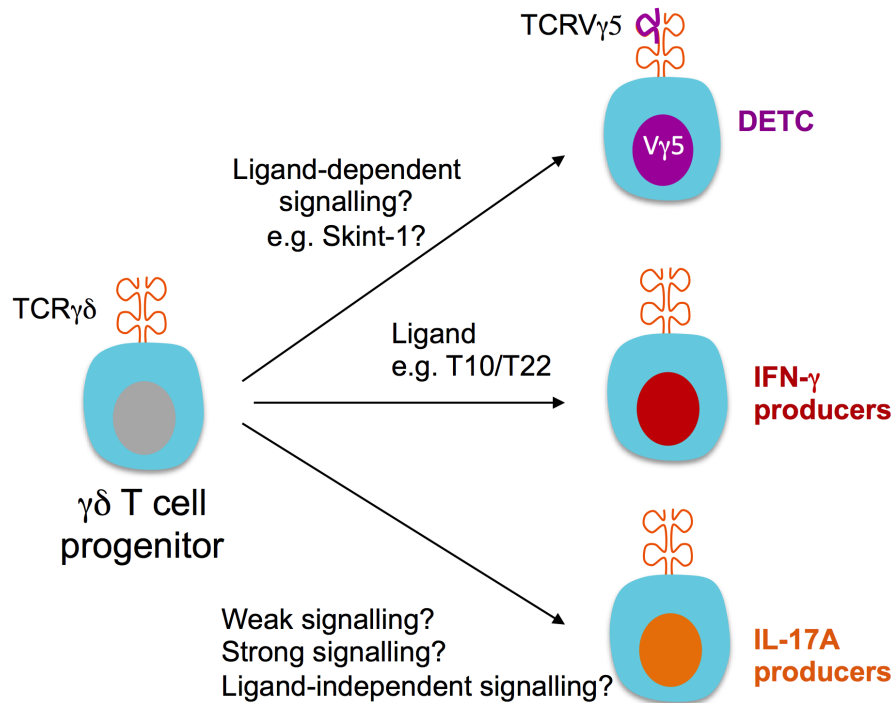
Figure 1.18 Schematic representation of the current uncertainty regarding γδ T cell development. It has been proposed that TCRγδ engagement of T10 and T22 favours the development of IFN-γ-producing γδ T cells. By contrast, ligand-independent signalling or recognition of currently unknown ligands may drive the development of IL-17A producing γδ T cells. Skint-1 may also be a ligand involved in DETC development. Finally, using SKG mice, the Hayday lab suggested that strong signalling was required for development of IL-17A-secreting γδ T cells while weak signalling favoured IFN-γ-producing cells.

1.5 Summary

TCR signalling is a central pillar of T cell development. There is increasing evidence that TCR signal strength in DN thymocytes is fundamentally important for dictating T cell fate (e.g. at the β-selection or T cell selection checkpoints). Importantly, the TCR signalling machinery is able to translate quantitatively different signals (driven or not by ligands) into qualitatively different signals that serve to instruct cell survival versus death during T cell selection, or $\alpha\beta$ versus $\gamma\delta$ lineage commitment at the DN3 stage. Moreover, it may also determine subsequent $\gamma\delta$ cell effector fate (i.e. IL-17A versus IFN-γ secretion).

However, several aspects of a signal-strength-driven model of T cell development remain to be elucidated. For example, at the DP stage, how does a "strong" TCR$\alpha\beta$ signal dictate two seemingly opposite fates; to die by apoptosis or to differentiate into an unconventional T cell subset. Perhaps, DP thymocytes constitute a heterogeneous population potentially pre-committed to a conventional or unconventional T cell fate. If this were the case, the factors responsible for establishing this heterogeneity are yet to be determined. It is known that DP thymocytes arise from DN3 cells following the successful expression of the preTCR at the β-selection checkpoint. The preTCR exists as two possible isoforms; preTCR^a and preTCR^b, but very little work has been carried out to investigate their individual roles due to the perhaps mis-placed idea that they have redundant functions at the β-selection checkpoint. Indeed, both pTα isoforms (pTα^a and pTα^b) have been conserved across evolution and

are found in human, chicken, and mice, likely demonstrating that they have been selectively kept for an important non-redundant role in T cell development. Finally, in the context of $\gamma\delta$ T cell development, the relationship between strong and weak signalling, and ligand-dependent and ligand-independent signalling are still not clear. Nor are signalling pathways that translate these differences in signalling intensity into distinct developmental outcomes.

1.6 Working hypotheses of the work presented in this thesis

1.6.1 General hypothesis

We hypothesise that both quantitative and qualitative differences in TCR signalling at the early stages of T cell development have fundamental consequences for subsequent T cell development and influence the type of T cell subsets generated by the thymus.

1.6.2 Sub-hypothesis 1

We hypothesise that preTCR^a and preTCR^b deliver qualitatively and/or quantitatively different signals responsible for establishing heterogeneity at the DP stage, that has a fundamental impact on the subsequent development of $\alpha\beta$ T cells.

1.6.3 Sub-hypothesis 2

We hypothesise that quantitative differences in TCR$\gamma\delta$ signalling in DN thymocytes recruits qualitatively different signalling pathways that drive the differential development of IFN-γ- versus IL-17-A- secreting $\gamma\delta$ T cell subsets.

The work presented in this thesis focuses on testing these hypotheses. The work on the preTCR^a and preTCR^b represents the largest part of this thesis (four chapters), whereas the $\gamma\delta$ T cell project was undertaken in collaboration with other members of the lab (Dr. J. Pang and Dr. Nital Sumaria) and thus is represented by only a single chapter.

1.7 Aims

- To characterise the expression of $pT\alpha^a$ and $pT\alpha^b$ isoforms of the $pT\alpha$ gene at the single cell level during T cell development.

- To investigate the role of $preTCR^a$ and $preTCR^b$ during T cell development in *vivo* using BAC-transgenic mice.

- To investigate the development of unconventional T cells using various strains of mice (C57Bl/6, FVB/n, BALB/c).

- To investigate how quantitative differences in $TCR\gamma\delta$ signalling are translated into the differential development of IFN-γ- versus IL-17A-secreting $\gamma\delta$ T cell.

- To investigate the role of PI3K signalling in $\gamma\delta$ T cell development

Chapter 2

Materials and methods

2.1 Molecular biology

2.1.1 Gel electrophoresis

Agarose gel electrophoresis was used to separate DNA molecules according to their molecular weight (size). It was used mainly to visualize PCR products, fragmented DNA molecules following enzymatic digestion, or in order to extract DNA fragments. The concentration of the agarose gel determines how tightly packed the polymers are between themselves. Therefore, the concentration of an agarose gel needs to be appropriately chosen depending on the size of the DNA fragment to be visualised. DNA fragments smaller than 1500bp were run on a 1.5% gel at 110V for 40mins. Isolation of BAC DNA fragments for subsequent pronuclear injection was achieved by running the DNA sample on a 0.5% gel at 40V for 2 to 3 hours. A 1.5% gel was made by dissolving 3g of Agarose (Sigma-Aldrich) in 200mL of 1x TAE buffer, diluted from 50X TAE buffer (Table 2.1).

The mixture was heated in a microwave for 1min, gently shaken and heated again for an extra minute to allow full dissolution of the agarose powder.

For visualization of PCR products without subsequent sequencing or cloning, 10μl of Ethidium Bromide (VWR) was added to the mixture once cooled down.

Alternatively, if the DNA sample was to be extracted for pronuclear injection or sequencing, 15 to 20µl of the non-mutagenesis nucleic acid gel stain, GelRed (Biotium), was used instead of Ethidium Bromide.

50X TAE buffer	242g Trizma base (Sigma-Aldrich)
	57.1ml Glacial Acetic Acid (Sigma-Aldrich)
	100ml 0.5M EDTA, PH 8.0 (Gibco, Invitrogen)
	dH$_2$0 to total volume of 1L

Table 2.1 Components of the 50X TAE buffer The table shows the reagents used for preparing 1L of 50X TAE buffer.

Once thoroughly mixed, the solution was poured onto a tray and was left for 30min at room temperature to solidify. Gels were run in 1x TAE buffer. DNA samples were mixed with 6X TriTrack Loading dye (Invitrogen) at a 1:6 dilution before loading on an agarose gel. To determine the size of DNA in the samples, a 1kb ladder (Fermentas) was used for PCR products with a size below 10kb. Alternatively, the GeneRuler high range DNA ladder (New England Bioscience, NEB) was used for products with a size between 10kb and 40kb.

2.1.2 Polymerase Chain Reaction (PCR)

Polymerase chain reaction (PCR) is a very sensitive technique allowing the amplification of a DNA sequence of interest. Using oligonucleotides or primers, the DNA region of interest is flanked and replicated by a polymerase. Each PCR step occurs at a specific temperature to allow denaturation of the DNA strands, primer binding, and elongation. The DNA is copied twice at each cycle, because of the presence of two strands, and therefore the quantity can be determined at each cycle by 2^n where n represents the number of cycles. Three

types of PCR reactions are presented in this section; Semi-quantitative PCR where the PCR products are visualized at the end of the reaction by running the PCR mix on an agarose gel; real-time PCR, which allows precise quantitation of the DNA throughout the reaction; and the single-cell PCR where semi-quantitative PCR is carried out on a single cell.

To avoid contamination, pipettes (Gilson), tubes (Starlab), and tube racks were kept separately and not used for other experiments. All equipment and workspaces were wiped with 1M sodium hydroxide (NaOH) solution and 70% Ethanol (Sigma-Aldrich) prior to setting up the PCR reaction. Gloves (SLS) were changed frequently throughout the experiment.

2.1.3 Semi-quantitative PCR

Unless indicated in the text, a common PCR master mix was used when setting up a semi-quantitative PCR (Table 2.2). The primers were designed in-house and ordered from Eurofins MWG Operon. The dNTP mix was obtained with the Taq polymerase (NEB) and was diluted to a final working concentration of 2.5mM. A common PCR programme was used for each cycle (Table 2.3). The elongation time is dependent on the size of the expected PCR band. Conventionally, 1min extension is used for every 1kb to amplify. The annealing temperature used for each primer was approximately 3°C below the manufacturer's recommended temperature. In some cases a gradient PCR was set up to determine the ideal annealing temperature. The PCRs were carried out in a Peqstars thermocycler (Peqlab).

Components	Volume for each reaction
Forward primer (25μM)	4μl
Reverse primer (25μM)	4μl
dNTPs (2.5mM)	2.5μl
Taq Buffer (10X)	2.5μl
Taq Polymerase	0.2μl
RNAse and DNAse Free Water	10.8μl
DNA (1ng to 1μg)	1μl
Total volume of the reaction	**25μl**

Table 2.2 List of the components constituting the PCR master mix. The table shows the common PCR master mix used for semi-quantitative PCRs. Primers were purchased from Eurofins MWG Operon. dNTPs, Taq polymerase and the Taq Buffer are supplied by NEB.

Step	Temperature	Time
Initial denaturation	95°C	5min
38 Cycles	95°C Primer Tm 72°C	30s 30s 1kb/min
Final extension	72°C	5min
Storage	4°C	∞

Table 2.3 Semi-quantitative PCR cycle. The first step consists of 95°C, which allows the two strands of DNA to come apart. The annealing temperature (Tm) is primer-specific and was generally 3°C under the recommended temperature. 72°C represent the temperature at which Taq polymerase proceeds to the elongation.

2.1.4 Single-cell PCR

Single-cell PCR was carried out in two steps using different set of primers (Table 2.4) (Eurofins MGW Operon). The first round PCR amplified the entire pTα cDNA regardless of its isoform by using a set of primers (M-pTageneF and M-pTageneR) recognizing a region located in exons 1 and 4 present in both pTα isoforms (pTα[a] and pTα[b]).

The second round PCR amplified $pT\alpha^a$ (M-pTaaF and M-pTaaR) or $pT\alpha^b$ (M-pTabF and M-pTabR) cDNAs, respectively, by using a set of primers recognizing the exon boundaries present only in $pT\alpha^a$ or only in $pT\alpha^b$ cDNAs. The first PCR cycle followed the same steps as the one described in Table 3 with only 34 cycles. The second round PCR was carried out using 2μl from the 1st PCR and the PCR cycle was repeated 25 times. The PCR was run in a Biorad thermocycler and the result was visualized on a 96-well 1% agarose gel (Biorad).

	Exon binding site	Primer Sequence (5' to 3')	Tm (°C)
M-pTageneF (Forward)	1	TAGGACATGGCTGCTGCTGC	61.4
M-pTageneR (Reverse)	4	GTCCAAATTCTGTGGGTGGGAG	62.1
M-pTaaF (Forward)	1-2	GCTCTACCATCAGGCATCGC	61.4
M-pTaaR (Reverse)	2-3	GATTCCCCTGACAGCTGGAG	61.4
M-pTabF (Forward)	1-3	GCTCTACCATCAGGGGAATCTTC	62.4
M-pTabR (Reverse)	4	GCTCAGCCACAGTACCTGC	61.0

Table 2.4 Primers used for the single-cell PCR. M-pTageneF recognises a sequence found in exon 1 and M-pTageneR in the un-translated region of exon 4 of pTα. Both were used to amplify total pTa cDNA during the first round PCR. M-pTaaF binds at the exon1-2 boundaries while M-pTaaR binds at the exon 1-3 boundaries. Therefore, this set of primers can only recognise $pT\alpha^a$ cDNA during the second round PCR. Finally, M-pTabF flanks a region at the exon1-3 boundaries and M-pTabR recognises a DNA sequence in exon 4, and were used to identify the $pT\alpha^b$ isoform during the second round PCR.

2.1.5 Real-time PCR

In contrast to semi-quantitative PCR, real-time PCR allows quantification of a PCR product as the reaction progresses. A fluorescent dye is incorporated in the newly generated DNA making it fluorescent and allowing the thermocycler

to monitor the number of DNA copies present at each cycle. As a result, real-time PCR is a very useful technique to compare differences in cDNA quantity across different samples. Because of its high sensitivity, it is also a useful tool to detect very low amounts of DNA.

The real-time PCR was set up using the Power SYBR green PCR Master Mix (Applied Biosystems) according to the manufacturer's instructions. Briefly, 1µl of each 10µM forward and reverse primers were mixed with 10µl of the 2X power SYBR Green PCR Master Mix and 2µl of cDNA was added to a final volume of 20µl. The reaction was set up in a MicroAmp® Optical 96-Well Plate (Applied Biosystems) and run on a 7500 Real-Time PCR system (Applied Biosystems). The primers were designed in-house and ordered from Eurofins MWG Operon. The primers were tested for their efficiency, which was calculated using a standard curve generated from a 1:2 serial dilution of the cDNA template. The standard curve was obtained by plotting the dilution factor against the Ct value determined during the amplification of each dilution. The amplification efficiency was calculated in percentage using the equation below:

$$\% \, Efficiency = (E - 1) \times 100$$

Where E is the amplification efficiency as defined by

$$E = 10^{-(\frac{1}{Slope})}$$

And where the slope of the curve can be calculated using the following equation:

$$Slope = \frac{yb - ya}{xb - xa}$$

An optimal amplification efficiency should lie between 95 and 105%.

The Ct values were defined by setting up the Ct threshold manually above the background noise.

	pTα exon binding site	Primer Sequence (5' to 3')	Tm (°C)
qpTaaF (Forward)	1-2	GGCTCTACCATCAGGCATCGC	61.9
qpTaaR (Reverse)	2	CGAGGACCAGGCAAACCACC	63.4
qpTabF (Forward)	1-2	GCTCTACCATCAGGGGAATCTTC	62.4
qpTabR2 (Reverse)	2-3	CCGCTGTGTCCCCCCG	62.0
qGAPDH (Forward)	NA	GGCTCATGACCACAGTCCATGC	64.0
qGAPDH (Reverse)	NA	AGAGGGGCCATCCACAGTCT	63.7

Table 2.5 Primers were designed in-house and ordered from Eurofins MWG Operon. Each primer amplified a region smaller than 120bp to allow efficient reaction. qpTaaF and qpTaaR were used to detect the pTα[a] cDNA while qpTabF and qpTabR detected the pTα[b] cDNA. GAPDH was used as the endogenous control and was detected using qGAPDHF and qGAPDHR.

2.1.6 Genomic DNA extraction for genotyping

Genomic DNA was isolated from ear-punch biopsies from 3 week-old pups. The tissues were placed in 100μl of autoclaved 0.05M NaOH (Sigma-Aldrich) in 1.5mL eppendorf tubes (Starlab, UK) and incubated for 1hr at 95°C. Following incubation, 10μl of Tris-EDTA buffer (PH 8.0, Sigma-Aldrich) was added to the samples. To allow separation of DNA from the remaining skin fragments, the tubes were centrifuged in a bench-top centrifuge at 400g for 5mins at 4°C. Samples were either used straight away for PCR or stored at -20°C for subsequent use. 1μl was used during PCRs.

2.1.7 Bacterial artificial chromosome (BAC)

a. Maxi prep

The QIAGEN Large-Construct Kit was used to generate large quantities of pTα^b BAC according to manufacturer's instructions. The pTα^b BAC was subsequently used for pro-nuclear injection in order to generate pTα^b-expressing transgenic animals. Prior to starting the procedure, Buffer P3 was placed at 4°C and a water bath was set at 37°C. A single colony of SW102 *E.coli* bacteria previously transformed with the pTα^b BAC was inoculated overnight at 32°C with vigorous shaking (300rpm) in 5mL of LB broth (Sigma-Aldrich) containing chloramphenicol (Sigma-Aldrich) at a 12.5μg.mL$^{(-1)}$ concentration. The following day, 1mL of this culture was incubated for 16hrs into 500mL of 12.5μg.mL$^{(-1)}$ chloramphenicol LB broth at 32°C with vigorous shaking (300rpm). The bacterial cells were harvested the next day by centrifugation at 6000g for 5mins at 4°C using a plus centrifuge (Sorvall RC 6+) and the supernatant was removed by inversion. The pellet was fully re-suspended by vortexing with 20mL of Buffer P1 and 20mL of Buffer P2 was added for further lysis of the cells. Tubes were inverted 4 to 6 times and incubated at room temperature for no more than 5mins. The precipitation of the proteins and the cell debris was achieved by mixing the solution with 20mL of pre-chilled Buffer P3. The sample was centrifuged at 20,000g for 30min at 4°C and supernatant was removed by inversion. The supernatant, containing the DNA, was filtered through a pre-moistened folded filter-paper and DNA was precipitated by adding 0.6 volume of room-temperature isopropanol. Samples were mixed and centrifuged at 15,000g for 30mins at 4°C and supernatant was removed by inversion. The DNA pellet was washed with 5mL of 70% ethanol and centrifuged at 15,000g

for 15mins. Supernatant was removed by inversion and the pellet was air-dried by placing the tube upside down on a clean paper towel. Once dried, the DNA was re-suspended in 9.5mL of Buffer EX and mixed gently to fully dissolve the DNA. Removal of genomic DNA and nicked BAC was achieved by adding 200µl of ATP-dependent exonuclease and 300µl of ATP solution to the DNA, and incubating in a water bath at 37°C for 60mins. After incubation, 10mL of Buffer QS was added to the DNA and the whole solution was applied to a QIAGEN-tip 500 previously equilibrated with 10mL of Buffer QBT. The DNA was allowed to travel through the resin by gravity. The QIAGEN-tip 500 was subsequently washed twice with 30mL of Buffer QC and the DNA was eluted with 15mL of pre-warmed Buffer QF. The DNA was precipitated by adding 0.7 volumes of room-temperature isopropanol and centrifuged at 15,000g for 30mins at 4°C. Supernatant was removed by inversion and 5mL of 70% ethanol was added to the sample followed by centrifugation at 15,000g for 15mins. The DNA pellet was air dried for 5 to 10mins and re-dissolved in 500µL of TE buffer.

b. Restriction digest

The transgene used for pro-nuclear injection lacks the backbone of the BAC. The latter is removed through restriction digest using the restriction endonucleases SpeI (NEB). 10µg of pTα^b BAC was digested overnight at 37°C. Each reaction consisted of 5µl of the restriction endonucleases SpeI (NEB) and 5µl of the 10x CutSmart Buffer (NEB) in a final volume of 50µl. The SpeI enzyme recognizes the following sequences:

```
5' – A CTAGT – 3'
3' – TGATC A – 5'
```

The reaction was subsequently run on a 0.5% agarose gel (Sigma-Aldrich).

c. Gel extraction

The pTα^b BAC fragments obtained by restriction digestion were mixed with 6x TriTrack DNA loading dye (Thermo Scientific) at a 1:6 dilution and run on a 0.5% agarose gel (Sigma-Aldrich) at 40V for 5hrs containing 15μl of GelRed (Biotium). 0.6μg of the GeneRuler high range DNA ladder (Thermo Scientific) was run alongside the samples to determine the band size. DNA gel extraction was performed using the Qiagen QIAEX II Gel Extraction Kit. In summary, the DNA band of interest was visualized on a UV trans-illuminator and excised from the gel using a clean sharp disposable scalpel (Scientific laboratory supplies, SLS). The gel slice was transferred to a 1.5mL eppendorf tube and weighed. Three volumes of buffer QX1 was added for each volume of gel. DNA was absorbed using 30ul of QIAEX II silica particles following 10mins of incubation at 50°C. The samples were centrifuged at 3000g and the supernatant was removed by pipetting. The pellet was washed with 500μl of Buffer QX1 followed by two washes with 500μl of Buffer PE. Once the supernatant was removed, the pellet was air-dried for up to 15mins until it became visibly white. DNA was eluted by adding 20μl of 10mM Tris-Cl (PH 8.5) and incubated at 50°C for 10mins. Supernatant was removed and transferred to a fresh tube. DNA quality and concentration was determined by running 2μl on a 1% agarose gel.

Alternatively, for smaller DNA products, the GeneJET gel extraction kit (Fermentas) was used according to the manufacturer's instructions. The band of interest was visualized on a UV trans-illuminator, cut with a sharp disposable scalpel (SLS) and transferred into a pre-weighed 1.5mL eppendorf tube. 1 volume of Binding Buffer was added and the sample was incubated at 50°C for

10mins until the gel was fully dissolved. The solution was transferred onto a GeneJET purification column and centrifuged for 1min at 13,000g. The column was washed with 100μl of the Binding Buffer if the sample was to be sent for sequencing and further washed with 700μl of Wash Buffer. Finally, the DNA was eluted into a 1.5mL eppendorf tube with 30μl of Elution Buffer.

2.1.8 RNA extraction

RNA extraction from thymocytes was performed to investigate the level of transcription of the two pTα isoforms, pTα^a and pTα^b.

Thymocytes were re-suspended in 200μl of TRIZOL (Invitrogen) and 40μl of chloroform (SLS) in a 1.5mL eppendorf tube. The sample was shaken vigorously at 300rpm for 15mins at room temperature before centrifugation at 400g for 3mins. The clear aqueous phase was carefully transferred to a fresh 1.5mL eppendorf tube and an equal volume of 70% ethanol was added. Each solution was applied onto a QIAGEN RNeasy Mini-Column and centrifuged for 30seconds at 15,000g in a bench-top centrifuge. The flow-through was discarded and the column was washed twice with 600μl of Buffer RW1. Genomic DNA was removed by incubating the column for 15mins at room temperature with 80μl of the DNAse1/RDD stock solution (QIAGEN) prepared according to the manufacturer's instructions. The RNA was washed twice with 500μl of Buffer RPE before being air-dried and eluted into a 1.5mL eppendorf tube using 25μl of RNAse-free water (Roche). The samples were stored at -80°C for no more than 1 month. The quality of the RNA was evaluated using Nanodrop ND-100 spectrophotometer TM8000 (Labtech International).

2.1.9 DNA and RNA quantitation

The concentration of DNA or RNA was determined by measuring the absorbance of 1μl of the sample using the Nanodrop ND-100 spectrophotometer TM8000 (Labtech International) at a wavelength of 260nm. The quality of the sample was considered good if both the 230mn/260mn and 260mn/280mn ratios were equal to 2.0.

Alternatively, the concentration of the DNA sample was determined by running 2μl of the sample on an agarose gel. The intensity of the band was compared to the one from the ladder where the DNA quantity for each band is known. The intensity between the bands was analysed using ImageJ software.

2.1.10 cDNA synthesis

Single-stranded cDNA was generated using the High Capacity cDNA Reverse Transcription Kit (Life technologies) and was used during PCR. Up to 2μg of RNA was retro-transcribed into a final volume of 20μl. 9μl of the eluted RNA was mixed with 1μl of the 20X RT enzyme mix (Life technologies) and 10μl of the 10x RT reaction Buffer provided. The sample was incubated at 37°C for 1hr and the enzyme was denatured at 95°C for 5mins. The samples were subsequently stored at -20°C.

Alternatively, for single-cell PCR, both cDNA synthesis and RNA retro-transcription took place in a 96 well-plate and RNA using specific reverse primers. The reaction consisted of 0.15μl of the MMLV-RT enzyme (Invitrogen) and 1μl of the 5X MMLV-RT Buffer mixed with 0.5μl of 2.5mM dNTPs (Ambion) and 0.1μl of 100μM reverse pTα primer M-pTageneR (Table 2.4) (Thermo Scientific or Eurofins MWG Operon). 1μl of 20% Triton-X allowed cell lysis and

exposure of the RNA whereas 0.25μl of RNAseOUT (Invitrogen) was required to prevent RNA degradation prior to cDNA synthesis. The plate was incubated at 37°C for 2hrs and denaturation of the enzyme was achieved by heating at 70°C for 10mins.

2.1.11 Sequencing

DNA fragments or PCR products were sent for sequencing to Source BioScience. 5μl of DNA at a concentration of 100ng.μl$^{(-1)}$ (for plasmid DNA) or 1 ng.μl$^{(-1)}$ /100bp (for PCR product) was transferred to a 1.5mL Eppendorf tube. Adequate primers were provided at a 3.2pmol/μl concentration. Analysis of the sequencing results was performed using the software Chromas (Technelysium) and Cluster W2.

2.2 Cell Biology

2.2.1. Isolation of lymphocytes from thymuses and from lymph nodes

Thymuses and lymph nodes (brachial, axillary and inguinal) were dissected and placed in ice-cold RPMI-1640 (Invitrogen). The tissues were homogenised and strained through an 80μm metal mesh (Sefar Ltd., UK) into a 15mL falcon tube (SLS) with fluorescence-activated cell sorting (FACS) buffer to obtain a single-cell suspension.

FACS Buffer	1X Phosphate-Buffered Saline (PBS, Invitrogen)
	2% Heat-Inactivated Fetal Calf Serum (HI-FCS, Invitrogen)
	5mM Ethylenediaminetetraacetic acid (EDTA, Invitrogen)

Table 2.6 Composition of FACS Buffer The table shows the composition of FACS buffer. The buffer was prepared under sterile conditions and was filtered before use.

2.2.2. Isolation of splenocytes

Adult mouse spleens were obtained by dissection and placed in ice-cold RPMI-1640 (Invitrogen). Splenocytes were isolated by homogenizing the spleen and straining through an 80μm metal mesh (Sefar Ltd., UK) into a 15mL tube (SLS) to obtain a single-cell suspension. Cells were pelleted by centrifugation at 400g for 5mins at 4°C. Red blood cells were osmotically lysed in 500μl of ACK lysis buffer (Invitrogen) by incubating the sample for 10mins at room temperature. Splenocytes were then washed twice with FACS buffer to remove any residual lysis buffer.

Alternatively, red blood cells were removed by gradient centrifugation. The cell suspension was under-laid with 4mL of Lymphocyte Separation Medium (LSM, Fischer) and tubes were centrifuged at 450g for 25mins with no brake at room temperature. The interphase containing the splenocytes was aspirated using a Pasteur glass pipette (VWR) and transferred to a fresh tube. Splenocytes were subsequently washed with FACS buffer before staining for extra-cellular markers.

2.2.3. Isolation of intra-epithelial lymphocytes

Small intestines from adult mice were dissected and placed in cold RPMI-1640 supplemented with 10% Newborn Calf Serum (NCS, Invitrogen). Fecal material

was flushed out from the small intestines with ice-cold PBS using an oral gavage needle attached to a 10mL syringe. Fatty tissues, vasculature and Peyer's patches were removed, and the intestine was opened longitudinally to expose the lumen side. The organ was cut into small pieces of approximately 0.5cm in length and transferred to a 50mL beaker with 40mL of 10% NCS RPMI-1640 and 5mM EDTA. The pieces of tissue were subsequently agitated for 60min at room temperature to encourage cell isolation.

Nylon wool columns (1column/small intestine) were previously prepared by packing 0.7g of finely separated nylon fibers (Polysciences, USA) into a 20mL syringe up to the 20mL mark. The columns were covered in foil and autoclaved at 121°C for at least 20mins. Cell suspensions were subsequently passed through an autoclaved nylon wool column previously equilibrated with RPMI-1640 with 38 mM HEPES (Life technologies). Flow-through was collected in a fresh tube and was washed with 10%NCS RPMI-1640. IELs were enriched on a discontinuous Percoll gradient (40% and 80% isotonic Percoll) (Amersham Biosciences). IELs were removed from the 40%-80% interphase by aspirating with a glass pasteur pipette and transferred to a fresh tube. The cells were washed with 10%NCS RPMI-1640 by centrifuging at 400g before being stained for FACS analysis.

2.2.4. Foetal thymic organ culture (FTOC)

Mouse E15 embryos were cut transversely using scissors and washed in 5mL of 1X PBS in a petri dish before the lungs, and the heart were removed using Dumont tweezers to expose the thymuses. Thymic lobes were dissected under a dissecting microscope and transferred to a drop of 1X PBS on a petri dish. Up to 5 lobes were cultured on a nucleopore membrane filter (Whatman) in 3mL of

filtered FTOC media (Table 2.7) in 6-well plates. In some experiments the following antibodies or inhibitors were added to the FTOC media: PP2 (Sigma), GL3 (Sigma). FTOCs were incubated at 37°C in 5%CO_2 for 7-9 days (or as specified in the text).

FTOC medium	RPMI-1640 without Glutamax (Invitrogen)
	10% HI-FCS Amnion cell tested (PAA)
	2mM L-Glutamine (Invitrogen)
	50μM 2-mercaptoethanol (Invitrogen)
	1% Penicillin-Streptavidin (Invitrogen)

Table 2.7 Composition of the FTOC medium The table shows the components of the FTOC medium, which was prepared under sterile conditions to minimise contamination in FTOC.

2.2.5. Staining protocols for Fluorescent Activated Cell sorting (FACS)

a. Extracellular-staining

Between 2 to 10 million lymphocytes were filtered through a 40μm strainer (BD) and transferred to a FACS tube (Becton, Dickinson and Company, BD). The tubes were centrifuged and cells were resuspended in 50μl of FACS buffer. Unless stated in the text, all antibodies were used at 1:100 dilution and samples were stained on ice, in the dark for 30 to 45 minutes. After staining, lymphocytes were washed twice with 1ml of FACS buffer. Prior to running the samples on the LSR-II flow cytometer (BD Bioscience), the cells were resuspended in 200μl of FACS buffer and 3μl of 4',6-Diamidino-2-Phenylindole, Dihydrochloride (DAPI, 2.5mg.mL$^{(-1)}$; Invitrogen) was added to the sample to allow the detection of dead cells.

b. Intracellular staining of cytokines

For intracellular staining of cytokines, 5 to 10 million thymocytes were transferred to a FACS tube and resuspended in 1mL of FTOC medium. The

lymphocytes were stimulated with 50ng.mL$^{(-1)}$ of phorbol 12-myristate 13-acetate (PMA, Sigma-Aldrich) and 1μg.mL$^{(-1)}$ of Ionomycin (Sigma-Aldrich) for 4hours at 37°C with intermittent mixing every 30mins. To prevent secretion of the cytokines, two protein transporter inhibitors, Monensin (eBioscience) and Brefeldin A (eBioscience) were added during the last 2hours at a final concentration of 2μM and 10μg.mL$^{(-1)}$, respectively. Post-stimulation, the samples were washed with FACS buffer by centrifugation at 400g for 5mins at 4°C and stained for extracellular cell surface markers (refer to section 5.1.1) and with the Zombie Aqua™ Fixable Viability dye (1:100 dilution; Biolegend) for dead cell exclusion. Cells were subsequently washed with FACS buffer by centrifugation at 400g for 5mins at 4°C, supernatant was removed by inversion and the pellet was disaggregated by vortexing. The cells were fixed by drop-wise addition of 250μl of the IC fixation buffer (eBioscience) while the sample was vortexed. The tube was incubated on ice, in the dark, for 15mins. The samples were then washed twice with 1 mL Permeabilisation buffer (eBioscience), previously diluted from a 10X stock in dH$_2$O, by centrifugation at 400g for 5mins at 4°C. Intracellular cytokines were stained by fluorochrome-conjugated antibody diluted at 1:100 in 1X Permeabilization buffer. The samples were incubated at 4°C for 45mins in the dark. Prior to analysis on the LSR-II flow cytometer (BD Bioscience), the cells were washed once with 1X Permeabilization buffer and once with FACS buffer by centrifugation at 400g for 5mins at 4°C.

c. Intracellular staining of transcription factors

For intracellular detection of transcription factors, 10 million cells were transferred into a FACS tube and stained for extracellular markers as described

in section 5.1.1 and with the Zombie Aqua™ Fixable Viability dye (Biolegend) for dead cell exclusion. The Fixation/Permeabilization concentrate (eBioscience) was diluted 1:4 using the Fixation/Permeabilization diluent (eBiosicence) and the 10X Permeabilization buffer (eBioscience) was diluted 1:10 with dH_20. Following extracellular staining, cells were washed in FACS buffer by centrifugation at 400g for 5mins at 4°C. The pellet was disaggregated by vortexing and the cells were resuspended in 1mL of the diluted Fixation/Permeabilization buffer. Cells were incubated for at least 30mins at 4°C in the dark and subsequently washed with 1mL of 1X Permeabilization buffer (eBioscience). Cells were stained for transcription factors of interest using antibodies diluted 1:100 in 1X Permeabilization buffer for 45mins on ice, in the dark. Prior to analysis on the LSR-II flow cytometer (BD Bioscience), the cells were washed once with 1X Permeabilization buffer and once with FACS buffer by centrifugation at 400g for 5mins at 4°C.

d. Antibodies used throughout this thesis

Protein	Clone	Fluorochrome	Company
TCRβ	H57-597	FITC	eBioscience
TCRβ	H57-597	PerCp5.5	eBioscience
TCRβ	H57-597	APCCy7	eBioscience
TCRδ	GL3	FITC	eBioscience
TCRδ	GL3	PE	eBioscience
TCRδ	GL3	PerCp5.5	eBioscience
TCRδ	GL3	APC	eBioscience
TCRvα2	B20.1	PE	eBioscience
CD3ε	145-2C11	V500	BD

CD3ε	145-2C11	PeCy5.5	eBioscience
CD4	RM4.5	Pacific blue	eBioscience
CD4	RM4.5	FITC	eBioscience
CD4	RM4.5	PeCy7	eBioscience
CD8α	53-6.7	Pacific blue	eBioscience
CD8α	53-6.7	FITC	eBioscience
CD8α	53-6.7	APCCy7	eBioscience
CD8β	H35-17.2	PE	eBioscience
CD25	PC61	PeCy7	eBioscience
CD25	PC61	APC	eBioscience
CD44	IM7	V500	eBioscience
CD44	IM7	Pacific blue	eBioscience
CD24	M1/69	Pacific blue	eBioscience
CD45RB	C363-16A	APCCy7	Biolegend
CD27	LG.7F9	PerCp5.5	eBioscience
CD5	53-7.3	PB	eBioscience
CD5	53-7.3	FITC	eBioscience
CD69	H1.2F3	APC	eBioscience
CD117 (cKit)	2B8	APC	eBioscience
Foxp3	FJK-16s	Pacific blue	eBioscience
Nur77	12.14	PE	eBioscience
Helios	22F6	APC	eBioscience
IL-17	Ebio17B7	APC	eBioscience
IFN-γ	XMG1.2	PeCy7	eBioscience
B220	RA3-6B2	FITC	eBioscience
CD11c	N418	FITC	eBioscience
NK1.1	PK136	FITC	eBioscience

Zombie Aqua	NA		Biolegend

Table 2.8 List of the antibodies used throughout this thesis The table shows the protein recognized by the antibody, the clone, the fluorochrome and the supplier. PE, Phycoerythrin and FITC, Fluorescein, APC Allophycocyanine

e. Compensation

In order to set up voltages accurately and compensate for overlapping spectrum between two fluorochromes, single colour controls were run before each experiment and compensations were carried out manually on FACS Diva software (BD) or semi-automatically on FlowJo software (Tree Star). When possible, thymocytes were used to generate single colour controls. Alternatively, 10μl of OneComp ebeads (eBioscience) were stained with 1μl of antibody in 100μl of FACS buffer.

f. Gating strategy

Lymphocytes were identified based on their size (Forward Scatter, FSC) and their granularity (Side Scatter, SSC). Doublets were visualized and gated out by looking at scatter-height and scatter-area for both forward and side scatters (FSC-H versus FSC-A & SSC-H versus SSC-A). Dead cells were gated out using DAPI (Invitrogen) or Zombie Aqua™ Fixable Viability dye (Biolegend).

2.2.6 FACS sorting

a. FACS sorter

Sorting of cells was performed on a FACSAria II cell sorter (BD Bioscience). Single cell sorting was performed on a MoFlo sorter (Beckman Coulter).

b. Depletion of thymocytes expressing CD4 and CD8 co-receptor molecules

In order to save time while sorting DN subsets and therefore minimize cell-death, CD4 and CD8 expressing thymocytes, which constitute over 80% of the thymus, were depleted by complement-mediated lysis. Adult mouse thymuses were dissected, homogenised and strained through an 80μm metal mesh into a 15mL tube with 7mL of RPMI-1640. 250μl of each CD4 and CD8 hybridoma supernatant was added to the cell suspension and incubated for 10mins at 37°C. The CD4 and CD8 hybridoma supernatants consist of anti-CD4 and anti-CD8 IgM isotype antibodies, respectively. Complement powder (Cedarlane Laboratories) was resuspended in 1mL of ice-cold water. It was subsequently added to the cell suspension and mixed by inversion. The samples with complement were incubated at 37°C for an additional 30mins to allow components of the complement system to recognise antibody-bound cells and mediate cell lysis.

In order to isolate live DN cells from the lysed CD4$^{(+)}$ and CD8$^{(+)}$ cells, the cell suspensions were under-laid with 4mL of lymphocyte separation media (LSM, Fisher) and centrifuged at 450g for 25mins at room temperature with no brake. Live thymocytes were aspirated from the interphase using a glass Pasteur pipette (VWR) and transferred to a fresh tube. The cells were washed with FACS buffer by centrifugation at 400g for 5mins at 4°C before staining for extracellular markers as described in section 5.1.1.

2.2.7 Flow cytometry acquisition

The acquisition of the flow cytometry data was done using a LSRII flow cytometer (BD Bioscience) through the FACSDIVA software (BD Bioscience).

2.2.8 Flow cytometry analysis

Analysis of the FACS data was done using the Flow Jo software Version X (Tree Star).

2.2.9 Cell count

Dead cells were excluded from the cell counts by diluting $10\mu l$ of a cell suspension with $10\mu l$ of 0.4% trypan blue (Invitrogen), which is known to enter cells with a fractured cell membrane. $10\mu l$ of the diluted cell suspension was subsequently loaded onto a heamocytometer and the number of cells per mL was determined as follow:

$$\text{Number of cells.mL}^{(-1)} = \text{Number of cells counted x Dilution factor x } 10^{4}$$

2.2.10 Mice

C57Bl/6 and FVB mice were purchased from Charles River Laboratories. $pT\alpha^{-/-}.pT\alpha^{a}$ mice on a C57Bl/6 background were generated in-house. $pT\alpha^{-/-}$ and OT-II transgenic mice on a C57Bl/6 background were obtained from Jackson Laboratories. $pT\alpha^{-/-}$ x $TCR\delta^{-/-}$ were generated in-house by crossing a $pT\alpha^{-/-}$ with a $TCR\delta^{-/-}$ animal and backcrossing onto a C57Bl/6 background for four generations. Embryos were obtained by setting up timed-pregnancies. All animals were bred and maintained in Individually Ventilated Cages (IVC) at Barts and The London School of Medicine and Dentistry, ensuring a pathogen-free environment. All experiments involving animals were performed in

compliance with relevant laws and institutional guidelines and were approved by a local ethics committee. PPL is 70/7191.

2.2.11. Statistical Analysis

Unless specified in the text, all statistical analysis was done using the GraphPad Prism software. When comparing two groups, an unpaired Student's *t*-test with a two-tailed p value with 95% confidence intervals was performed. Alternatively, when comparing three or more groups, a one-way analysis of variance (ANOVA) with Tukey post hoc was carried out. Data are presented as mean ± standard deviation (SD). *P*>0.05 is not-significant (ns); * *P*<0.05; ** *P*<0.001; *** *P*<0.0001.

Chapter 3

T cell development in pTα^a-only transgenic mice

3.1 Introduction

It is still unclear why some DP progenitors undergo apoptosis following agonist recognition by TCR$\alpha\beta$ during T cell selection while others differentiate into unconventional $\alpha\beta$ T cells. This could suggest that DP thymocytes are a heterogeneous subset that do not possess an equal potential to adopt a conventional or an unconventional $\alpha\beta$ T cell fate. All DP thymocytes arise from the DN3 stage after having efficiently traversed the β-selection checkpoint. This transition is governed by expression of the preTCR, made by inclusion of one of the alternatively-spliced pTα isoforms (pTα^a or pTα^b). Very little is understood about the role of each isoform during T cell development. We know that the two pTα isoform; have been conserved across evolution and are found in humans and mice (Smelty et al., 2010), can form functional preTCRs (Gibbons et al., 2001), and differently affect the cell-surface expression of TCRβ, potentially resulting in quantitatively or qualitatively different preTCR signals (Barber et al., 1998). In support of this, previous work *in vitro* performed by Juliet Mahtani-Patching, a former PhD student in the lab, demonstrated differential expression for each pTα isoform across various thymocytes subsets. Furthermore, ectopic expression of each isoform in FTOCs *in vitro* promoted different T cell development likely due to the different qualitative, quantitative or temporal

120

signals at the β-selection checkpoint. Thus, we hypothesised that differences in preTCR^a and preTCR^b signalling at the β-selection checkpoint may be responsible for establishing heterogeneity at the DP stage that would be subsequently important for the generation of different $\alpha\beta$ T cell subsets following positive selection. Here, we first investigate the pattern of expression of each pTα isoform at the single cell level in pre- and post-β-selected thymocytes and subsequently investigate the role of the pTα^a isoform at the β-selection checkpoint *in vivo*.

3.2 pTα^a and pTα^b are differently expressed during T cell ontogeny – Data generated by Juliet Mahtani-Patching

A differential pattern of expression for the two pTα isoforms throughout T cell ontogeny was demonstrated by Juliet Mahtani-Patching during her Ph.D. Using semi-quantitative PCR on Fluorescence Activated Cell (FAC) sorted DN2 (CD25$^{(+)}$CD44$^{(-)}$), DN3 (CD25$^{(+)}$CD44$^{(-)}$), DN4 (CD25$^{(-)}$CD44$^{(-)}$), ISP (CD8$^{(+)}$TCR$\beta^{(-)}$), DP (CD4$^{(+)}$CD8$^{(+)}$) and CD4$^{(+)}$ T cell subsets (Figure 3.1), she demonstrated:

- A peak of expression for both pTα^a and pTα^b in the DN3 and DN4 T cell subsets that corresponds to cells traversing the β-selection checkpoint.

- An unexpected expression of pTα^b but not pTα^a at the DP stage of T cell development where rearrangement of the TCRα gene is thought to silence pTα expression.

- Sustained pTα^b expression in mature T cells (e.g. CD4$^{(+)}$ T cells).

Thus, it was concluded that expression of $pT\alpha^a$ and $pT\alpha^b$ appears to be differentially regulated throughout T cell development, favouring the idea that these isoforms have a non-redundant role in T cell development.
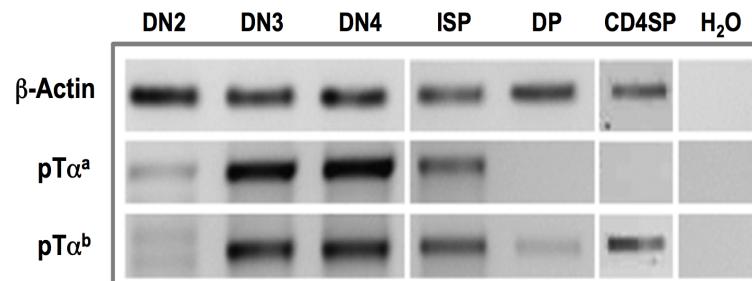
Figure 3.1 $pT\alpha^a$ and $pT\alpha^b$ are differentially expressed in the thymus. Semi-quantative PCR for $pT\alpha^a$ or $pT\alpha^b$ was carried out on cDNA obtained from sorted DN2, DN3, DN4, ISP, DP and CD4[(+)] T cell subsets. Loading was normalised with β-actin. From Juliet Mahtani-Patching's thesis.

3.3 Individual C57Bl/6 DN3 and DN4 thymocytes can express $pT\alpha^a$, $pT\alpha^b$, or both isoforms simultaneously

Although Juliet's data suggested a difference in the regulation of $pT\alpha^a$ and $pT\alpha^b$ expression at the level of thymocyte subsets, we next sought to investigate whether each $pT\alpha$ isoform was expressed simultaneously or individually in developing thymocytes. Thus, using single-cell PCR, we investigated the pattern of expression of each isoform in individual DN3 and DN4 thymocytes from C57Bl/6 animals. C57Bl/6 thymuses were dissected and single cells were individually FAC-sorted into 96 well plates. Ten cells were placed in the first well (A1) and none in the last (H12) so they could be used as positive and negative controls, respectively. For the sort, lymphocytes were identified according to

their size and doublets were gated out using the SSC-Width (SSC-W) and SSC-Area (SSC-A) (Figure 3.2).

Using a cocktail of antibodies, cells were then excluded based on the expression of B220 (B cells), NK1.1 (NKT and NK cells), CD11c (Dendritic cells), TCRδ (γδ T cells) and CD4, CD8α, CD8β and TCRβ (late αβ lineage thymocyte). DN3 and DN4 subsets were identified by expression of CD25 and CD44; DN3 cells are CD25$^{(+)}$CD44$^{(-)}$ and DN4 cells are CD25$^{(-)}$CD44$^{(-)}$ (Figure 3.2).
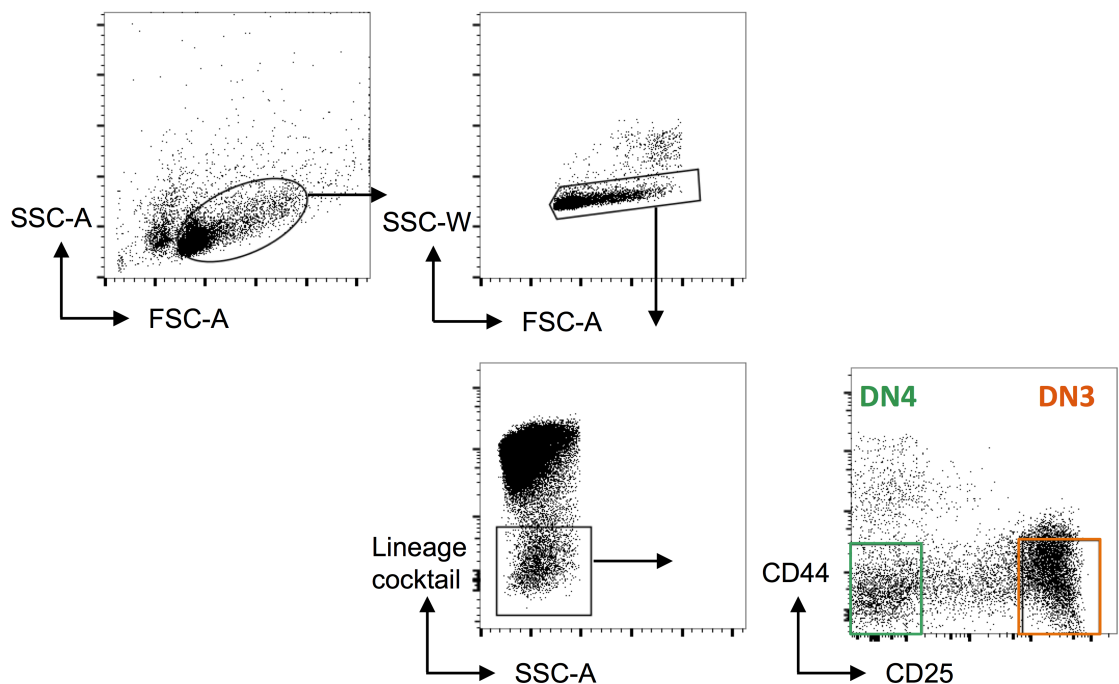
Figure 3.2 Gating strategy for single-cell FAC-sort of DN3 and DN4 thymocytes. Lymphocytes are initially identified by size before doublets are removed using FSC-A versus SSC-W. Lineage$^{(+)}$ cells (B220$^{(+)}$, CD11c$^{(+)}$, NK1.1$^{(+)}$, CD4$^{(+)}$, CD8α$^{(+)}$, CD8β$^{(+)}$, TCRδ$^{(+)}$, TCRβ$^{(+)}$) were gated out before DN3 and DN4 subsets were identified by expression of CD44 and CD25. FSC-A, Forward scatter area; SSC-A, side scatter area; SSC-W, Side scatter width.

Cells were sorted into 10μl of reverse transcription mix containing pTα-targeting primers. Due to the potentially low expression of pTα transcripts in a single cell, all pTα transcripts were first amplified using the M-pTageneF and M-pTageneR primers that recognise sequences within exon 1 and exon 4 of the pTα gene
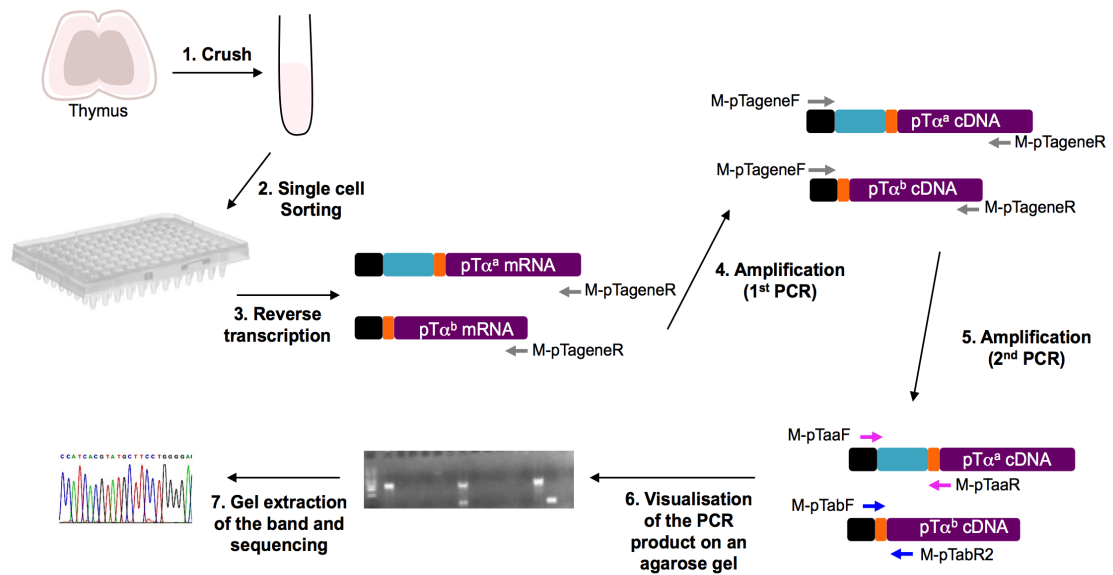
Figure 3.3 Overview of the methodology of single-cell PCR. Thymocytes from C57Bl/6 mice were FAC-sorted into 96 well-plates. Reverse transcription was performed using primers targeting pTα transcripts specifically. All pTα transcripts were then amplified using MpTageneF and M-pTageneR primers. This PCR product then underwent a second round of nested PCR using either M-pTaaF and M-pTaaR to amplify pTα^a, or M-pTabF and M-pTabR2 to amplify pTα^b. The PCR products were visualised on agarose gels and bands were extracted to be sent for sequencing to confirm the specificity of the PCR reaction.

that are shared by both pTα isoforms (Figure 3.3).

Specific amplification of pTα^a or pTα^b isoforms was performed using a second nested PCR reaction. This used primers that amplified sequences unique to either isoform. The pTα^a forward primer (MpTaaF) was homologous to 13bp located at the 3' end of Exon 1 and the first 7bp at the 5' end of exon 2. The

$pT\alpha^a$ reverse primer (M-pTaaR) was homologous to the last 13bp of exon 3 and the first 7bp of exon 4. Because exon 2 is absent from $pT\alpha^b$ transcripts, these primers amplified $pT\alpha^a$ only. Recognition of $pT\alpha^b$ transcripts followed a similar strategy where the $pT\alpha^b$ forward primer (M-pTabF) traversed the exon 1:3 boundary absent from $pT\alpha^a$ transcripts; M-pTabF recognises 13bp located at the 3' end of exon 1 and the first 10bp of exon 3. The $pT\alpha^b$ reverse primer was homologous to 19bp of exon 4. The data was visualised by running the products on agarose gels. The results suggested that DN3 and DN4 thymocytes could express $pT\alpha^a$-only, $pT\alpha^b$-only or both $pT\alpha$ transcripts simultaneously (Figure 3.4).
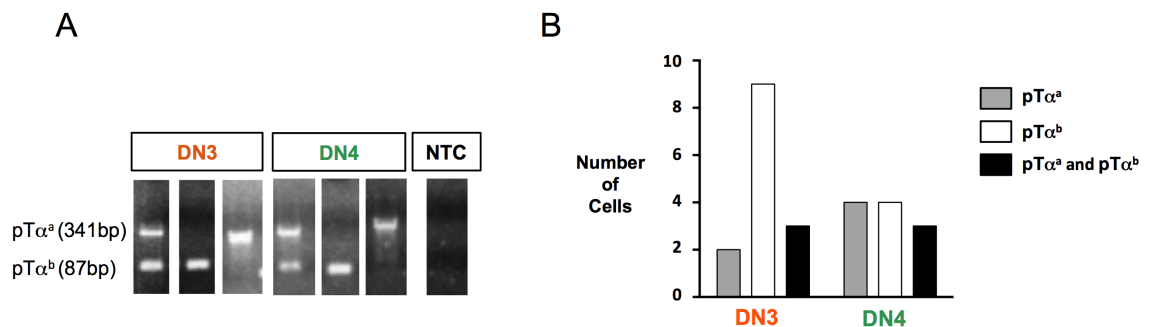
Figure 3.4 C57Bl/6 DN3 and DN4 thymocytes can express $pT\alpha^a$, $pT\alpha^b$ or both $pT\alpha$ isoforms simultaneously. (A) An example of a PCR result obtained from single-cell PCR for $pT\alpha^a$ and $pT\alpha^b$. The expected band for $pT\alpha^a$ is 341bp and for $pT\alpha^b$ it is 87bp (B) Data summarising the numbers of cells detected to express one or the other isoform.

Out of 47 wells containing DN3 cells, two wells were detected to express $pT\alpha^a$-only, against nine expressing $pT\alpha^b$-only. Three cells expressed both $pT\alpha$ isoforms. Similarly, out of 47 wells that contained DN4 cells, four expressed $pT\alpha^a$-only, or $pT\alpha^b$-only, while both $pT\alpha$ transcripts were amplified in three

wells. This cannot be considered as a quantitative result. Instead, it simply illustrates that cells could contain either $pT\alpha^a$, $pT\alpha^b$, or both isoforms. The relatively low efficiency of the experiment (only 25 out of 94 wells (~26.6%) gave us a result) could be due to sorting issues or to some degree of competition between each set of primers. It could also indicate that some cells do not express the preTCR.

To confirm the specificity of the PCR, bands corresponding to $pT\alpha^a$ (341bp) and $pT\alpha^b$ (87bp) were extracted and sent for sequencing. Band extraction and sequencing of the 341bp product corresponding to the $pT\alpha^a$ isoform was efficient and successful (Figure 3.5). The sequence matched 100% the $pT\alpha^a$ cDNA sequence obtained on the PubMed website (http://www.ncbi.nlm.nih.gov/pubmed).

By contrast, despite the successful extraction of $pT\alpha^b$ bands, sequencing efficiency was poor and did not allow us to align it successfully to the $pT\alpha^b$ cDNA sequence. The reason for this was unclear. Nonetheless, the size of the band (87bp) gave us some confidence that the PCR product was specific for $pT\alpha^b$.

In conclusion, this suggested that individual DN3 or DN4 thymocytes could express $pT\alpha^a$, $pT\alpha^b$ or both $pT\alpha$ mRNA simultaneously at the β-selection checkpoint.
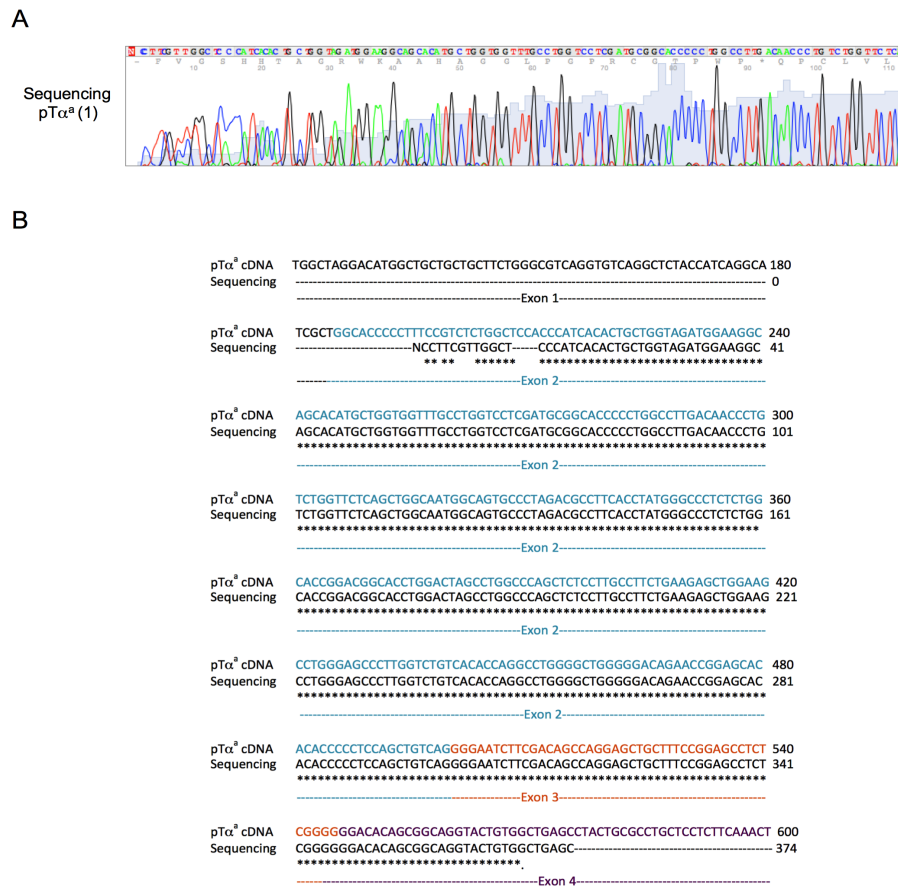
Figure 3.5 The pTαᵃ isoform was successfully amplified during single-cell PCR reaction as shown by sequencing. (A) Chromatogram obtained from the sequencing of pTαᵃ. (B) The alignment of the sequencing result with pTαᵃ confirmed the specificity of the PCR.

3.4 Overview of the generation of pTαᵃ transgenic mice (work initiated by Juliet Mahtani-Patching)

Data obtained from FTOCs *in vitro* from the PhD of Juliet Mahtani-Patching had suggested that pTαᵃ and pTαᵇ could have non-redundant differential roles in T cell development at the β-selection checkpoint (Mahtani-Patching, 2010). However, expression of the pTα isoforms in these studies was under the

control of a retroviral promoter, rather than the physiologically relevant pTα promoter, which could result in non-physiological pTα expression. To overcome this issue, a bacterial artificial chromosome (BAC) pTα[a]-only transgenic mouse line was generated in-house to investigate the role of pTα[a] (only) at the β-selection checkpoint. A BAC consists of a large DNA vector containing a targeted piece of genomic DNA that includes a gene of interest (here pTα), and the regulatory elements required for its physiological expression. Thus, BAC transgenic animals are likely to express the transgene at the right place and at the right time during T cell development (Heintz, 2001; Sharan et al., 2009). pTα transgenic mice have been generated previously but under the control of the proximal Lck promoter which is unlikely to reproduce normal pTα expression (Gibbons et al., 2001). Additionally, the role of each isoform in the generation of different T cell subsets was not investigated (Gibbons et al., 2001). The BAC used in the generation of BAC pTα[a] transgenic mice (BMQ452P20) consists of 41Kb of C57Bl/6 chromosome 17, that includes 8.5kb of the pTα gene. Using a recombination-mediated genetic engineering technique (recombineering) exons 1 and 2 were fused to prevent splicing out of exon 2 thus forcing the expression of only pTα[a] (Figure 3.6).
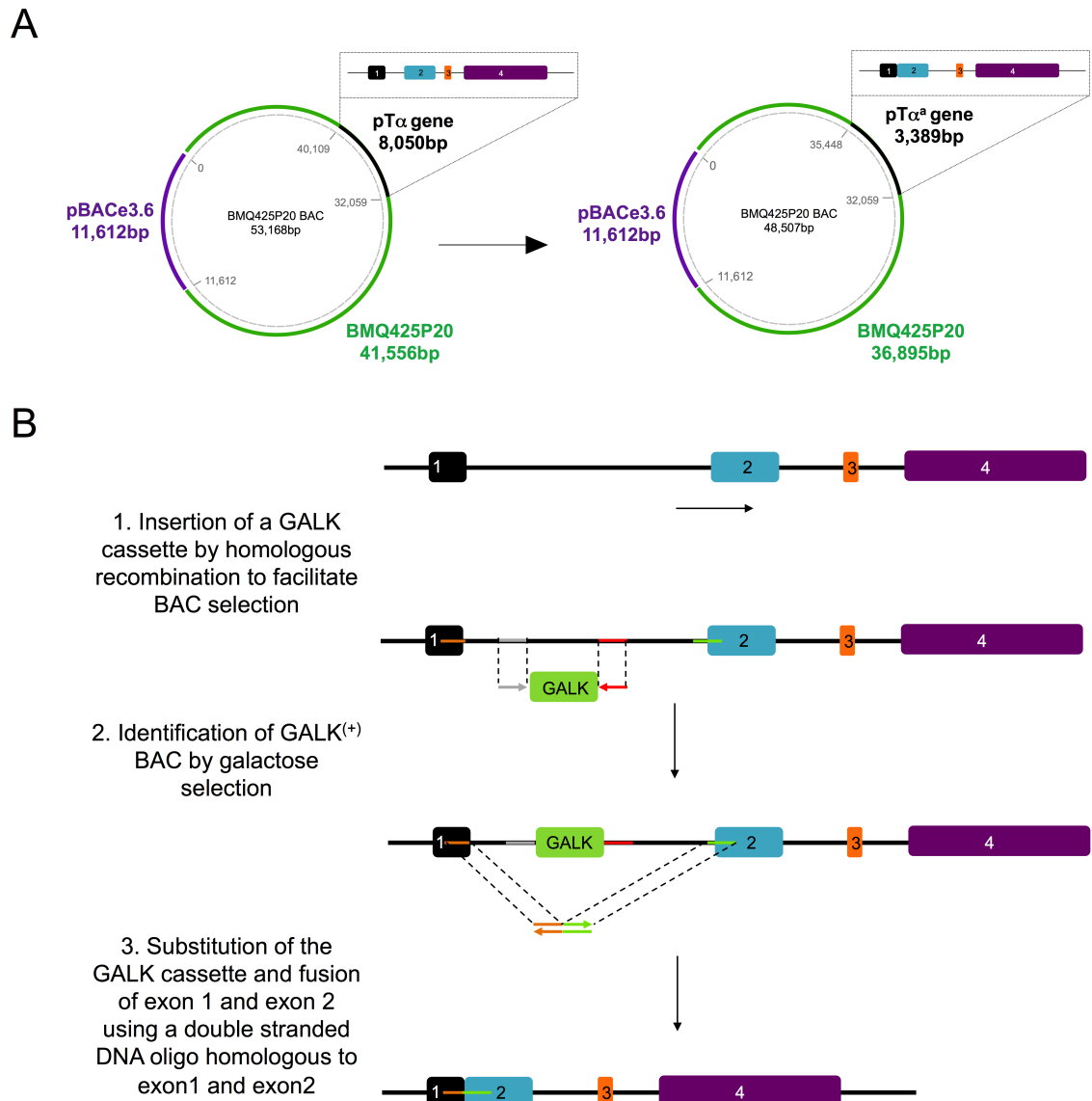
Figure 3.6 Schematic representation of the pTα^a BAC transgene. (A) A BAC containing the pTα gene (top panel) was purchased from the Ensembl organisation and underwent several steps of recombineering where exon 1 and 2 were fused to prevent alternative splicing resulting in a pTα gene that can generate only pTα^a (bottom panel). (B) A GALK cassette was amplified by PCR using primers sharing some homology with the GALK sequence and intron 1. Insertion of the GALK cassette within intron 1 was catalysed by the bacteriophage λ Red system. Successful transformants were identified by growing bacteria onto a galactose-containing plate. Removal of GALK and fusion of exon 1 and 2 happened simultaneously in a subsequent stage. Oligos homologous to exon 1 and 2 were annealed to one another and used to remove intron 1 through homologous recombination resulting in a pTα gene unable to undergo alternative splicing following transcription. Thus, pTα^a only will be generated.

BAC-pTα^a-transgenic founders were bred onto a pTα-deficient background and pups were weaned at 3 weeks of age as required by home office regulations. The pTα^a.pTα$^{-/-}$ colony was established and sustained for subsequent experiments by breeding a pTα^a.pTα$^{-/-}$ transgenic animal with a pTα$^{-/-}$ animal resulting in ~50% of pTα^a.pTα$^{-/-}$ pups. Genotyping was performed by PCR using ears snips. To control for the quality of the genomic DNA a PCR was run using primers recognising a 466bp DNA sequence located 9.5Kb upstream of the pTα gene (Figure 3.7). A second PCR amplified a 450bp sequence across exon 1 and 2 of the pTα gene, which was specific for the pTα^a-only transgene.
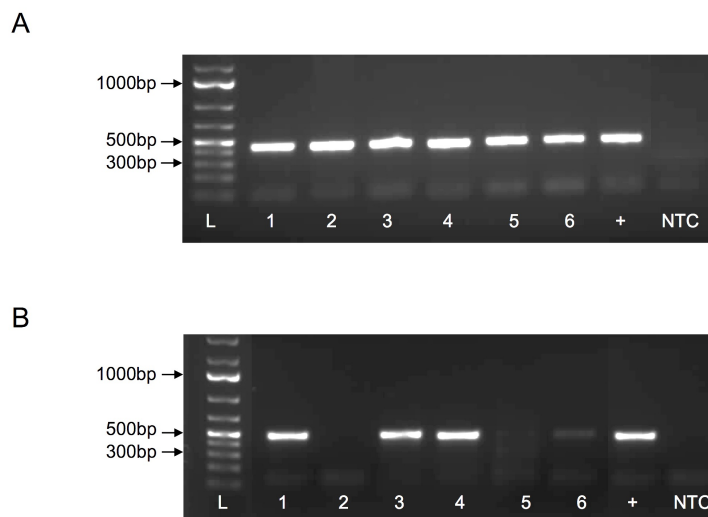
Figure 3.7 pTα^a.pTα$^{-/-}$ transgenic litters were genotyped by PCR. (A) PCR amplifying a 466bp sequence upstream of the pTα gene was used to assess the quality of the DNA. The positive control was obtained from previously genotyped mice. (B) A second PCR was carried out on the same samples using primers amplifying specifically the pTα^a transgene. Here, out of six pups genotyped, three are positive for the transgene. L, 1Kb Ladder; NTC, no template control

3.5 The pTα[a] transgene successfully drives transition of DN thymocytes across the β-selection checkpoint

PreTCR signalling at the DN3 stage is known to drive developing thymocytes towards an αβ T cell fate. Indeed, absence of the preTCR in pTα-deficient mice results in a severe depletion of αβ T cells and the accumulation of γδ T cells (Fehling et al., 1995; Neilson, 2004). In light of this, we first investigated whether the pTα[a] transgene was able to promote the DN3→DN4→DP transition (in a pTα^{-/-} background) and to divert DN3 thymocytes away from a γδ fate. All flow cytometry analyses throughout this thesis share a common initial gating strategy (Figure 3.8); lymphocytes are first identified by size using forward scatter area (FSC-A) and by granularity using side scatter area (SSC-A); doublets are removed by sequentially gating on FSC-A and FSC-H and SSC-A and SSC-Height (SSC-H). Finally, live thymocytes are then identified by exclusion of the DNA-bound dye 4',6-diamidino-2-phenylindole (DAPI) (Figure 3.8).
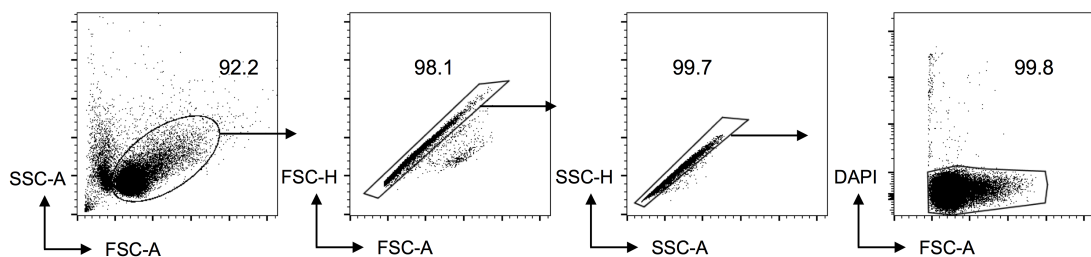
Figure 3.8 The initial steps of the gating strategy shared across all flow cytometry analysis. Lymphocytes are initially identify according to their size on the SSC-A and FSC-A profile before doublets are removed by visualising the cells on a FSC-H versus FSC-A plot and subsequently using SSC-H versus SSC-A. Dead cells are removed using the auto-fluorescent DAPI dye. FSC, forward scatter; SSC, side scatter; A, area, H, height; DAPI, 4',6-diamidino-2-phenylindole.

Flow cytometry analysis of the thymus from $pT\alpha^a.pT\alpha^{-/-}$ mice revealed that the $pT\alpha^a$ transgene was expressed as it largely rescued the profound block in $\alpha\beta$ T cell development observed in $pT\alpha$-deficient mice. Not only did the CD4 vs CD8 plots from $pT\alpha^a.pT\alpha^{-/-}$ mice resemble wild-type (WT) controls (rather than $pT\alpha^{-/-}$ mice) but there was also significant reduction of $\gamma\delta$ T cells (to ~2.5%) compared to $pT\alpha^{-/-}$ mice (~18%) although not quite as low as WT animals (~0.5%) (Figure 3.9). Upon analysis of cell numbers, we noted that although thymus cellularity was significantly greater in $pT\alpha^a.pT\alpha^{-/-}$ thymuses (~50×10^6 cells) compared to $pT\alpha^{-/-}$ animals (~5×10^6 cells), it was nevertheless 3-fold lower than C57Bl/6 mice (~170×10^6 cells) (Figure 3.10). This partial rescue could be due to the absence of the second $pT\alpha$ isoform ($pT\alpha^b$) or possibly to a subtle timing issue of transgene expression.
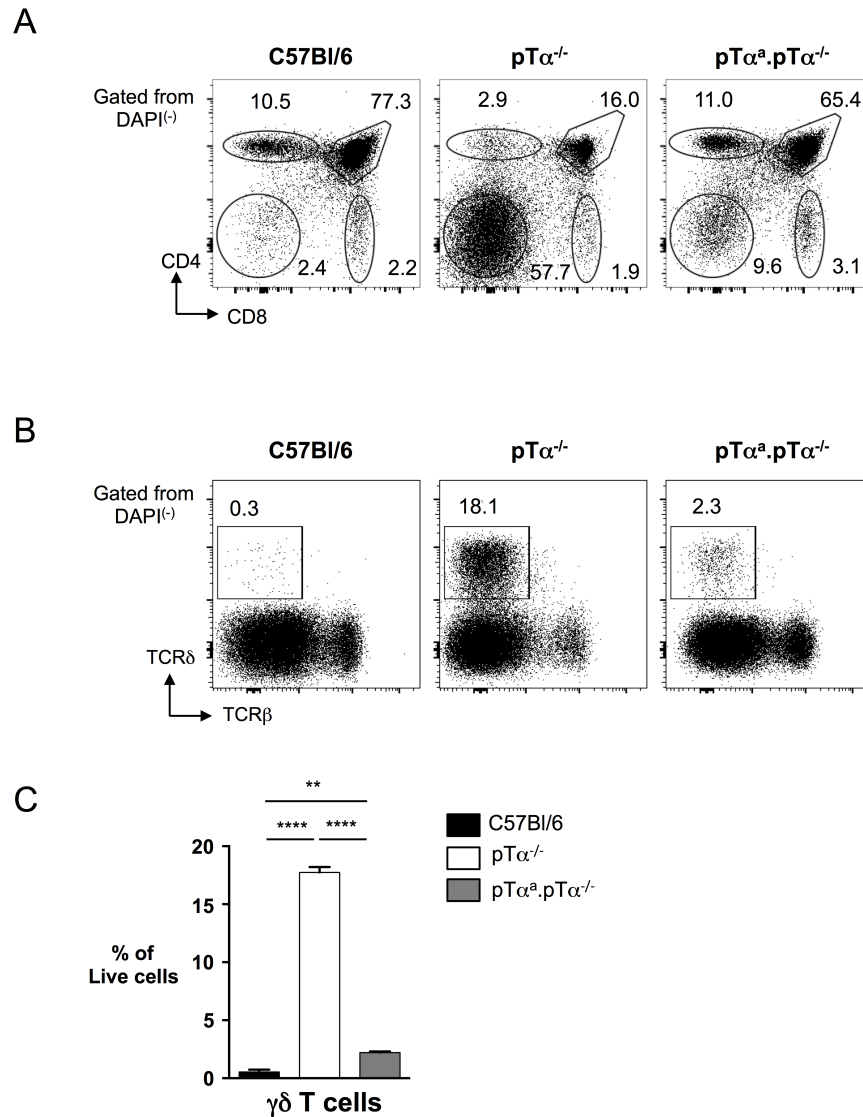
Figure 3.9 The pTα^a transgene significantly rescues αβ T cell development in a pTα^{-/-} background. (A) Representative flow cytometry plots (from n>10) from thymuses of C57Bl/6, pTα^{-/-} and pTα^a.pTα^{-/-} mice showing showing CD4 versus CD8 profiles (B) Representative flow cytometry plots (from n>10) from C57Bl/6, pTα^{-/-} and pTα^a.pTα^{-/-} transgenic mice shown TCRδ versus TCRβ profiles (C) Summary bar charts of the percentages of γδ T cells as a percentage of all living cells from thymus of C57Bl/6, pTα^{-/-} and pTα^a.pTα^{-/-} transgenic mice. ****p<0.0001; ** p<0.01; *** p<0.001 error bar is SD.
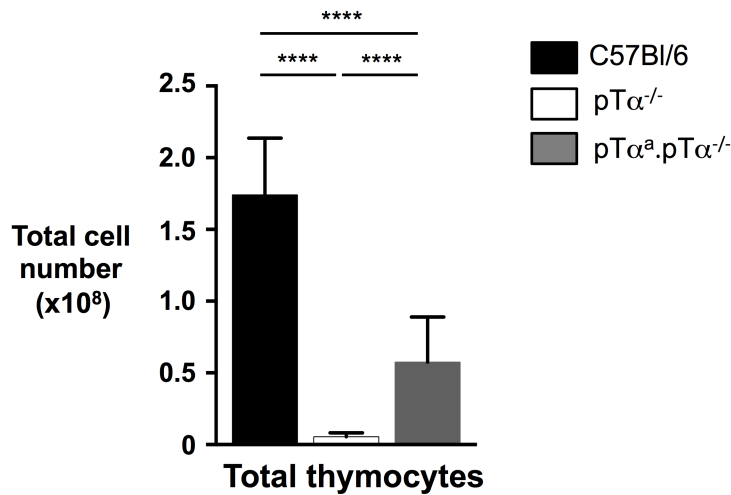
Figure 3.10 Total number of thymocytes in C57Bl/6, pTα$^{-/-}$ and pTα^{a}.pTα$^{-/-}$ mice Summary bar charts (from n>10) showing the total number of thymocytes from the thymuses of C57Bl/6, pTα$^{-/-}$ and pTα^{a}.pTα$^{-/-}$ transgenic mice. ****p<0.0001; error bar is SD.

3.6 The development of mature TCRβ$^{(+)}$CD4$^{(+)}$ and TCRβ$^{(+)}$CD8$^{(+)}$ T cells is rescued in lymph nodes from pTα^{a}.pTα$^{-/-}$ mice compared to pTα-deficient animals.

The data presented above suggested that the pTα^{a} transgene largely rescued qualitatively αβ T cell development in a pTα$^{-/-}$ background. This prompted us to assess whether the number of mature αβ T cells was also restored in the periphery of pTα^{a}.pTα$^{-/-}$ animals. As shown in figure 3.11, flow cytometry analysis of lymph nodes demonstrated that expression of pTα^{a} largely rescues the proportion and cell number of peripheral CD4$^{(+)}$ and CD8$^{(+)}$ T cells.

Indeed, while pTα-deficient animals harbour about ~5.0×10^5 CD4$^{(+)}$ T cells, pTα^a.pTα$^{-/-}$ mice had on average about 5-6 times more cells (~2.8×10^6 cells). Similarly, pTα-deficient animals have a largely lymphopenic CD8$^{(+)}$ compartment with only ~2.0×10^5 cells against ~3.0×10^6 cells in pTα^a.pTα$^{-/-}$ animals (compared with ~3.9×10^6 cells in C57Bl/6 mice) (Figure 3.11).
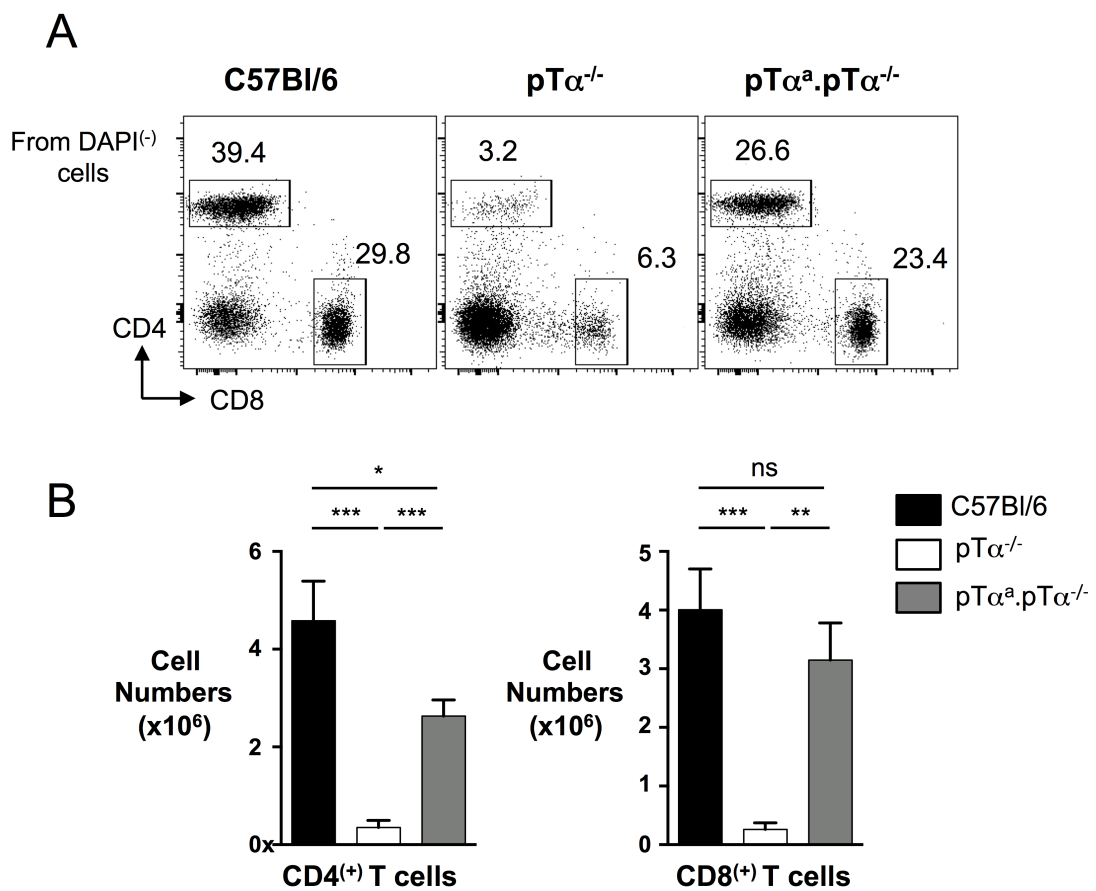
Figure 3.11 The pTα^a transgene successfully rescues the development of mature CD4$^{(+)}$ and CD8$^{(+)}$ T cells in a pTα$^{-/-}$ background. (A) Representative flow cytometry plots (from n>10) showing CD4 versus CD8 profiles from lymph nodes from C57Bl/6, pTα$^{-/-}$ and pTα^a.pTα$^{-/-}$ mice. (B) Summary bar charts of total numbers of CD4$^{(+)}$ and CD8$^{(+)}$ lymphocytes in all three strains.****$p<0.0001$; *** $p<0.001$; ** $p<0.01$; ns is non significant; error bar is SD.

Thus, the pTα^a transgene was able to largely rescue conventional CD4$^{(+)}$ and CD8$^{(+)}$ T cell development in a pTα$^{-/-}$ background (Figure 3.11).

3.7 The pTα^a transgene does not rescue the development of unconventional TCRαβ$^{(+)}$CD8αα$^{(+)}$ IELs

As documented in the introduction, we had previously hypothesised that signalling events at the β-selection checkpoint might be responsible for establishing heterogeneity amongst DP thymocytes that could then impact on subsequent T cell selection. Because conventional CD4$^{(+)}$ and CD8$^{(+)}$ T cells appeared largely rescued in thymus and LN from pTα^a.pTα$^{-/-}$ transgenic mice we sought to investigate whether this was also the case for agonist-selected T cells. The lab has had an ongoing interest in understanding the development of agonist-selected unconventional TCRαβ$^{(+)}$CD8αα$^{(+)}$ intra-epithelial lymphocytes (IELs), which prompted us to investigate their development in pTα^a.pTα$^{-/-}$ mice. pTα-deficient animals, which cannot express a preTCR, also lack TCRαβ$^{(+)}$CD8αα$^{(+)}$ IELs, implicating β-selection as an important checkpoint in their development (Fehling et al., 1995). Small intestines from C57Bl/6, pTα$^{-/-}$ and pTα^a.pTα$^{-/-}$ mice were dissected, epithelial lymphocytes were isolated and cells were analysed by flow cytometry. Because we were mainly interested in CD8$^{(+)}$ IELs, CD4$^{(+)}$ cells were gated out and populations of γδ and αβ IELs were identified using anti-TCRδ and anti-TCRβ antibodies. CD8α and CD8β were then used to look at three populations of interest; conventional

$TCR\alpha\beta^{(+)}CD8\alpha\beta^{(+)}$ IELs; unconventional $TCR\alpha\beta^{(+)}CD8\alpha\alpha^{(+)}$ IELs; and unconventional $TCR\gamma\delta^{(+)}CD8\alpha\alpha^{(+)}$ IELs.

Although great care is taken to obtain a pure population of epithelial lymphocytes, we observed significant variability (up to five-fold) regarding the number of cells that were isolated per small intestine. This has somewhat restricted our analysis of total cell number, and effectively forced us to mainly concentrate on cell proportions (**Figure 3.12**).
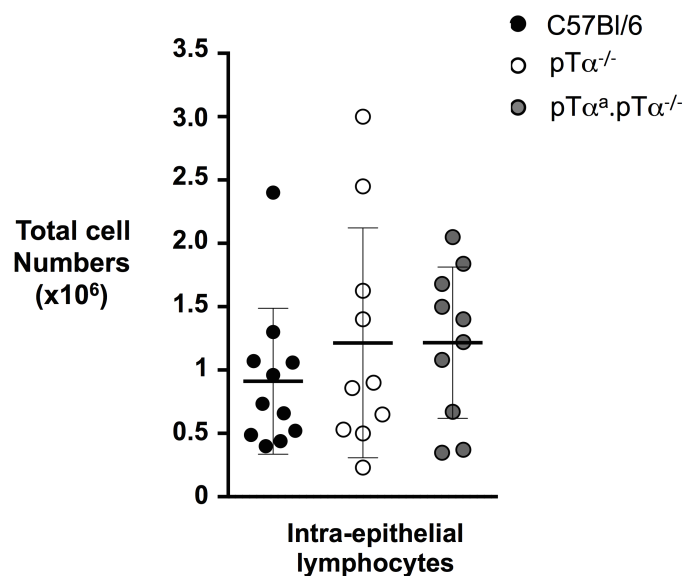
Figure 3.12 The total number of intra-epithelial lymphocytes (IEL) varies significantly across different experiments. Summary dot plot showing the total number of cells obtained from the small intestine of C57Bl/6, $pT\alpha^{-/-}$, and $pT\alpha^{a}.pT\alpha^{-/-}$ mice. Cell numbers varied significantly between experiments.

On analysis of the small intestine of the three groups of mice, it was evident that $pT\alpha^{a}.pT\alpha^{-/-}$ mice had a significant reduced proportion of $TCR\alpha\beta^{(+)}$ IELs when compared to WT animals. This proportion was more similar to that seen in $pT\alpha^{-/-}$

mice, suggesting that expression of the transgenic pTα^a had not efficiently rescued development of this subset. Importantly, this depletion of TCR$\alpha\beta^{(+)}$ IELs was restricted to the unconventional TCR$\alpha\beta^{(+)}$CD8$\alpha\alpha^{(+)}$ IEL subset as proportions of conventional TCR$\alpha\beta^{(+)}$CD8$\alpha\beta^{(+)}$ IELs or TCR$\gamma\delta^{(+)}$ IELs were largely rescued by the pTα^a transgene. Indeed, TCR$\alpha\beta^{(+)}$CD8$\alpha\beta^{(+)}$ IELs and TCR$\gamma\delta^{(+)}$CD8$\alpha\alpha^{(+)}$ IELs constitute on average 15% and 25% of the CD4$^{(-)}$ subset in both C57Bl/6 and pTα^a.pT$\alpha^{-/-}$ transgenic mice. Thus, the TCR$\alpha\beta^{(+)}$ IEL ratio of conventional TCR$\alpha\beta^{(+)}$CD8$\alpha\beta^{(+)}$ IELs to unconventional TCR$\alpha\beta^{(+)}$CD8$\alpha\alpha^{(+)}$ IELs that is ~1.5 in WT animals, and is almost 20 in pT$\alpha^{-/-}$ mice, is still significantly raised in pTα^a.pT$\alpha^{-/-}$ mice with a ratio of ~8 (Figure 3.13).

Thus, although the development of conventional T cells seems to be largely rescued by the pTα^a transgene in both the lymph node and to a slightly lesser extent the gut, the availability of only the pTα^a isoform at the β-selection checkpoint appears to disproportionately affect the development of agonist-selected TCR$\alpha\beta^{(+)}$CD8$\alpha\alpha^{(+)}$ IELs.
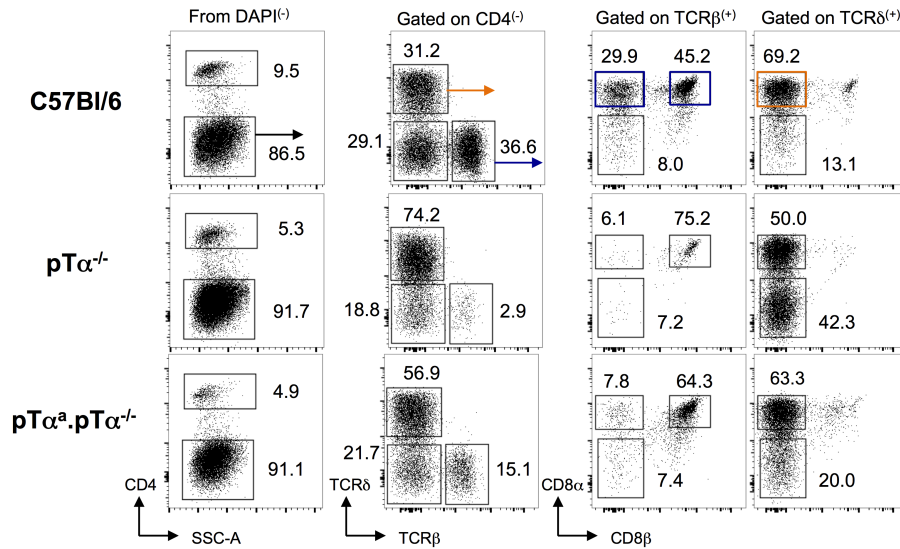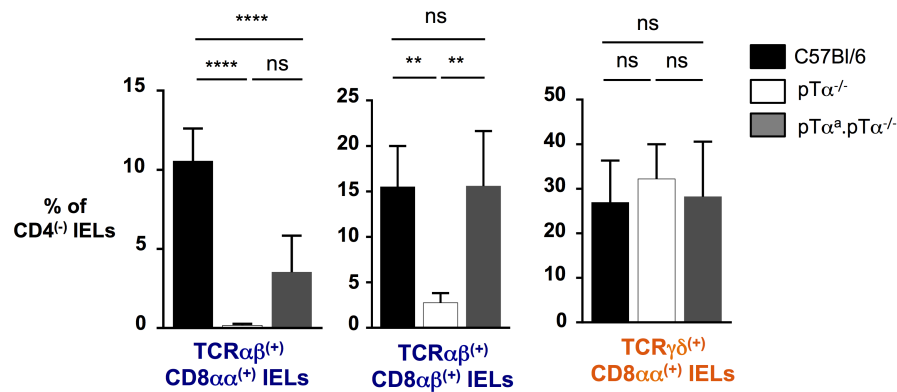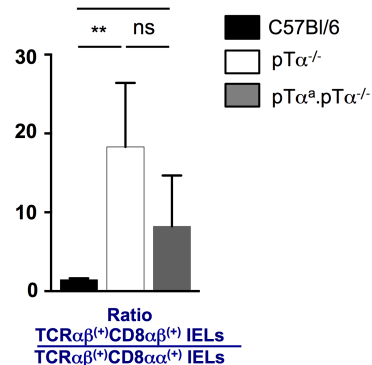
Figure 3.13 The TCRαβ⁽⁺⁾CD8αα⁽⁺⁾ IELs are not rescued by the pTα^a transgene.

(A) Representative flow cytometry plots (n>8) looking at IEL populations in the small intestine of C57Bl/6, pTα$^{-/-}$ and pTα$^{a.}$pTα$^{-/-}$ mice. Percentages of cells are indicated near each gate. (B) Summary bar graphs (n>8) of the proportion of TCRαβ$^{(+)}$CD8αα$^{(+)}$, TCRαβ$^{(+)}$CD8αβ$^{(+)}$ and TCRγδ$^{(+)}$CD8αα$^{(+)}$IELs out of CD4$^{(-)}$ IELs (C) Summary bar graph (n>8) of the ratio of conventional TCRαβ$^{(+)}$CD8αβ$^{(+)}$ IELs to unconventional TCRαβ$^{(+)}$CD8αα$^{(+)}$ IELs. **** $p< 0.0001$ *** $p < 0.001$, **$p < 0.01$, * $p < 0.05$, ns is for not significant. Error bars are SD.

3.8 The pTα^a transgene does not fully rescue the development of thymic TCRαβ$^{(+)}$CD8αα$^{(+)}$ IEL progenitors.

The reduced proportion of TCRαβ$^{(+)}$CD8αα$^{(+)}$ IELs in the small intestine of pTα^a.pTα$^{-/-}$ transgenic animals led us to then assess the development of their progenitors in the thymus that have been defined by Hilde Cheroutre's lab as TCRδ$^{(-)}$ DN (CD4$^{(-)}$CD8$^{(-)}$) CD5$^{(+)}$TCRβ$^{(+)}$ (Lambolez et al., 2007). In WT C57Bl/6 mice the percentage of these progenitors (as a proportion of all DN cells) was ~11%. In pTα$^{-/-}$ mice, these cells were largely absent, representing only 0.2% of DN cells. However, in pTα^a.pTα$^{-/-}$ mice this subset was ~4% of DN cells suggesting that the transgene is capable of rescuing their development to some extent (Figure 3.14). Of note, the large disparity in the size of the DN population between the three groups (for example, 1.5%, 60.0%, 8.5% in C57Bl/6, pTα$^{-/-}$, and pTα^a.pTα$^{-/-}$ mice, respectively (Figure 3.9) is likely to affect the calculation of IEL progenitors.

To try to clarify whether thymic IEL progenitors were reduced in pTα$^{-/-}$.pTα^a mice, we looked at TCRαβ$^{(+)}$CD8αα$^{(+)}$ IEL progenitors based on the recently described phenotype of CD4^{low}CD8^{low} (DP^{dull}), CD5$^{(+)}$, CD69$^{(+)}$, PD1$^{(+)}$ and CD122$^{(+)}$ (McDonald et al., 2014). Preliminary analysis led to a similar conclusion as that above; that there is a reduction of TCRαβ$^{(+)}$CD8αα$^{(+)}$ IEL progenitors in pTα^a.pTα$^{-/-}$ mice (~8% of DP^{dull}) compared to C57Bl/6 mice (~16% of DP^{dull}) (Figure 3.15).
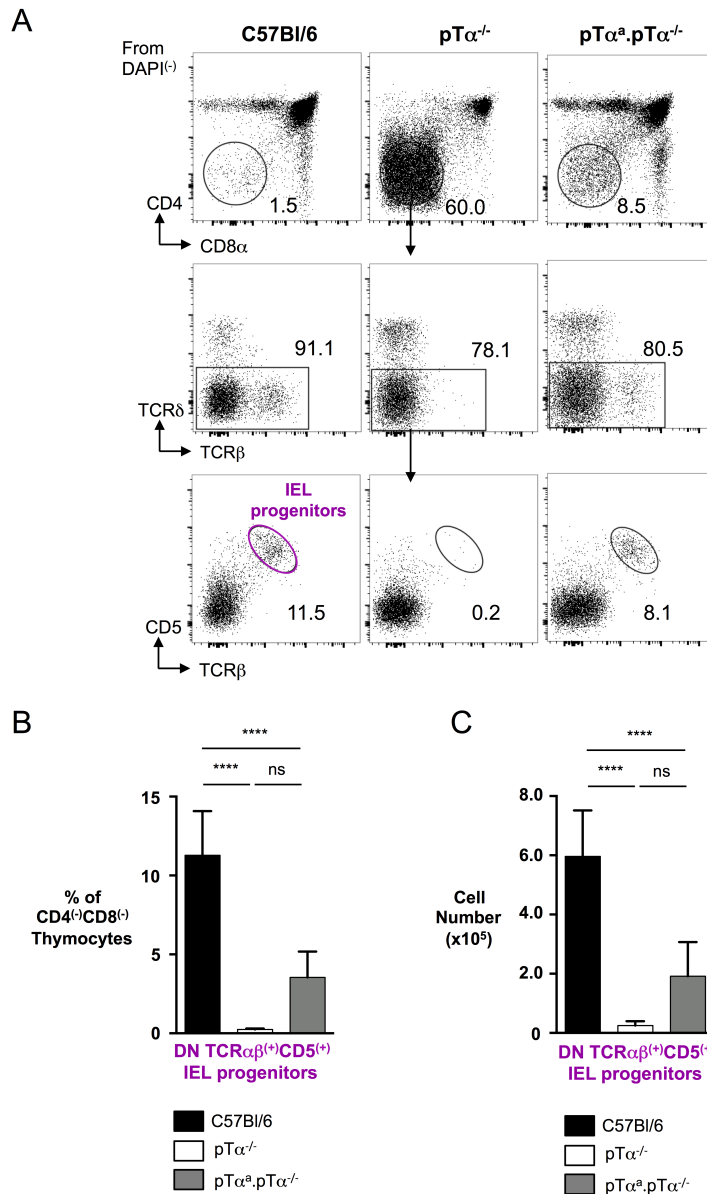
Figure 3.14 pTαª.pTα⁻/⁻ mice harbour a reduced compartment of thymic TCRαβ⁽⁺⁾CD8αα⁽⁺⁾IEL progenitors. (A) Representative flow cytometry plots (n>10) looking at CD4⁽⁻⁾CD8⁽⁻⁾,TCRαβ⁽⁺⁾,CD5⁽⁺⁾ IEL progenitors in the thymus of C57Bl/6, pTα⁻/⁻ and pTαª.pTα⁻/⁻ mice. Percentages of cells are indicated near each gate. (B) Summary bar graph (n>10) of the proportion of CD4⁽⁻⁾CD8⁽⁻⁾TCRαβ⁽⁺⁾CD5⁽⁺⁾ IEL progenitors in C57Bl/6, pTα⁻/⁻ and pTαª.pTα⁻/⁻ mice (C) Summary bar graph (n>10) of the total cell number of CD4⁽⁻⁾CD8⁽⁻⁾TCRαβ⁽⁺⁾CD5⁽⁺⁾ IEL progenitors in C57Bl/6, pTα⁻/⁻ and pTαª.pTα⁻/⁻ mice. DN is Double negative (CD4⁽⁻⁾CD8⁽⁻⁾) **** p<0.0001 *** p < 0.001.
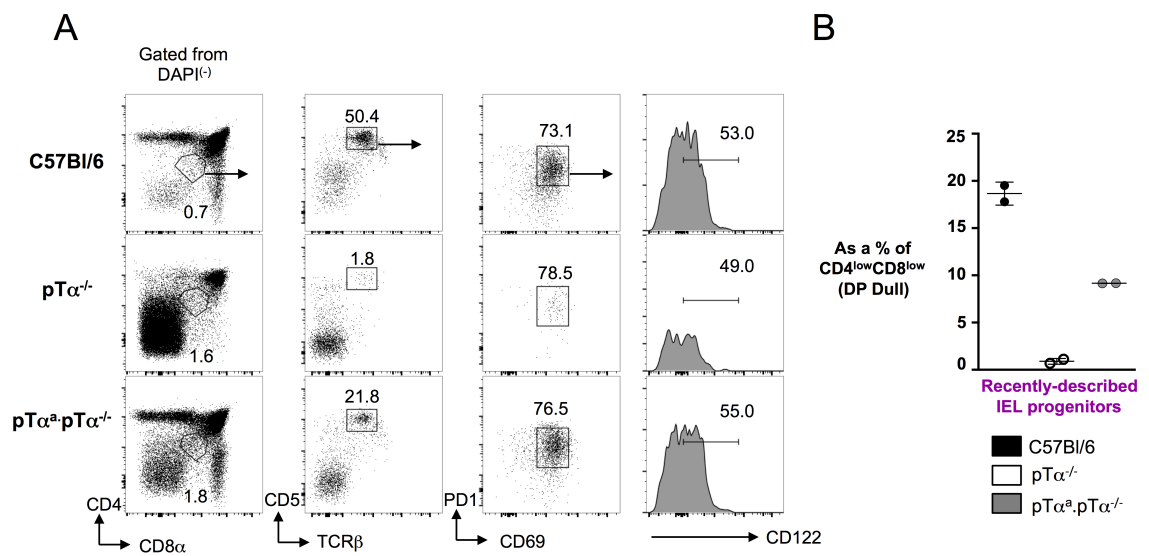
Figure 3.15 pTα^a.pTα^{-/-} transgenic mice harbour a reduced compartment of recently described TCRαβ$^{(+)}$CD8αα$^{(+)}$IEL progenitors. (A) Representative flow cytometry plots (n=2) looking at DP^{dull}, CD5$^{(+)}$, CD69$^{(+)}$, PD1$^{(+)}$ and CD122$^{(+)}$ IEL progenitors in the thymus of C57Bl/6, pTα$^{-/-}$ and pTα^{a}.pTα$^{-/-}$ transgenic mice. Percentages of cells are indicated near each gate. (B) Summary graph (n=2) of the proportion of DP^{dull}, CD5$^{(+)}$, CD69$^{(+)}$, PD1$^{(+)}$ and CD122$^{(+)}$ IEL progenitors in C57Bl/6, pTα$^{-/-}$ and pTα^{a}.pTα$^{-/-}$ mice. DP dull is (CD4^{low}CD8^{low});

3.9 Characterisation of TCR$\alpha\beta^{(+)}$ and TCR$\gamma\delta^{(+)}$ IEL populations in the small intestine of C57Bl/6, FVB/n, and BALB/c mice.

It had previously been noted in the lab that different strains of WT mice (C57Bl/6, FVB/n, BALB/c) had different ratios of conventional TCR$\alpha\beta^{(+)}$CD8$\alpha\beta^{(+)}$ to unconventional TCR$\alpha\beta^{(+)}$CD8$\alpha\alpha^{(+)}$ IELs, that was somewhat reminiscent of that observed in pTα^{a}.pT$\alpha^{-/-}$ mice when compared to C57Bl/6 mice. Importantly, these are WT strains and have been extensively used as "controls" in numerous studies (Kunisawa et al., 2007; Mysorekar et al., 2002; Panwala et al., 1998). Comparing T cell subsets in different strains of WT mice has, on some occasions, allowed scientists to gain a particular insight into T cell development or function (Barbee et al., 2011; Turchinovich and Hayday, 2011). This is well demonstrated by identification of Skint-1 required for dendritic epidermal $\gamma\delta$ T cells (DETC) development and maintenance in the murine skin. The importance of Skint-1 came to light following the comparison of two different strains of FVB/n mice (Barbee et al., 2011). Indeed, it was noted that FVB/n mice from the supplier Taconic farms (FVB/n-Tac) lacked DETC compared to FVB/n mice from the Jackson laboratories (FVB/n-Jax). Transfer of FVB/n-Tac thymocytes to FVB/n-Jax thymic stroma restored DETC development suggesting that a developmental determinant was present in non-haematopoietic cells (Barbee et al., 2011). Genetic comparison of the two strains revealed a mutation in the *Skint-1* gene resulting in premature termination of translation and thus a mutated protein (Barbee et al., 2011).

To investigate the IEL compartments of the three WT strains, lymphocytes were isolated from the small intestine and analysed by flow cytometry. (Figure 3.16). The first notable difference in IEL populations between the three strains was a significant reduction in TCR$\alpha\beta^{(+)}$ IELs in BALB/c mice compared to the other two strains (~5% of CD4$^{(-)}$ IELs compared to ~30% in C57Bl/6 and ~40% in FVB/n mice). By contrast, the TCR$\gamma\delta^{(+)}$IEL compartment was not significantly different (~40% of CD4$^{(-)}$ cells for all three strains).
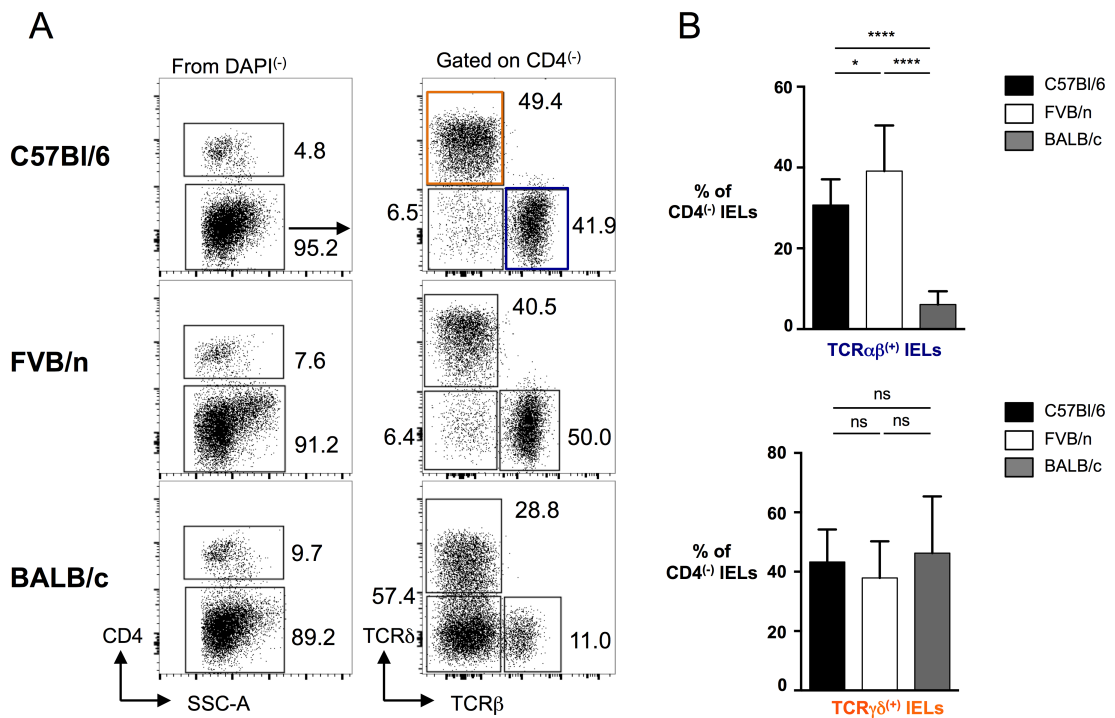
Figure 3.16 BALB/c mice harbour a reduced proportion of TCR$\alpha\beta^{(+)}$ IELs but not TCR$\gamma\delta^{(+)}$ IELs compared to C57Bl/6 and FVB/n mice. (A) Representative flow cytometry plots (from n>6) looking at the IEL populations in the small intestine of C57Bl/6, FVB/n and BALB/c mice. (B) Summary bar graphs (n>6) of the proportions of TCR$\alpha\beta^{(+)}$ and TCR$\gamma\delta^{(+)}$ IELs out of CD4$^{(-)}$IELs in the small intestines of C57Bl/6, FVB/n and BALB/c mice. **** p< 0.0001, * p < 0.05, ns is for not significant.

Analysis of the proportions of each $TCR\alpha\beta^{(+)}$ IEL population (that is the $TCR\alpha\beta^{(+)}CD8\alpha\beta^{(+)}$, $TCR\alpha\beta^{(+)}CD8\alpha\alpha^{(+)}$, and $TCR\gamma\delta^{(+)}CD8\alpha\alpha^{(+)}$ subsets) revealed that $TCR\alpha\beta^{(+)}CD8\alpha\alpha^{(+)}$ IELs were found in lower proportions in FVB/n mice (~7% of $CD4^{(-)}$ cells) and BALB/c mice (~3%) compared to C57Bl/6 mice (~13%) (Figure 3.17). $TCR\alpha\beta^{(+)}$ IELs were then analysed further by calculating the ratio of conventional $TCR\alpha\beta^{(+)}CD8\alpha\beta^{(+)}$ IELs to unconventional $TCR\alpha\beta^{(+)}CD8\alpha\alpha^{(+)}$ IELs. For C57Bl/6 mice this ratio was ~1.0, with roughly equal proportions of the two types of $TCR\alpha\beta^{(+)}$IELs. However, for BALB/c mice this ratio was nearer 0.5, while FVB/n mice had a ratio of conventional to unconventional IELs that approached 6.0 (Figure 3.17). Thus, in three strains of WT mice, housed in the same facility, and purchased from the same supplier, the proportion of conventional and unconventional IELs varied significantly. Of particular interest were FVB/n mice as these mice appear to have a significantly reduced unconventional $TCR\alpha\beta^{(+)}CD8\alpha\alpha^{(+)}$ IEL pool. We hypothesised at this point that this reduction in unconventional gut IELs in FVB/n mice may be due to compromised thymic development of unconventional IEL progenitors.
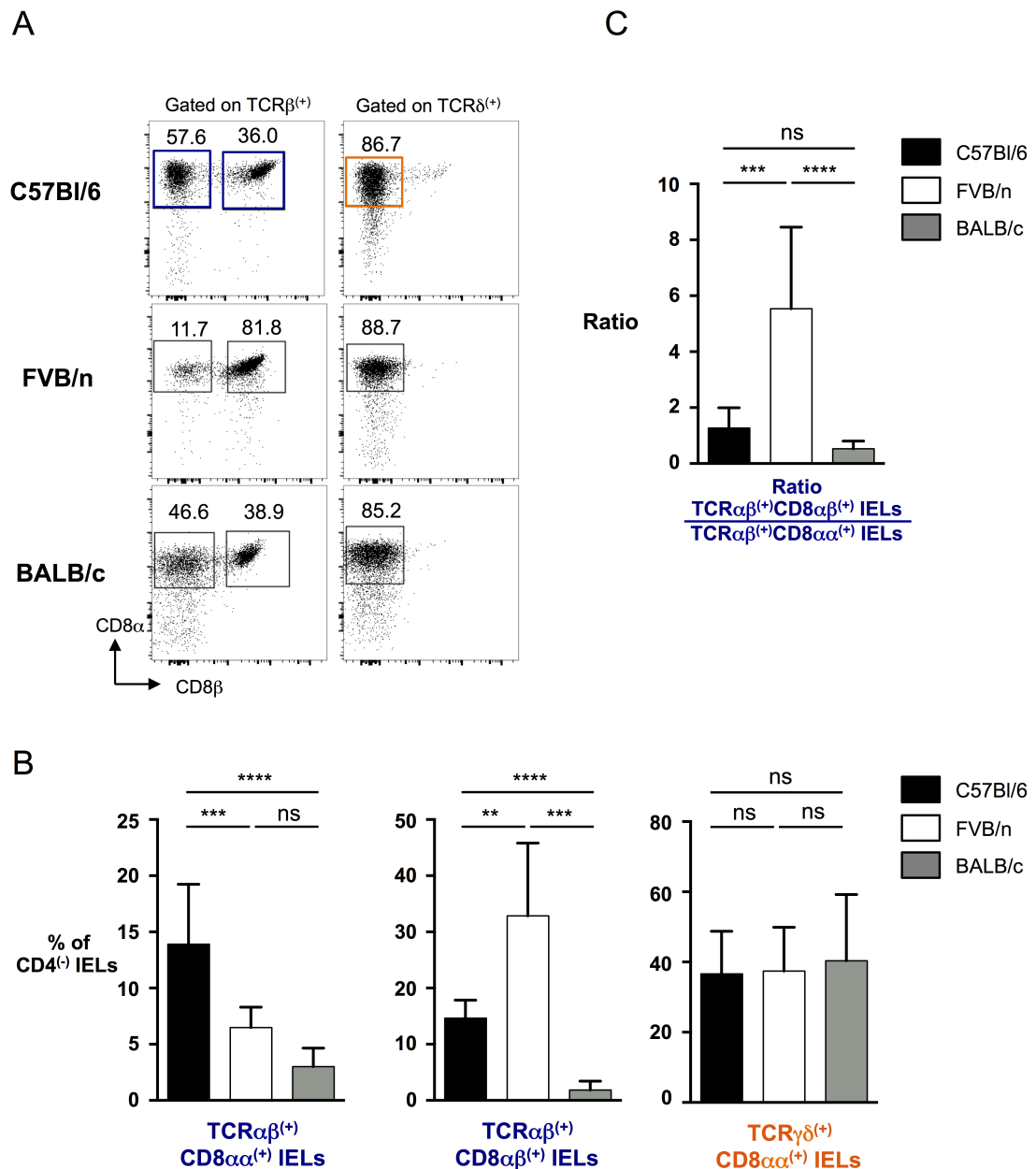
Figure 3.17 C57Bl/6, FVB/n and BALB/c mice harbour different proportions of TCRαβ$^{(+)}$CD8αα$^{(+)}$ IELs. (A) Representative flow cytometry plots (from n>6) looking at the IEL populations (TCRαβ$^{(+)}$CD8αα$^{(+)}$, TCRαβ$^{(+)}$CD8αβ$^{(+)}$ and TCRγδ$^{(+)}$CD8αα$^{(+)}$IELs) in the small intestine of C57Bl/6, FVB/n and BALB/c mice. Percentages of cells are indicated near each gate. (B) Summary bar graphs (n>6) of the percentages (of total CD4$^{(-)}$ IELs) of TCRαβ$^{(+)}$CD8αα$^{(+)}$, TCRαβ$^{(+)}$CD8αβ$^{(+)}$ and TCRγδ$^{(+)}$CD8αα$^{(+)}$IELs (C) Summary bar graph (n>6) of the ratio of TCRαβ$^{(+)}$CD8αβ$^{(+)}$ to TCRαβ$^{(+)}$CD8αα$^{(+)}$ IELs. **** p< 0.0001 *** p < 0.001, **p < 0.01, ns is for not significant.

3.10 Characterisation of IEL progenitors in the thymus of adult C57Bl/6, FVB/n and BALB/c mice.

The relative decrease or increase in $TCR\alpha\beta^{(+)}CD8\alpha\alpha^{(+)}$ IELs in the small intestines of FVB/n and BALB/c mice respectively, led us to investigate whether this was mirrored by the pool of thymic IEL progenitors from 6-week old adult mice. On average, C57Bl/6 mice had ~4.0×10^5 $CD4^{(-)}CD8^{(-)}TCR\beta^{(+)}CD5^{(+)}$ (so-called) unconventional IEL progenitors that represented ~12% of the thymic DN pool. By comparison, FVB/n mice had only ~2.0×10^5 cells (~9% of the DN subset), while BALB/c mice had significantly more (5.0×10^5 cells) that were almost 20% of the DN compartment (Figure 3.18). Thus, the numbers and proportions of thymic unconventional IELs progenitors mirrored the relative proportions of unconventional IELs in the three strains of WT mice, suggesting that a possible reason for the reduced or increased proportions of unconventional IELs in FVB/n or BALB/c mice may be related to T cell development in the thymus.
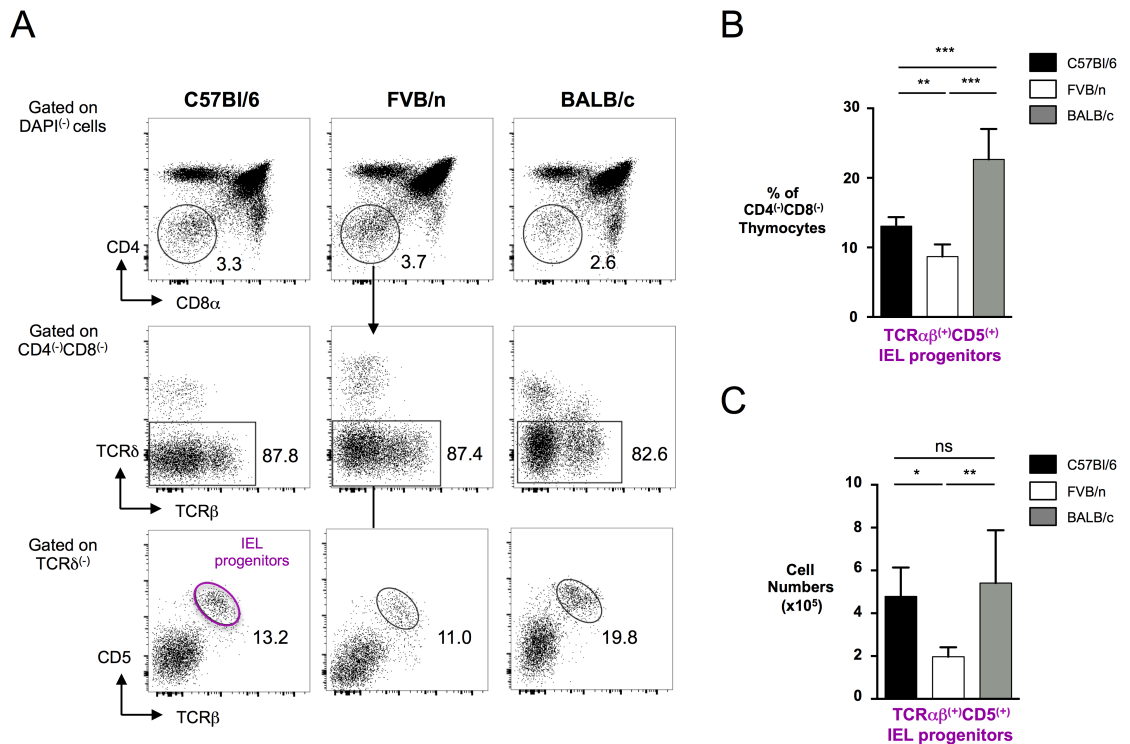
Figure 3.18 TCRαβ$^{(+)}$ CD5$^{(+)}$ IELs progenitors are reduced in FVB/n mice compared to C57Bl/6 and BALB/c mice. (A) Representative flow cytometry plots (n>5) of CD4$^{(-)}$CD8$^{(-)}$TCRαβ$^{(+)}$CD5$^{(+)}$ IEL progenitors in the thymus of C57Bl/6, FVB/n and BALB/c mice. Percentages of cells are indicated near each gate. (B) Summary bar graph (n>5) of the percentage (from CD4$^{(-)}$CD8$^{(-)}$cells) of CD4$^{(-)}$CD8$^{(-)}$TCRαβ$^{(+)}$CD5$^{(+)}$ IEL progenitors in C57Bl/6, FVB/n and BALB/c mice (C) Summary bar graph (n>5) of total cell number for CD4$^{(-)}$CD8$^{(-)}$TCRαβ$^{(+)}$CD5$^{(+)}$ IEL progenitors in C57Bl/6, FVB/n and BALB/c mice *** p< 0.001, **p< 0.01, * p< 0.05, ns is not significant. DN is double negative for CD4 and CD8α.

3.11 Characterisation of recently-described IEL progenitors in the thymus of adult C57Bl/6, FVB/n and BALB/c mice

To provide support for the findings above, the thymuses of C57Bl/6, BALB/c, and FVB/n mice were also analysed for the recently described subset of thymic IEL progenitors that are DP^{dull} TCRαβ$^{(+)}$CD5$^{(+)}$PD1$^{(+)}$CD69$^{(+)}$CD122$^{(+)}$.

Consistent with the previous analysis, FVB/n mice contained a decreased compartment of these cells (~16% of the DP^{dull} subset, and 2.0x10^5 cells) when compared to C57Bl/6 mice (~19% of DP^{dull} cells, 3.5x10^5 cells) (Figure 3.19). Although this failed to reach statistical significance, somewhat surprisingly BALB/c mice also showed a reduced proportion (9.3% of DP^{dull} cells) and number of these IEL progenitors (2.0x10^5 cells) when compared to C57Bl/6 mice. Thus, taken together, the data appear to support a hypothesis in which FVB/n mice have reduced unconventional gut IELs with a concomitant decrease in thymic IEL progenitors, when compared to C57Bl/6 mice.

A

Gated on DAPI$^{(-)}$

C57Bl/6   0.8   47.6   71.0   43.9

FVB/n   0.7   41.9   70.5   44.7

BALB/c   1.3   43.5   50.3   43.1

CD4 — CD8α CD5 — TCRβ PD1 — CD69   CD122

B

Cell numbers (10^5)

Newly described IEL progenitors

- C57Bl/6
- FVB/n
- BALB/c
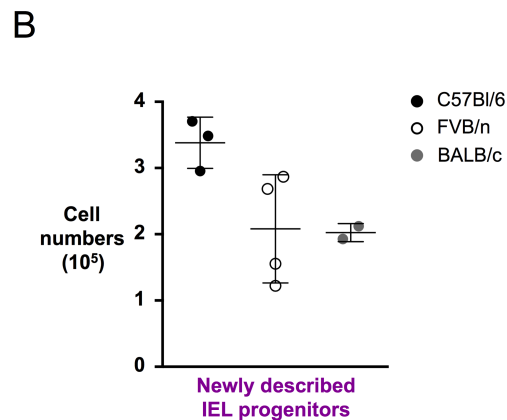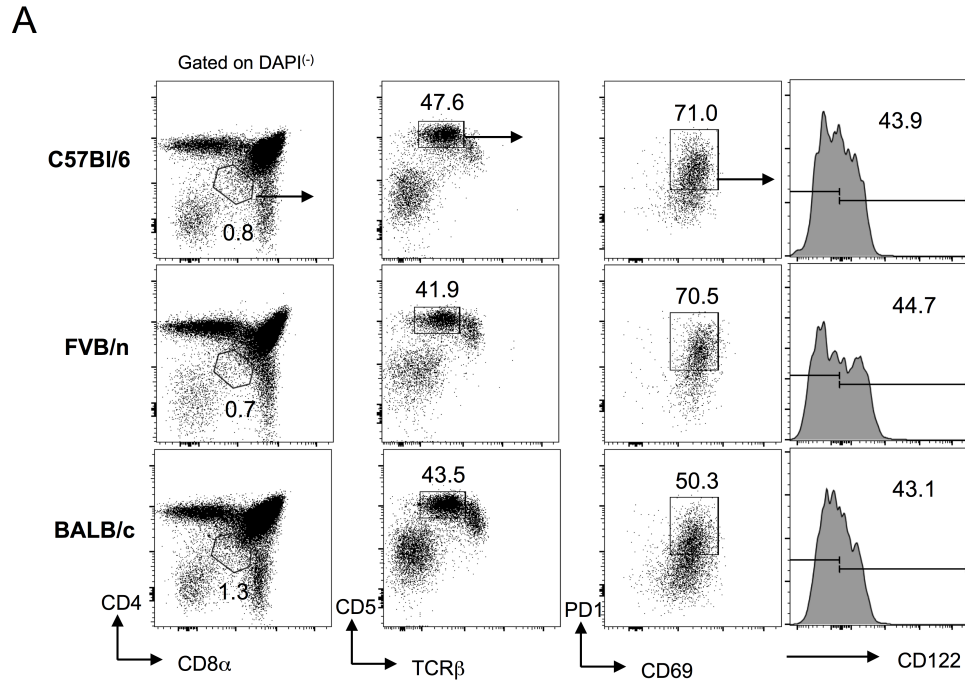
Figure 3.19 Preliminary analysis of recently-described DP^{dull} TCR$\alpha\beta^{(+)}$CD5$^{(+)}$ PD1$^{(+)}$CD69$^{(+)}$CD122$^{(+)}$IEL progenitors. (A) Representative flow cytometry plots (n>2) looking at recently-described DP^{dull},TCR$\alpha\beta^{(+)}$,CD5$^{(+)}$, PD1$^{(+)}$,CD69$^{(+)}$, CD122$^{(+)}$ IEL progenitors in the thymus of C57Bl/6, FVB/n and BALB/c mice. Percentages of cells are indicated near each gate. (B) Summary dot plot of total number of DP^{dull},TCR$\alpha\beta^{(+)}$,CD5$^{(+)}$, PD1$^{(+)}$,CD69$^{(+)}$, CD122$^{(+)}$ IEL progenitors in C57Bl/6, FVB/n and BALB/c mice. DP is double positive for CD4 and CD8α.

3.12 Characterisation of thymic IEL progenitors in seven day FTOCs of C57Bl/6 and FVB/n thymuses

Foetal thymic organ culture (FTOC) is a useful technique to follow the kinetics of T cell development over a certain period of time (Jenkinson and Owen, 1990). E15 foetal thymuses, from timed pregnant C57Bl/6 or FVB/n females, were dissected and cultured for 7 days in FTOC media. It was actually challenging to get embryos from all three strains (C57Bl/6, FVB/n and BALB/c strains) simultaneously, so we subsequently focused our analysis on C57Bl/6 and FVB/n mice. Flow cytometry analysis of these cultures showed a decreased proportion and cell number of $CD4^{(-)}CD8^{(-)}CD5^{(+)}TCR\beta^{(+)}$ thymic IEL progenitors in FVB/n mice (~0.4% of DN cells, 250 cells in total) compared with C57Bl/6 mice (~0.6% as of DN cells, $1.0x10^3$ cells in total) (Figure 3.20).

Thus, the data presented in the last few sections suggest that in comparison to C57Bl/6 mice, FVB/n mice have significantly fewer unconventional $TCR\alpha\beta^{(+)}CD8\alpha\alpha^{(+)}$ IELs. Moreover, rather than being a consequence of the gut environment, these data suggest that in FVB/n mice thymic IEL progenitors do not develop to the same extent as for C57Bl/6 animals.
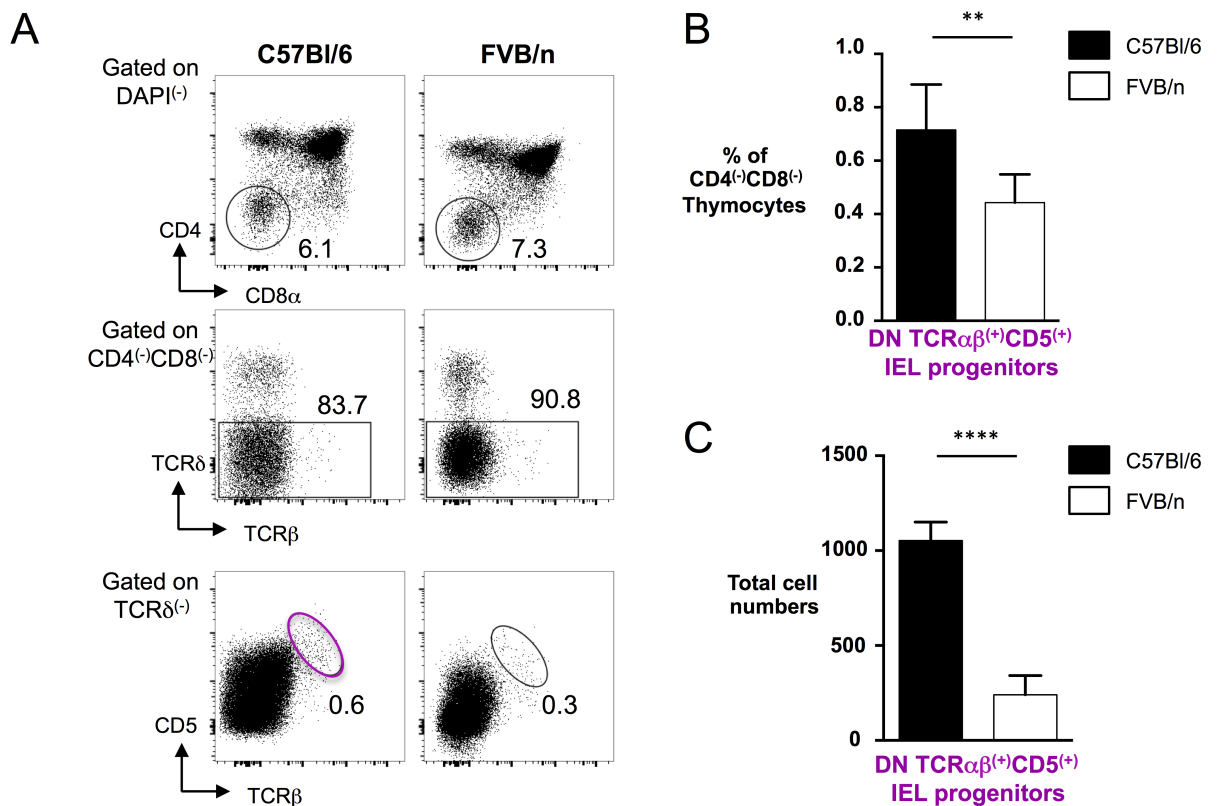
Figure 3.20 Investigating the development of TCRαβ$^{(+)}$CD5$^{(+)}$ IEL progenitors in foetal thymic organ cultures (FTOC). (A) show represensative flow cytometry plots (from n>5) of E15 C57Bl/6 and FVB/n lobes cultured for 7 days. (B) shows a summary bar chart of the proportion of CD4$^{(-)}$CD8$^{(-)}$TCRαβ$^{(+)}$CD5$^{(+)}$ IEL progenitors in FTOC run in (A) for 7days. (C) shows the total number of TCRαβ$^{(+)}$CD5$^{(+)}$ thymic IEL progenitors in a 7-day FTOC. ****p<0.0001 **p < 0.01, error bars are SD.

3.13 Investigating the early stages of T cell development in C57Bl/6 and FVB/n mice

Data presented from both the thymus and the gut of C57Bl/6 and FVB/n mice suggest that in comparison to C57Bl/6 mice, FVB/n animals have fewer IEL

progenitors and fewer unconventional TCR$\alpha\beta^{(+)}$CD8$\alpha\alpha^{(+)}$ cells that is similar to the phenotype of pTα^a.pT$\alpha^{-/-}$ mice when compared to wild-type controls. Because the key feature of pTα^a.pT$\alpha^{-/-}$ mice is the expression of pTα^a only and thus preTCR^a only, this prompted us to investigate the early stages of T cell development in FVB/n mice with a particular focus on the DN3 to DN4 transition where the preTCR is expressed. Analysis of the DN compartment first requires the removal of CD4$^{(+)}$ and CD8$^{(+)}$ thymocytes (using antibodies against CD4 and CD8α), as well as other mature T cells such as NKT cells and $\gamma\delta$ T cells (using both anti-TCRβ and anti-TCRδ antibodies). The DN3 and DN4 subsets are subsequently identified through the differential expression of CD25 and CD44, being CD25$^{(+)}$CD44$^{(-)}$ for DN3 cells and CD25$^{(-)}$CD44$^{(-)}$ for DN4 cells. Using this approach we compared the DN3 to DN4 transition in C57Bl/6 and FVB/n mice. C57Bl/6 mice had a ratio of DN3 cells to DN4 cells of ~1.8, which represents an expected distribution of DN3 to DN4 cells judging by previous studies(Yui, 2010). By contrast, analysis revealed what appeared to be a partial block in the DN3 to DN4 transition in FVB/n mice with an increased proportion of DN3 thymocytes (~60%) and a 3-fold increase in the DN3 to DN4 ratio (~4.5) (Figure 3.21).
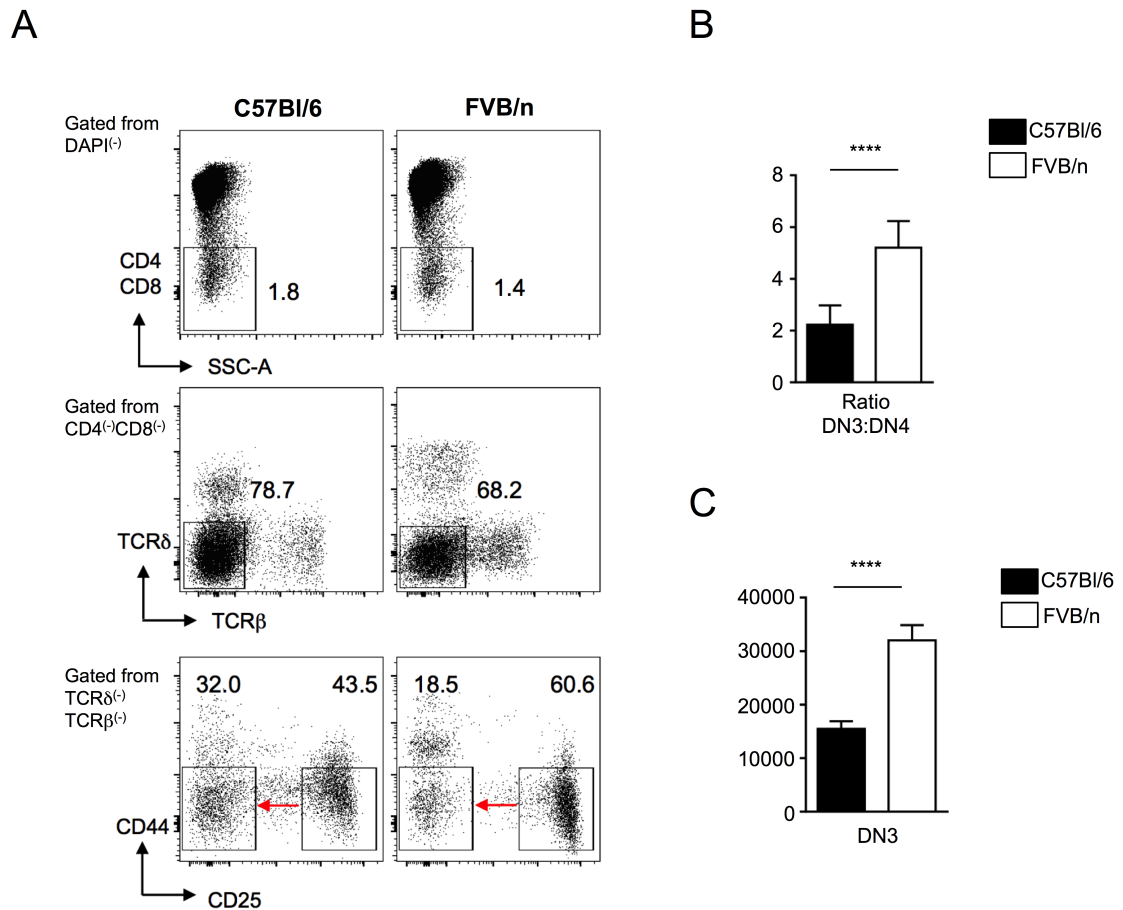
Figure 3.21 FVB/n mice have an impaired DN3 to DN4 transition compared to C57Bl/6 animals. (A) Representative flow cytometry plots looking at the thymic DN3 and DN4 subsets in C57Bl/6 and FVB/n mice. The transition from the DN3 to the DN4 stage is represented by a red arrow. Percentages of cells are indicated near each gate. The ratio of DN3 to DN4 thymocytes obtained from at least 5 experiments is summarised in a summary bar graph in (B). (C) Summary bar graph (n>5) showing CD25 mean fluorescent intensity (MFI) on DN3 cells from C57Bl/6 mice and FVB/n mice **** $p < 0.0001$, ***$p < 0.001$.

A block at the DN3 to DN4 transition of thymocyte development is also indicated by increased CD25 expression on DN3 cells, as observed in pTα-deficient mice where the absence of the preTCR leads to a large accumulation of DN3 cells with significantly greater CD25 expression (Fehling et al., 1995). On analysis of CD25 levels on DN3 cells from C57Bl/6 and FVB/n mice, a 2-fold

increase of CD25 expression was observed on FVB/n DN3 thymocytes (~3200 MFI units) compared to C57Bl/6 DN3 cells (~1500 MFI units) (Figure 3.21). Thus, these data suggest that in comparison to C57Bl/6 mice, FVB/n mice have an inefficient DN3 to DN4 transition.

3.14 FVB/n DN3 thymocytes over-express pTα^a compared to C57Bl/6 DN3 cells

The data presented above suggest an inefficient DN3 to DN4 transition in FVB/n mice. This partial impairment could be the result of inappropriate expression of one of the pTα isoforms (and thus the preTCR) at the β-selection checkpoint. To test this idea, we examined the level of expression of each pTα isoform in the DN3 and DN4 subsets of C57Bl/6 and FVB/n mice using real-time PCR (qPCR). The methodology used is summarised in figure 3.22. As pTα^b is generally omitted from studies, it was not possible to set up a TaqMan qPCR as the TaqMan probe available from ABI does not discriminate between the two pTα isoforms. As an alternative, we set up SYBR green qPCR, in which the SYBR dye binds to newly-generated double-stranded DNA resulting in the emission of a fluorescent signal detectable by the PCR thermocycler (Becker et al., 1996).
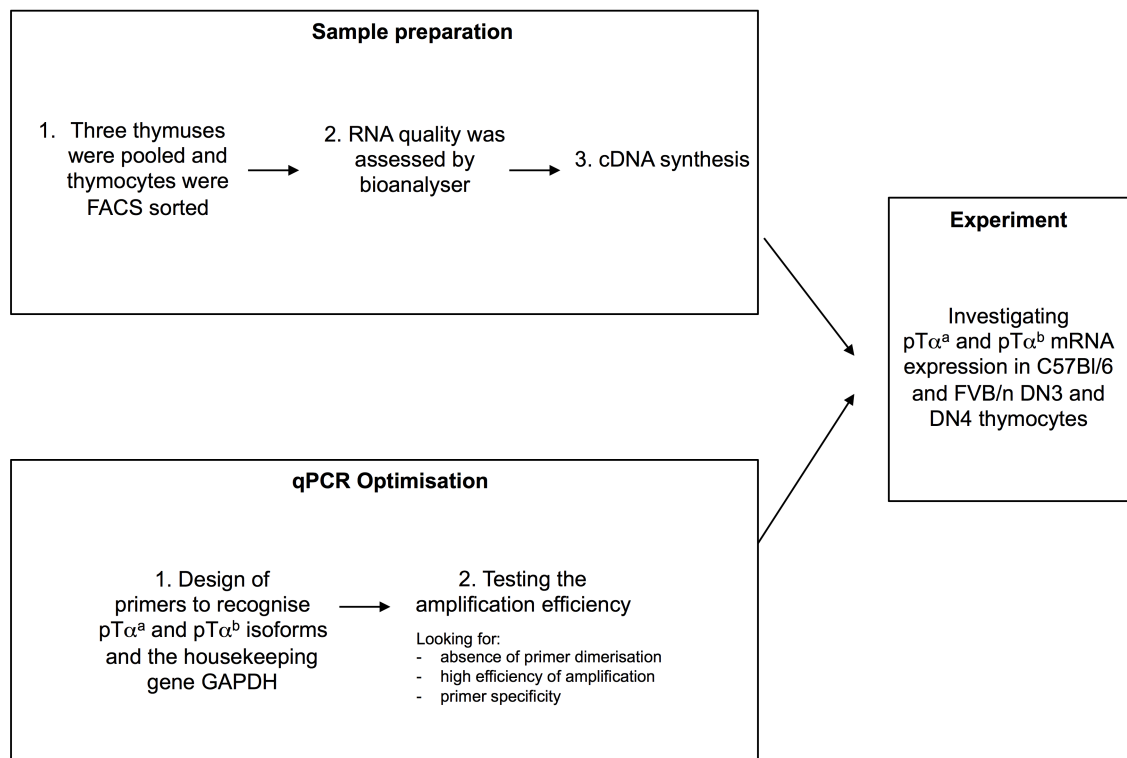
Figure 3.22 Overview of the steps taken for investigating the level of pTα^a and pTα^b transcripts in DN3 and DN4 thymocytes from C57Bl/6 and FVB/n mice.

We used three individual sets of in-house designed primers recognising pTα^a, pTα^b, and glyceraldehyde-3-phosphate dehydrogenase (GAPDH; as a reference gene). The amplicon size for qPCR is usually kept below 200bp to ensure high efficiency during the amplification process. pTα^a transcripts were amplified using a forward primer (qpTaaF) traversing the exon1:2 boundary, being homologous to 14bp at the 3' end of exon-1 and 6bp at the 5' end of exon-2. The reverse primer bound to a 20bp sequence found in exon-2 resulting in an amplicon of 106bp. The forward primer for pTα^b (qpTabF) was homologous to 13bp found at the 3' end of exon-1 and 10bp located at the 5' end of exon-3. The pTα^b reverse primer (pTabR2) was homologous to 20bp in exon-4 resulting in an amplicon of 87bp. GAPDH was amplified with a forward primer recognising 20bp in exon-4, while the reverse primer was homologous to

20bp in exon-5 resulting in an amplicon of 64bp. Because our experiment focused on the expression levels of pTα at steady state in DN3 and DN4 cells, it was considered that expression of GAPDH would be similar across the two subsets and could therefore be used as a reference gene. GAPDH has also been extensively used as a reference gene in other studies (Douglas et al., 2001; Goff and Huntington, 2009).

Before running our qPCR, several steps of optimisation were required. The qPCR reaction should yield a "linear curve" across serially-diluted samples with a coefficient of determination (R^2) above 0.98. Amplification efficiency was also assessed by generating a standard curve from a 1:2 serial dilution of template and their corresponding cycle threshold (C_T) values. The C_T threshold was manually determined. The data was visualised in a linear manner and the threshold was set up so that it would be above the baseline but within the exponential phase of the reaction (Figure 3.23).
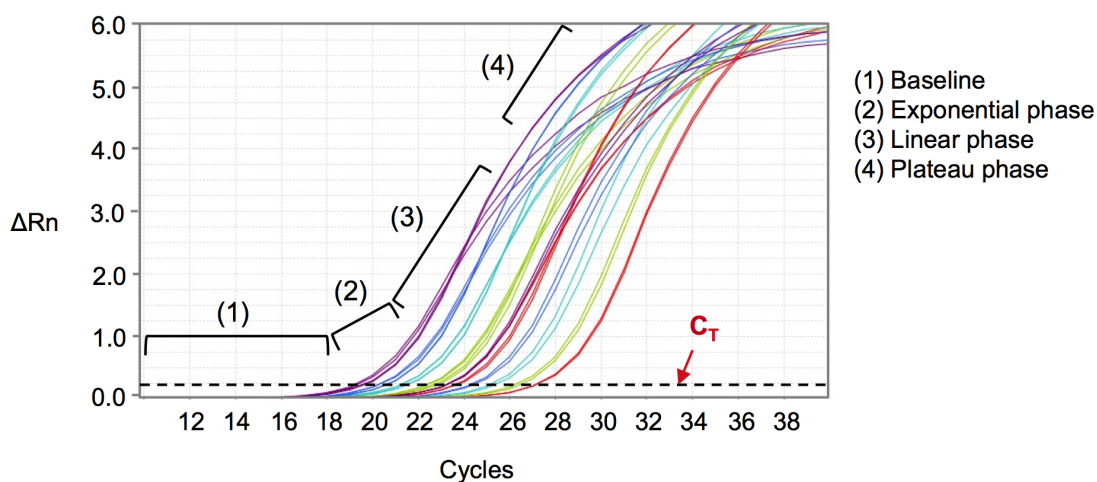
Figure 3.23 The cycle threshold (C_T) was determined manually The amplification plot can be divided into several phases (1) Corresponds to background fluorescence. It is conventionally called the baseline. (2) During the exponential phase the differences in cDNA concentration between each sample can be easily visualised. PCR products are increasing following a 2^n pattern, where n is the number of cycle. (3) During the linear phase the PCR product is still being amplified but the gap between each sample is not maintained like during the exponential phase. The PCR reaction subsequently reaches a plateau phase where the concentration of PCR products no longer increases as depicted by (4). Rn corresponds to the ratio between the fluorescence emission intensity of the reporter dye and the fluorescence emission intensity of the passive reference dye. ΔRN is Rn-Rn of the baseline. CT, cycle threshold

For this experiment, cDNA from DN3 cells from C57Bl/6 cDNA mice were serially-diluted four times at 1:2. A qPCR was run using primers detecting pTα[a]-only, pTα[b]-only or GAPDH in individual wells. Each dilution contains half the amount of cDNA than in the previous well, which means that the threshold cycle (C_T) value between each dilution should be separated by one C_T value if the reaction is 100% efficient. Indeed, the quantity of product is visualised as $\log_2(n)$ where n is the dilution factor. Thus, in our experiment, where samples were diluted 1 in 2, this results in $\log_2(2)$, which equals to 1 C_T value. The Power SYBR Green kit that we used allowed us to manipulate the final concentration

of our set of primers. We first tested 500nM as a final concentration. Each sample was run in duplicates and the melting curves were scrutinized to identify potential primer dimerisation or unspecific amplification. For each reaction, the software generates a peak indicating the melting temperature at which the primers target the cDNA sequence allowing its amplification. A very efficient PCR reaction should have a precise alignment between each peak demonstrating that each amplification took place at the same temperature. The peaks obtained for the GAPDH-targeted qPCR showed a precise overlap between the different peaks averaging around a temperature of 80°C, suggesting that the reaction was specific (Figure 3.24).
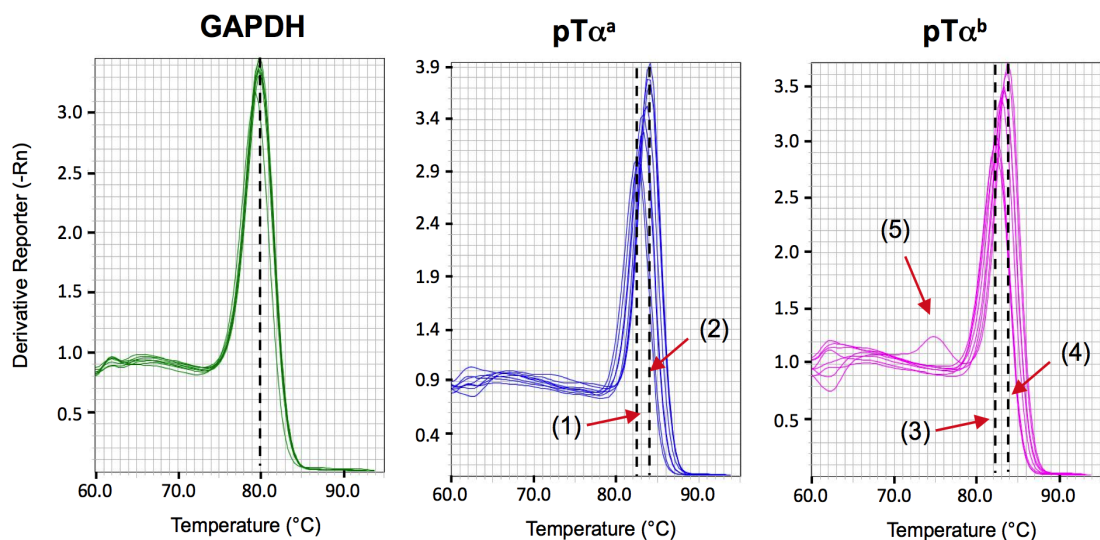
Figure 3.24 Melting curves obtained for each PCR reaction Melting curves are generated during qPCR reactions and can be indicative of primer dimerization (5) or unspecific product amplification (1),(2),(3),(4).

By contrast, the PCRs amplifying the pTα^a and the pTα^b isoforms gave different peaks with various melting temperature (1), (2), (3) and (4). The extra peak at a lower Tm (5) for pTα^b reflected the presence of unspecific product or primer dimerization (Figure 3.24).

Altogether, these observations indicated that the PCR reaction for pTα^a and pTα^b was not optimal as initially designed. To work out the percentage efficiency, each dilution factor was plotted on the x-axis (Log$_2$ Scale) while the C$_T$ values were plotted on the y-axis. Adjacent data points were joined to obtain a straight line. The reaction efficiency was calculated as;

$$\% \, Efficiency = (E - 1) \times 100$$

Where E is defined by;

$$E = 10^{-\left(\frac{1}{Slope}\right)}$$

And where slope can be defined as;

$$slope = \frac{y_b - y_a}{x_b - x_a}$$

Where a and b represent two points located on the line, y_a and y_b are their corresponding values on the y-axis and x_a, x_b the values on the x-axis.

While pTα^a and GAPDH PCRs had an efficiency of 102% and 103% respectively, pTα^b efficiency was 128%, considered to be above the acceptable range of 100%(+/-5%). Moreover, each R^2 value was below 0.98 consistent with a relatively poorly optimised reaction (Figure 3.25).

GAPHD
pTα^a
pTα^b

$y = -3.26x + 23.5$
$R^2 = 0.92$
$P_{Eff} = 102\%$

$y = -3.27x + 27.5$
$R^2 = 0.96$
$P_{Eff} = 103\%$

$y = -2.8x + 30.2$
$R^2 = 0.9175$
$P_{Eff} = 128\%$
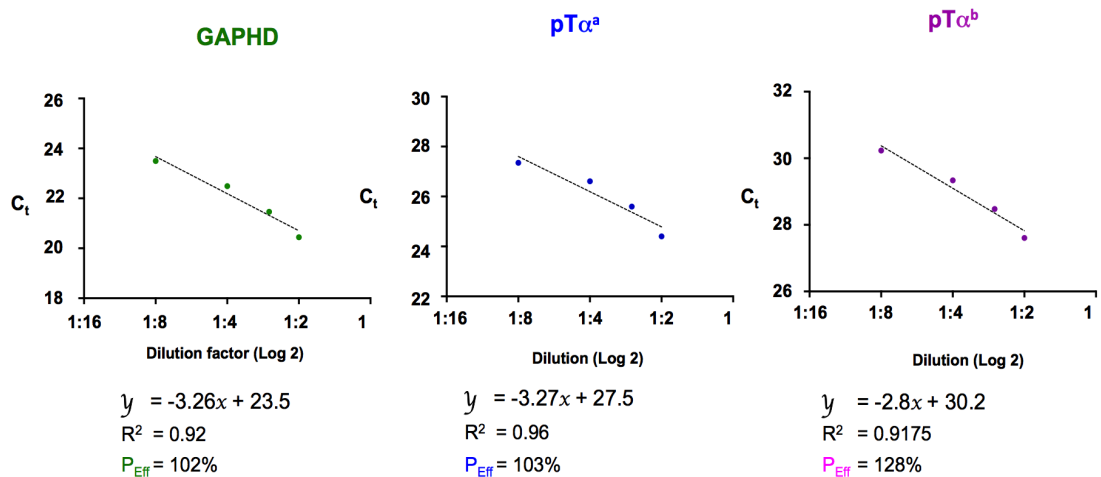
Figure 3.25 The amplification efficiency is not optimal for GAPDH, pTα^a and pTα^b qPCR reactions. A straight line is obtained by plotting the dilution factor of each sample on the x-axis and the corresponding C_T values on the y-axis. The slope is calculated the amplification efficiency is calculated with the formula described in the text. R^2, coefficient of determination; C_T, cycle threshold;

The unspecific amplification suggested by the non-overlapping melting curves for the pTα^a and pTα^b qPCR reactions could be due to the presence of too much primer that favours unspecific recognition. Thus, the experiment was repeated using half the primer concentration (to obtain a final concentration of 250nM). The pipetting error was very minor with less than a 0.2 difference between each C_T values resulting in a neat overlap of the amplification curves between each duplicate as well as a clean no template control (NTC) (Figure 3.26). Lowering the primer concentration produced a much higher specificity for the pTα^a and pTα^b qPCR reactions as seen by the alignment of all the melting curves at around 83°C for both pTα^a and pTα^b, and ~80°C for GAPDH (Figure 3.27).
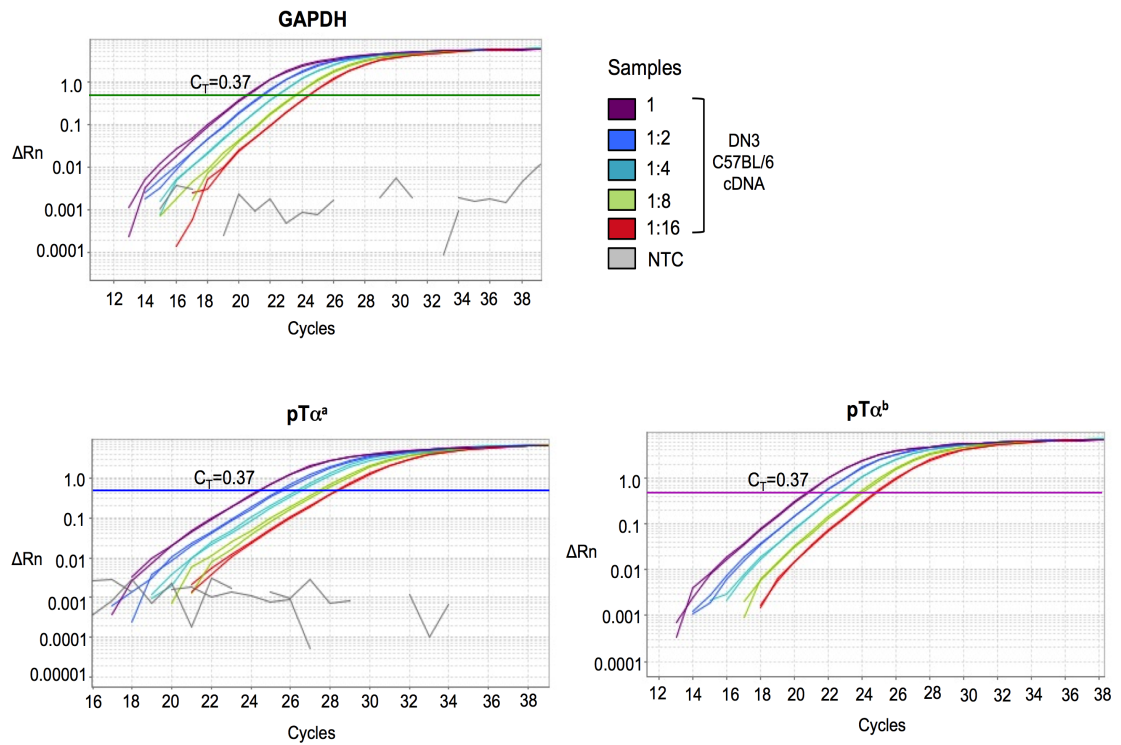
Figure 3.26 The pipetting error is minor between each duplicate in the GAPDH, pTα^a and pTα^b qPCR reactions. Amplification curves showing of the GAPH, pTα^a or pTα^b qPCRs showing the variation between each duplicate within the same diluted sample. The pipetting errors were minor as $C_T < 0.5$ between duplicates. The C_T was manually set up within the exponential phase. C_T, cycle threshold

New standard curves were generated that revealed an improved efficiency of reaction in all three cases with 102% efficiency for the pTα^a qPCR, 101% for GAPDH, and 96% for pTα^b (Figure 3.27). Moreover, each standard curve had a R^2 value of 0.99 indicating a high degree of reproducibility for these PCR reactions. Finally, to visualise the amplified PCR product, the samples were run on agarose gels to confirm the specificity of the amplification (Figure 3.27).
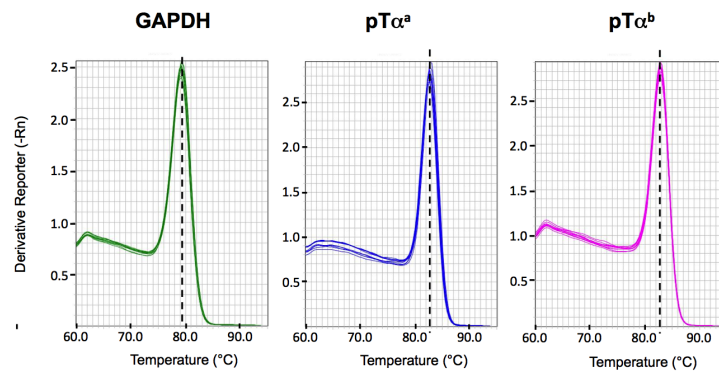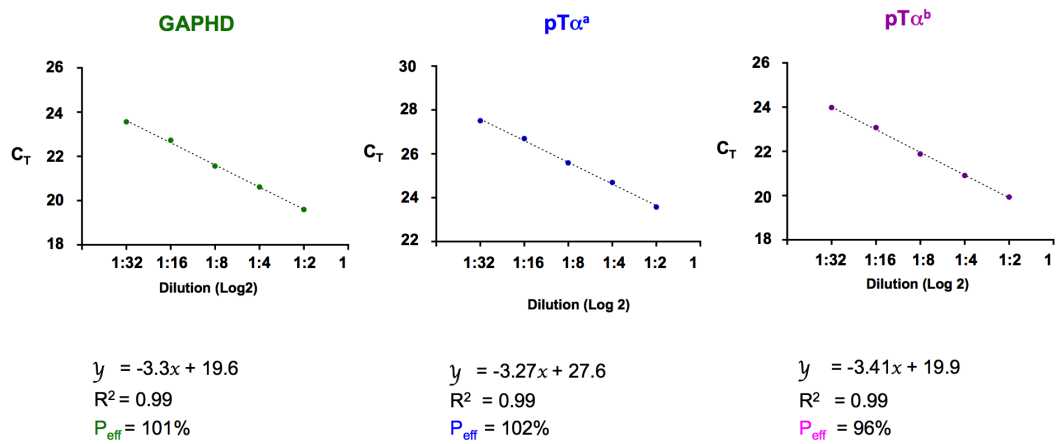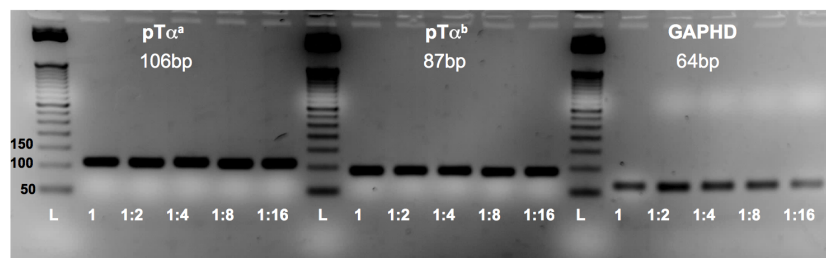
Figure 3.27 Using the lower final concentration of primers improved the qPCR reactions for GAPDH, pTα^a and pTα^b. (A) Melting curves obtained from the GAPDH, pTα^a and pTα^b qPCR run on serially diluted samples. (B) Standard curves were drawn and the amplification efficiency was calculated. The three PCR reactions showed an amplification efficiency within the acceptable range (+/-5%) (C) qPCR products were run onto an agarose gel to confirm the size of the amplicons.

For all reactions, bands of the expected size were observed; $pT\alpha^a$ = 106bp, $pT\alpha^b$ = 87bp, GAPDH = 64bp. Taken together, these data suggest that the qPCR reactions were reliable and could be used to analyse $pT\alpha^a$ and $pT\alpha^b$ expression.

The expression of $pT\alpha^a$ and $pT\alpha^b$ in DN3 and DN4 cells from C57Bl/6 and FVB/n mice was assessed using the optimised qPCR methodology described above. The data obtained were normalised against the reference gene GAPDH by following the formula below;

$$\Delta C_T = C_{T(pT\alpha)} - C_{T\ (GAPDH)}$$

This corresponds to the difference in expression between GAPDH and $pT\alpha^a$ or $pT\alpha^b$. Thus, the higher the expression of $pT\alpha^a$ and $pT\alpha^b$, the smaller the C_T value and therefore the smaller the ΔC_T. (This is because GAPDH transcripts are found at higher concentrations that $pT\alpha$ transcripts resulting in a GAPDH C_T value lower than $pT\alpha$ C_T) Thus, in order to visualise this in a more desirable manner, we plotted $\frac{1}{\Delta CT}$ value to allow an increase in gene expression to appear as a higher value in our results.

On running these reactions, $pT\alpha^a$ expression in DN3 cells was found to be significantly greater in FVB/n mice than in DN3 cells from C57Bl/6 animals. By contrast, $pT\alpha^b$ was expressed at a similar level in both DN3 and DN4 subsets in C57Bl/6 and FVB/n mice (Figure 3.28).
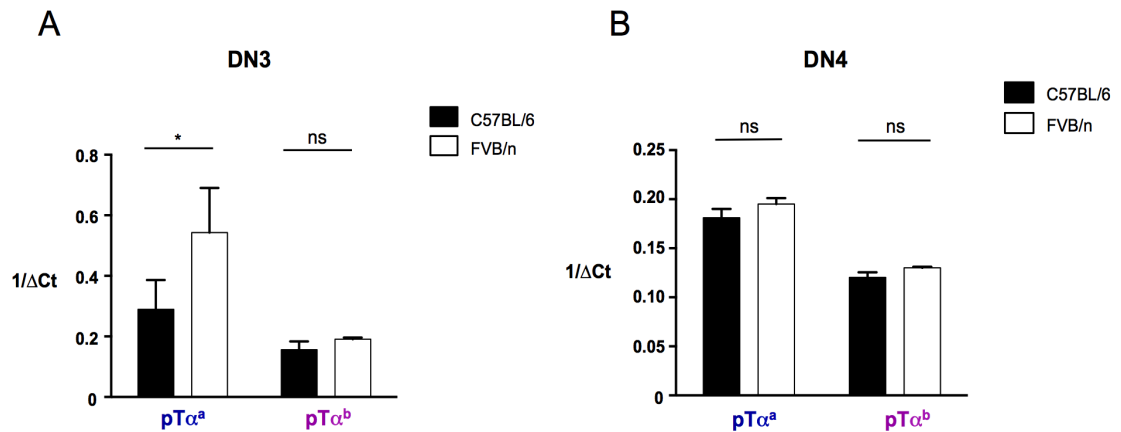
Figure 3.28 DN3 thymocytes from FVB/n mice express greater amounts of pTα^a but not pTα^b, in comparison with C57Bl/6 thymocytes. (A) The relative level of pTα^a and pTα^b transcripts expressed by the DN3 thymocytes or DN4 thymocytes (n>2) (B) from C57Bl/6 and FVB/n mice. ΔC_T corresponds to the normalised C_T value of the reaction according to the reference gene GAPDH. *p<0.05, ns is for not significant

Thus, unlike pTα$^{-/-}$ mice, which have a block at the DN3 to DN4 transition due to the inability to express any of the preTCRs, DN subsets in FVB/n mice appear to be able to express both pTα isoforms. However, the pTα^a isoform was found to be over-expressed (1/ΔC_T=0.55) in FVB/n DN3 cells when compared to C57Bl/6 mice (1/ΔC_T=0.3).

3.15 The pTα^a transgene only partially rescues the DN3 to DN4 transition in pTα^a·pTα$^{-/-}$ transgenic animals.

The data generated by Juliet Mahtani-Patching *in vitro* and discussed earlier in this chapter, suggested a dominant role for pTα^a over pTα^b in T cell development. Thus, over-expressing the pTα^a isoform might have a similar affect as having only pTα^a at the β-selection checkpoint. This idea linked the

two areas of investigation described so far in this chapter; namely thymic development in both $pT\alpha^a.pT\alpha^{-/-}$ mice, and in FVB/n vs C57Bl/6 mice. Indeed, the reduced IEL compartment and reduced IEL progenitors in FVB/n mice were reminiscent of the phenotype described for $pT\alpha^a.pT\alpha^{-/-}$ animals. This prompted us to investigate the DN3 to DN4 transition in $pT\alpha^a.pT\alpha^{-/-}$ animals more closely, as FVB/n mice had displayed distinct features at the β-selection checkpoint (see Figure 3.21).

Flow cytometry analysis of adult C57Bl/6, $pT\alpha^{-/-}$ and $pT\alpha^a.pT\alpha^{-/-}$ revealed that $pT\alpha^a.pT\alpha^{-/-}$ animals have a partial block at the DN3 to DN4 transition reminiscent of the FVB/n mice. This was illustrated by an increased DN3:DN4 ratio (~5) and elevated CD25 levels on $pT\alpha^a.pT\alpha^{-/-}$ DN3 thymocytes (~3500 MFI units) compared to a ratio of ~1.5 in C57Bl/6 mice and a CD25 fluorescence intensity of ~2500 MFI units (Figure 3.29). Thus, the expression of only $pT\alpha^a$ in the BAC transgenic $pT\alpha^a.pT\alpha^{-/-}$ mice at the DN stage of T cell development was not sufficient to fully restore the transition through the β-selection checkpoint to that seen in wild type animals.
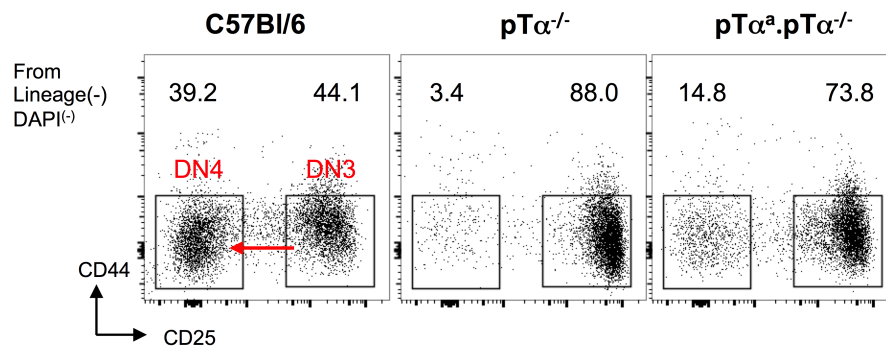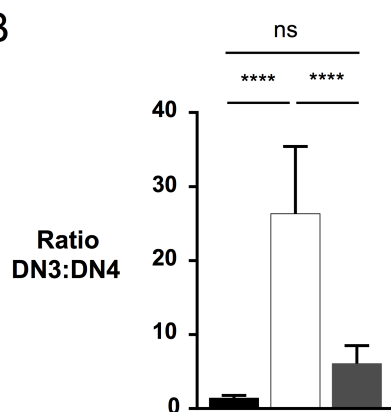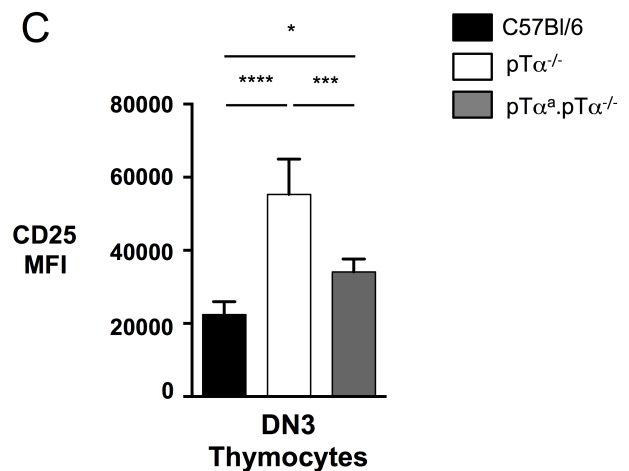
Figure 3.29 pTαᵃ.pTα⁻/⁻ transgenic mice have a partially impaired DN3 to DN4 transition. (A) Representative flow cytometry (n>10) profiles of DN3 and DN4 subsets from the thymus of C57Bl/6, pTα⁻/⁻ and pTαᵃ.pTα⁻/⁻ transgenic mice (B) Bar chart summarising the DN3 to DN4 ratio (n>10) observed in C57Bl/6, pTα⁻/⁻ and pTαᵃ.pTα⁻/⁻ transgenic mice (C) Summary bar of the mean fluorescence intensity (MFI) or CD25 on DN3 thymocytes from each strain of mice. .****p<0.0001; *** p<0.001; ** p<0.01; error bar is SD.

3.16 pTαᵃ signals weakly at the β-selection checkpoint

There is very little work exploring whether pTαᵃ and pTαᵇ convey different signals at the β-selection checkpoint during T cell development. Nonetheless, it has been shown that expression of pTαᵃ *in vitro* led to a marked reduction in

surface expression of TCRβ which was not the case for pTα^b (Barber et al., 1998). This was also demonstrated by Juliet Mahtani-Patching during her Ph.D, where retroviral transduction of pTα-deficient thymocytes with pTα^b-encoding viruses led to higher TCRβ expression than with transduction with pTα^a-encoding

viruses (Figure 3.30).

preTCR surface expression:
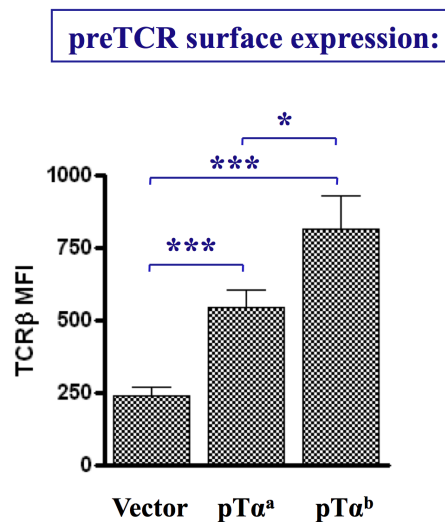
Figure 3.30 preTCR^a is expressed at lower surface levels than preTCR^b. Summary bar graph (n>3) of the mean fluorescence intensity of TCRβ on pT$\alpha^{-/-}$ thymocytes transduced with vector only, pTα^a or pTα^b. *** $p<0.001$; * $p<0.05$; error bar is SD. Juliet Mahtani-Patching's work

The level of TCRβ expression should correlate with the strength of signal delivered to the cell, which would suggest that preTCR^a signals more weakly than preTCR^b. Interestingly, differences in signal strength are widely accepted to result in qualitatively different signals that drive commitment of developing thymocytes to either the $\alpha\beta$ or $\gamma\delta$ lineages (Hayes et al., 2005). Moreover, these differential signals could potentially establish heterogeneity amongst DP

thymocytes. Thus, we sought to investigate the strength of signal received by β-selected thymocytes in our various strains of wild type and transgenic mice.

The strength of signal received by DP progenitors during positive selection is conventionally visualised by the level of cell-surface expression of CD5 on naïve TCR$\alpha\beta^{(+)}$CD4$^{(+)}$ and TCR$\alpha\beta^{(+)}$CD8$^{(+)}$ SP thymocytes (Azzam et al., 1998). Signalling through the preTCR also results in the cell-surface expression of CD5. Indeed, Paul Love and his lab demonstrated that DN4 thymocytes, which have undergone β-selection, showed a modest up-regulation of CD5 expression consistent with the weak signalling capacity of the preTCR. compared to TCR$\gamma\delta$ (Azzam et al., 1998). Thus, using CD5, we first investigated the strength of signal received by β-selected DN3 thymocytes, specifically focusing on FVB/n and pTα^{a}·pT$\alpha^{-/-}$ mice. The lack of a robust commercially available directly-conjugated pTα antibody rendered the task of accurately identifying preTCR-expressing DN3 thymocytes difficult and prompted us to find an alternative strategy. β-selected DN3 have been reported to undergo a c-Myc-dependent burst of proliferation as they traverse the β-selection checkpoint (Laurent et al., 2004). It was later reported by others that the transferrin receptor, CD71, is up-regulated during proliferation in a c-Myc-dependent manner with its level of expression being proportional to the degree of proliferation (Janas et al., 2010). In addition, preTCR-expressing DN3 cells will be expressing TCRβ chains, which should be readily detectable intracellularly (i.c.) despite the low surface expression of the preTCR. Thus, we combined CD71 with i.c.TCRβ in order to distinguish β-selected DN3 cells (Brekelmans et al., 1994; Larrick and Cresswell, 1979). Surface TCRβ^{high} and TCR$\delta^{(+)}$ thymocytes were first gated out as they represent mature $\alpha\beta$ and $\gamma\delta$ T cells

169

respectively, before looking at the DN3 subset defined as $CD25^{(+)}CD44^{(-)}$. Unexpectedly, gating on β-selected DN3 cells from C57Bl/6, $pT\alpha^{-/-}$ and $pT\alpha^a·pT\alpha^{-/-}$ mice using CD71 and i.c.TCRβ did not reveal evidence of the impaired DN3-DN4 transition described previously for $pT\alpha^a·pT\alpha^{-/-}$ mice when compared to wild type controls, as $CD71^{(+)}$i.c.$TCR\beta^{(+)}$ cells were found in similar proportions in $pT\alpha^a·pT\alpha^{-/-}$ transgenic and C57Bl/6 mice (~12%) (Figure 3.31).

We next evaluated CD5 levels on β-selected $CD71^{(+)}$i.c.$TCRb^{(+)}$ DN3 thymocytes from C57Bl/6, $pT\alpha^{-/-}$ and $pT\alpha^a·pT\alpha^{-/-}$ mice. CD5 on β-selected DN3 thymocytes from $pT\alpha^a·pT\alpha^{-/-}$ mice was nearly half (~700 units) to that of the similar subset of C57Bl/6 thymocytes (~1400 units) suggesting that these cells had received a weaker signal through $preTCR^a$ than when both pTα isoforms are available at the β-selection checkpoint. We then applied this analysis to FVB/n DN3 thymocytes to investigate whether the apparent over-expression of $pT\alpha^a$ would correlate with lower CD5 expression compared to C57Bl/6 DN3 thymocytes. We gated on the DN3 subset in a similar manner as described before and compared CD5 expression on DN3 $CD71^{(+)}$i.c.$TCR\beta^{(+)}$ thymocytes between C57Bl/6 and FVB/n mice. We found that (albeit not reaching statistical significance) FVB/n DN3 $CD71^{(+)}$ i.c.$TCR\beta^{(+)}$ thymocytes displayed a lower CD5 expression than similarly gated C57Bl/6 DN3 thymocytes across two independent experiments (Figure 3.32). Thus, CD5 levels on β-selected DN3 thymocytes from FVB/n mice (when compared to those levels in C57Bl/6 mice) are consistent with a weaker signal from the preTCR during β-selection.
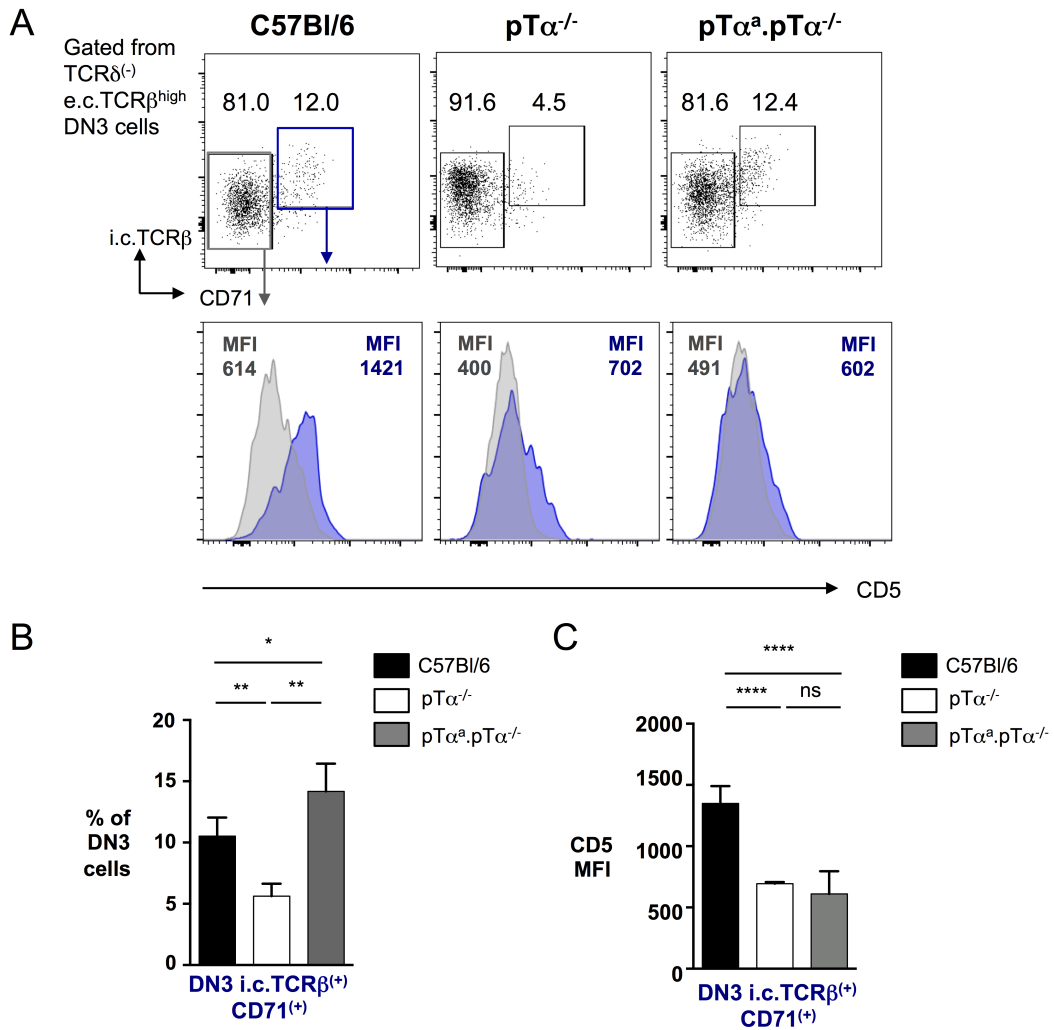
Figure 3.31 Analysis of the β-selection checkpoint with CD71 and i.c.TCRβ. (A) Representative flow cytometry profiles (n=4) of DN3 cells and representative flow cytometry histograms of CD5 on CD71[(+)]i.c.TCRβ[(+)] (in blue) or CD71[(-)]i.c.TCRβ[(-)] (in grey) in the thymus of C57Bl/6, pTα^{-/-} and pTα[a].pTα^{-/-} transgenic mice. (B) is a summary bar chart of the percentage of DN3 cells that are CD71[(+)]i.c.TCRβ[(+)]. (C) shows summary bar charts of the mean fluorescence intensity of CD5 on DN3 CD71[(+)]TCRβ[(+)] cells (n>4). ****p<0.0001; ** p<0.01; * p<0.05 ns, non-significant error bar is SD; MFI, Mean fluorescence intensity; i.c., intracellular; e.c. extracellular.
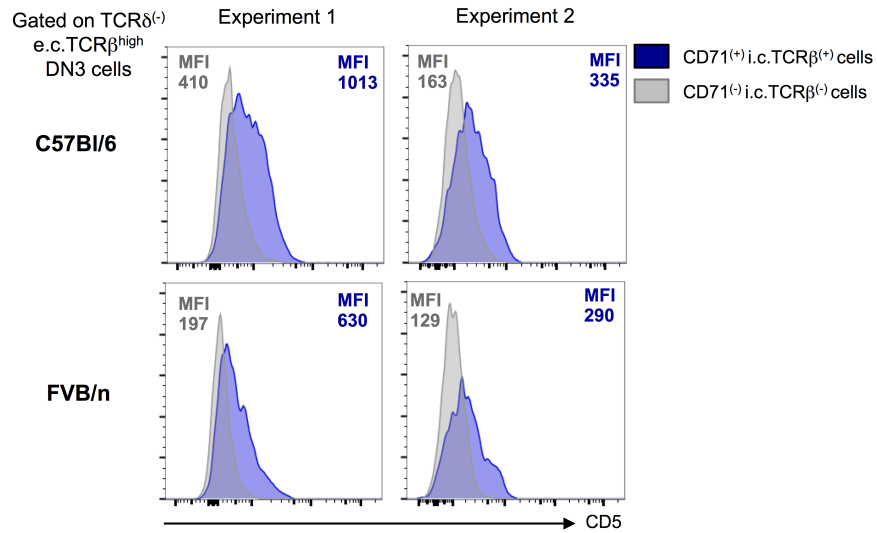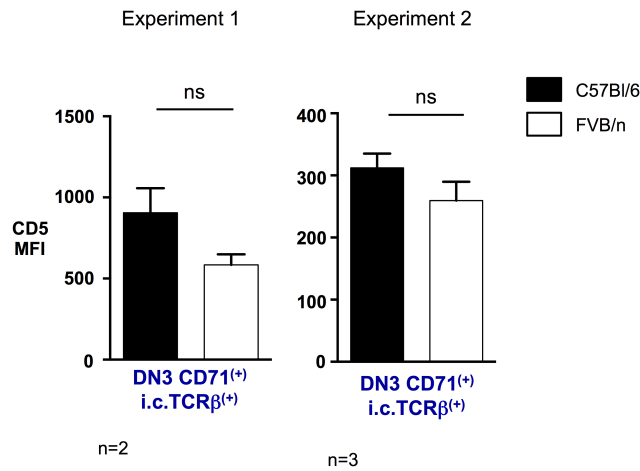
Figure 3.32 DN3 β-selected cells express lower levels of CD5 in FVB/n compared to C57Bl/6 mice. (A) Representative histograms of CD5 cell surface expression in thymic DN3 CD71$^{(+)}$i.c.TCR$\beta^{(+)}$ cells (blue) and CD71$^{(-)}$ cells (grey) in C57Bl/6 and FVB/n animals (B) Bar graph summarising (from n>2) CD5 MFI on DN3 CD71$^{(+)}$i.c.TCR$\beta^{(+)}$ thymocytes. MFI, mean fluorescence intensity; i.c., intracellular; e.c. extracellular; ns, non-significant

3.17 Investigating IEL development in TCR$\alpha\beta$ transgenic OT-II mice

The set of data presented above highlight a correlation between a weak TCR signal at the DN stage of T cell development and a reduced compartment of unconventional TCR$\alpha\beta^{(+)}$CD8$\alpha\alpha^{(+)}$ IELs. This prompted us to explore whether strong signalling at the β-selection checkpoint would correlate with an increased TCR$\alpha\beta^{(+)}$CD8$\alpha\alpha^{(+)}$ IEL compartment. To do this we utilised TCR$\alpha\beta$ transgenic mice that have been shown to express their transgene TCRα chain prematurely in DN thymocytes due to the promoter they use to express the transgene. Because TCRα displays a greater affinity for TCRβ than pTα, it preferentially binds TCRβ when both are co-expressed at the DN stage, resulting in the expression of a TCR$\alpha\beta$ complex instead of preTCR (Trop et al., 2000). Although early TCR$\alpha\beta$ signalling has been associated with an inefficient DN to DP transition, a substantial pool of DP progenitors are generated and mature CD4$^{(+)}$ and CD8$^{(+)}$ T cells are found in the periphery suggesting that early TCR$\alpha\beta$ expression is not completely incompatible with T cell development (Bruno et al., 1996; Huang and Kanagawa, 2004; Lacorazza et al., 2001). Finally, TCR$\alpha\beta$ is thought to deliver a stronger signal than the preTCR primarily due to its much higher surface expression and its ability to bind self-peptide/MHC ligands. Indeed, transgenic TCR$\alpha\beta$ expressed in DN cells can drive $\gamma\delta$ T cell development (Bruno et al., 1996).

We therefore decided to use TCR$\alpha\beta$ transgenic animals to assess whether strong signalling from the transgenic TCR at the DN stage would preferentially favour TCR$\alpha\beta^{(+)}$CD8$\alpha\alpha^{(+)}$ IEL development. Previous experiments undertaken in MHC I or MHC II-restricted TCR$\alpha\beta$ transgenic animals (e.g. AND, H-Y and OT-I) had demonstrated an increased proportion of TCR$\alpha\beta^{(+)}$CD8$\alpha\alpha^{(+)}$ IELs, and it was suggested that TCR$\alpha\beta^{(+)}$CD8$\alpha\alpha^{(+)}$ IELs develop following agonist selection (Leishman et al., 2002). However, delaying the expression of the transgenic TCRα to the DP stage in H-Y mice through a CD4-cre-lox recombineering system, resulted in an unchanged proportion of TCR$\alpha\beta^{(+)}$CD8$\alpha\alpha^{(+)}$ IELs in male H-Y mice (with ligand present), implicating the timing of TCRα expression as critical (Baldwin et al., 2005).

In this study, OT-II mice were used, which express a single type of MHC-II-restricted TCR$\alpha\beta$ complex comprising a Vβ5$^{(+)}$TCRβ chain and a Vα2$^{(+)}$ TCRα chain. This TCR$\alpha\beta$ complex specifically recognises the ovalbumin 323-339 (OVA$_{323-339}$) peptide presented by MHC-II and are often used to study positive selection in the thymus.

We first explored the DN3 to DN4 transition in OT-II mice. CD4$^{(+)}$,CD8$^{(+)}$ and TCR$\delta^{(+)}$ T cells were gated out before visualising the DN3 and DN4 subsets based on expression of CD25 and CD44 (DN3: CD25$^{(+)}$CD44$^{(-)}$; DN4 CD25$^{(-)}$CD44$^{(-)}$). Although various studies have reported an impaired DN to DP transition in TCR$\alpha\beta$ transgenic mice, both OT-II and C57Bl/6 mice showed a DN3 to DN4 ratio of ~1.5 suggesting an efficient DN3 to DN4 transition (Figure 3.33).
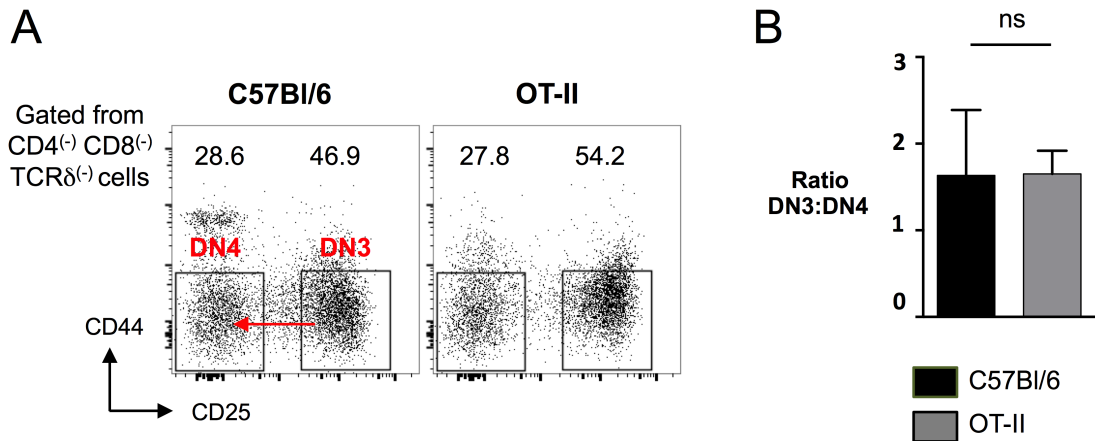
Figure 3.33 The DN3 to DN4 transition appears efficient in OT-II mice. (A) Representative flow cytometry profiles (n=4) of thymic DN3 and DN4 subsets from C57Bl/6 and OT-II mice. The DN3 to DN4 transition is shown by the red arrow (B) Summary bar chart of the ratio of DN3 to DN4 thymocytes in thymuses from C57Bl/6 and OT-II mice. ns; non-significant

To check that signalling through the TCR$\alpha\beta$ transgene was strong in DN thymocytes, CD5 levels were analysed on DN3 cells that expressed the transgenic TCR$\alpha\beta$ (compared with DN3 cells that did not express the transgenic TCR$\alpha\beta$ and $\gamma\delta$ T cells). This analysis revealed that about 30% of T cells expressed the transgenic TCR$\alpha\beta$ identified through the use of the Vα_2-specific antibody marker (Figure 3.34). Interestingly, we observed that V$\alpha2^{(-)}$ cells were mainly restricted to the DN3 subset (CD25$^{(+)}$CD44$^{(-)}$) while V$\alpha2^{(+)}$ cells were found within the DN4 subset suggesting a rapid progression through the β-selection checkpoint once the transgene TCR$\alpha\beta$ was expressed. Upon CD5 analysis, the transgenic TCR$\alpha\beta$ appeared to signal at a similar level to TCR$\gamma\delta$ with a CD5 MFI of ~1600 and ~1900 MFI units, respectively. This seemed to indicate that expression of a TCR$\alpha\beta$ transgenic complex in DN cells did indeed transduce a strong TCR signal.
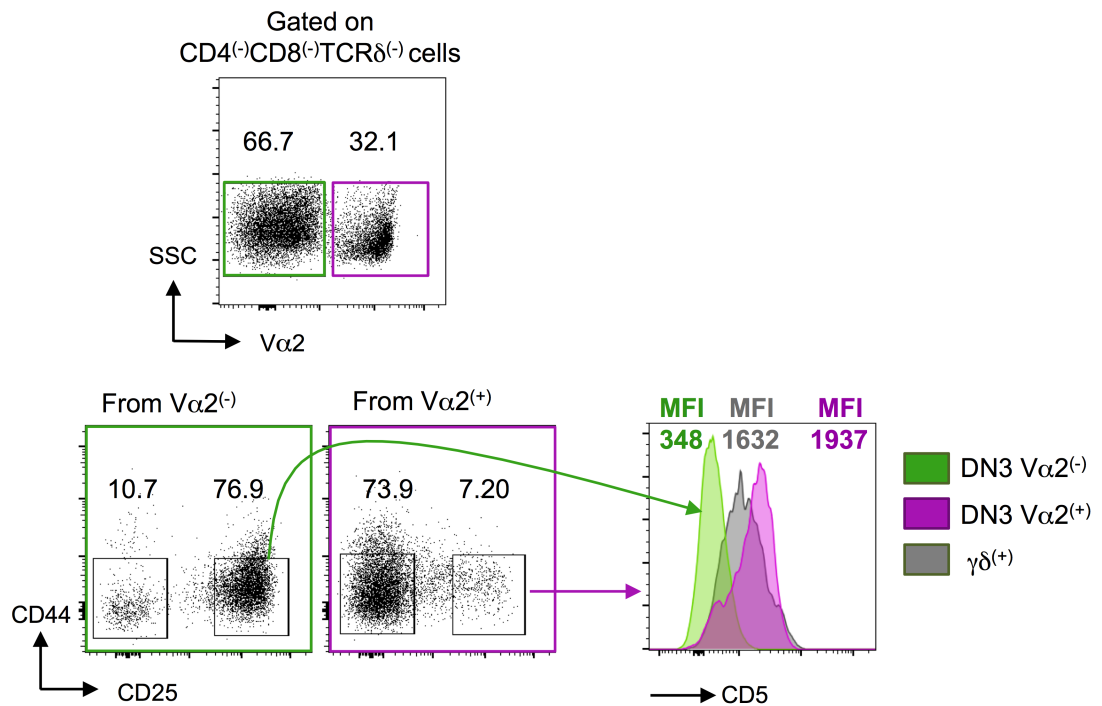
Figure 3.34 OT-II thymocytes expressing the transgenic TCRαβ signal strongly at the DN stage of T cell development. Representative flow cytometry profiles (from n=4) of OT-II thymocytes showing DN3 (CD25$^{(+)}$CD44$^{(-)}$) and DN4 (CD25$^{(-)}$CD44$^{(-)}$) thymocyte subsets from Vα2$^{(+)}$ and Vα2$^{(-)}$ populations. Cell surface expression of CD5 is then showed on a histogram to investigate signal strength. This shows that transgenic TCRαβ signals strongly compared to cells negative for the transgene. MFI; mean fluorescence intensity

3.18 OT-II mice have an increased proportion of TCRαβ$^{(+)}$ CD8αα$^{(+)}$ IELs

The data presented above suggest that DN cells from OT-II mice that express the transgenic TCRαβ receive a strong signal presumably due to the early expression of the TCRα chain. We therefore sought to investigate the

proportions of TCR$\alpha\beta^{(+)}$CD8$\alpha\alpha^{(+)}$ IELs in the small intestine of OT-II compared to C57Bl/6 mice. OT-II mice showed a 2.5-fold increase in TCR$\alpha\beta^{(+)}$CD8$\alpha\alpha^{(+)}$ IELs (~30% of CD4$^{(-)}$ IELs) compared to C57Bl/6 mice (~12%). This was very obviously evident when the ratio of conventional TCR$\alpha\beta^{(+)}$CD8$\alpha\beta^{(+)}$ to unconventional TCR$\alpha\beta^{(+)}$CD8$\alpha\alpha^{(+)}$ was assessed. For OT-II mice, this was ~0.4 whereas it was ~1.5 for control animals (Figure 3.35).
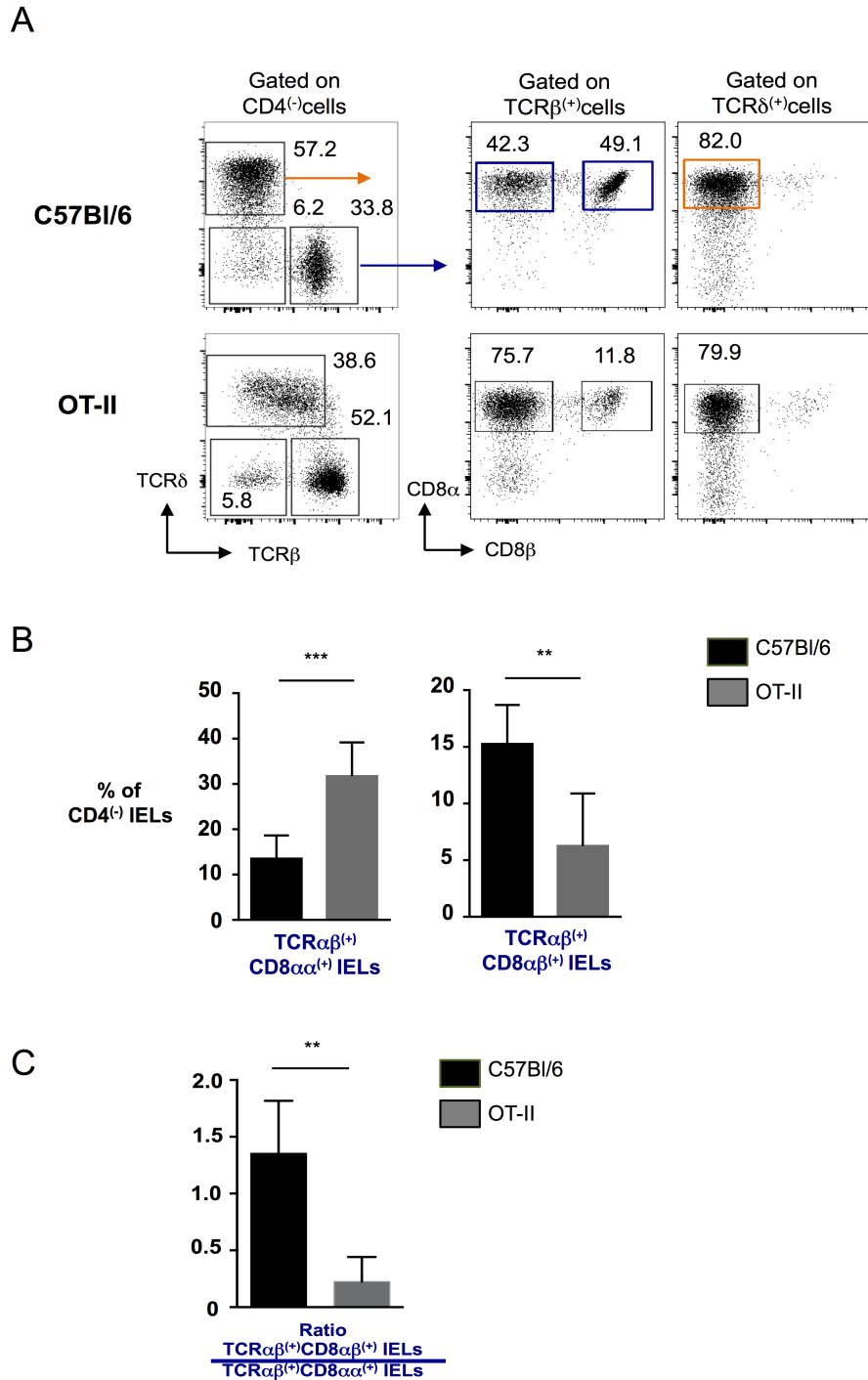
Figure 3.35 OT-II mice have an increased proportion of TCRαβ$^{(+)}$CD8αα$^{(+)}$ IELs. (A) Representative flow cytometry plots (n=4) looking at IEL populations in the small intestine of C57Bl/6 and OT-II mice. Percentages of cells are indicated near each gate. (B) Summary bar graph (n=4) of TCRαβ$^{(+)}$CD8αα$^{(+)}$ and TCRαβ$^{(+)}$CD8αβ$^{(+)}$ IELs in C57Bl/6 (black) and OT-II mice (grey). (C) Summary bar graph (n=4) of the ratio of conventional TCRαβ$^{(+)}$CD8αβ$^{(+)}$ to unconventional TCRαβ$^{(+)}$CD8αα$^{(+)}$ IELs. Error bars are SD. *** p < 0.001, **p < 0.01.

3.19 Early TCRα expression in pT$\alpha^{-/-}$.TCR$\delta^{-/-}$ mice

Although we used OT-II mice to investigate the role of increased TCR signal strength at the DN stage of T cell development on TCR$\alpha\beta^{(+)}$CD8$\alpha\alpha^{(+)}$ IEL development, the TCR$\alpha\beta$ transgene is obviously restricted to a single Vβ_5/Vα_2 combination. Thus, we sought to expand this analysis to a system where different TCRα chains could be expressed early at the DN stage during T cell development. The lab has had a colony of pTα-deficient by TCRδ-deficient (pT$\alpha^{-/-}$.TCR$\delta^{-/-}$) animals that were first generated to be used as a background strains for the pTα^a transgenic mice described previously. However, upon analysis of the thymus of these mice, we could unexpectedly detect (considering these mice cannot generate either preTCR or TCR$\gamma\delta$) a considerable proportion of DP thymocytes (~14% of total cells), compared to pTα-deficient (~12%) and C57Bl/6 mice (~83%) (Figure 3.36).

As pT$\alpha^{-/-}$.TCR$\delta^{-/-}$ mice cannot express the preTCR or the TCR$\gamma\delta$ the only possible TCR chain that could pair with TCRβ at the β-selection checkpoint would be a TCRα chain, presumably expressed prematurely at the DN stage. Because TCRα and TCRδ share the same locus, this prompted us to examine how the TCRδ-deficient animals were generated by Tonegawa's lab in 1993 (Itohara et al., 1993). In order to "knockout" the TCRδ chain, the constant region of TCRδ was disrupted through homologous recombination with a pPMKO vector containing a phosphoglycerate kinase I promoter (PGK) and a Neomycin cassette (Neo). The latter is required during the positive selection of embryonic

stem cells (ES) that have successfully integrated the vector and therefore disrupted the TCRδ constant region.
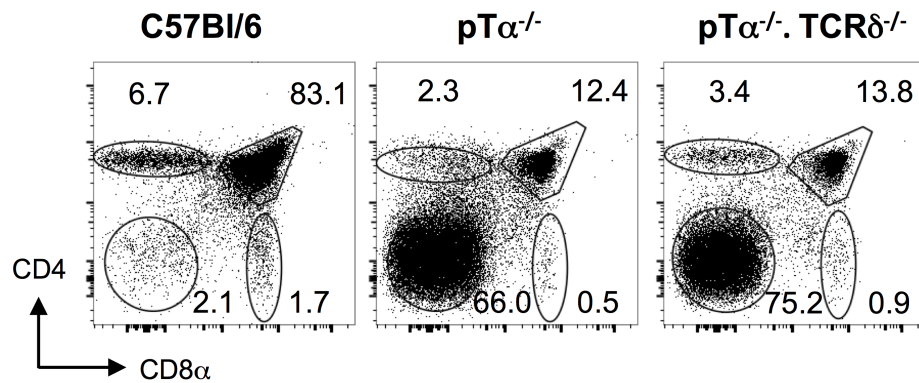
Figure 3.36 FACS profile of C57Bl/6, pTα$^{-/-}$ and pTα$^{-/-}$.TCRδ$^{-/-}$ thymuses. Representative flow cytometry plots (n=4) of DN, DP, and SP cells from C57Bl/6, pTα$^{-/-}$ and pTα$^{-/-}$.TCRδ$^{-/-}$ mice. Despite the absence of both the preTCR and the TCRγδ to drive progression through the DN to DP stages, pTα$^{-/-}$.TCRδ$^{-/-}$ mice have a significant proportion of DP thymocytes. Percentages of cells are indicated near each gate. DN, CD4$^{(-)}$CD8$^{(-)}$; DP, CD4$^{(+)}$CD8$^{(+)}$; SP, CD4$^{(+)}$ or CD8$^{(+)}$

It was subsequently reported that the presence of a PGK-Neo cassette can alter the regulation of adjacent genes through mechanisms that are presumably related to the PGK promoter binding numerous transcription factors (it is generally considered to be a strong promoter) (Pham et al., 1996). Thus, TCRα expression may be dis-regulated in TCRδ$^{-/-}$ animals, due to the presence of the PGK promoter, resulting in early TCRα expression (Figure 3.37).
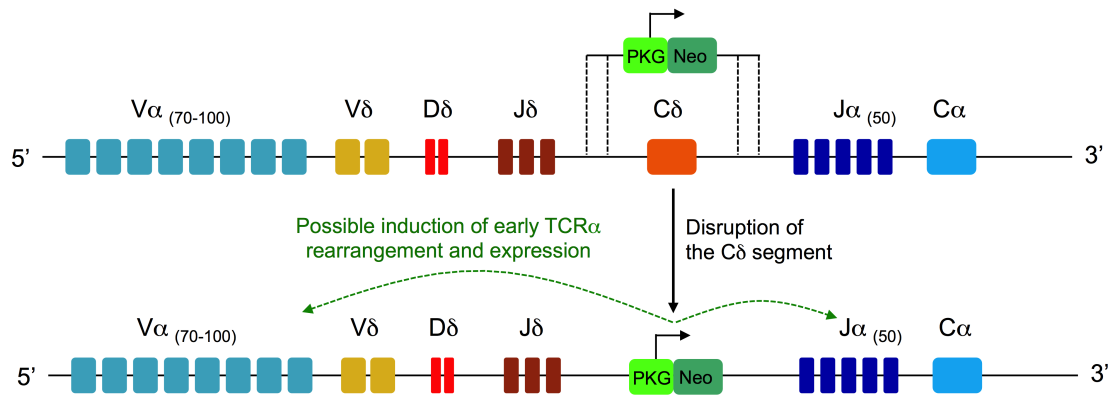
Figure 3.37 Schematic overview of the mutated TCRδ locus The TCRδ locus is embedded within the TCRα locus. The constant region of the TCRδ locus was targeted with a pPMKO vector sharing some homology to the regions on each side of the constant region and containing a PGK-Neo cassette. As recombination took place, the TCRδ constant region was replaced by the PGK-Neo cassette. The latter has been reported to influence expression of neighbouring genes and might be the reason why pTα$^{-/-}$.TCRδ$^{-/-}$ mice generate DP thymocytes, despite the lack of both TCRγδ and pre TCR complexes.

To test this idea, the presence of TCRαβ complexes in post-selected DN4 thymocytes in pTα$^{-/-}$.TCRδ$^{-/-}$ mice was assessed. Unfortunately, a pan-anti-TCRα antibody is not commercially available. Thus, we limited our analysis to three anti-Vα antibodies targeting the Vα2, Vα8 and Vα11. Flow cytometry analysis of surface TCRβ and TCRVα2/8/11 on thymic DN4 cells (CD25$^{(-)}$CD44$^{(-)}$) from C57Bl/6, pTα$^{-/-}$ and pTα$^{-/-}$.TCRδ$^{-/-}$ mice showed that in C57Bl/6 mice (~1.1%) and pTα$^{-/-}$ mice (0.3%) only very few cells expressed the TCRα chains in question. However, 10.7% DN4 cells from pTα$^{-/-}$.TCRδ$^{-/-}$ mice expressed the Vα2/8/11chains. Futhermore, a clear TCRβ$^{(+)}$ population can be seen in the DN4 subset of pTα$^{-/-}$.TCRδ$^{-/-}$ mice probably corresponding to TCRαβ complexes that are using Vα segments not detected by our analysis (Figure 3.38)
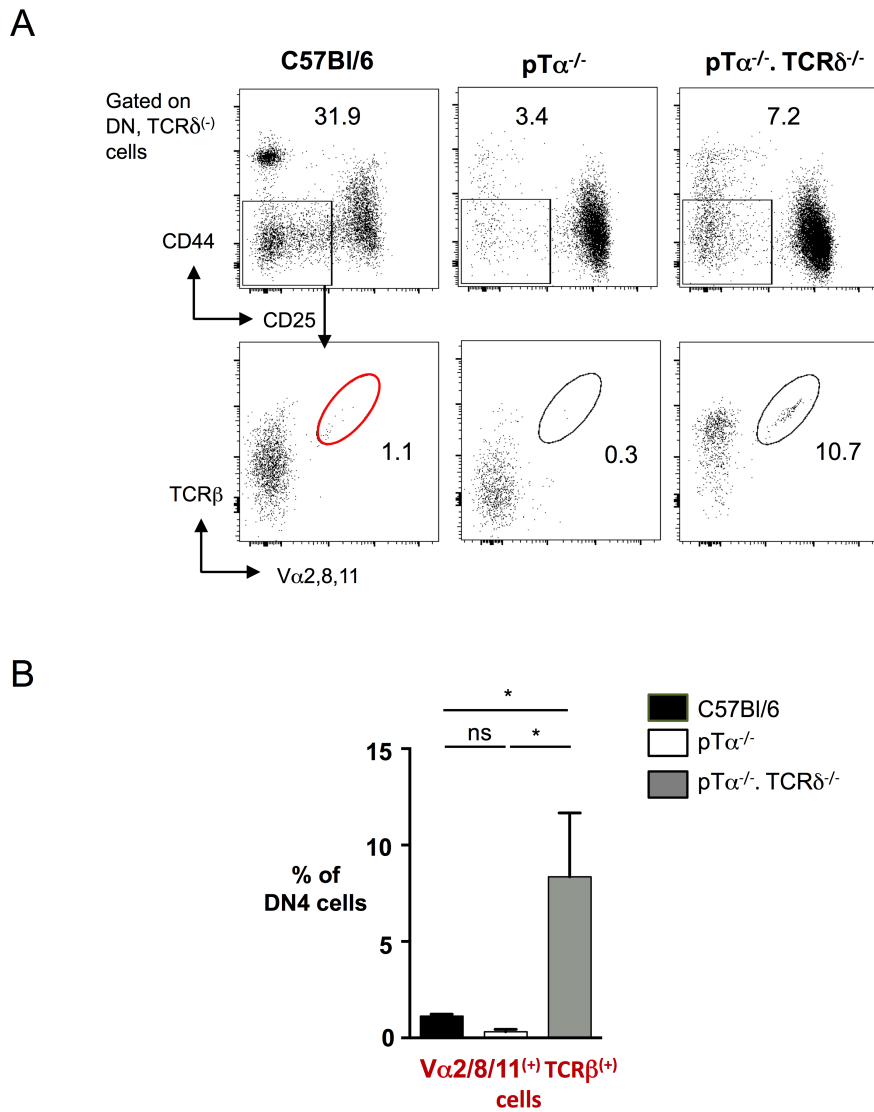
Figure 3.38 TCRα is expressed early in pTα⁻ᐟ⁻.TCRδ⁻ᐟ⁻ mice Representative flow cytometry plots (n=4) of DN3 and DN4 subsets from C57Bl/6, pTα⁻ᐟ⁻ and pTα⁻ᐟ⁻ .TCRδ⁻ᐟ⁻ mice. pTα⁻ᐟ⁻.TCRδ⁻ᐟ⁻ mice have an increased proportion of TCRβ$^{(+)}$Vα2/8/11$^{(+)}$ cells at the DN4 stage of T cell development. DN, CD4$^{(-)}$CD8$^{(-)}$. Ns is for not significant; * p<0.05

3.20 pT$\alpha^{-/-}$.TCR$\delta^{-/-}$ mice have an increased proportion of TCR$\alpha\beta^{(+)}$CD8$\alpha\alpha^{(+)}$ IELs

As pT$\alpha^{-/-}$.TCR$\delta^{-/-}$ mice have expression of a heterogeneous set of TCR$\alpha\beta$ complexes at the DN stage of T cell development, this strain was used as an alternative to OT-II mice to assess the effect of strong TCR signalling at the DN to DP transition, specifically with regard to the development of TCR$\alpha\beta^{(+)}$CD8$\alpha\alpha^{(+)}$ IELs. Interestingly and supporting our view that strong signalling at the β-selection checkpoint favours the subsequent development of unconventional IELs, pT$\alpha^{-/-}$.TCR$\delta^{-/-}$ mice (like OT-II mice), had almost a 3-fold increase in the proportion of TCR$\alpha\beta^{(+)}$CD8$\alpha\alpha^{(+)}$ IELs when compared to C57Bl/6 mice (~30% versus ~10% respectively of all CD4$^{(-)}$ IELs) (Figure 3.39). Moreover, the ratio of conventional IELs to unconventional IELs also differed, being ~1.2 in C57Bl/6 mice but lowering to ~0.4 in pT$\alpha^{-/-}$.TCR$\delta^{-/-}$ mice. Thus, unconventional IEL development again appears favoured by strong TCR signalling at the β-selection checkpoint.

3.21 Conclusion

Here, we showed that pTα^{a}-only transgenic mice and WT-FVB/n mice have a compromised unconventional TCR$\alpha\beta^{(+)}$CD8$\alpha\alpha^{(+)}$ IEL compartment compared to C57Bl/6 mice. This is associated with a reduced pool of thymic IEL progenitors and a partially inefficient thymic DN3 to DN4 transition.
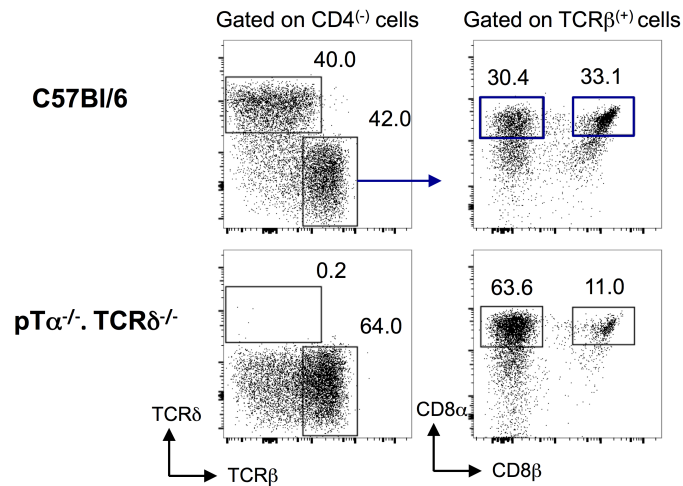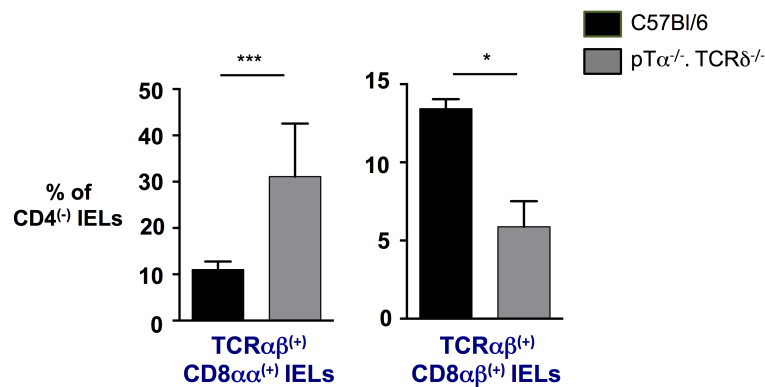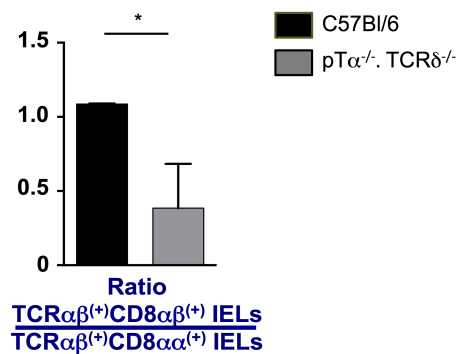
Figure 3.39 pTα$^{-/-}$.TCRδ$^{-/-}$ mice have a greater proportion of TCRαβ$^{(+)}$CD8αα$^{(+)}$ IELs than C57Bl/6 mice. (A) Representative flow cytometry plots (n=4) looking at the IEL population in the small intestine of C57Bl/6 and pTα$^{-/-}$.TCRδ$^{-/-}$ mice. Percentage of cells are indicated near each gate. (B) Summary bar graph (n=4) of TCRαβ$^{(+)}$CD8αα$^{(+)}$ and TCRαβ$^{(+)}$CD8αβ$^{(+)}$IELs as a proportion of CD4$^{(-)}$IELs (C) Ratio of TCRαβ$^{(+)}$CD8αβ$^{(+)}$ to TCRαβ$^{(+)}$CD8αα$^{(+)}$ IELs in C57Bl/6 and pTα$^{-/-}$.TCRδ$^{-/-}$ mice. Error bar is SD. *** p < 0.001, * p < 0.05

Whereas pTα^a-only transgenic mice lack pTα^b, we show that FVB/n DN3 thymocytes over-express pTα^a compared to pTα^b. Importantly, evidence suggests that pTα^a signals weakly at the DN stage through the analysis of CD5 levels. Finally, strong signalling (as depicted by CD5 levels) at the DN stage of T cell development (through prematurely expressed TCR$\alpha\beta$ complexes) appears to favour unconventional TCR$\alpha\beta^{(+)}$CD8$\alpha\alpha^{(+)}$ IELs development. Taken together, these data argue that the strength of signal received through TCR complexes at the β-selection checkpoint correlate strongly with the subsequent development of unconventional IELs.

Chapter 4

T cell development in $pT\alpha^b$-only transgenic mice

4.1 Introduction

FVB/n and $pT\alpha^a$-only transgenic mice, in which $pT\alpha^a$ signalling is dominant or exclusive respectively, show a reduced proportion of $TCR\alpha\beta^{(+)}CD8\alpha\alpha^{(+)}$ IELs. This was associated with an inefficient thymic DN3 to DN4 transition and lower CD5 cell-surface expression. This is in line with previously published data suggesting that $pT\alpha^a$ signals weakly compared to the other truncated $pT\alpha$ isoform ($pT\alpha^b$). Indeed, expression *in vitro* of $pT\alpha^b$ results in higher $TCR\beta$ expression than $pT\alpha^a$, which appears to result in stronger preTCR signalling (Barber et al., 1998). Importantly, despite its truncated form, $pT\alpha^b$ was shown capable of directing DN progenitors through the β-selection checkpoint *in vivo* confirming its ability to signal (Barber et al., 1998; Gibbons et al., 2001; Irving et al., 1998; Mahtani-Patching et al., 2011). Thus, we decided to investigate whether $preTCR^b$ signalling at the DN stage would rescue, and even favour the development of $TCR\alpha\beta^{(+)}CD8\alpha\alpha^{(+)}$ IELs. To test this idea, we generated BAC $pT\alpha^b$-only transgenic animals that were crossed onto a $pT\alpha^{-/-}$ background such that they express only $pT\alpha^b$ at the β-selection checkpoint, and assessed $TCR\alpha\beta^{(+)}CD8\alpha\alpha^{(+)}$ IEL development.

4.2 Overview of the generation of pTα^b–only transgenic mice

A similar procedure as described in the previous chapter was undertaken by Dr.J.Mahtani-Patching to generate the construct that was used to produce BAC pTα^b–only transgenic mice. The BAC (purchased from Ensembl Organisation) was manipulated so that exon 1 and exon 3 were fused, and exon 2 removed to prevent alternative splicing, and to enforce expression of only the pTα^b isoform only (Figure 4.1). The recombineering steps were similar to those described previously; a GALK sequence was incorporated by homologous recombination between exons 1 and 2 allowing positive selection of the successful recombinants by selection on galactose. The second cloning steps differed slightly from before as it involved simultaneous replacement of both the GALK cassette and intron 2, resulting in the fusion of exons 1 and 3 (Figure 4.1).

Two primers of 100bp sharing a homology to 85bp of the 3' end of exon 1 and of the 5' end of exon 3 were designed and annealed to create a double stranded DNA. The latter was electroporated into GALK$^{(+)}$BAC$^{(+)}$SW102 bacteria resulting in the fusion of exons 1 and 3 following homologous recombination. GALK$^{(-)}$ pTα^b-only BAC transformants were identified by growing bacteria on a deoxy-galactose containing plate.
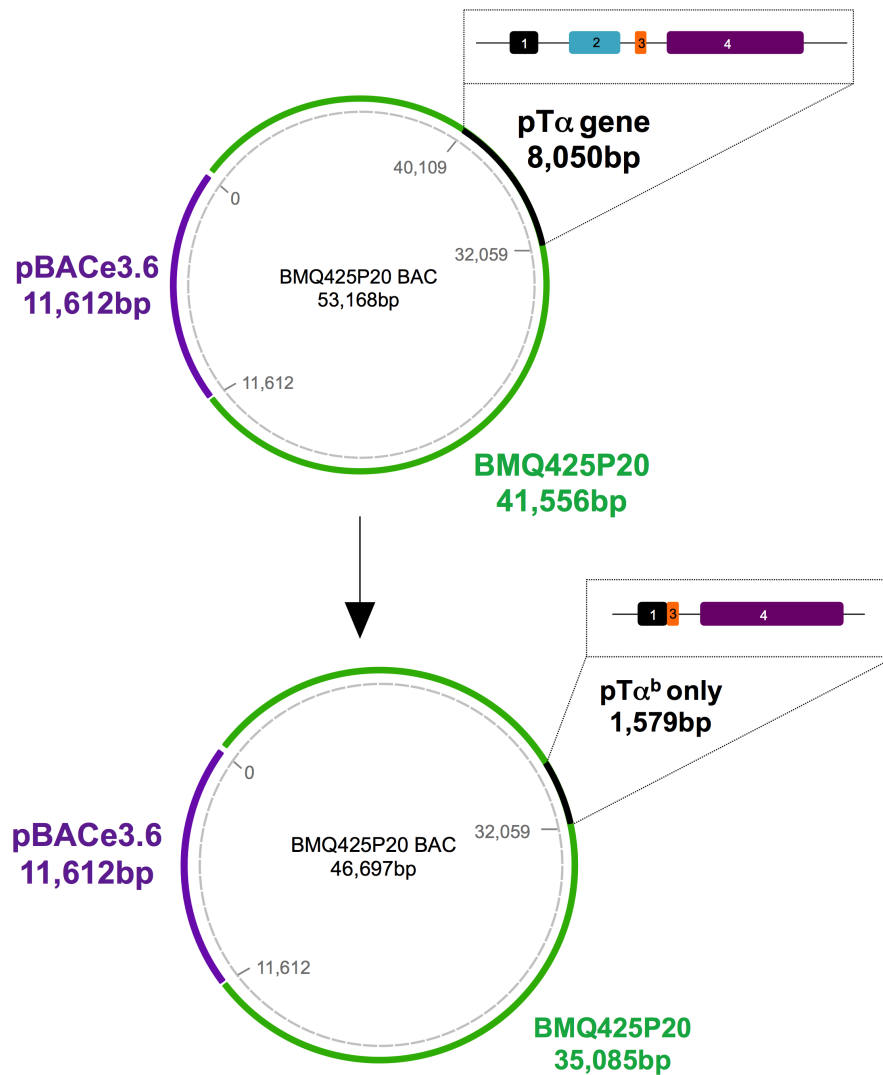
Figure 4.1 Schematic overview of the pTα^b-only BAC. A BAC containing the pTα gene (top panel) was purchased from the Ensembl organisation. Several recombineering steps were performed to fuse exons 1 and 3 to prevent alternative splicing. Thus, the pTα gene can only generate the pTα^b isoform.
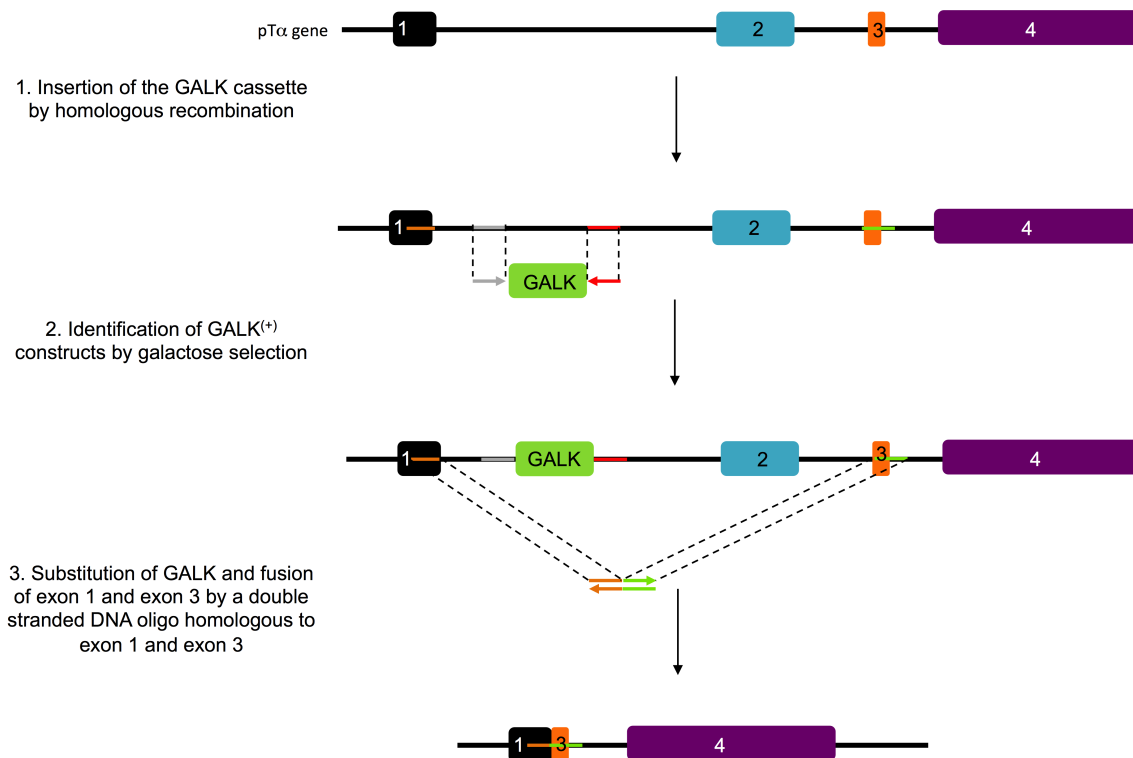
Figure 4.2 Schematic overview of the recombineering steps undertaken to fuse exons 1 and 3 to generate the pTαb-only BAC transgene. A GALK cassette was amplified by PCR using primers sharing some homology with the GALK sequence and some with intron 1. Insertion of the GALK cassette within intron 1 was catalysed by the bacteriophage λ Red system. Successful transformants were identified by growing bacteria on a galactose-containing plate. Removal of GALK and fusion of exon 1 and 3 happened simultaneously in a subsequent stage. Oligos homologous to exon 1 and 3 were annealed to one another and used to cut out intron1, exon 2 and intron 2 through homologous recombination. Thus the remaining pTα gene is unable to undergo alternative splicing following transcription and can only generate the pTαb isoform.

4.3 Successful juxtaposition of exon 1 and 3 was validated by PCR and sequencing.

Before passing the pTαb-only transgene to the transgenic facility for pro-nuclear injection, the GALK(-) pTαb-only BAC was tested for successful fusion of exons 1 and 3. This was first verified by PCR. We used the forward primer pTa15s

189

homologous to 24bp found 194bp upstream of exon 1 and the reverse primer

pTa20s homologous to 24bp located 394bp downstream of exon 3. PCR

products were run on an agarose gel. We obtained a 810bp band suggesting

that exon 1 and 3 had been correctly fused (Figure 4.3A).

This band was extracted from the gel, purified and then sent for sequencing

using the same primers (pTa15s and pTa20s) (Figure 4.3B). The sequencing

was successful and the result was aligned to a $pT\alpha^b$ sequence in which exons 1

and 3 are fused (Figure 4.4). Upon analysis, we found a point mutation where a

thymine nucleotide had been replaced by a cytosine residue. However, once
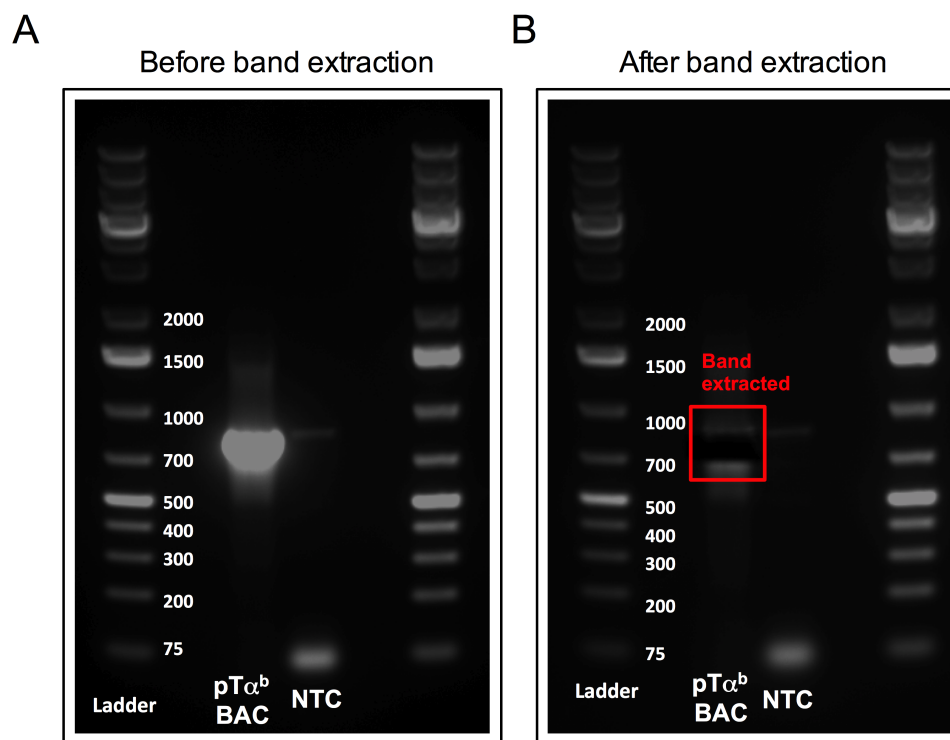
Figure 4.3 Exons 1 and 3 were successfully fused in the $pT\alpha^b$ only BAC. (A)
The PCR amplified a 810bp sequence spanning the exon 1 and 3 boundary. The
PCR result was visualised on a 1.5% agarose gel (B) The 810bp band was
extracted (red box) so that the DNA sequence could be validated by sequencing.
NTC, no template control

the sequence was translated into amino acids, the resulting protein matched 100% with the pTα^b protein sequence from PubMed. This is due to a redundant genetic code where the GCC or GCT codons both encode the amino acid alanine (A). To continue the analysis of the pTα^b-only BAC, it was subsequently digested by the restriction endonuclease SpeI, which cuts DNA following recognition of a ACTAGT sequence. This was to make sure there had been no major changes in the structure of the BAC and to prepare the fragment containing pTα^b for injection. Digestion of the BAC was expected to result in six products with a 26.8kb band corresponding to the fragment containing pTα^b-only transgene (Figure 4.5A&B). Figure 4.5B and 4.5C demonstrate that the expected bands were observed at roughly the correct intensitites (for their size). The fragment containing pTα^b (The 26.8Kb band) was then carefully extracted and purified. A small sample was then run on a 0.5% gel to confirm the integrity of the DNA molecule, before passing it onto the transgenic facility of Liverpool University for pro-nuclear injection (Figure 4.5C).

A

```
                                                                    Start
pTα^b        CAGGTAGCTCCTGGCTGCAACTGGGTC[ATG]CTTCTCCACGAGTGGGCCATGGCTAGGACA
Sequencing   CAGGTAGCTCCTGGCTGCAACTGGGTCATGCTTCTCCACGAGTGGGCCATGGCTAGGACA
             ************************************************************
             -------------------------Exon 1---------------------------

pTα^b        TGGCTGCTGCTGCTTCTGGGCGTCAGGTGTCAGGC(TC)TACCATCAGGGGAATCTTCGACA
Sequencing   TGGCTGCTGCTGCTTCTGGGCGTCAGGTGTCAGGC(C)TACCATCAGGGGAATCTTCGACA
             ***********************************  ************************
             ------------Exon 1------------------------------------------

pTα^b        GCCAGGAGCTGCTTTCCGGAGCCTCTCGGGGGTAAGTCACCAGTGGGTGAGGGAGGGACG
Sequencing   GCCAGGAGCTGCTTTCCGGAGCCTCTCGGGGGTAAGTCACCAGTGGGTGAGGGAGGGACG
             ************************************************************
             ----------Exon 3--------------

pTα^b        GTGGCTGGGAACAAGAATCTCAGCACTGGTACCCGGCAGGTAGCATTCAGCTCTAATTCA
Sequencing   GTGGCTGGGAACAAGAATCTCAGCACTGGTACCCGGCAGGTAGCATTCAGCTCTAATTCA
             ************************************************************
```

B

```
Protein encoding exon 1&3     MARTWLLLLLGVRCQ(A)LPSGESSTARSCFPEPLG
Sequencing result             MARTWLLLLLGVRCQ(A)LPSGESSTARSCFPEPLG
                              ***********************************
```

Figure 4.4 Although the pTα^b-only BAC carries a point mutation, this does not affect the sequence of the pTα^b protein. (A) The sequencing result (bottom line) was aligned to the pTα^b cDNA sequence (top line) obtained from PubMed. The point mutation where a thymine residue has been mutated to a cytosine base is shown by the red circle. The start codon (ATG) is indicated in green (B) The protein encoding exon 1 and 3 was aligned to the reference sequence from PubMed. The mutation previously identified is indicated by the red circle. Due to the redundancy in the genetic code both GCC or GCT codons encode for an alanine residue.
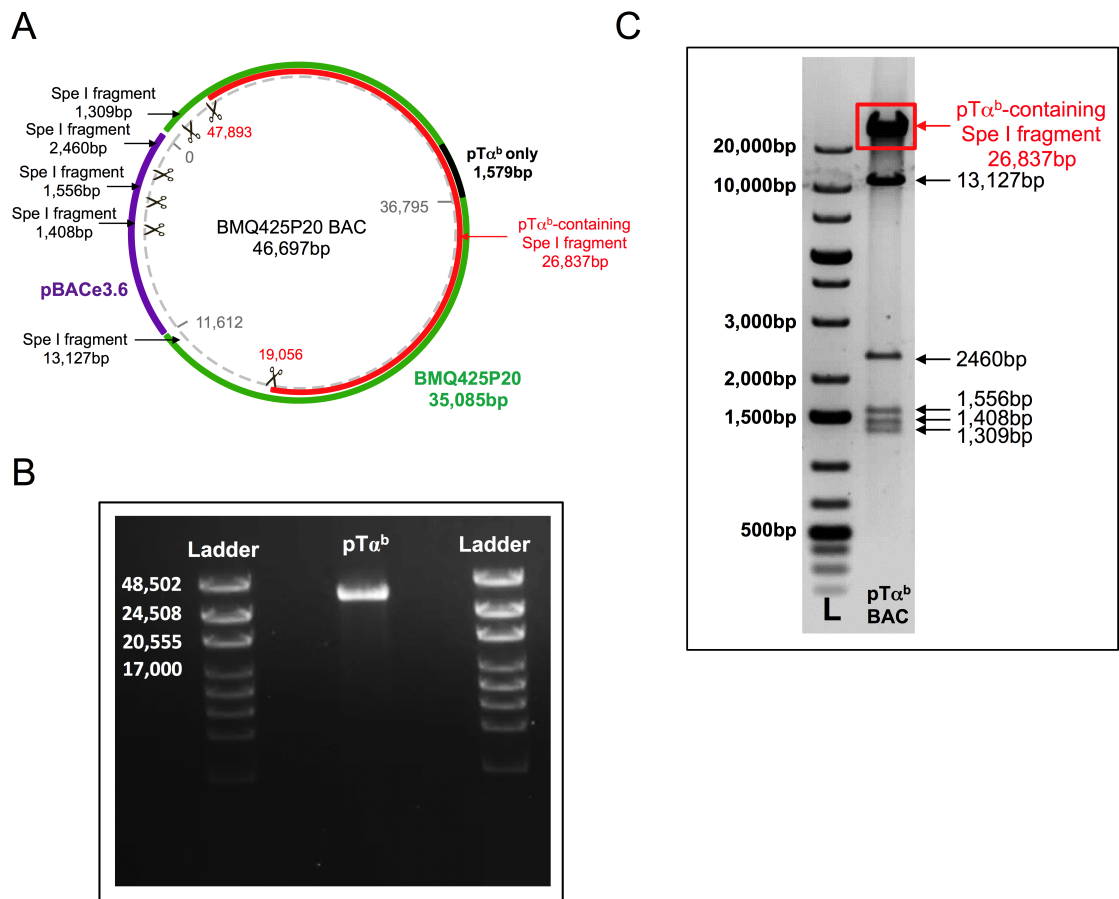
Figure 4.5 Preparation of the pTα^b-only transgene for pro-nuclear injection (A) Schematic representation of the pTα^b-only BAC and the six cutting sites of the SpeI enzyme (B) The digested pTα^b-only BAC was run on a 0.5% gel to allow the separation of the six bands and identification of the 26.8Kb band containing the pTα^b-only gene (C) Following extraction of the band, 2μl of the sample was run onto a 0.5% gel to assess the quality of the DNA before being passed onto the transgenic facility at Liverpool University for pro-nuclear injection. L; Ladder

4.4 pTα^b-only transgenic founders were identified by PCR

At weaning age, 16 pups born after pro-nuclear injection of C57Bl/6 fertilized oocytes were transferred to the Barts and the London School of Medicine animal facility and were ear-snipped for genotyping. DNA was extracted and two independent PCRs were carried out. The first PCR tested the integrity of the DNA following extraction and consisted of the pTa1s and pTa2 primers amplifying a 466bp sequence located 9.5Kb upstream of the pTα gene (Figure 4.6A). The second PCR amplified a 492bp sequence specific to the pTα^b-only construct. For this, the forward primer (F1-3) was homologous to 24bp spanning the exon 1 and 3 boundary while the reverse primer, pTa20s, recognised 394bp downstream of exon 3 (Figure 4.6B).
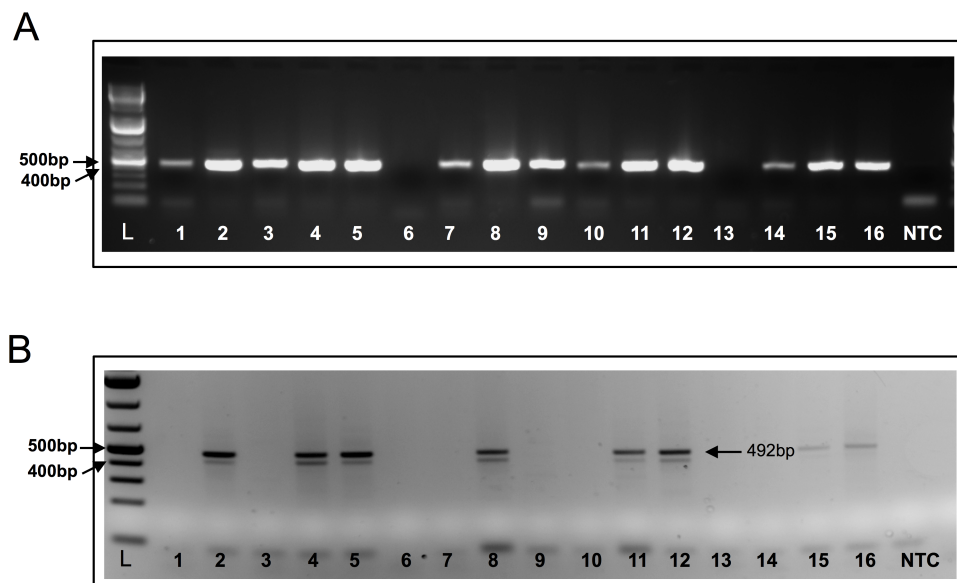
Figure 4.6 PCR to identify possible founders for the pTα^b-only transgene. (A) PCR amplifying a 466bp sequence located upstream of the pTα gene to assess the quality of the DNA. (B) A second PCR on the same samples using primers amplifying a 492bp sequence specific to the pTα^b transgene. Eight pups were identified as carrying the pTα^b transgene. L, Ladder; NTC, no template control

We found that out of 16 pups, eight were positive for the transgene. Two of these animals were subsequently bred onto a $pT\alpha^{-/-}$ background to prevent expression of the endogenous $pT\alpha$ isoforms.

4.5 Preliminary investigation of the small intestine of the first generation of $pT\alpha^{b}$-only transgenic mice

Founders positive for the BAC $pT\alpha^{b}$-only transgene also carry two copies of the intact wild-type endogenous $pT\alpha$-gene (WT-$pT\alpha$). Thus, in order to generate a colony of mice expressing $pT\alpha^{b}$-only at the β-selection checkpoint, founders were bred with $pT\alpha$-deficient mice. Animals obtained from the first generation were all carrying one endogenous $pT\alpha$-deficient allele, one WT-$pT\alpha$ allele and about 50% of them also carried the $pT\alpha^{b}$-only transgene resulting in two possible genotypes: $pT\alpha^{-/+}$ or $pT\alpha^{-/+}.pT\alpha^{b}Tg$. Importantly, at this stage, transgenic animals carry the $pT\alpha^{b}$-only transgene in addition to the WT-$pT\alpha$ allele, which can generate both $pT\alpha^{a}$ and $pT\alpha^{b}$ following alternative splicing. Thus, we considered these animals to be essentially over-expressing $pT\alpha^{b}$, as they express one more copy of $pT\alpha^{b}$ rather than $pT\alpha^{a}$ when compared to non-transgenic littermates.

We showed in chapter 3 that FVB/n mice, which appear to over-express the weakly signalling $pT\alpha^{a}$ isoform at the DN stage of T cell development, have a reduced $TCR\alpha\beta^{(+)}CD8\alpha\alpha^{(+)}$ IEL compartment. Indeed, the ratio of conventional $TCR\alpha\beta^{(+)}CD8\alpha\beta^{(+)}$ to unconventional $TCR\alpha\beta^{(+)}CD8\alpha\alpha^{(+)}$ IELs is ~5 in these

mice as opposed to ~1.3 in C57Bl/6 mice. This led us to hypothesise that perhaps over-expression of the $pT\alpha^b$ isoform in $pT\alpha^{-/+}.pT\alpha^bTg$ mice might favour generation of unconventional $TCR\alpha\beta^{(+)}CD8\alpha\alpha^{(+)}$ IELs. Unfortunately, there was limited time to analyse these mice before the end of my PhD. Nonetheless, preliminary flow cytometry analysis of the IEL compartment revealed no significant differences between the over-expressing $pT\alpha^b$-only mice ($pT\alpha^b.pT\alpha^{-/+}$) and the littermate controls ($pT\alpha^{-/+}$) negative for the $pT\alpha^b$-transgene (Figure 4.7). Despite the lack of statistical significance, both conventional and unconventional $TCR\alpha\beta^{(+)}$ IELs appeared slightly reduced on average in $pT\alpha^b.pT\alpha^{-/+}$ mice (~10% and ~13% respectively as of all $CD4^{(-)}$ IELs) compared to littermate controls (~12.5% and ~15.5% as of all $CD4^{(-)}$ IELs respectively). However this resulted in a similar ratio (~1.3) of $TCR\alpha\beta^{(+)}CD8\alpha\beta^{(+)}$ to $TCR\alpha\beta^{(+)}CD8\alpha\alpha^{(+)}$ IELs between $pT\alpha^b.pT\alpha^{-/+}$ and $pT\alpha^{-/+}$ mice, which is also similar to that observed in WT C57Bl/6 controls.

Thus, this preliminary experiment did not reveal any definitive phenotype related to whether over-expression of $pT\alpha^b$ at the β-selection checkpoint influences $TCR\alpha\beta^{(+)}CD8\alpha\alpha^{(+)}$ IELs development.
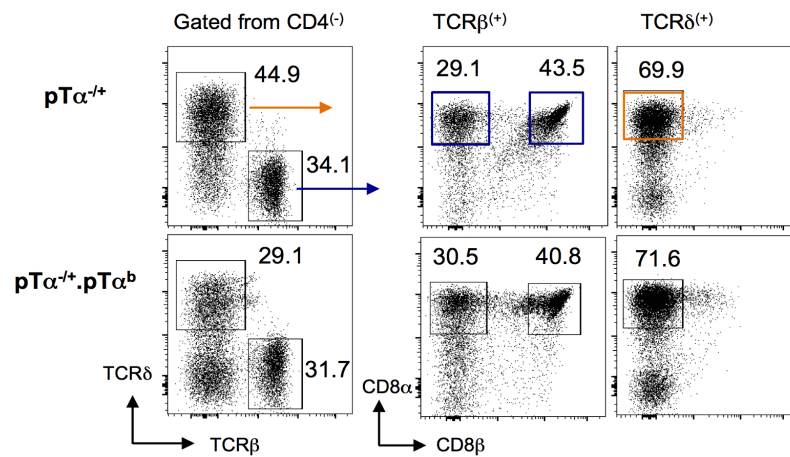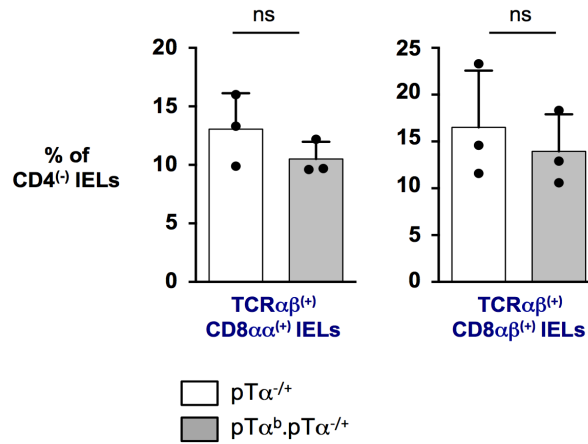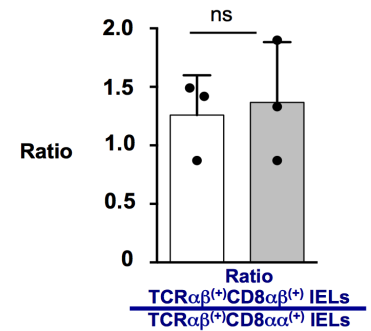
Figure 4.7 Preliminary analysis of the small intestine of pTα^b.pTα^-/+ mice. (A) Representative flow cytometry plots (n=3) looking at the IEL population in the small intestine of pTα^b.pTα^-/+ and pTα^-/+ mice. Percentages of cells are indicated near each gate. (B) Representative bar graphs (n=3) of TCRαβ$^{(+)}$CD8αα$^{(+)}$ and TCRαβ$^{(+)}$CD8αβ$^{(+)}$ IELs (C) Representative bar graph (n=3) of the ratio of TCRαβ$^{(+)}$CD8αβ$^{(+)}$ to TCRαβ$^{(+)}$CD8αα$^{(+)}$ IELs. ns is not significant.

4.6 Preliminary investigation of thymic T cell development in pTα^b.pT$\alpha^{-/+}$ mice

Despite the lack of a clear phenotype in the small intestines of pTα^b.pT$\alpha^{-/+}$ mice, we subsequently assessed whether over-expression of pTα^b influences thymic T cell development in pTα^b.pT$\alpha^{-/+}$ animals compared to pT$\alpha^{-/+}$ littermate controls. Analysis of the total number of thymocytes averaged around 2×10^8 cells in both pTα^b.pT$\alpha^{-/+}$ and pT$\alpha^{-/+}$ mice (Figure 4.8A). Thus, over-expression of pTα^b does not appear to influence thymus size. PreTCR signalling competes at the DN stage with TCR$\gamma\delta$. We therefore sought to investigate whether $\gamma\delta$ T cell development was affected. However, flow cytometry analysis of TCR$\delta^{(+)}$ cells showed no significant differences between pTα^b.pT$\alpha^{-/+}$ mice(~0.25% of all lymphocytes) and pT$\alpha^{-/+}$ mice (~0.25% of all lymphocytes) (Figure 4.8B&C).

One of our main hypotheses is that signalling at the DN stage of T cell development through pTα^a or pTα^b may be responsible for establishing DP heterogeneity that subsequently allows different T cell subsets to develop. We therefore assessed whether T cell development in pTα^b-transgenic mice favoured the generation of certain $\alpha\beta$ T cells subsets. Analysis of DP (CD4$^{(+)}$CD8$^{(+)}$) or DN(CD4$^{(-)}$CD8$^{(-)}$) cells in pTα^b.pT$\alpha^{-/+}$ and littermate pT$\alpha^{-/+}$ mice did not reveal any differences between the two strains with ~80% of DP cells and ~2% of DN thymocytes as a proportion of total lymphocytes (Figure 4.8).
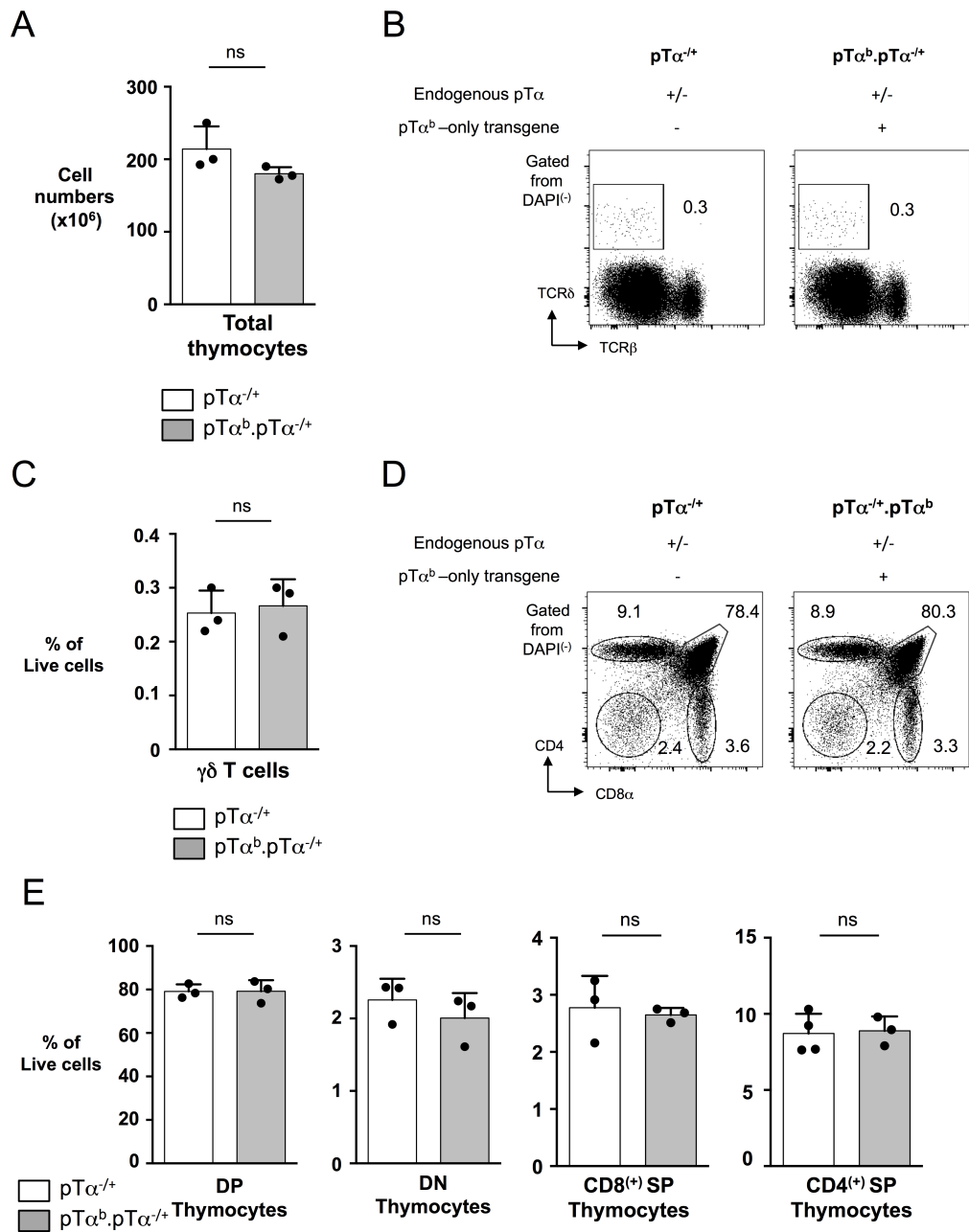
Figure 4.8 Preliminary analysis of the thymus of pTα^b.pTα$^{-/+}$ mice

(A) Representative bar graph (n=3) of the total number of thymocytes from pTα^b.pTα$^{-/+}$ and pTα$^{-/+}$ mice. (B) Representative FACS profile (n=3) of total γδ thymocytes from pTα^b.pTα$^{-/+}$ and pTα$^{-/+}$ mice and the corresponding summary bar chart in (C). (D) shows representative flow cytometry profiles of CD4$^{(+)}$ and CD8$^{(+)}$ T cells in pTα^b.pTα$^{-/+}$ and pTα$^{-/+}$ mice. (E) Summary bar charts of the proportions of DP, DN and CD4$^{(+)}$SP and CD8$^{(+)}$SP thymocytes in pTα^b.pTα$^{-/+}$ and pTα$^{-/+}$ mice. ns, non-significant; error bar is SD; DN, double negative for CD4 and CD8α; DP, Double positive for CD4 and CD8α proteins.

4.7 Conclusion

Together, these preliminary analyses of $pT\alpha^b$-transgenic mice on a $pT\alpha^{-/+}$ background did not reveal any significant differences in thymus size, thymic T cell subset representation, or unconventional $TCR\alpha\beta^{(+)}CD8\alpha\alpha^{(+)}$ IEL development. Importantly, the presence of the one endogenous WT-allele is likely responsible for the "normal" phenotype of these mice, especially considering evidence from our lab (and others) that $pT\alpha^a$ is dominant to $pT\alpha^b$. Nonetheless, the ideal scenario would be to analyse these animals on a $pT\alpha$-deficient background. Unfortunately, time ran out on my PhD before these breedings were possible.

Chapter 5

Investigating the DP-to-SP transition in FVB/n and pTα^a transgenic animals

5.1 Introduction

A central hypothesis of this thesis has been that different signalling events occurring at the DN stage of T cell development could be responsible for promoting subsequent differential development of T cell subsets (eg. conventional versus unconventional TCR$\alpha\beta^{(+)}$ T cell subsets). Consistent with this, we identified in chapter 3 a correlation between the strength of signal delivered at the DN stage of T cell development and the ratio of conventional TCR$\alpha\beta^{(+)}$CD8$\alpha\beta^{(+)}$ IELs to unconventional TCR$\alpha\beta^{(+)}$CD8$\alpha\alpha^{(+)}$ IELs found in the small intestine of mice. Whereas "weaker" signalling at the β-selection checkpoint seems to oppose unconventional TCR$\alpha\beta^{(+)}$CD8$\alpha\alpha^{(+)}$ IEL development in FVB/n and pTα^a.pT$\alpha^{-/-}$ mice, "stronger" signalling through an early-expressed TCR$\alpha\beta$ or TCR$\gamma\delta$ complex seemed to favour their development as suggested in OT-II and pT$\alpha^{-/-}$.TCR$\delta^{-/-}$ mice. To extend this idea, the DP-to-SP transition in FVB/n and pTα^a.pT$\alpha^{-/-}$ mice, where positive and negative selection of T cells occurs, was explored further, as this represents a branching point at which different subsets of conventional and unconventional T cell subsets develop.

5.2 Investigating the proportion of positively selected DP thymocytes in FVB/n and pTα^a.pTα$^{-/-}$ mice

Positive selection of DP thymocytes triggers cell-surface expression of the activation marker CD69 and post-selected DP cells represent between 3 to 5% of all DP thymocytes (Yamashita et al., 1993). To investigate positive selection, we first defined the proportion of newly positively selected DP thymocytes that we identified as CD4$^{(+)}$CD8$^{(+)}$CD69$^{(+)}$ in C57Bl/6, FVB/n and pTα^a.pTα$^{-/-}$ mice.
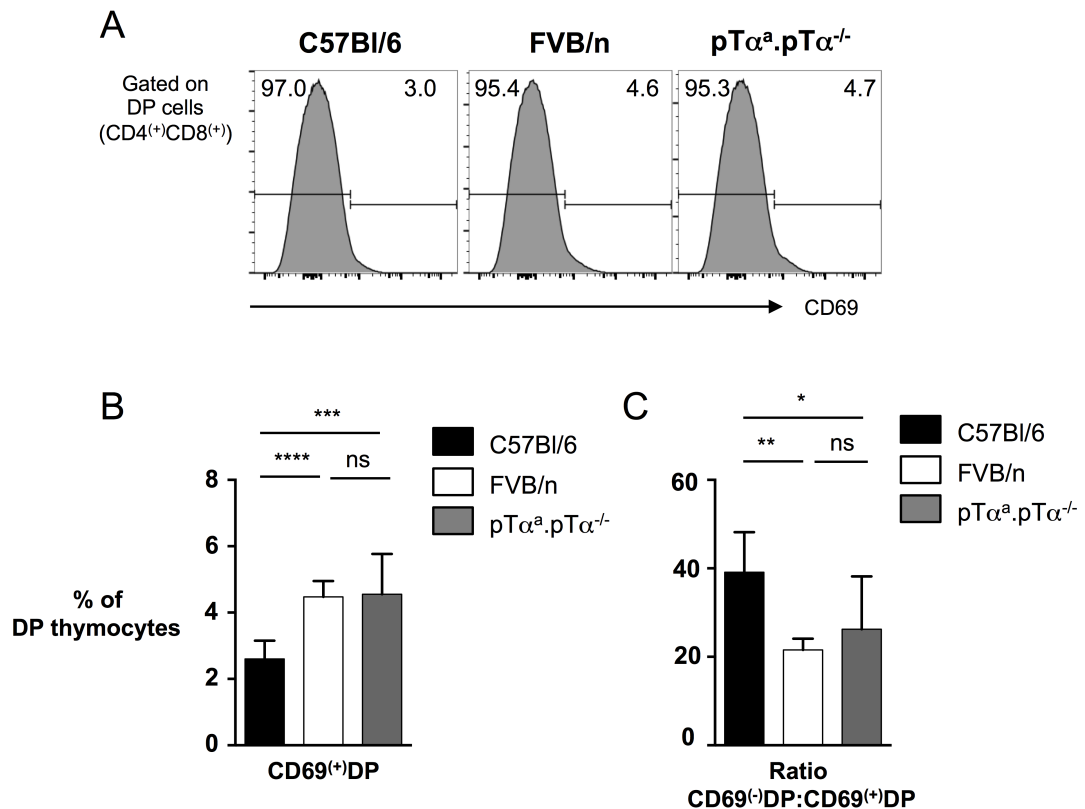
Figure 5.1 Analysis of positively selected DP thymocytes in FVB/n and pTα^a.pTα$^{-/-}$ mice. (A) Representative histograms (from n>4) of CD69 expression on DP thymocytes from C57Bl/6, FVB/n and pTα^a.pTα$^{-/-}$ mice (B) Summary bar chart (from n>4) of the percentage of CD69$^{(+)}$ DP cells from C57Bl/6, FVB/n and pTα^a·pTα$^{-/-}$ mice (C) Summary bar chart (from n>4) of the ratio of pre-selected (CD69$^{(-)}$) to post-selected CD69$^{(+)}$DP thymocytes. DP is Double positive (CD4$^{(+)}$CD8$^{(+)}$); Error bars are SD; **** p<0.0001, *** p<0.001; *p<0.05; ns is for not significant.

Flow cytometry analysis revealed a significantly increased proportion of positively selected DP thymocytes (~4.0% of DP cells) in both FVB/n and pTα^a.pT$\alpha^{-/-}$ mice compared to that of C57Bl/6 mice (~2.5% of DP cells) (Figure 5.1).

Indeed, the ratio pre-selected DP cells (CD69$^{(-)}$) to positively selected DP thymocytes (CD69$^{(+)}$) was of ~20 for FVB/n and pTα^a.pT$\alpha^{-/-}$ mice, but nearly double that in C57Bl/6 mice with a ratio of ~40 (Figure 5.1). Thus, these data appear to suggest that positive selection of DP thymocytes is favoured or "accelerated" in FVB and pTα^a·pT$\alpha^{-/-}$ mice, compared to controls.

5.3 Conventional thymic TCR$\alpha\beta^{(+)}$CD4$^{(+)}$ and TCR$\alpha\beta^{(+)}$CD8$^{(+)}$ T cells are found in greater proportions in FVB/n and pTα^a·pT$\alpha^{-/-}$ transgenic mice

As a greater proportion of DP thymocytes appeared to be showing evidence of positive selection in FVB/n and pTα^a.pT$\alpha^{-/-}$ mice compared to C57Bl/6 controls, we sought to analyse the relative proportions of mature thymic CD4$^{(+)}$ and CD8$^{(+)}$ T cells. FVB/n and pTα^a.pT$\alpha^{-/-}$ mice had on average a significantly increased proportion of TCR$\alpha\beta^{(+)}$CD4$^{(+)}$ T cells (~9% of all thymocytes) compared to C57Bl/6 mice (~5%). TCR$\alpha\beta^{(+)}$CD8$^{(+)}$ T cells were increased by 2-fold in pTα^a·pT$\alpha^{-/-}$ (~3% of total thymocytes), but not in FVB/n mice (~1.5%), compared to C57Bl/6 animal (~1.5%) (Figure 5.2). These changes in SP

thymocyte percentages were also partialy reflected in the proportion of total DP cells in these animals, for example in $pT\alpha^a.pT\alpha^{-/-}$ mice, in which the DP pool accounted for only 65% of total thymocytes compared to 80% for C57Bl/6 mice. Indeed, the DP-to-SP ratio in FVB/n and $pT\alpha^a.pT\alpha^{-/-}$ mice was significantly different to that seen in C57Bl/6 mice, being 6 for $pT\alpha^a.pT\alpha^{-/-}$ animals, 7 for FVB/n mice, but nearly 11 in C57Bl/6 controls (Figure 5.3).

Taken together, these data suggest that for a given pool of DP cells, FVB/n and $pT\alpha^a.pT\alpha^{-/-}$ mice appear to generate a greater number of mature SP thymocytes than in C57Bl/6 animals.
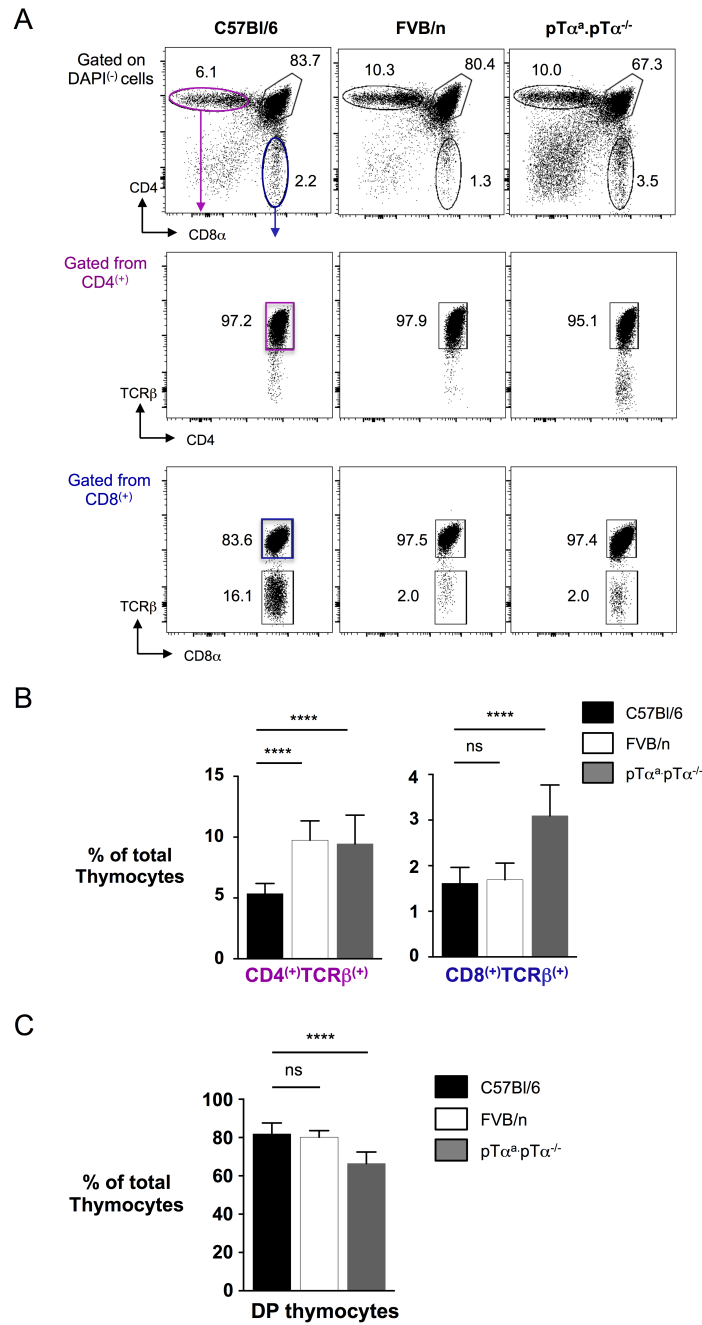
Figure 5.2 FVB/n and pTαᵃ.pTα⁻/⁻ mice harbor a greater proportion of SP thymocytes. (A) Representative flow cytometry profiles (from n>5) of TCRαβ$^{(+)}$CD4$^{(+)}$ (pink) and TCRαβ$^{(+)}$CD8$^{(+)}$ thymocytes (blue) from FVB/n, C57Bl/6 and pTαᵃ.pTα⁻/⁻ mice (B) Summary bar chart of the percentages of TCRαβ$^{(+)}$CD4$^{(+)}$ and TCRαβ$^{(+)}$CD8$^{(+)}$ thymocytes from FVB/n, C57Bl/6 and pTαᵃ.pTα⁻/⁻ mice. (C) Summary bar chart of the percentages of DP thymocytes from FVB/n, C57Bl/6 and pTαᵃ.pTα⁻/⁻ mice. DP is double positive (CD4$^{(+)}$CD8$^{(+)}$); **** p<0.0001; ns is for not significant
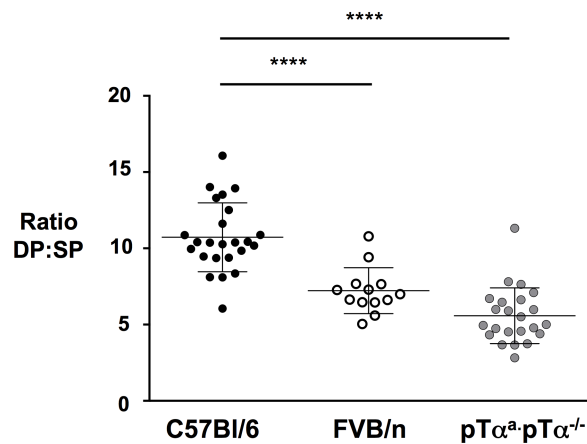
Figure 5.3 Analysis of the DP-to-SP ratio in C57Bl/6, FVB/n and pTα^{a}.pTα$^{-/-}$ mice. Summary dot plot (n>13) showing the DP-to-SP ratio in C57Bl/6, FVB/n and pTα^{a}.pTα$^{-/-}$ mice. DP, Double Positive CD4$^{(+)}$CD8$^{(+)}$; SP Single positive TCRαβ$^{(+)}$CD4$^{(+)}$ or TCRαβ$^{(+)}$CD8$^{(+)}$ thymocyte; **** $p<0.0001$

5.4 The DP-to-SP ratio does not correlate with thymus size in C57Bl/6, FVB/n, or pTα^{a}.pTα$^{-/-}$ mice

Upon analysis of the thymus in chapter 3, we noticed that in pTα^{a}.pTα$^{-/-}$ mice, the pTα^{a} transgene only partially rescued the total number of thymocytes on a pTα$^{-/-}$ background. Indeed, pTα^{a}.pTα$^{-/-}$ mice had on average only approximately 5×10^{6} thymocytes, whereas C57Bl/6 and FVB/n thymuses contained about 1.6×10^{8} cells (Figure 3.10). Published data has suggested that the efficiency of positive selection is affected by the availability of peptide-MHC complexes in stromal niches (Prockop et al., 2002). We therefore investigated whether the

"enhanced" DP-to-SP transition that we described for $pT\alpha^a.pT\alpha^{-/-}$ mice could be due, at least in part, to a greater availability of selecting stromal niches, that would be present in a thymus with reduced cellularity. Thus, we looked for correlation between the ratio of DP-to-SP thymocytes and thymus size (as a surrogate for the number of stromal niches). Although when all mice in the study were analysed, the larger thymuses from C57Bl/6 mice had a higher DP-to-SP ratios, and the smaller $pT\alpha^a.pT\alpha^{-/-}$ thymus has the lowest DP-to-SP ratios, no correlations were observed when only mice of a certain type were assessed; with R^2 values of 0.02 for C57Bl/6, 0.08 for FVB/n mice and 0.05 for $pT\alpha^a.pT\alpha^{-/-}$ mice (Figure 5.4). Thus, differences in DP-to-SP ratios in the different strains of mice cannot be explained by a difference in the size of the thymus.
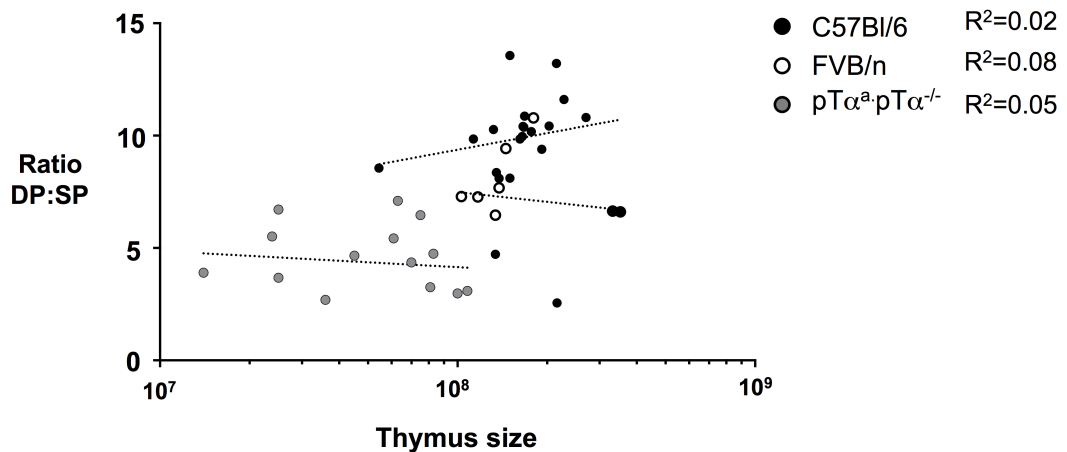
Figure 5.4 The thymic DP-to-SP ratio is not correlated to thymus size. The DP-to-SP ratio is plotted on the y-axis while total thymic cell number is found on the x-axis (Log scale).

5.5 Investigating the role of CD5 in conventional versus unconventional T cell development.

We have suggested that "weaker" signalling at the DN stage of T cell development results in low CD5 expression that was associated with reduced development of unconventional $TCR\alpha\beta^{(+)}CD8\alpha\alpha^{(+)}$ IELs in the gut of FVB/n and $pT\alpha^a.pT\alpha^{-/-}$ mice compared to C57Bl/6 mice. By contrast, "stronger" signalling at the DN stage, for instance through early-expressed transgenic $TCR\alpha\beta$ complexes, triggers a higher surface expression of CD5 and correlated with a greater proportion of unconventional $TCR\alpha\beta^{(+)}CD8\alpha\alpha^{(+)}$ IELs in the small intestine of OT-II and $pT\alpha^{-/-}.TCR\delta^{-/-}$ mice compared to C57Bl/6 mice. Thus, this led us to investigate whether the level of CD5 expression was directly responsible for altered DP cell sensitivity to positive selection, which would explain the accelerated DP-to-SP transition and the differences in the ratio of unconventional versus conventional IELs in the small intestines of FVB/n and $pT\alpha^a.pT\alpha^{-/-}$ mice. Indeed, CD5 has previously been shown to influence T cell fate during development and was demonstrated to regulate cell sensitivity to TCR stimulation (Azzam et al., 2001; Tarakhovsky et al., 1995). To investigate this idea, thymuses and small intestines from four CD5-deficient ($CD5^{-/-}$), four CD5 over-expressing (CD5Tg) mice and one littermate WT control were kindly shipped to us on ice within 48hrs by Professor Paul Love from NIH in Bethesda (US). Unfortunately upon reception, the small intestines from all mice had undergone a damaging degree of self-digestion, a commonly observed phenomenon when these organs are not processed within 12 hours of dissection. This forced us to focus our analysis on the thymus, which appeared

largely unaffected by cell death based on DAPI staining that we routinely do. Due to the presence of only one C57Bl/6 littermate control, we also included data obtained from C57Bl/6 mice bred at Queen Mary University (QMUL) (named here after C57Bl/6 QMUL) in order for us to draw meaningful conclusions. CD5$^{-/-}$ mice had on average a greater proportion of total single positive CD4$^{(+)}$ (~14%) and CD8$^{(+)}$ (~2%) T cells than the C57Bl/6 USA control mouse (Figure 5.6). However, they harboured a similar absolute number of cells with ~6x10^6 CD4$^{(+)}$ and ~0.8x10^6 CD8$^{(+)}$ T cells. By contrast, CD5 over-expressing mice (CD5Tg) harboured similar proportions of CD4$^{(+)}$ and CD8$^{(+)}$ T cells compared to the C57Bl/6 USA control mouse. However, analysis of cells numbers revealed a largely reduced number of CD4$^{(+)}$ and CD8$^{(+)}$ T cells in CD5Tg mice compared to C57Bl/6 USA mice (Figure 5.5).

Finally, the ratio of DP-to-SP thymocytes was assessed in the various groups of mice. This revealed a reduced DP-to-SP ratio in CD5-deficient animals (~5) that was similar to the ratio observed in FVB/n and pTα^a·pT$\alpha^{-/-}$ mice, and approximately 2-fold less than that seen in C57Bl/6 mice (~11). This supports a tentative hypothesis that reduced CD5 expression at the DP stage (caused by weaker signalling at the DN stage) could permit DP cells to be more sensitive to positive selecting TCR$\alpha\beta$ signals that would reduce the DP-to-SP ratio. However, CD5Tg mice also had a reduced DP-to-SP ratio averaging around 6, which at face value argues against such a conclusion.
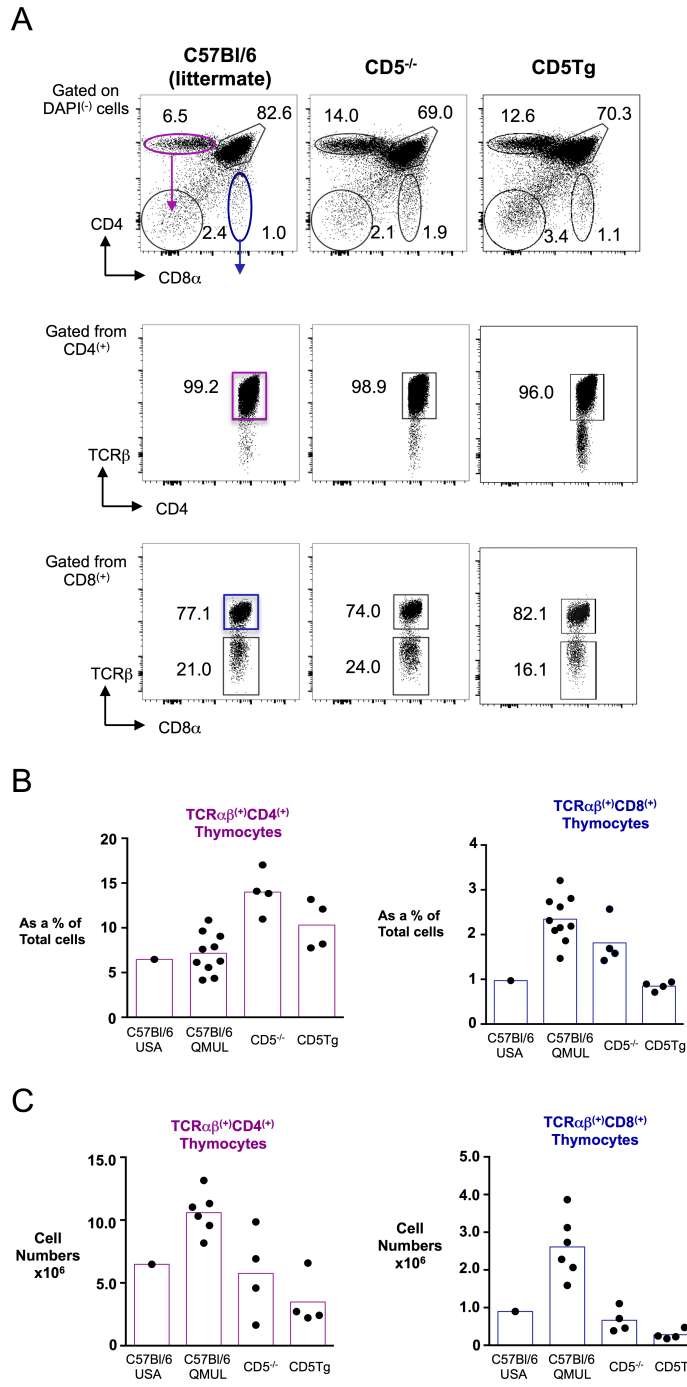
Figure 5.5 Preliminary analysis of CD5-deficient and CD5 overexpressing mice
(A) Representative flow cytometry profiles of CD4 versus CD8 expression for thymocytes from one C57Bl/6 CD5Tg littermate control received from the US, CD5-deficient (CD5$^{-/-}$) and CD5 overexpressing (CD5Tg) transgenic mice (B) Summary bar chart of the percentages of TCRαβ$^{(+)}$CD4$^{(+)}$ and TCRαβ$^{(+)}$CD8$^{(+)}$ thymocytes from one C57Bl/6 littermate control, C57Bl/6 mice from QMUL, CD5$^{-/-}$ and CD5Tg mice (C) Summary bar graphs of cell number for TCRαβ$^{(+)}$CD4$^{(+)}$ and TCRαβ$^{(+)}$CD8$^{(+)}$ thymocytes in C57Bl/6, CD5$^{-/-}$ and CD5Tg mice.
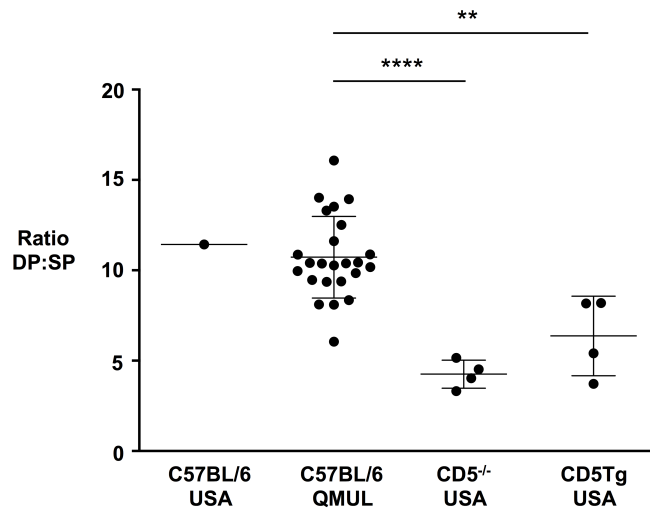
Figure 5.6 DP-to-SP ratios in C57Bl/6, CD5$^{-/-}$ and CD5Tg mice Summary dot plot showing the DP-to-SP ratio in one C57Bl/6 CD5Tg littermate control received from the US, C57Bl/6 mice from QMUL, CD5-deficient (CD5$^{-/-}$) mice and CD5-overexpressing (CD5Tg) transgenic mice. DP, Double Positive CD4$^{(+)}$CD8$^{(+)}$; SP Single positive TCR$\alpha\beta^{(+)}$CD4$^{(+)}$ or TCR$\alpha\beta^{(+)}$CD8$^{(+)}$ thymocytes

Nonetheless, expression of the CD5 transgene was under the regulation of the CD2 promoter that results in the early expression of CD5 during the DN phase of T cell development and hence to a reduced cell sensitivity to TCR signalling at the β-selection checkpoint. Thus, CD5Tg mice might not represent an ideal model to test this hypothesis.

5.6 Conclusion

Here we show that FVB/n and pTα^a.pT$\alpha^{-/-}$ mice have a lower DP-to-SP ratio compared to C57Bl/6 mice suggesting an enhanced transition from the DP stage to the SP stage; a transition driven by positive selection. Importantly, this does not appear to result from differences in thymus size, which prompted us to

postulate that differences in CD5 expression resulting from quantitatively different signals at the DN stage might be responsible for influencing subsequent positive selection events. Consistent with this, we show that preliminary analysis of the thymuses of CD5-deficient animals reveals that they too have a lower DP-to-SP ratio. Analysis of the small intestines of these mice has yet to be carried out to investigate whether this also correlates with a greater ratio of conventional $TCR\alpha\beta^{(+)}CD8\alpha\beta^{(+)}$ to unconventional $TCR\alpha\beta^{(+)}CD8\alpha\alpha^{(+)}$ IELs. Thus, this chapter presents preliminary evidence to suggest that signalling events at the DN stage could be responsible for subsequent T cell selection. If supported by further studies, this would reveal a previously unpredicted role for $pT\alpha$ and the preTCR at the β-selection checkpoint.

Chapter 6

Investigating the role of TCRγδ signalling in γδ T cell development

_____

6.1 Introduction

There are substantial data supporting a model, now widely accepted, that γδ T cell lineage commitment is dictated by strong signalling delivered by TCRγδ (Hayes et al., 2005). Strong signals are commonly associated with ligand engagement by the TCR, in contrast to the weak signal delivered by the preTCR in a ligand-independent manner. However, it remains unclear which factors (e.g. ligands, cytokine, etc) are responsible for driving the development of different γδ T cell subsets, especially the thymic generation of IFN-γ versus IL-17A-producing γδ T cells. TCR signal strength has a central role throughout αβ T cell development in driving T cell differentiation (e.g. CD4$^{(+)}$ versus CD8$^{(+)}$ T cells). As a result and by analogy, a similar idea has been applied to the role of TCRγδ in γδ T cell development. However, the lack of known ligands for a majority of murine γδ T cells (~99%) has rendered the task complicated (Crowley et al., 1997). In contrast to αβ T cell development, which can be characterised using previously well-defined cell-surface markers, a consensus nomenclature is yet to be defined for developing thymic γδ T cell subsets. Thus, we have first sought to characterise different γδ T cell subsets and their cytokine potential using a combination of previously published cell-surface markers

(Coffey et al., 2014; Jensen et al., 2008; Michel et al., 2012; Prinz et al., 2006; Ribot et al., 2009). We then investigated the role TCRγδ in γδ T cell development using foetal thymic organ culture (FTOC) supplemented with the selective inhibitors or antibodies (Figure 6.1). Importantly, this project was carried out in collaboration with other members of the lab and thus the data presented here represent only a small fraction of the whole work.
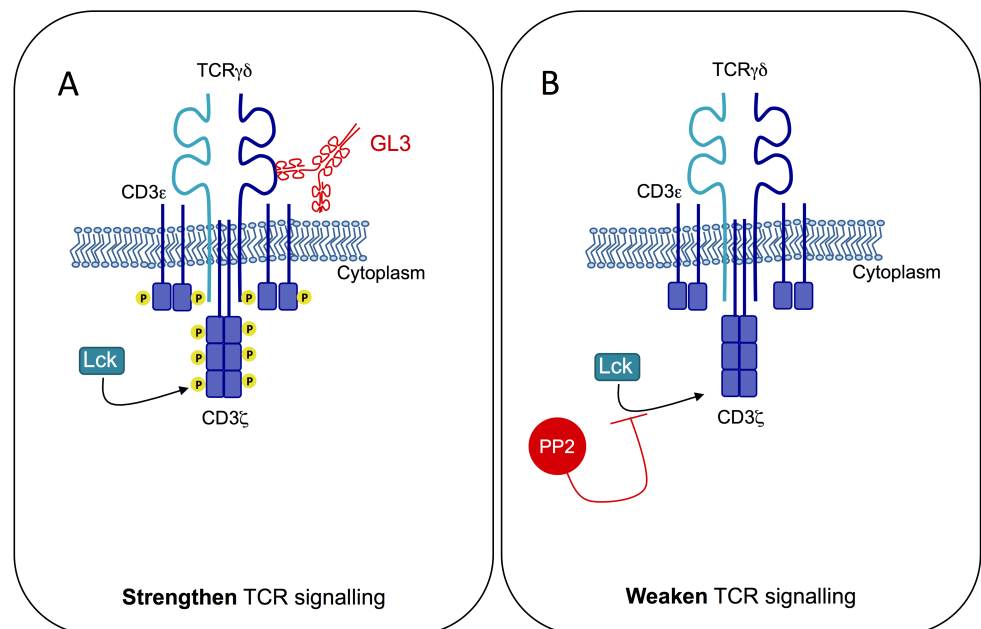
How does TCRγδ signal strength affect development of IL-17A-secreting or IFN-secreting γδ T cell subsets?

Figure 6.1 Experimental approach. The role of TCRγδ signalling in γδ T cell development will be investigated by (A) using the TCRδ-crosslinking antibody (GL3) widely recognised to strengthen TCR signalling or by (B) using a src-kinase inhibitor PP2 which inhibits Lck and therefore prevents phosphorylation of the ITAMs thus resulting in a weakened TCR signal. Indeed, TCR signalling involves the phosphorylation of ITAMs (yellow circle) by Lck.

6.2 Characterisation of six γδ T cell subsets from lymph nodes of C57Bl/6 mice

Various cell surface markers have been used across numerous studies to characterise γδ T cell subsets, but a precise nomenclature that robustly distinguishes IL-17A versus IFN-γ-producing γδ T cells had yet to be defined. For example, although expression of the TNF-receptor family member CD27 is commonly used to identify IFN-γ secreting γδ T cells, some CD27$^{(-)}$ γδ T cells have also been shown to produce a small amount of IFN-γ following stimulation (Ribot et al., 2009). Thus, we first sought to characterize γδ T cells from lymph nodes (LN) of C57Bl/6 mice based on the combined expression of CD24, CD44, the protein phosphatase CD45RB, NK1.1 and the interleukin 7 receptor α (IL-7α) chain CD127. We first sub-divided γδ T cells into immature (CD24$^{(+)}$, or subset 1) and mature (CD24$^{(-)}$, or subset 2) subsets and subsequently identified six subsets based on CD44 and CD45RB expression (that we have named 1a, 1b, and 2a to 2d) (Figure 6.2).
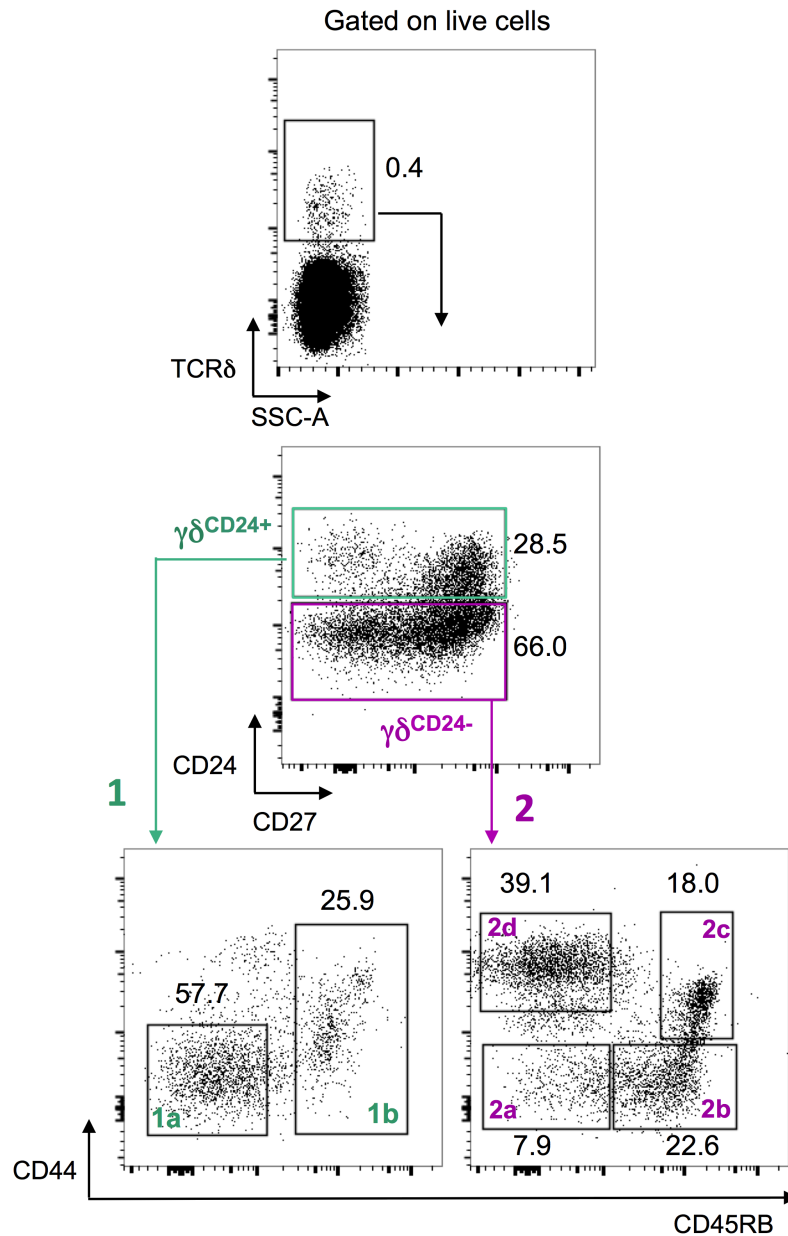
Figure 6.2 Six distinct γδ T cell subsets can be identified from lymph nodes of C57Bl/6 mice. (A) Representative flow cytometry profiles (n=3) of γδ T cells obtained from lymph nodes of adult (>6 weeks) C57Bl/6 mice, where different γδ T cell subsets can be identified using CD24, CD27, CD44, and CD45RB The immature population (γδ^{CD24+}, green) can be further divided into two subsets 1a (CD44$^{(-)}$CD45RB$^{(-)}$) and 1b (CD44$^{(-)}$CD45RB$^{(+)}$) while four subsets can be identified in the mature population (γδ^{CD24-}, purple): 2a (CD44$^{(-)}$CD45RB$^{(-)}$), 2b (CD44$^{(-)}$CD45RB$^{(+)}$), 2c (CD44^{low}CD45RB$^{(+)}$), and 2d (CD44$^{(+)}$CD45RB$^{(-)}$)

We next assessed these subsets for expression of CD27, IL-7Rα and NK1.1 as well as their cytokine potential following 4hr stimulation at 37°C using phorbol myristate acetate (PMA) and ionomycin to activate the cells unspecifically (Chatila et al., 1989). Subset 1a (CD44$^{(-)}$CD45RB$^{(-)}$) represents approximately two third of the immature subset (65%) and mainly expressed CD27 while subset 1b (CD45RB$^{(+)}$) consists of approximately 35% of all immature cells and displays a heterogenous surface expression of CD27. Both the 1a and 1b subsets do not express NK1.1 or IL-7Rα. While subset 1a has very little cytokine-secreting capacity, subset 1b displays some IFN-γ-secreting potential. Four subsets can be identified within the mature subset (2); subset 2a (CD44$^{(-)}$CD45RB$^{(-)}$) mainly expresses CD27 but no NK1.1 nor IL-7Rα and appears to display limited cytokine secretion capacity (Figure 6.3). Subset 2b (CD44$^{(-)}$CD45RB$^{(+)}$) and 2c (CD44$^{(+)}$CD45RB$^{(+)}$) express CD27 but no IL-7Rα and both secrete IFN-γ with ~22% and ~62% of IFN-γ producing cells respectively. The 2c subset appears to be the only subset with a heterogenous expression of NK1.1. Finally, subset 2d (CD44$^{(+)}$CD45RB$^{(-)}$) does not express CD27, nor NK1.1 but does express the IL-7Rα and up to ~50% of the cells display a IL-17A secreting potential making it the greater source of IL-17A cytokine (Figure 6.3).
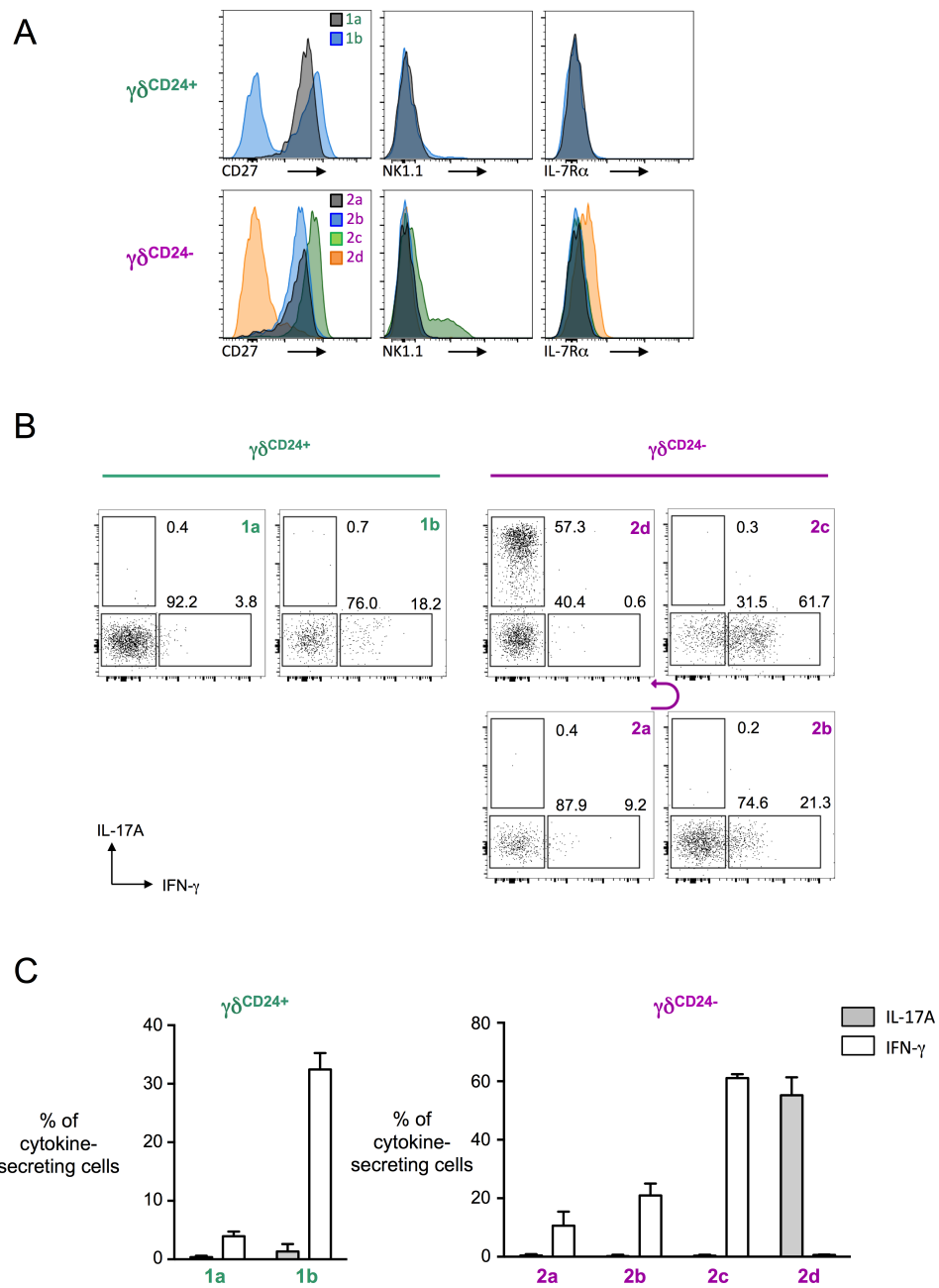
Figure 6.3 Six distinct γδ T cell subsets with different cytokine-secreting potential can be identified in the lymph nodes of C57Bl/6 mice. (A) Representative histograms of CD27, NK1.1, and IL-7Rα on 1a, 1b, 2a, 2b, 2c, and 2d subsets (B) Representative flow cytometry plots (n>3) of intracellular IL-17A and IFN-γ cytokines. Percentages of IL-17A[(+)] and IFN-γ[(+)] cells are indicated near each gate. (C) Representative bar charts (n=3) of the cytokine contribution from the γδ[CD24-] subset 1a and 1b as well as γδ[CD24+] subset 2a, 2b, 2c and 2d in lymph nodes of C57Bl/6 mice. Error bars are SD; **** p<0.0001, *** p<0.001; *p<0.05; ns is for not significant.

6.3 The six γδ T cells subsets identified from the lymph nodes can be found in the thymus of C57Bl/6 mice.

Having identified six peripheral γδ T cell subsets based on CD24, CD27, CD44 and CD45RB surface expression, we subsequently sought to investigate whether these populations could also be found in the adult thymus. Using the same gating strategy as above, a large proportion of γδ T cells were found with an immature phenotype with up to 90% of the cells expressing CD24 (Figure 6.4).
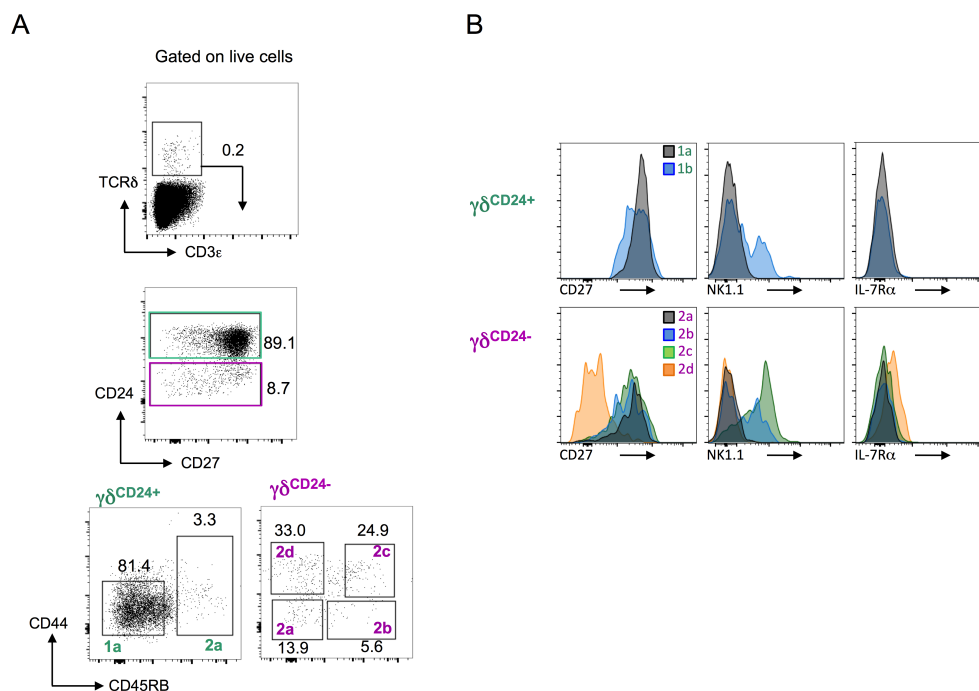
Figure 6.4 The six γδ T cell subsets identified previously from the lymph nodes can be found in the adult thymus (A) Representative flow cytometry profiles (n=3) of γδ T cells obtained from thymus of adult (>6 weeks) C57Bl/6 mice, where different γδ T cell subsets can be identified using CD24, CD44, CD27 and CD45RB. The γδ^{CD24+} subset can be further divided into two subsets 1a (CD44$^{(-)}$CD45RB$^{(-)}$) and 1b (CD44$^{(-)}$CD45RB$^{(+)}$) while four subsets can be identified in the γδ^{CD24-}population: 2a (CD44$^{(-)}$CD45RB$^{(-)}$), 2b (CD44$^{(-)}$CD45RB$^{(+)}$), 2c (CD44$^{(+)}$CD45RB$^{(+)}$), 2d (CD44$^{(+)}$CD45RB$^{(-)}$) (B) Representative histograms of CD27, NK1.1, and IL-7Rα on 1a, 1b, 2a, 2b, 2c, and 2d subsets.

In contrast to $\alpha\beta$ T cells, $\gamma\delta$ T cells commit to effector function before egressing the thymus (Prinz et al., 2013). Thus, we investigated the cytokine secreting potential of each thymic $\gamma\delta$ T cell subset following stimulation with PMA and Ionomycin. Whereas subset 1a displayed in the lymph node a small IFN-γ-secreting potential, it appears in the thymus to be skewed towards an IL-17A-secreting fate with 8% of cells displaying an IL-17A-secreting potential. On the other hand, the 1b subset mainly harbored IFN-γ-secreting cells constituting about 10% of the subset. Amongst the $\gamma\delta^{CD24(+)}$ subset, the pattern of expression of CD27 and IL-7Rα recapitulated what had been seen in the LN. While only the 2c subset in the LN showed a small NK1.1$^{(+)}$ population, the thymic 2b and 2c subsets largely expressed NK1.1. Similar to the LN, the 2c and 2d subsets harboured a large proportion of IFN-γ (25%) and IL-17A-secreting cells (65%) respectively (Figure 6.5). While 15% of the 2a cells displayed an IFN-γ-secreting potential in the LN, they were mainly skewed towards an IL-17A secreting potential in the adult thymus.

Thus, the data collected here suggest that the $\gamma\delta$ T cell subsets identified from LN of C57Bl/6 mice can also be found in the thymus and display a largely similar phenotype.
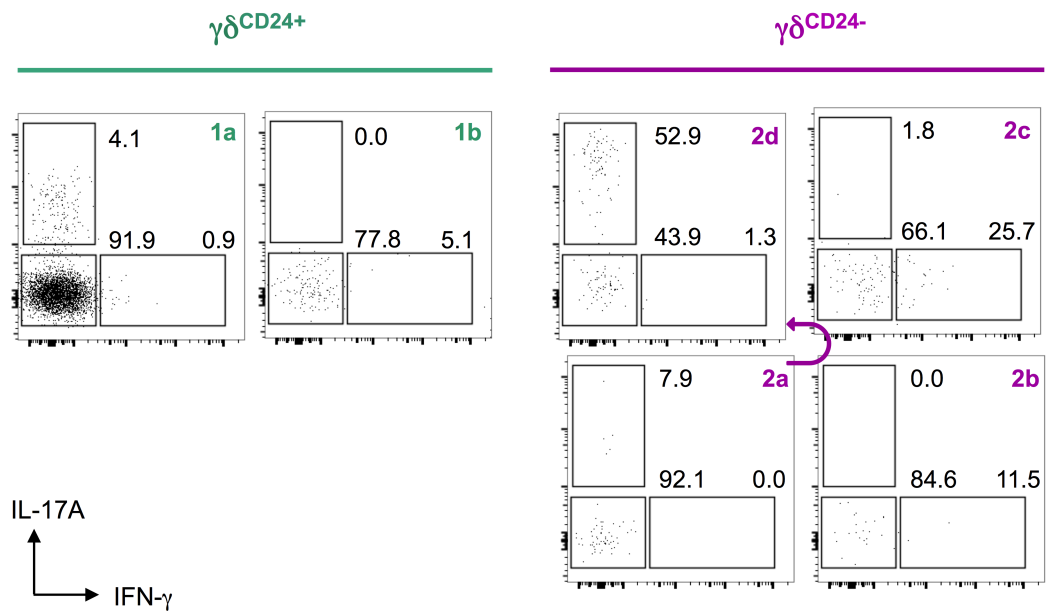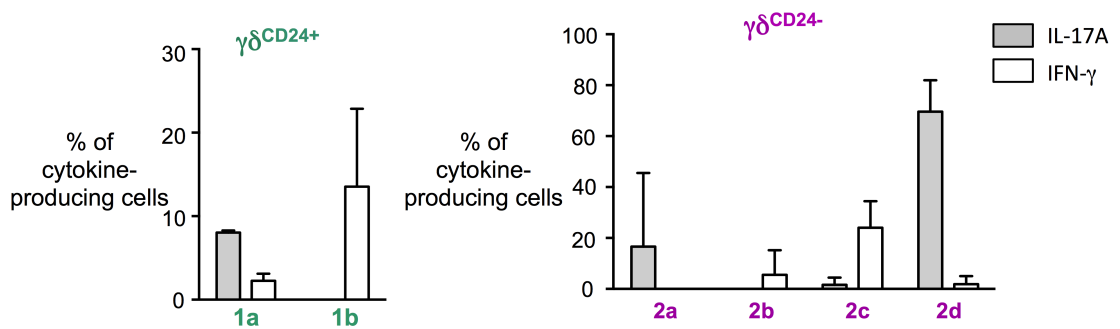
Figure 6.5 The six γδ T cell subsets identified previously from the lymph nodes can be found in the thymus. (A) Representative flow cytometry plots (n>3) of intracellular IL-17A and IFN-γ cytokines following stimulation with PMA and ionomycin for 4hrs at 37°C. Percentages of IL-17A[(+)] and IFN-γ[(+)] cells are indicated near each gates. (B) Representative bar graph (n=3) of the cytokine contribution from the immature γδ[CD24-] subset 1a and 1b as well as the mature γδ[CD24+] subset 2a, 2b, 2c and 2d in the thymus of C57Bl/6 mice. Error bars are SD.

6.4 Investigating the consequences of augmenting TCRγδ signal strength in γδ T cell development

γδ T cell subsets develop in waves. Indeed, unlike αβ T cells, certain γδ T cell subsets develop within certain windows of time from embryonic life onwards. Vγ5-expressing γδ T cells (or DETC) constitute the first γδ T cell subset to arise at day 13.5 of embryonic life (E13.5) and continue their development until about E16, which partially overlaps with the Vγ6[(+)] γδ subset that develop from about E15 (Figure 6.6). Finally, Vγ4[(+)] and Vγ1[(+)] γδ T cells develop from the neonatal period onwards (Carding and Egan, 2002; Prinz et al., 2013) (Figure 6.6).
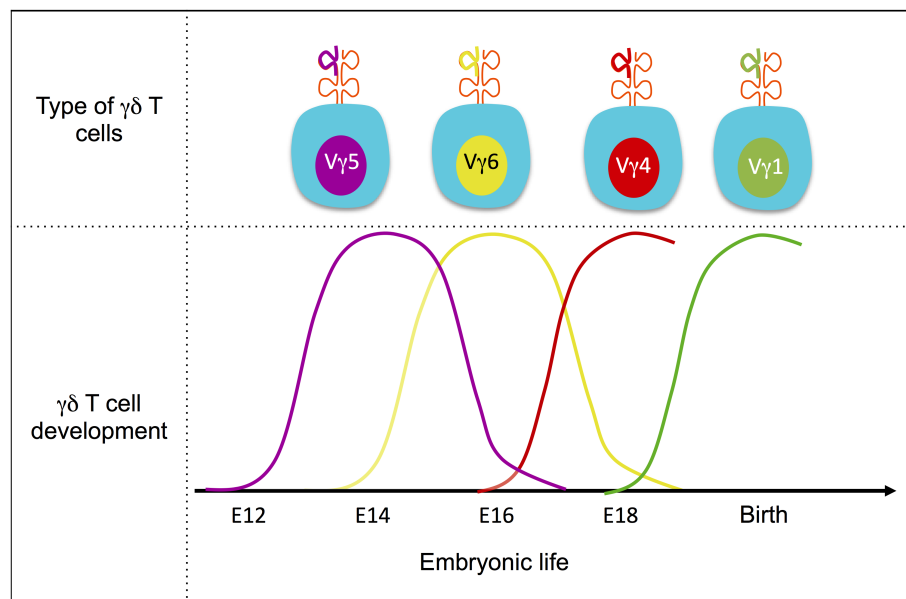
Figure 6.6 Thymic-derived γδ T cells develop in waves Vγ5[(+)]cells are the first γδ cells arising from day 12-15 of embryonic life (E12-E15). Vγ6[(+)]γδ T cells arise subsequently around E16 and are followed by Vγ4[(+)] and Vγ1[(+)]γδ T cells, which develop during the neonatal period. Vγ7[(+)]γδ T cells are not represented here as there is some debate as to whether they develop extrathymically.

Because of these early waves, FTOC represents an ideal tool to investigate γδ T cell development. Moreover, FTOC has been shown to faithfully recapitulate T cell development *in vitro* (Jenkinson et al., 1992).

Strong TCR signal is often associated with ligand engagement and full phosphorylation of the ITAMs found on CD3 and TCRζ molecules. Despite the lack of known ligands for murine γδ T cells, strong signalling can be mimicked by cross-linking the TCRγδ using anti-TCRδ antibodies, such as the clone known as GL3. Thus, to investigate the effect of increasing TCRγδ signal strength on γδ T cell development, we cultured E15 thymic lobes with 1μg.mL$^{(-1)}$ of GL3 for 7 days with one day of rest to allow potentially down-regulated TCRγδ to be re-expressed on the cell-membrane. At the end of these cultures, flow cytometry analysis revealed a significant reduction in both the proportions and cell number of the CD44$^{(+)}$CD45RB$^{(-)}$ "2d" population in the presence of GL3 compared to control cultures (Figure 6.7B & C). Upon stimulation with PMA/ionomycin and analysis of cytokine-secreting potential, we found that the CD44$^{(+)}$ CD45RB$^{(-)}$cells that did develop in the presence of GL3, had a significant decrease in IL-17A-secreting capacity on a per cell basis as judged by decreased IL-17A MFI levels (Figure 6.7E & G). By contrast, numbers of IFN-γ-secreting cells were largely unchanged in GL3-supplemented FTOC (Figure 6.7F). This set of data suggests that increasing signal strength during γδ T cell development by cross-linking TCRδ appears incompatible with the development of IL-17A-secreting γδ T cells while it allows CD45RB$^{(+)}$ γδ subsets to develop similarly to the control. Thus, development into an IL-17A-secreting γδ T cell fate does not appear to be driven by strong signalling through TCRγδ suggesting that instead, a weak TCRγδ signal might be required.
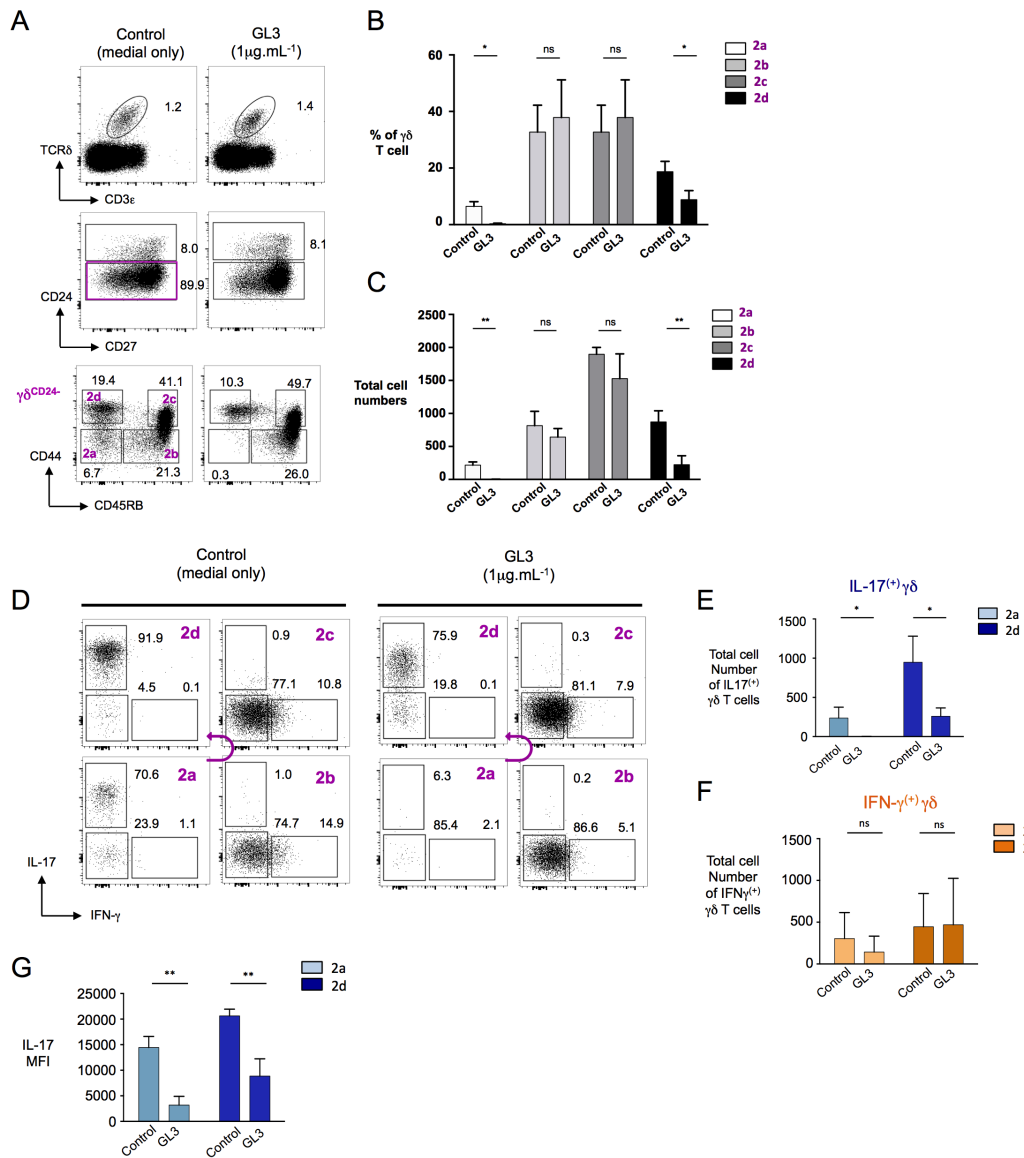
Figure 6.7 Increasing TCRγδ signal strength impairs IL-17A-producing γδ T cell development. (A) Representative flow cytometry profiles (n>3) of γδ T cells obtained from E15 FTOC following 7days supplemented with GL3. Summary bar chart (n>3) of the proportion (B) and cell numbers (C) of each mature subset 2a, 2b, 2c, and 2d subsets. (D) Representative flow cytometry plots (n>3) of intracellular IL-17A and IFN-γ cytokines. Percentages of IL-17A$^{(+)}$ and IFN-γ$^{(+)}$ cells are indicated near each gates. (E) Summary bar graph (n>3) of the numbers of IL-17A-secreting γδ T cells amongst the 2a and 2d subset in control and GL3-supplemented FTOCs. (F) Summary bar graph (n>3) of the numbers of IFN-γ-secreting γδ T cells amongst the 2b and 2c subset in control and GL3 cultures. (G) Summary bar graph (n>3) of the mean fluorescence intensity (MFI) of IL-17A cytokine in the 2a and 2d subset. Error bars are SD; ** $p<0.01$; *$p<0.05$; ns is for not significant.

6.5 Investigating the effect of weakening TCRγδ signalling in γδ T cell development.

The data presented above suggest that strong signalling through TCRγδ impairs IL-17A-secreting γδ T cell development. This prompted us to investigate whether weakening of the TCRγδ signal would, by contrast, favour the development of this subset. TCR signalling is initiated through the phosphorylation of tyrosine residues in the ITAM domains of the CD3 proteins and TCRζ by the src-family tyrosine kinase Lck. This creates a docking site for Zap-70 (Straus and Weiss, 1993; Wang et al., 2010; Wange et al., 1993). Importanty, for our studies, Lck activity can be inhibited by the src-kinase inhibitor PP2 (1-*tert*-Butyl-3-(4-chlorophenyl)-1*H*-pyrazolo[3,4-*d*]pyrimidin-4-amine) (Alice et al., 2012). Thus, we supplemented FTOCs with increasing concentrations of PP2 and followed the development of γδ T cells for 7 days. Somewhat surprisingly on analysis we observed that the proportion and cell number of the 2a and 2d γδ subsets decreased as the concentration of PP2 increased suggesting that weakening TCRγδ signal strength compromises their development (Figure 6.8). By contrats, at the highest concentration of PP2, the only subset that developed was the CD45$^{(+)}$CD44$^{(+)}$ "2c" subset. This suggests that normally, cells destined to develop to this fate signal strongly, so that in the presence of PP2 they can still develop. The 2c subset was shown by other members of the lab to harbor a large proportion of Vγ5$^{(+)}$ cells, which are thought to require strong ligand-dependent TCRγδ signals to develop (Barbee et al., 2011). Alternatively, Vγ5$^{(+)}$ cells γδ cells commence their development at

day 14 of embryonic development, and as our FTOC system uses E15 lobes, some Vγ5$^{(+)}$ cells may have developed prior to the addition of PP2.

Next, cytokine-secreting potential was assessed upon stimulation of the cells with PMA and ionomycin. This revealed a reduction in IL-17A-secreting cells that mirrored the reduction of the 2d subset, yet the MFI of those cells committed to IL-17A secretion remained similar to controls. IFN-γ cells were largely un-affected up to a concentration of 1.0μM. At 1.5μM, while numbers of IFN-γ-producing cells decreased in the 2b subset, the 2c subset remained largely unaffected (Figure 6.9).

Collectively, these data suggest that while strong TCR$\gamma\delta$ signalling triggered by anti-TCRδ antibody cross-linking was incompatible with the development of IL-17A-secreting $\gamma\delta$ T cells, weakening of TCR$\gamma\delta$ signalling by inhibiting Lck activity did not appear to favour their development either. This is somewhat paradoxical. However, taken at face value, one could argue that IL-17A-secreting $\gamma\delta$ cells require a specific window of Lck activity for their development. Thus, increasing (with GL3) or decreasing (with PP2) this activity outside of this Lck window are both incompatible with the development of IL-17A-secreting $\gamma\delta$ T cells.
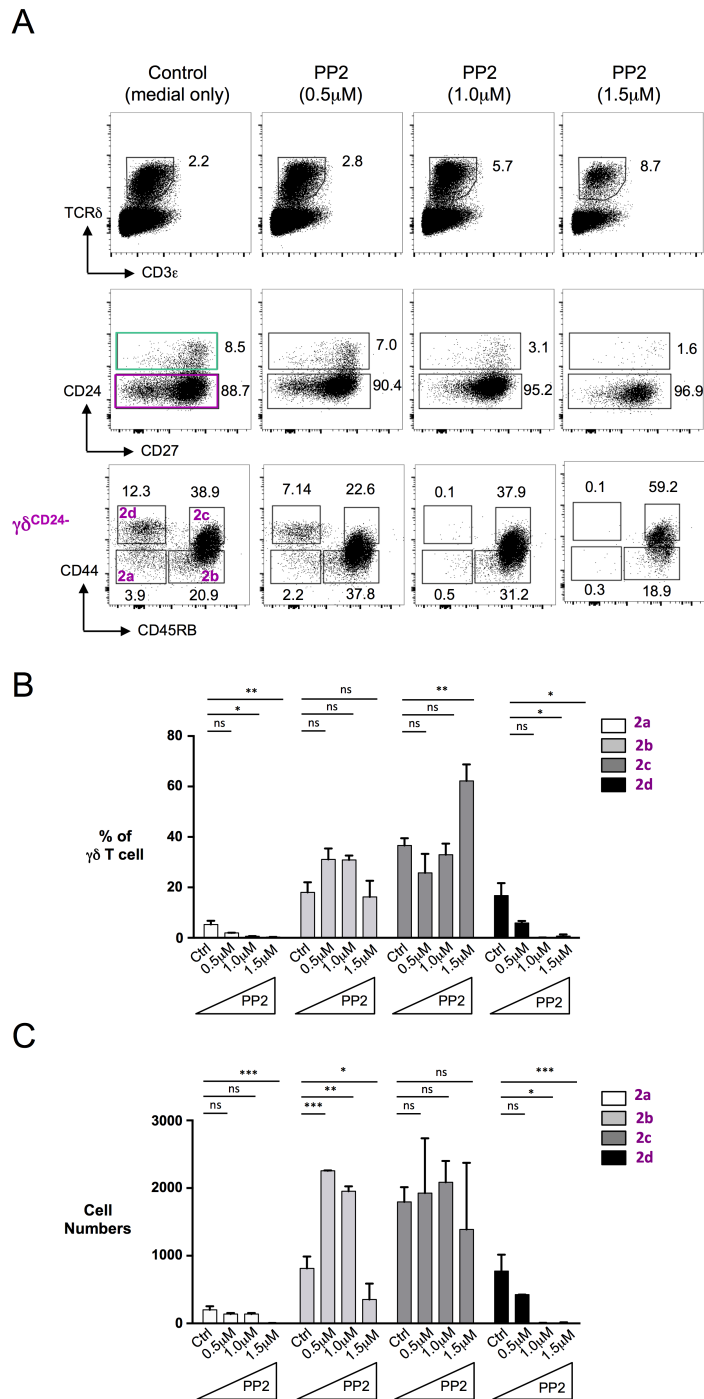
Figure 6.8 Reduced TCRγδ signalling impairs the development of IL-17A-secreting γδ T cells. (A) Representative flow cytometry profiles (2≤n<4)of γδ T cell subsets following 7-day culture of E15 C57Bl/6 thymic lobes supplemented with the Src-kinase inhibitor PP2 at various concentrations indicated underneath each column. Percentages are indicated next to the respective gate. (B) Summary bar chart of the proportion of mature γδ T cell or total cell number (C) following 7-day FTOC supplemented with PP2. Error bars are SD; *** p<0.001, **p<0.01; *p<0.05; ns is for not significant.
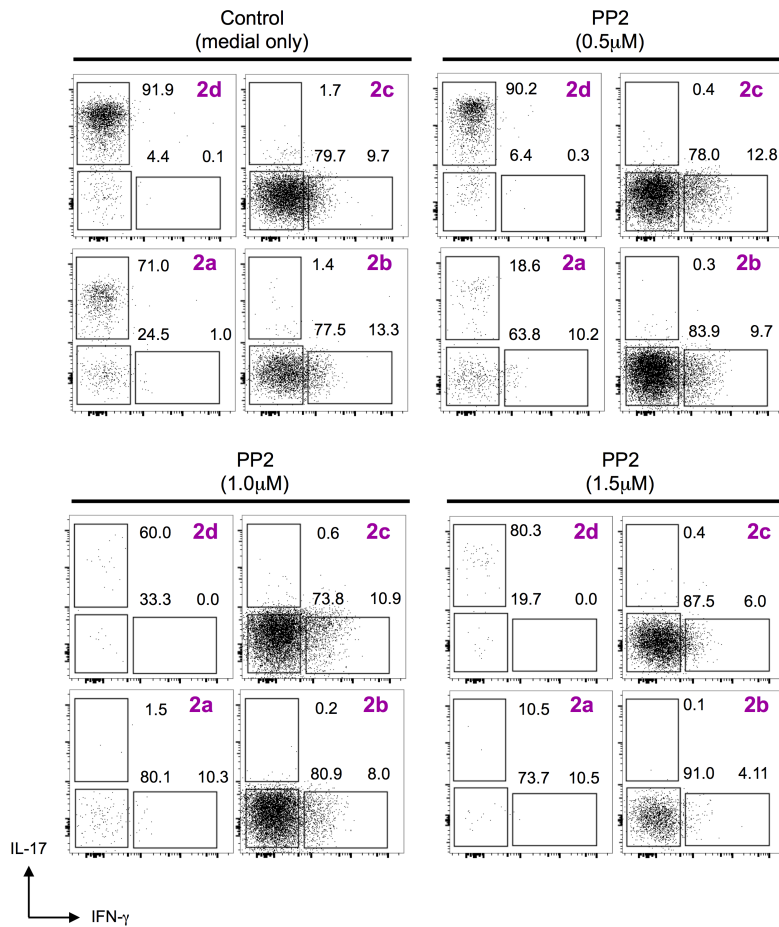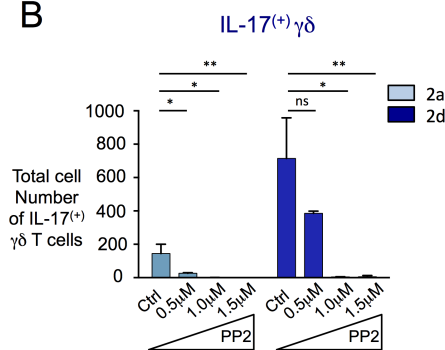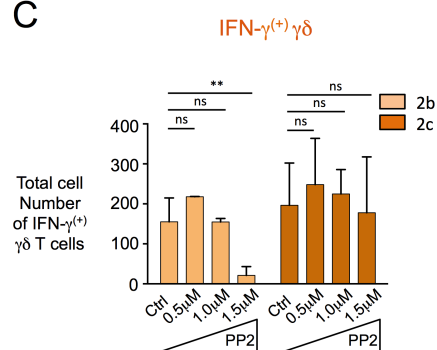
Figure 6.9 Inhibition of Lck impairs the development of IL-17A(+) γδ T cells. (A) Representative flow cytometry profiles (2≤n<4) of intracellular IL-17A and IFN-γ from the subsets 2a, 2b, 2c and 2d following 7-day FTOC supplemented with increasing concentrations of PP2 (B) Bar chart showing number of 2a and 2d IL-17A(+) γδ T cells following 7-day FTOC supplemented with PP2 (C) Bar chart showing number of IFN-γ(+) γδ T cells within the 2b and 2c subsets following 7-day FTOC supplemented with PP2. Error bars are SD; **p<0.01; *p<0.05; ns is for not significant.

6.6 Investigating the role of PI3K signalling in $\gamma\delta$ T cell development

The data presented above suggest that a certain windoaw of Lck activity is permissive for the developmet of IL-17A-secreting $\gamma\delta$ T cells. Thus, we hypothesized that this restricted Lck activity could activate a specific pathway that drives development of IL-17A-secreting $\gamma\delta$ T cells. This prompted investigation of alternative TCR signalling pathways that could be responsible for driving the development of IL-17A versus IFN-γ-secreting $\gamma\delta$ T cells. Phosphoinositide 3-kinase (PI3K) signalling represents a major signalling pathway in immune cells. Class IA PI3Ks are PI3Kα, PI3Kβ, and PI3Kδ, while PI3Kγ is a class IB PI3K (Okkenhaug and Vanhaesebroeck, 2003). PI3K signalling has been implicated in development of certain B cell subsets demonstrating its importance in lymphocyte development (Ramadani et al., 2010). Moreover, knocked-out PI3Kδ and PI3Kγ animals, where signallling through PI3Kδ and PI3Kγ was absent, were largely protected from imiquidod-induced psioriasis-like dermatitis, which was associated with reduced IL-17A in the lesion and a reduction in IL-17A-secreting $\gamma\delta$ T cells in the draining lymph node, suggesting that PI3K signalling is required for IL-17A cytokine secretion by $\gamma\delta$ T cells (Roller et al., 2012). Thus, this prompted us to investigate whether PI3K signalling could play a central role in the development of IL-17A-secreting $\gamma\delta$ T cells. To test this idea, we cultured E15 C57Bl/6 thymic lobes for 7-days supplemented with the pan-PI3K inihibitor ZSTK474. Inhibition of PI3K signalling largely supported our hypothesis, as the treatment

resulted in a significant reduction in the development of the IL-17A-committed « 2d » subset (Figure 6.10). Moreover, these cultures appeared to favour expansion of CD45RB$^{(+)}$CD44$^{(-)}$ « 2b » cells, and interestingly allowed both the 2b and 2c subsets to commit to IFN-γ secretion at far greater levels than control (Figure 6.10D).

Finally, to investigate the additive effects of TCR$\gamma\delta$ signalling (that reduces IL-17A-commited $\gamma\delta$ cell development) and PI3K inhibiton (that also reduces the generation of IL-17-specific $\gamma\delta$ T cells), we co-cultured E15 lobes with the pan-PI3K inhibitor and the TCRδ crosslinking antibody GL3. This resulted in an increased proportion of both 2b and 2c cells while the development of the 2a and 2d subsets was significantly compromised. Upon stimulation of the cells with PMA/ionomycin, we saw a clear reduction in IL-17A-producing $\gamma\delta$ cells, while the development of IFN-γ-producing $\gamma\delta$ T cells was largely favoured. This suggested that while PI3K signalling is required for IL-17A$^{(+)}$ $\gamma\delta$ T cell development, it also appears to inhibit commitment to IFN-γ-secretion in CD45RB$^{(+)}$ $\gamma\delta$ cells suggesting that a different signalling pathway is implicated in their development. Importantly, addition of GL3 and the PI3K inhibitor were additive, severely impairing IL-17A$^{(+)}$ $\gamma\delta$ T cell development.
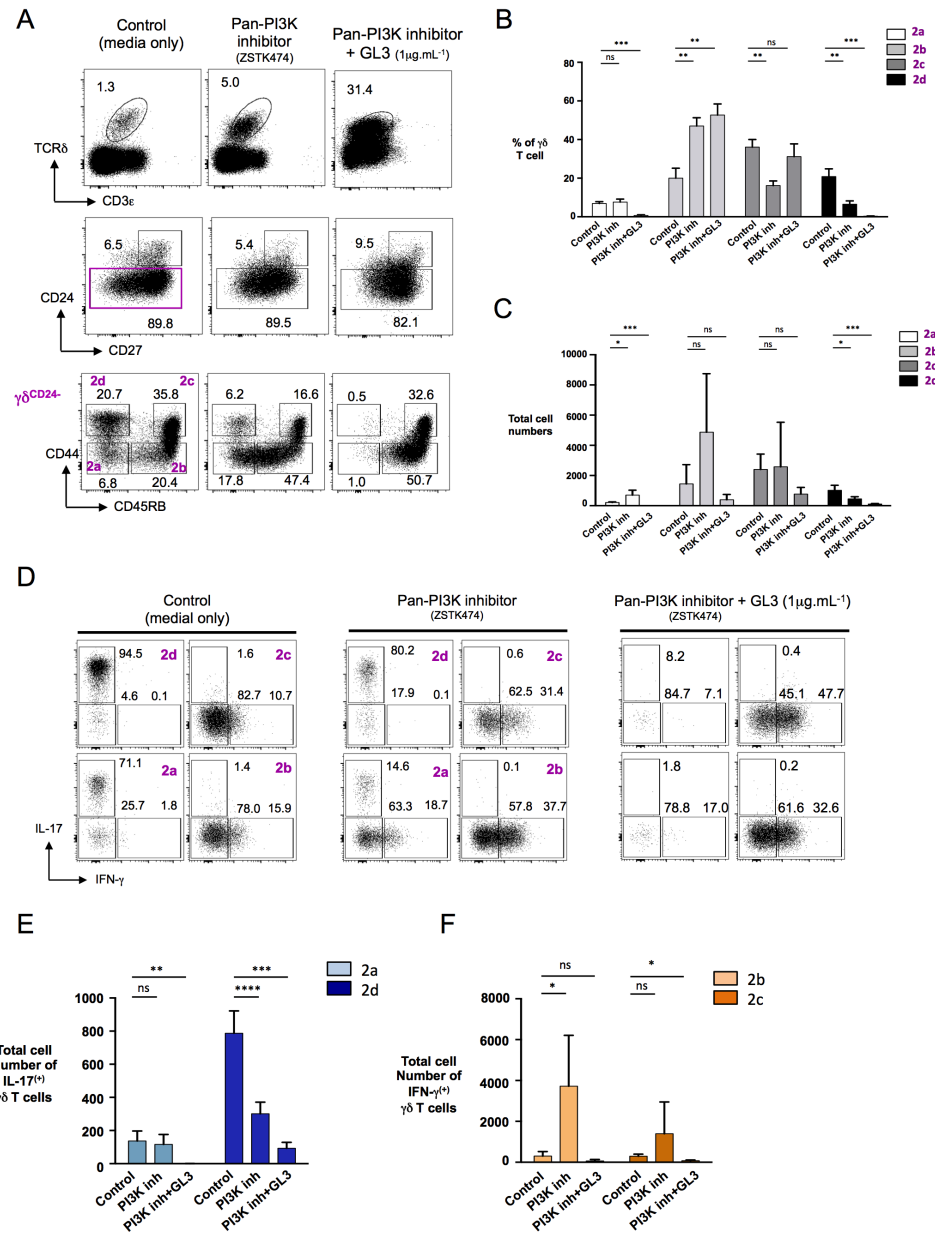
Figure 6.10 PI3K signalling is required for IL-17A$^{(+)}$γδ T cell development. (A) Representative flow cytometry profiles (n>3) of γδ T cells obtained from E15 FTOC following 7-day culture with pan-PI3K inhibitor alone or in addition to GL3. Summary bar graph (n>3) of the proportion (B) and total cell number (C) of each subset 2a, 2b, 2c, and 2d. (D) Representative flow cytometry plots (n>3) of intracellular IL-17A and IFN-γ. Percentages of IL-17$^{(+)}$ and IFN-γ$^{(+)}$ cells are indicated near each gates. (E) Summary bar graph (n>3) of the numbers of IL-17A-secreting γδ T cells amongst the 2a and 2d subset in control, Pan-PI3K inhibitor alone and in addition to GL3. (F) Summary bar graph (n>3) of the numbers of IFN-γ-secreting γδ T cells amongst the 2b and 2c subset in Pan-PI3K inhibitor and Pan-PI3K inhibitor plus GL3. Error bars are SD; ****p<0.0001, **p<0.01; *p<0.05; ns is for not significant.

6.7 Conclusion

Using previously published cell surface markers, we have identified six peripheral $\gamma\delta$ T cell subsets that were also found in the thymus of C57Bl/6 mice. We have investigated the role of TCR$\gamma\delta$ signal strength in the development of these different subsets and more specifically in the development of IL-17A$^{(+)}$ versus IFN-$\gamma^{(+)}$ $\gamma\delta$ T cells. We showed that strong TCR$\gamma\delta$ signalling was incompatible with the development of IL-17$^{(+)}$ $\gamma\delta$ T cells but that un-predictably, reducing TCR$\gamma\delta$ signal strength did not favour their development either. Instead, we have identified a previously unknown role for PI3K signalling in driving IL-17A$^{(+)}$ $\gamma\delta$ T cell development that at the same time restricts commitment of CD45RB$^{(+)}\gamma\delta$ T cells to IFN-γ secretion.

Chapter 7

Discussion and future work

Part I – $\alpha\beta$ T cell development

7.1 Introduction

TCR signalling is fundamentally important throughout T cell development as it participates in the generation of heterogeneous T cell subsets critical for immune responses against a wide range of infections. TCR signalling is widely accepted to instruct cell fate ($\alpha\beta$ or $\gamma\delta$ fate) at the DN3 stage of T cell development, as well as T cell survival (or death) at the DP stage during conventional $\alpha\beta$ T cell selection (Haks et al., 2005; Hayes et al., 2005). Although these developmental choices are often explained by a signal-strength-model, it remains unclear how seemingly equivalent "strong" signals through the TCR can instruct different cell fates. For example, strong agonist TCR$\alpha\beta$ signals at the DP stage of T cell development, can instruct either death by apoptosis or development into unconventional T cell subsets (Ashton-Rickardt et al., 1994; Jordan et al., 2001; Oh-Hora et al., 2013; Yamagata et al., 2004). Because all DP cells arise from DN3 cells that have successfully undergone β-selection, this led us to hypothesise that different signalling events at the DN stage of T cell development may contribute to the establishment of a heterogeneous DP pool, imprinting DP cells with different potentials to adopt alternative T cell fates. Traversing the β-selection checkpoint requires cell

surface expression of the preTCR complex composed of a rearranged TCRβ chain and an invariant pTα chain (Fehling et al., 1995). Importantly, pTα can generate two isoforms following alternative splicing; pTα^a or pTα^b (Barber et al., 1998). Although $\alpha\beta$ T cell development is undoubtedly severely impaired in the absence of pTα, very little is known about the differential roles of the pTα isoforms during T cell development (Gibbons et al., 2001). Despite having both been shown to efficiently form a preTCR complex, they differently affect cell-surface expression of TCRβ, and appear to be differentially expressed during T cell development possibly resulting in qualitatively, quantitatively or temporally different preTCR signals (Barber et al., 1998; Campese et al., 2009; Ramiro et al., 2001). This led us to hypothesise that differential use of the two pTα isoforms could have important consequences for the subsequent development of different T cell subsets by contributing to the generation of a heterogeneous DP subset.

Thus, this thesis has principally focused on understanding whether signalling events occurring at the DN stage of thymocyte development could be responsible for establishing a heterogenous DP subset; more precisely by generating DP cells that do not possess equal potential to adopt a conventional versus unconventional T cell fate. To directly test this hypothesis, we first assessed pTα isoform expression at the single cell level at the β-selection checkpoint. Then, with a focus on pTα^a, we subsequently investigated conventional T cell versus unconventional T cell development in BAC transgenic animals expressing pTα^a-only or FVB/n mice that we show over-express pTα^a compared to pTα^b. Finally, we have attempted to understand the

impact of "strong" signalling at the DN stage for conventional versus unconventional T cell development.

7.2 Alternative splicing of pTα^a and pTα^b is differently regulated during T cell development

Using PCR on single-sorted DN3 and DN4 thymocytes, we demonstrated that they can express pTα^a only, pTα^b only, or both isoforms simultaneously. This suggests that splicing to produce the two isoforms of pTα can be differentially regulated in single thymocytes despite them being at the same developmental stage. This could suggest that some degree of heterogeneity already exists among preTCR-expressing cells. As pTα^b transgenic mice have generally been shown to support early T cell development at the DN3 to DN4 transition (Gibbons et al., 2001), our results support our initial hypothesis that pTα^a and pTα^b may have different roles at the β-selection checkpoint. This is further supported by data generated by Juliet Mahtani-Patching (a former PhD student in the lab) who showed during her PhD that murine thymocyte subsets express variable amounts of pTα^a or pTα^b throughout T cell development (Mahtani-Patching, 2010). Whereas pTα^a expression is terminated at the DP stage of T cell development, Juliet showed that pTα^b expression is maintained up to the CD4[(+)] SP stage (Mahtani-Patching, 2010). In addition, Campese *et al.* (Campese et al., 2009) have shown that thymic CD4[(+)]CD25[(+)] T cells (which consist mainly of Foxp3[(+)] cells and thus are T regulatory cells) have a 2.7-fold increase in pTα^b expression compared to conventional CD4[(+)] T cells, and that

$pT\alpha^b$ was preferentially expressed over $pT\alpha^a$ in these cells. Moreover, data obtained by real-time PCR on human intra-thymic T cell subsets revealed a differential pattern of $pT\alpha$ isoform expression throughout human T cell development (Ramiro et al., 2001). The data presented in these studies were obtained by PCR carried out at the level of thymocyte subsets and could be investigated at the single-cell level with the optimized assay that we have developed. Thus, future work should focus on investigating $pT\alpha^a$ and $pT\alpha^b$ expression in murine ISP, DP, CD4SP and CD8SP subsets, as well as in IEL progenitors (DP^{dull} CD5$^{(+)}$TCR$\beta^{(+)}$PD-1$^{(+)}$CD69$^{(+)}$), and T regulatory cells. This could shed some insight onto the importance of each isoform for the development of certain subsets of T cells.

Interestingly, we show that FVB/n DN3 cells over-express $pT\alpha^a$ compared to C57Bl/6 cells. This difference is however not maintained at the DN4 stage of T cell development. These data add further weight to our idea that $pT\alpha$ isoforms are differently regulated throughout T cell development. This appears to be strain-dependent and should be considered when FVB/n mice are used as controls to study T cell development as it might have implications for some T cell development (e.g.FVB/n vs C57Bl/6).

Alternative mRNA splicing is a critical biological process, which allows the coding diversity of the genome to be significantly increased while being finely regulated. However, the regulators of alternative splicing during T cell development remain largely unstudied. It was recently described that an increase in expression of the RNA binding protein CELF2 (CUGBP, Elav-Like

Family Member 2) results in changes in mRNA splicing during T cell development (Mallory et al., 2015). Unfortunately, although CELF2 expression appeared to increase from the β-selection checkpoint up to the DP stage, alternative splicing of pTα isoforms was not investigated (Mallory et al., 2015). Conditional ablation in mice of the splicing regulator SC35 using a Lck-driven Cre/Loxp strategy showed a partial block in the DN to DP transition. Moreover, analysis of the DN compartment showed a slight increase in DN3 cells compared to WT controls reminiscent of the partial DN3 to DN4 block observed in our pTα^a.pT$\alpha^{-/-}$ mice. The authors attributed this phenotype to a clear reduction in expression of the alternative spliced CD45 isoform CD45RB, and preTCR isoforms were unfortunately not investigated (Wang et al., 2001).

Altogether these data support our initial hypothesis that pTα^a and pTα^b may have different roles at the β-selection checkpoint, but their physiological relevance during T cell development remains to be ascertained. Moreover, identifying alternative splicing regulators implicated in pTα regulation using a microarray approach should provide novel insight into the early stages of T cell development.

7.3 The timing of expression of the pTα^a transgene in pTα^a.pTα$^{-/-}$ mice

pTα^a.pTα$^{-/-}$ transgenic mice had been previously generated by the Hayday laboratory (Gibbons et al., 2001). However, pTα^a transgene expression was under the regulation of the Lck promoter, which despite being turned on as early as the DN3 stage of T cell development remains active during subsequent DP and SP stages of T cell development, during which pTα expression should normally be terminated (Mingueneau et al., 2013; Shimizu et al., 2001). We felt it was of critical importance to recapitulate physiological pTα expression for our transgenic mice. Indeed, the sustained expression of pTα has been associated with leukemogenesis and pTα transcripts were detected in human T-acute lymphoblastic leukaemias (T-ALL) (Bellavia et al., 2002). To circumvent such issues, we chose to investigate the role of pTα^a in T cell development using BAC transgenic mice that were generated in-house by a previous PhD student. Because the pTα^a BAC consists of a large piece of genomic DNA carrying both the pTα gene and its regulatory elements, choosing this approach should have faithfully recapitulated pTα expression during T cell development (Heintz, 2001). Constitutive pTα^a expression in FTOC was shown to be associated with ISP accumulation, a feature that was not observed in pTα^a.pTα$^{-/-}$ mice, supporting the idea that the expression of the pTα^a transgene is regulated to some extent throughout T cell development (Mahtani-Patching, 2010). We also show that the severely impaired DN to DP transition observed in pTα-deficient animals appear to be largely rescued by the pTα^a transgene. The proportion of

γδ T cells is also largely restored, suggesting that the pTα^a transgene efficiently signals (with TCRβ) to divert thymocytes away from a γδ T cell fate. By contrast, total thymic cellularity remains significantly lower in pTα^a.pTα$^{-/-}$ mice compared to C57Bl/6 mice and more in-depth analysis of the DN subsets revealed a subtle block at the DN3 to DN4 transition. Although the lack of pTα^b in pTα^a.pTα$^{-/-}$ mice could be a possible explanation for the phenotype described here, these data could also be due to non-physiological pTα^a expression. Thus, this raises the possibility of a timing of expression issue with our pTα^a transgene in pTα^a.pTα$^{-/-}$ mice. Although this possibility was considered during my PhD, I have been unable to fully investigate it due to optimization problems with the real time PCR assay described earlier, when assessing pTα^a expression in FVB/n DN3 and DN4 subsets. This may be due to the presence of truncated WT pTα transcripts in pTα^a.pTα$^{-/-}$ mice (where exon 3 and 4 have been replaced by a neomycin gene), creating some form of competition, and impeding good target amplification. Future work should focus on assessing transgene expression during T cell development in both the WT and transgenic mice. If the pTα^a transgene is shown to be expressed either earlier or later than it would normally be expressed, it would suggest that some of the phenotypes observed in these mice may be due to this issue.

7.4 PreTCR^a signals more weakly than preTCR^b

FVB/n mice, which over-express pTα^a transcripts in DN3 cells compared to C57Bl/6 cells, have a partially impaired DN3 to DN4 transition and a lower CD5

expression on post-β-selected DN cells. Similar data were obtained with pTα^a.pT$\alpha^{-/-}$ mice, which only express pTα^a at the DN stage of T cell development. Levels of CD5 are modulated throughout T cell development and are considered to positively represent the strength of TCR signal received by a particular cell (Azzam et al., 1998). Post-β-selected DN3 cells from FVB/n and pTα^a.pT$\alpha^{-/-}$ mice both express lower cell surface levels of CD5 compared to WT C57Bl/6 cells. Thus, we suggest that post-β-selected DN3 cells from FVB/n and pTα^a.pT$\alpha^{-/-}$ mice have received a weaker signal than in "normal" WT C57Bl/6 mice. Although this idea could and should be validated by other approaches such as the phosphorylation state of TCRζ, it is consistent with the study of Barber *et al.* who demonstrated that transfection of pTα^a into TCRβ-expressing cells resulted in a reduction of TCRβ expression compared to pTα^b, highlighting that the different isoform of pTα regulate TCRβ expression to different extents. Furthermore, FTOC data generated in the lab have shown that cell surface expression of preTCR^b is greater than preTCR^a (Mahtani-Patching, 2010). Indeed, differences in TCR cell surface expression is often thought to translate into quantitatively different and thus perhaps also qualitatively different intracellular signals (Hayes et al., 2005). Thus, one could hypothesise that preTCR^a and preTCR^b deliver qualitatively different signals at the β-selection checkpoint, which might account for differences in subsequent T cell development (further discussed below).

7.5 Signal strength at the DN stage and acquired CD5 levels may influence subsequent T cell selection

Paul Love and colleagues have shown using transgenic TCR$\alpha\beta$ mice that the levels of CD5 expression on developing thymocytes could affect DP cell sensitivity during positive/negative selection (Azzam et al., 2001). Indeed, using both MHC-I- and MHC-II-restricted transgenic TCR$\alpha\beta$ mice (P14, H-Y, D010.10 TCR, AND transgenic TCRs recognizing lymphocytic choriomeningitis virus, a male antigen, ovalbumin peptide and pigeon cytochrome c respectively) they showed that over-expression of CD5 resulted in a decrease of SP cells whereas ablation of CD5 "accelerated" SP development (Azzam et al., 2001; Azzam et al., 1998; Kaye et al., 1989; Murphy et al., 1990; Pircher et al., 1989). Indeed, increasing cell sensitivity to MHC/self-peptide interactions by reducing CD5 levels allowed positive selection of previously un-selected TCRs resulting in a greater proportion of SP thymocytes. This can be explained by the fact that TCR affinity for MHC/self-peptide is believed to adopt a pyramid-like shape (as suggested by work carried out on T regulatory cells) (Hogquist et al., 2005; Jordan et al., 2001). Thus, a larger number of DP cells express TCRs with very weak affinity to MHC/self-peptide while very few display TCRs with high affinity to MHC/self-peptide. Altogether, this study supports a model where CD5 levels on DP thymocytes affect positive selection and in turn development of SP thymocytes.

In this thesis, CD5 levels are used to suggest that pTα^a signals weakly at the β-selection checkpoint, as shown in FVB/n and pTα^a.pT$\alpha^{-/-}$ mice compared to

C57Bl/6 mice (discussed above). This is associated in the gut with a reduced proportion of unconventional TCR$\alpha\beta^{(+)}$CD8$\alpha\alpha^{(+)}$IELs, whereas conventional T cells appear largely rescued, in comparison with pT$\alpha^{-/-}$ and C57Bl/6 mice. Importantly, unconventional TCR$\alpha\beta^{(+)}$CD8$\alpha\alpha^{(+)}$IELs are thought to express TCRs with high(er) affinity to MHC/self-peptide and undergo "agonist" selection in the thymus (Yamagata et al., 2004). Conversely, "stronger" signalling at the DN stage of T cell development through the premature expression of TCR$\alpha\beta$ complexes in OT-II and pT$\alpha^{-/-}$.TCR$\delta^{-/-}$ mice was associated with increased CD5 expression at the DN stage and an increased relative proportion of unconventional TCR$\alpha\beta^{(+)}$CD8$\alpha\alpha^{(+)}$IELs. This led us to hypothesise that the strength of signal "recorded" by developing thymocytes at the β-selection checkpoint would dictate subsequent CD5 expression levels, which in turn would influence DP sensitivity to TCR signals during positive/negative selection. Thus, weak signalling at the DN stage would translate to low CD5 and a greater cell sensitivity to TCR signals. This would potentially select a larger proportion of SP thymocytes as seen in FVB/n and pTα^a.pT$\alpha^{-/-}$ mice. Consistent with this, we show that FVB/n and pTα^a.pT$\alpha^{-/-}$ mice have a reduced CD69$^{(-)}$DP to CD69$^{(+)}$DP ratio suggesting that a greater proportion of DP thymocytes have been positively selected compared to C57Bl/6 mice. This also correlated with a decrease DP-to-SP ratio in FVB/n and pTα^a.pT$\alpha^{-/-}$ mice compared to C57Bl/6 mice. By contrast, stronger signalling at the DN stage, through either preTCR[b] (possibly-yet to be confirmed experimentally) or through prematurely-expressed TCR$\alpha\beta$ complexes like in OT-II and pT$\alpha^{-/-}$.TCR$\delta^{-/-}$ mice, triggers greater CD5 upregulation that decreases DP cell sensitivity to TCR signals. This would partially impede positive selection of conventional T cells, but would perhaps

favour unconventional T cell development. This hypothesis could explain why a seemingly equivalent "strong" signal at the DP stage can in one case trigger positive selection of unconventional T cells, while also promoting apoptosis and death of conventional T cells. This hypothesis is supported by our data from CD5$^{-/-}$ mice which have a reduced DP-to-SP ratio compared to C57Bl/6 mice. However, the reduced DP-to-SP ratio in CD5-overexpressing mice would not be consistent with this hypothesis. Importantly, expression of the CD5 transgene in CD5Tg mice is under the regulation of the CD2 promoter and is thus expressed early in T cell development (Azzam et al., 2001). This might have affected signal strength in DN3 cells and thus might not have been the ideal model to investigate our hypothesis.

To assess and compare the sensitivity of DP thymocytes in C57Bl/6, FVB/n and pTα^a.pT$\alpha^{-/-}$ strains we thought to measure the amplitude of Ca$^{(2+)}$ signalling following TCR cross-linking as this is known to correlate with TCR signal strength (Mariathasan et al., 1998). Thus, we hypothesised that DP cells from FVB/n and pTα^a.pT$\alpha^{-/-}$ mice would be more sensitive to TCR cross-linking than C57Bl/6 cells and would in turn flux greater amounts of Ca$^{(2+)}$. Unfortunately, due to technical issues, we were unable to carry out this experiment. Indeed, we were unable to visualise calcium influx following anti-CD3 crosslinking by flow cytometry in control C57Bl/6 cells.

A similar approach could be undertaken by crossing FVB/n and pTα^a.pT$\alpha^{-/-}$ mice with Nur77-GFP mice, which express GFP under the control of the Nur77 promoter and has been shown to be a good indicator of the TCR signal

received by cells(Moran et al., 2011). Thus, this could be a useful read out of the DP sensitivity. One would expect Nur77 expression to be greater in CD69$^{(+)}$DP cells from FVB/n and pTα^a.pT$\alpha^{-/-}$ mice compared to C57Bl/6 mice.

The sensitivity of the cell could also be investigated in terms of negative selection, which can be assessed by superantigen-mediated deletion of cells that expressed certain TCR-Vβ chains. Superantigens derive from the "remains" of endogeneous retroviruses belonging to the mouse mammary tumour virus family (MMTV) that have long ago integrated into the mouse genome. Recognition of thymus-associated superantigens through TCRβ/MHC interactions triggers a very strong TCR signal resulting in the negative selection of developing DP cells expressing specific TCR-Vβ chains. Thus for instance, recognition of Mtv9 results in the deletion of TCRVβ8-expressing T cells (Acha-Orbea et al., 1991).

Superantigens represent a useful tool to analyse negative selection. However, C57Bl/6 mice, and thus pTα^a.pT$\alpha^{-/-}$ mice (on a C57Bl/6 background), lack the MHC-II I-Eα chain involved in superantigen presentation and thus superantigen-specific T cells do not undergo negative selection in these animals. To overcome this issue, β-selected DN3 thymocytes from pTα^a.pT$\alpha^{-/-}$ mice, expressing low CD5 levels, could be sorted and used to repopulate thymic lobes obtained from mice sufficient for I-Eα, such as BALB/c mice. I-Eα-expressing stromal cells should then present superantigens and induce negative selection in pTα^a.pT$\alpha^{-/-}$-derived DP cells. The Vβ usage of SP thymocytes could then be assessed, which could be used as a read out of

effective negative selection was and to ascertain whether their sensitivity to TCR signalling is altered.

We show in this thesis that the "accelerated" DP-to-SP transition in FVB/n and $pT\alpha^a.pT\alpha^{-/-}$ mice does not correlate with the size of the thymus. However, this could be due to environmental cues from the thymic stroma. To confirm that this feature is cell-intrinsic, future work could generate mixed bone marrow chimeras where C57Bl/6 and $pT\alpha^a.pT\alpha^{-/-}$ -derived bone marrow are used to reconstitute irradiated C57Bl/6 mice. Investigating T cell development in these reconstituted animals should allow us to confirm that this altered DP-to-SP transition is cell intrinsic.

In summary, we propose a model where the strength of signal at the β-selection checkpoint subsequently affects positive/negative selection of $\alpha\beta$ T cells at the DP stage (Figure 7.1). This supports our original hypothesis that signalling events at the DN stage of T cell development may be responsible for establishing heterogeneity in the DP subset.
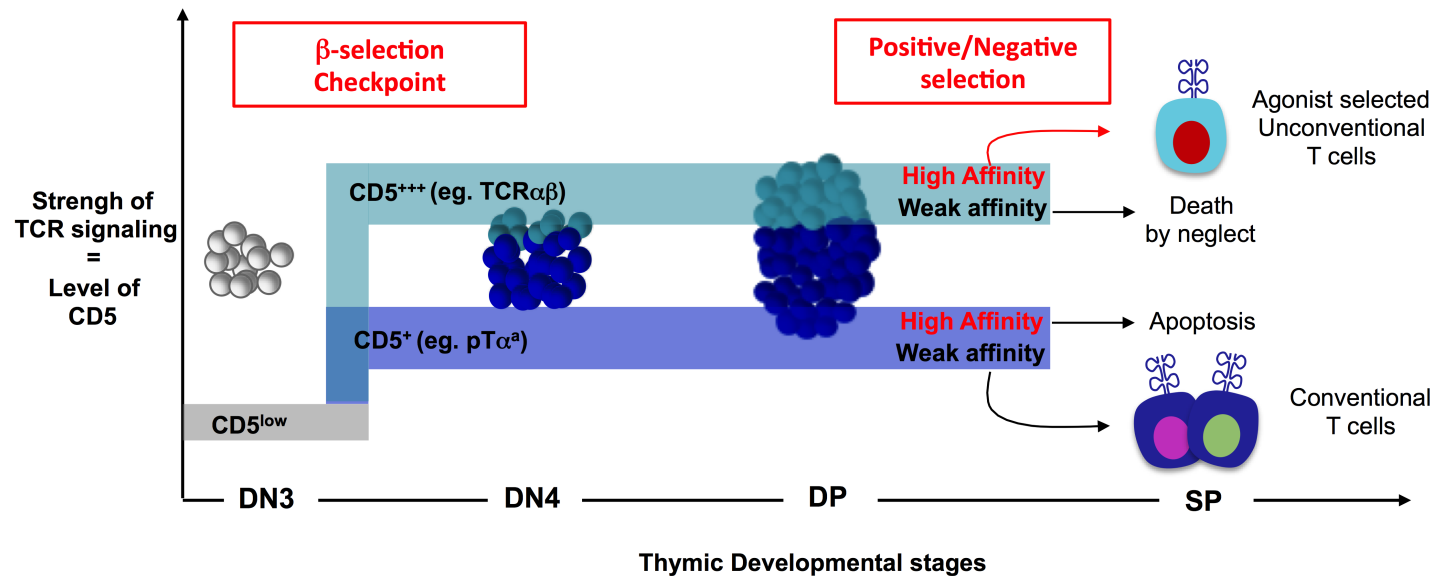
Figure 7.1 A possible model: Signal strength at the DN stage finely tunes DP cell sensitivity and subsequently impacts on the positive/negative selection of DP cells in the DP-to-SP transition. We propose that DN3 cells (that are CD5^{low}) expressing pTα^a at the β-selection checkpoint would express lower CD5 levels than cells expressing stronger signalling TCR complexes such as TCR$\alpha\beta$, which then finely tunes their sensitivity to subsequent T cell selection. Low-CD5 expressing cells interacting with agonist self-peptide/MHC complex would undergo negative selection and die by apoptosis while interactions with weaker affinity peptide/MHC should drive DP cells to adopt a conventional T cell fate. By contrast, high CD5-expressing cells, which should be less sensitive to strong signals, should now be positively selected on agonist-selecting ligands and thus adopt an unconventional T cell fate. Altogether, this hypothesis suggests that signalling events occurring at the DN stage of T cell development would participate in the establishment of a heterogenous DP subset.

7.6 PreTCR^a signalling may be dominant to that of preTCR^b

Interestingly, despite expressing the same level of pTα^b transcripts as C57Bl/6 DN3 cells, FVB/n cells express lower levels of CD5 similar to pTα^a.pT$\alpha^{-/-}$ mice. This suggests that over-expression of pTα^a leads to a dominant phenotype when co-expressed with pTα^b. These data are in agreement with those from Juliet Mahtani-Patching showing that co-expression of pTα^a and pTα^b in FTOC promoted accumulation of ISPs to a similar extent as FTOC with pTα^a only. These results suggest that pTα^b may need to be expressed alone or in excess to be able to exert its effect. If revealed to be true, it also raises the question of how weak signals can be dominant over stronger ones. This may be due to the high endocytosis rate of pTα^a over pTα^b. Once paired with TCRβ, the whole preTCR^a complex is likely to be endocytosed resulting in a lower cell surface expression and thus a reduced signal strength.

7.7 Signal strength at the DN stage may influence T cell proliferation, which may subsequently affect T cell development

Recent transcriptional analysis of pre- and post-β-selected DN3 cells revealed that progression through the β-selection checkpoint was associated with a dramatic shift in the thymocyte transcriptome with most of the identified genes

implicated in metabolism and proliferation (>48% of upregulated genes were linked to proliferation) (Mingueneau et al., 2013). Indeed, signalling through the preTCR together with notch and IL-7Rα signalling triggers a c-myc-dependent burst of proliferation important for subsequent T cell development (Ciofani et al., 2004; Kreslavsky et al., 2012; Maillard et al., 2006; Sicinska et al., 2003).

The significantly reduced thymic cellularity (and thus DP cell numbers) described in this thesis for the pTα^{a}.pT$\alpha$$^{-/-}$ mice does not appear to result from an inability of the pTα^{a} transgene to signal as part of the preTCR, as pTα^{a}.pT$\alpha$$^{-/-}$ mice have a reduced proportion of $\gamma\delta$ T cells, a substantial pool of DP cells, and mature thymic and peripheral CD4$^{(+)}$ and CD8$^{(+)}$ T cells compared to pTα-deficient mice. An altered ability for T cell precursors to undergo proliferation may thus be an explanation for the reduced thymic cellularity of pTα^{a}.pT$\alpha$$^{-/-}$ mice. Indeed, cyclin D3-deficient mice have an impaired proliferation of immature DN4 and ISP cells resulting in reduced thymic cellularity, reminiscent of the phenotype observed in pTα^{a}.pT$\alpha$$^{-/-}$ mice (Sicinska et al., 2003). Interestingly, Kreslavsky *et al*. recently demonstrated that differentiation and proliferation were actually two intertwined processes triggered at the β-selection checkpoint through preTCR signalling (Kreslavsky et al., 2012). In this study, only DN3 cells that had undergone four or more rounds of division in the presence of the preTCR efficiently progressed to the DP stage of T cell development in a OP9-DL1 system (Kreslavsky et al., 2012). Based on this study, the presence of DP cells and mature SP cells in pTα^{a}.pT$\alpha$$^{-/-}$ mice suggests at least in some DN cells the pTα^{a} transgene successfully induced proliferation (at least four rounds). The transferrin receptor, CD71, is up-

regulated in a c-myc dependent manner when cells increase their metabolism, for example during proliferation (Brekelmans et al., 1994). We show that proportions of CD71$^{(+)}$i.c.TCRβ$^{(+)}$DN3 cells are similar between C57Bl/6 and pTα^a.pTα$^{-/-}$ mice suggesting that the pTα^a transgene successfully enhanced metabolism and proliferation (Janas et al., 2010; O'Donnell et al., 2006). However, we show that FVB/n and pTα^a.pTα$^{-/-}$ mice have a higher DN3/DN4 ratio than C57Bl/6 mice that could illustrate a lack of proliferation in DN4 cells. Consistent with this idea, some preliminary data suggest that there is a lower proportion of DN4 CD71$^{(+)}$ cells in FVB/n and pTα^a.pTα$^{-/-}$ mice compared to C57Bl/6 mice. This is likely to reflect a reduced proliferative state of certain DN4 cells. Thus, further investigation of the proliferation state of post-β-selected DN3 and DN4 pTα^a.pTα$^{-/-}$ cells compared to C57Bl/6 cells using a CFSE assay, or by measuring Ki67 expression should be considered.

Importantly, pTα^a.pTα$^{-/-}$ mice lack a substantial proportion of unconventional TCRαβ$^{(+)}$CD8αα$^{(+)}$ IELs. Thus, one could hypothesise that pTα^a transgene-induced proliferation is insufficient to generate DP cells that can subsequently differentiate into unconventional TCRαβ$^{(+)}$CD8αα$^{(+)}$ IELs. Increasing TCR signal strength with increasing doses of anti-CD3 cross-linking antibody or by using increasing doses of OVA in OT-II mice, was recently shown to positively correlate with the burst of proliferation (Au-Yeung and Zikherman, 2014). Thus, greater TCR signal appears to trigger greater proliferation. β-selected DN3 cells from pTα^a.pTα$^{-/-}$ mice express significantly lower CD5 than C57Bl/6 mice suggesting that preTCR signalling was weaker in these animals. Thus, one could consider that weak signalling through the preTCR^a transgene induces less

proliferation that is sufficient for development of conventional T cells but not for unconventional TCR$\alpha\beta^{(+)}$CD8$\alpha\alpha^{(+)}$ IEL development. By contrast, stronger signalling could induce greater proliferation allowing DN and subsequently DP cells to acquire a certain phenotype that permits unconventional TCR$\alpha\beta^{(+)}$CD8$\alpha\alpha^{(+)}$ IEL development (Au-Yeung and Zikherman, 2014). Data obtained with FVB/n mice support this hypothesis as DN3 cells also express lower CD5 levels than C57Bl/6 DN3 thymocytes. Thus, we propose a model where the proliferative state of DN cells subsequently affects their ability to adopt a conventional versus unconventional T cell fate.

7.8 pTα^b transgenic mice

One of the aims of this thesis was to investigate the role of pTα^b in T cell development using BAC-transgenic mice. Although the pTα^b transgenic animals were generated towards the end of my PhD, it took significant time to backcross these mice onto a background that was deficient for the two endogeneous pTα alleles. Thus, preliminary results were obtained from pTα^b BAC transgenic animals onto a pT$\alpha^{-/+}$ background. Based on our initial hypothesis, "stronger" signalling at the DN stage of T cell development, potentially delivered by pTα^b, should have skewed T cell development towards an unconventional T cell fate resulting in a reduced ratio of TCR$\alpha\beta^{(+)}$CD8$\alpha\beta^{(+)}$ to TCR$\alpha\beta^{(+)}$CD8$\alpha\alpha^{(+)}$ IELs. Unfortunately, this was not the case as pTα^b.pT$\alpha^{-/+}$ mice had a phenotype very similar to pT$\alpha^{-/+}$ controls in terms of thymic cellularity, proportion of $\gamma\delta$ T cells, the efficiency of the DN to DP transition and proportion of TCR$\alpha\beta^{(+)}$CD8$\alpha\beta^{(+)}$

and $TCR\alpha\beta^{(+)}CD8\alpha\alpha^{(+)}$ IELs. This is likely due to the presence of WT-$pT\alpha$ allele. These animals will be further investigated once the strains have been backcrossed onto a "pure" $pT\alpha$-deficient background.

7.9 C57Bl/6, BALB/c and FVB/n mice have different ratios of conventional $TCR\alpha\beta^{(+)}CD8\alpha\beta^{(+)}$ IELs to unconventional $TCR\alpha\beta^{(+)}CD8\alpha\alpha^{(+)}$ IELs

One of the aims of this thesis was to use different strains of WT mice, here C57Bl/6, BALB/c and FVB/n, to shed light on unconventional $TCR\alpha\beta^{(+)}CD8\alpha\alpha^{(+)}$ IEL development. We show in this thesis that FVB/n mice have an increased ratio of conventional $TCR\alpha\beta^{(+)}CD8\alpha\beta^{(+)}$ IELs to unconventional $TCR\alpha\beta^{(+)}CD8\alpha\alpha^{(+)}$ IELs compared to C57Bl/6 and BALB/c mice, whereas this ratio is largely reduced in BALB/c mice compared to C57Bl/6 and FVB/n mice. Importantly, no differences were observed for $TCR\gamma\delta^{(+)}$ IELs. This gut phenotype was mirrored in the thymus with a decrease or increase of $CD4^{(-)}CD8^{(-)}TCR\beta^{(+)}CD5^{(+)}$ IEL progenitors for FVB/n and BALB/c mice respectively (compared to C57Bl/6 mice). Due to time constraints, we principally used FVB/n mice to understand the role of "weak" signalling at the DN stage of T cell development and its impact on conventional versus unconventional $TCR\alpha\beta^{(+)}CD8\alpha\alpha^{(+)}$ IEL development, but future work should further focus on BALB/c mice. Importantly, these data were unpredicted and demonstrate that different strains of WT mice are different to one another and may be useful tools when studying immunopathologies of the gut. Despite all three strains being

purchased from Charles River, one could hypothesise that this phenotype occurs because of differences in gut microbiota rather than differences in TCR$\alpha\beta^{(+)}$CD8$\alpha\alpha^{(+)}$ IEL development. To investigate this idea, two WT strains could be bred together (e.g. C57Bl/6 and BALB/c) and the gut IEL populations analysed. A similar experiment where offspring from one strain could be "cross-fostered" with the mother of the other strain would allow us to assess the role of microbiota on TCR$\alpha\beta^{(+)}$CD8$\alpha\alpha^{(+)}$ IEL proportions and maintenance as it is thought that the mother is responsible for shaping the microbiota of her pups (Daft et al., 2015).

The developmental pathway of unconventional TCR$\alpha\beta^{(+)}$CD8$\alpha\alpha^{(+)}$ IELs has been the source of lengthy debate. Thus, FVB/n, BALB/c and C57Bl/6 mice may be useful models to understand the developmental requirements for unconventional TCR$\alpha\beta^{(+)}$CD8$\alpha\alpha^{(+)}$ IELs by, for instance, carrying out a microarray assay on the newly described IEL progenitor DP^{dull} TCR$\alpha\beta^{(+)}$CD5$^{(+)}$PD1$^{(+)}$CD69$^{(+)}$CD122$^{(+)}$ cells from these three strains. This experiment would allow the identification of genes that are differently expressed and that may be implicated in unconventional TCR$\alpha\beta^{(+)}$CD8$\alpha\alpha^{(+)}$ IEL development.

7.10 Conclusion part I

Here, we show that single DN3 and DN4 cells can express pTα^{a}-only, pTα^{b}-only or both isoforms simultaneously suggesting that each isoform might have a non-redundant role at the β-selection checkpoint. We also show that β-selected

DN3 thymocytes from FVB/n and $pT\alpha^a.pT\alpha^{-/-}$ mice express lower levels of CD5 compared to C57Bl/6 cells, suggesting that they have received a "weaker" signal at the β-selection checkpoint. This is associated in the gut with a reduced $TCR\alpha\beta^{(+)}CD8\alpha\alpha^{(+)}$ IEL compartment. By contrast, premature expression of $TCR\alpha\beta$ complexes at the DN stage, generates a "stronger" signal as depicted by greater CD5 expression on DN thymocytes and is associated with an increased $TCR\alpha\beta^{(+)}CD8\alpha\alpha^{(+)}$ IEL compartment. Thus, quantitative different signals at the DN stage of T cell development appears to differently affect the development of conventional $TCR\alpha\beta^{(+)}CD8\alpha\beta^{(+)}$ IELs or unconventional $TCR\alpha\beta^{(+)}CD8\alpha\alpha^{(+)}$ IELs. We present two possible models to explain these observations: In the first model, we propose that the strength of signal recorded by developing DN cells positively correlate with CD5 levels, which in turn finely tunes the cell sensitivity to subsequent T cell selection events at the DP stage of T cell development, thus affecting development of conventional versus unconventional T cells. Our second model propose that the strength of signal delivered at the DN stage of T cell development is responsible for triggering different burst of proliferation which in turn imprint T cells to adopt a conventional or unconventional T cell fate. In sum, the data presented in this thesis support our initial idea that signalling events at the DN stage of T cell development may have fundamental consequences on subsequent T cell selection and development.

Part II – γδ T cell development

7.11 Introduction

αβ and γδ T cells share the immature DN stages of T cell development. Commitment to an αβ or γδ T cell fate occurs at around the DN3 stage and is generally accepted to be driven by quantitatively different signals delivered by preTCR or TCRγδ complexes, respectively (Hayes et al., 2005, Zarin et al., 2014). Indeed, the current consensus view suggests that "weak" signalling through the preTCR promotes αβ T cell development whereas "stronger" signalling through TCRγδ triggers DN3 progenitors to adopt a γδ T cell fate. Strong signals are generally thought to be the consequence of ligand recognition, exemplified during αβ T cell selection, but very few TCRγδ ligands have yet been identified, questioning their requirements for γδ T cell development. Indeed, The higher surface expression of TCRγδ compared to the preTCR, which is highly endocytosed and thus signals more weakly, could account for its increased signal strength even in the absence of ligand recognition (Azzam et al., 1998; Panigada et al., 2002). Moreover, it has remained unclear how a strong signal at the DN3 stage could first drive γδ T cell lineage commitment, but then have a differential influence of subsequent γδ T cell developmental outcome with respect to commitment to IL-17A versus IFN-γ-production (Prinz et al., 2013). Because investigation of these questions has been partially impeded by the lack of a very defined sequence of γδ T cell developmental stages, the lab has proposed a new combination of cell-surface

markers that precisely distinguishes the IL-17A- versus IFN-γ-specific $\gamma\delta$ T cell developmental pathways, which we have subsequently used to provide novel insight on the TCR$\gamma\delta$ signalling requirements for driving IL-17A versus IFN-γ-secreting $\gamma\delta$ T cell development.

7.12 IL-17A- versus IFN-γ-commited $\gamma\delta$ T cell developmental pathways can be identified through the combinatorial use of CD24, CD44 and CD45RB.

The lack of a consensus methodology to define thymic $\gamma\delta$ T cell subsets has partially impeded investigations into understanding the role of TCR$\gamma\delta$ at different stages of $\gamma\delta$ T cell development. Indeed, although cell surface expression of CD27 has widely been used to distinguish IL-17A or IFN-γ secreting $\gamma\delta$ T cells, some CD27$^{(-)}$ $\gamma\delta$ T cells do produce some IFN-γ upon stimulation (Ribot et al., 2009). Using new conbinations of previously published markers, the data in this thesis demonstrate the identification of two clear pathways of $\gamma\delta$ T cell development where CD24$^{(-)}$CD44$^{(-)}$CD45RB$^{(-)}$ $\gamma\delta$ T cell progenitors diverge by either up-regulating CD44 or CD45RB. This generates either CD24$^{(-)}$CD44$^{(+)}$CD45RB$^{(-)}$ or CD24$^{(-)}$CD44$^{(-)}$CD45RB$^{(+)}$ $\gamma\delta$ T cells, which clearly segregate with IL-17A or IFN-γ secreting potential, respectively. Consistent with IL-17A-secreting potential, CD24$^{(-)}$CD44$^{(+)}$CD45RB$^{(-)}$ cells but not CD24$^{(-)}$CD44$^{(-)}$CD45RB$^{(+)}$ cells express IL-7Rα (Michel et al., 2012). Conversely, consistent with an IFN-γ-secreting phenotype, CD24$^{(-)}$CD44$^{(int)}$CD45RB^{high} $\gamma\delta$ T cells express NK1.1 (Haas et al. 2009). Other

studies have suggested that IL-17-producing $\gamma\delta$ T cells can be defined by the transcription factors RORγt, and SOX13 whereas IFN-γ-producing $\gamma\delta$ T cells express T-bet (Gray et al., 2013; Turchinovich and Hayday, 2011). Thus, it would be interesting to investigate RORγt, SOX13 and T-bet expression in CD24$^{(-)}$CD44$^{(+)}$CD45RB$^{(-)}$ and CD24$^{(-)}$CD44$^{(-)}$CD45RB$^{(+)}$ $\gamma\delta$ T cells. Moreover, the B cell specific Src kinase, B lymphoid kinase (Blk) was recently implicated in IL-17-producing $\gamma\delta$ T cell development, and thus future work should confirm that its expression is confined to CD24$^{(-)}$CD44$^{(+)}$CD45RB$^{(-)}$ $\gamma\delta$ T cells (Laird et al JI. 2010). Finally, cell surface expression of CD73 was recently suggested to correlate with ligand engagement by $\gamma\delta$ T cells and CD73$^{(+)}$ $\gamma\delta$ T cells have been shown to principally secrete IFN-γ. Thus, CD73 expression could be analysed on CD24$^{(-)}$CD44$^{(int/-)}$CD45RB^{high} cells (Coffey et al., 2014).

Analysis appears to suggest that both CD24$^{(-)}$CD44$^{(+)}$CD45RB$^{(-)}$ and CD24$^{(-)}$CD44$^{(-)}$CD45RB$^{(+)}$ $\gamma\delta$ T cell subsets develop from a common CD24$^{(-)}$CD44$^{(-)}$CD45RB$^{(-)}$ progenitor and that an IL-17-A-secreting potential is gradually acquired following CD44 up-regulation whereas acquisition of an IFN-γ- secreting potential occurs through up-regulation of CD45RB and then (partially) CD44 following a CD24$^{(-)}$ CD44$^{(-)}$ CD45RB$^{(-)}$ $\rightarrow$ CD24$^{(-)}$ CD44$^{(-)}$ CD45RB$^{(+)}$ $\rightarrow$ CD24$^{(-)}$ CD44$^{(int)}$ CD45RB^{high} pathway. Development through these sequential steps should be further investigated and confirmed by analysing $\gamma\delta$ T cell subsets at different time points in mouse embryonic development or by culturing these different subsets on OP9-DL1 cells to follow their development (Holmes and Zuniga-Pflucker, 2009). OP9-DL1 cells are bone-marrow-derived stromal cells expressing delta like ligand 1 (DL1) and that

support T cell differentiation and development *in vitro*. Although further work is required to fully characterise these subsets (e.g. at the transcriptional level), a novel methodology has been developed using CD24, CD44 and CD45RB that precisely identifies the developmental pathways of IL-17A- versus IFN-γ producing $\gamma\delta$ T cells.

7.13 Strong TCR$\gamma\delta$ signalling does not favour commitment to an IL-17A-secreting $\gamma\delta$ T cell fate

It was suggested that thymic $\gamma\delta$ T cell progenitors that do not engage a thymic TCR$\gamma\delta$ ligand adopt an IL-17A-producing fate, whereas "ligand-experienced" $\gamma\delta$ T cell progenitors principally develop to secrete IFN-γ (Jensen et al., 2008). Consistent with this, we show that cross-linking of TCRδ with the anti-TCRδ antibody GL3, that is widely considered to increase signal strength and mimic TCR$\gamma\delta$ ligand engagement, inhibited development of IL-17A-secreting $\gamma\delta$ T cells, while favouring the CD45RB developmental pathway. Importantly, the few CD44$^{(+)}$CD45RB$^{(-)}$ cells that did develop under these conditions secreted significantly less IL-17A than controls further suggesting that cross-linking of TCR$\gamma\delta$ does not favour an IL-17A-secreting $\gamma\delta$ T cell fate. A possible explanation for the appearance of some CD44$^{(+)}$CD45RB$^{(-)}$ cells could be that FTOC were set up with thymic lobes dissected from E15 embryos, in which some IL-17A-producing $\gamma\delta$ T cells have already undergone some degree of development that renders them unresponsive to GL3. To investigate this idea, the E15/GL3 experiment should be repeated using thymuses from E14

embryos. One could also hypothesise that increasing concentrations of GL3 should correlate with progressively reduced appearance of IL-17A-secreting γδ T cells, which could be investigated by supplementing FTOCs with increasing doses of GL3. Moreover, because Vγ4- and Vγ6-expressing γδ T cells are the main IL-17A-producers (Carding and Egan, 2002), future work should confirm that these two populations are mainly found in the CD24[(-)] CD44[(+)] CD45RB[(-)] subset and that they are reduced under these cultures condition. Thus, development of IL-17A-secreting γδ T cells appears largely impeded by increased signalling through TCRγδ, suggesting perhaps that they instead develop using a ligand-independent pathway. In agreement with this, the lab previously published that a trunctated TCRγδ was sufficient to generate some γδ T cells when transfected into RAG-deficient DN2 thymocytes. This suggests that inititiation of TCR signalling can result from the simple oligomerization of the two TCR subunits and may not require ligand engagement.

7.14 Development of IL-17A-secreting γδ T cells is dependent on Lck/Zap-70 and PI3K signalling

The data from GL3-supplemented FTOCs suggest that IL-17A-producing γδ T cell development is not favoured by strong signalling through TCRγδ (discussed above). Unexpectedly, weakening of TCRγδ signal strength through a gradual increase in PP2, a src kinase inhibitor that would inhibit Lck, was associated with the gradual disappearance of IL-17A-producing γδ T cells. Although one could conclude that weak TCRγδ signalling is incompatible with their

development, this would directly contradict the conclusion from the GL3-treated FTOCS (above). Thus, we propose instead that it illustrates simply their Lck-dependence. In line with this, Wencker *et al*. recently showed that SKG mice, which harbor a mutation in Zap-70 resulting in reduced Zap-70 activity (Sakaguchi et al., 2003), had a highly reduced compartment of CD44$^{(+)}$CD27$^{(-)}$IL-7R$\alpha^{(+)}$ IL-17-secreting $\gamma\delta$ T cells, which corresponds to our CD24$^{(-)}$CD44$^{(+)}$CD45RB$^{(-)}$ subset. However, the authors concluded that strong Zap-70-mediated signalling, likely resulting from TCR$\gamma\delta$ ligand engagement, was responsible for driving IL-17$^{(+)}$ $\gamma\delta$ T cell development. To reconcile these data with ours, we propose simply that commitment to an IL-17-producing $\gamma\delta$ fate is both Lck and Zap-70-dependent, but that this does not necessarily imply that high activity of thee kinases is required. Instead we proposed that IL-17A-secreting $\gamma\delta$ T cells may required weak Lck/Zap-70 activity that may support signalling through another signalling pathway. It is possible that TCR$\gamma\delta$ may simply act as a scaffold in this case, providing Lck/zap-70 to another receptor such as the IL-7 receptor. Indeed, IL-7 has been demonstrated to be required for IL-17A-producing $\gamma\delta$ T cell development in an independent study (Michel et al., 2012) and IL7Rα subunits were shown to cluster with the preTCR:CD3ζ complex upon signalling in human T cells suggesting a possible cooperative role (Patel S., et al 2012). Recently, the spleen tyrosine kinase, Syk, a src kinase belonging to the same family as Zap-70, was shown to deliver signals emanating from the B-cell activating factor receptor (BAFFR) during B cell development, highlighting a previously unknown crosstalk between the B cell receptor (BCR) and BAFFR (Schweighoffer E., 2013). Importantly, stimulation of BAFFR was shown to result in greater phosphorylation of the PI3K signalling

pathway including protein kinase B (AKT). We show in this thesis that inhibiting PI3K signalling impedes development of IL-17A-producing $\gamma\delta$ T cells. Thus, we propose a model where IL-17A-secreting $\gamma\delta$ T cell development is driven by a Lck/Zap-70/PI3K axis triggered by an alternative receptor to TCR$\gamma\delta$. To further implicate a role for PI3K signalling in IL-17A but not IFN-γ secreting $\gamma\delta$ T cells, levels of phosphorylated ribosomal protein S6 (pS6) and AKT should be investigated in CD44$^{(+)}$CD45RB$^{(-)}$ versus CD45RB$^{(+)}$ cells and specific inhibitors to AKT (such as MK-2206 which prevents AKT auto-phosphorylation) could be supplemented in FTOC. The class I PI3K signalling family includes the subunits PI3Kα, PI3Kβ, PI3Kδ and PI3Kγ that were shown to play different role in B cell development (Okkenhaug and Vanhaesebroeck, 2003; Ramadani et al., 2010). Thus, future work should use isoform-targeting inhibitors in FTOC in order to dissect which isoform is implicated in IL-17A-producing $\gamma\delta$ T cell development. These data could also be further confirmed by using PI3K-deficient mice. Thus, we propose a new model where an alternative receptor would have access to Lck and Zap-70 downstream of TCR$\gamma\delta$ to signal through PI3K and support IL-17A-producing $\gamma\delta$ T cell development (Figure 7.2).
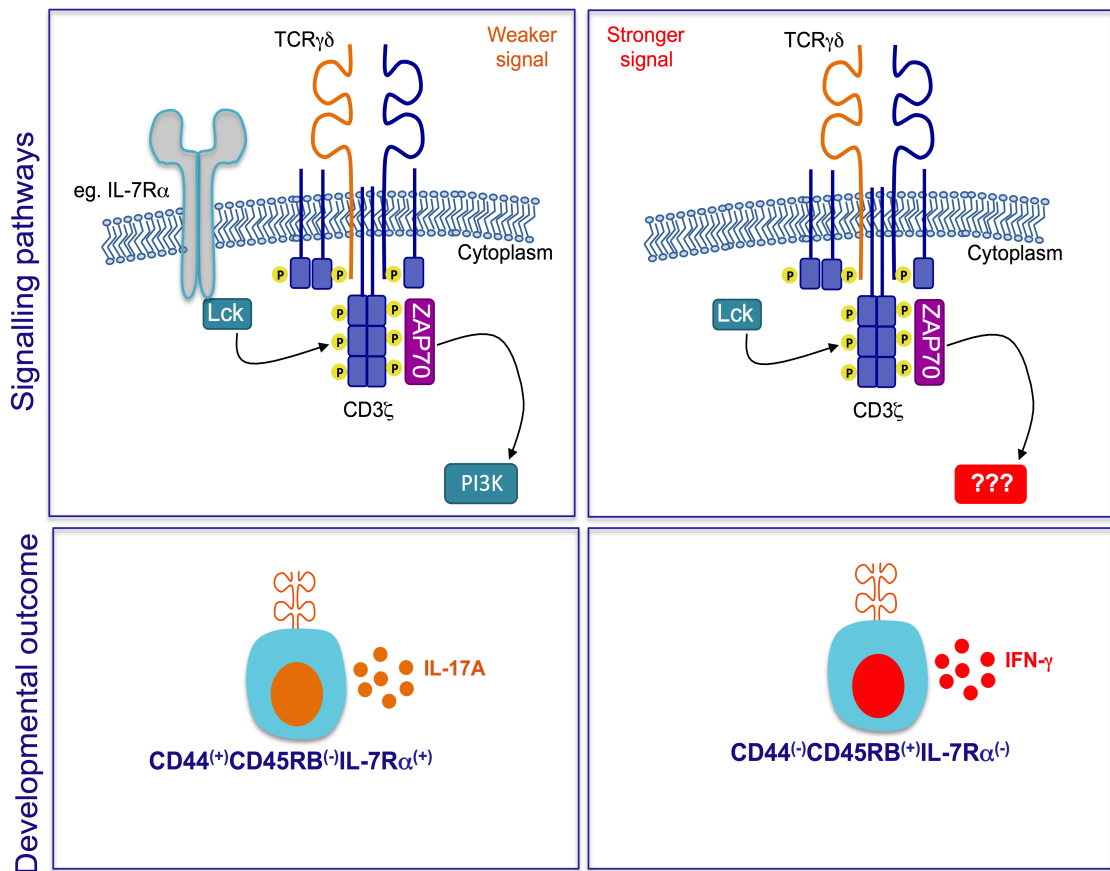
Figure 7.2 A schematic diagram to illustrate the current hypothesis that we propose to explain IL-17A- versus IFN-γ-secreting γδ T cell commitment. We propose that Lck/Zap-70 are used by an alternative receptor, possibly IL-7Rα, to signal through PI3K and support IL-17A-producing γδ T cell development. Conversely, we propose that IFN-γ-secreting γδ T cell development is supported by strong signals from TCRγδ that recruit a currently unknown signalling axis.

7.15 Commitment to an IFN-γ-secreting γδ T cell fate is supported by strong TCRγδ signalling that activates a currently unknown signalling pathway

Here we show that augmenting TCRγδ signal strength through the use of anti-TCRδ cross-linking antibody GL3 principally favour CD45RB$^{(+)}$ γδ T cell development. This development did not appear to occur through PI3K, as inhibiting PI3K signalling did not affect IFN-γ-secreting γδ T cells. Moreover, supplementing FTOC with GL3 in the presence of PI3K inhibitor drove CD45RB$^{(+)}$ γδ T cell development, suggesting that an alternative signalling pathway is implicated. We also show using PP2 that CD45RB^{high} cells were the only remaining cells at higher PP2 concentrations, suggesting that they survived because they are receiving the strongest signals (and are thus least affected). Nevertheless, these data suggest that an alternative signalling pathway activated by strong signals is likely to be supporting IFN-γ-secreting γδ T cell development. This should undoubtedly constitute a future area of research. The Hayday laboratory implicated the NFKB/NFAT/egr3 signalling pathway in the development of CD45RB$^{(+)}$Vγ5$^{(+)}$ γδ T cells (Turchinovich and Hayday, 2011) whereas inhibiting ERK signalling did not impede their development. Thus, future work could focus on using specific inhibitors of NFAT/NFKB and ERK to investigate their requirements for IL-17A- versus IFN-γ-secreting γδ T cell development.

7.16 Conclusion - part II

Here we propose a model in which strong TCR$\gamma\delta$ signalling would favour CD45RB$^{(+)}$ $\gamma\delta$ T cell development through a currently unknown signalling pathway, impeding IL-17A-secreting $\gamma\delta$ T cell development. Alternatively, if TCR$\gamma\delta$ signalling is weak, for example in the absence of TCR-ligand, signalling from an alternative receptor, such as the IL-7 receptor, could "hijack" TCR$\gamma\delta$-associated Lck/Zap-70 to activate PI3K and promote commitment to an IL-17A-secreting $\gamma\delta$ T cell fate (Figure 7.2).

Bibliography

Acha-Orbea, H., A.N. Shakhov, L. Scarpellino, E. Kolb, V. Muller, A. Vessaz-shaw, R. Fuchs, and K. Blochlinger. 1991. Clonal deletion of V β814-bearing T cells in mice transgenic for mammary tumour virus. *Nature* 350:207-211.

Acuto, O., V. Di Bartolo, and F. Michel. 2008. Tailoring T-cell receptor signals by proximal negative feedback mechanisms. *Nature Reviews Immunology* 8:699-712.

Aifantis, I., C. Borowski, F. Gounari, H.D. Lacorazza, J. Nikolich-Zugich, and H. von Boehmer. 2002. A critical role for the cytoplasmic tail of pTα in T lymphocyte development. *Nature Immunology* 3:483-488.

Aifantis, I., J. Buer, H. von Boehmer, and O. Azogui. 1997. Essential role of the pre-T cell receptor in allelic exclusion of the T cell receptor β locus. *Immunity* 7:601-607.

Alberola-Ila, J., K.A. Forbush, R. Seger, E.G. Krebs, and R.M. Perlmutter. 1995. Selective requirement for MAP kinase activation in thymocyte differentiation. *Nature* 373:620-623.

Alice, M.N., G. Himanshu, and J. Anjali. 2012. TCR‐induced T cell activation leads to simultaneous phosphorylation at Y505 and Y394 of p56lck residues. *Cytometry Part A* 81A:797-805.

Alt, F.W., G.D. Yancopoulos, T.K. Blackwell, C. Wood, E. Thomas, M. Boss, R. Coffman, N. Rosenberg, S. Tonegawa, and D. Baltimore. 1984. Ordered rearrangement of immunoglobulin heavy chain variable region segments. *The EMBO journal* 3:1209-1219.

Ara, T., M. Itoi, K. Kawabata, T. Egawa, K. Tokoyoda, T. Sugiyama, N. Fujii, T. Amagai, and T. Nagasawa. 2003. A role of CXC chemokine ligand 12/stromal cell-derived factor-1/pre-B cell growth stimulating factor and its receptor CXCR4 in fetal and adult T cell development in vivo. *Journal of Immunology* 170:4649-4655.

Arstila, T.P., A. Casrouge, V. Baron, J. Even, J. Kanellopoulos, and P. Kourilsky. 1999. A Direct Estimate of the Human T Cell Receptor Diversity. *Science* 286:958961.

Ashton-Rickardt, P.G., A. Bandeira, J.R. Delaney, L. Van Kaer, H.P. Pircher, R.M. Zinkernagel, and S. Tonegawa. 1994. Evidence for a differential avidity model of T cell selection in the thymus. *Cell* 76:651-663.

Au-Yeung, B.B., and J. Zikherman. 2014. A sharp T-cell antigen receptor signaling threshold for T-cell proliferation. *Proceedings of the National Academy of Sciences* 111:E3679-3688.

Autero, M., J. Saharinen, T. Pessa-Morikawa, M. Soula-Rothhut, C. Oetken, M. Gassmann, M. Bergman, K. Alitalo, P. Burn, and C.G. Gahmberg. 1994. Tyrosine phosphorylation of CD45 phosphotyrosine phosphatase by p50csk kinase creates a binding site for p56lck tyrosine kinase and activates the phosphatase. *Molecular and cellular biology* 14:1308-1321.

Azzam, H.S., J.B. DeJarnette, K. Huang, R. Emmons, C.S. Park, C.L. Sommers, D. El-Khoury, E.W. Shores, and P.E. Love. 2001. Fine Tuning of TCR Signaling by CD5. *The Journal of Immunology* 166:5464-5472.

Azzam, H.S., A. Grinberg, K. Lui, H. Shen, E.W. Shores, and P.E. Love. 1998. CD5 Expression Is Developmentally Regulated By T Cell Receptor (TCR) Signals and TCR Avidity. *The Journal of Experimental Medicine* 188:2301-2311.

Balciunaite, G., R. Ceredig, and A.G. Rolink. 2005. The earliest subpopulation of mouse thymocytes contains potent T, significant macrophage, and natural killer cell but no B-lymphocyte potential. *Blood* 105:1930-1936.

Baldwin, T.A., M.M. Sandau, and S.C. Jameson. 2005. The timing of TCRα expression critically influences T cell development and selection. *The Journal of Experimental Medicine* 202:111-121.

Barbee, S.D., M.J. Woodward, G. Turchinovich, J.J. Mention, J.M. Lewis, L.M. Boyden, R.P. Lifton, R. Tigelaar, and A.C. Hayday. 2011. Skint-1 is a highly specific, unique selecting component for epidermal T cells. *Proceedings of the National Academy of Sciences* 108:3330-3335.

Barber, D.F., L. Passoni, L. Wen, and L. Geng. 1998. Cutting edge: the expression in vivo of a second isoform of pTα: implications for the mechanism of pTα action. *The Journal of Immunology* 161:11-16.

Barth, R.J., J.J. Mulé, P.J. Spiess, and S.A. Rosenberg. 1991. Interferon γ and tumor necrosis factor have a role in tumor regressions mediated by murine CD8+ tumor-infiltrating lymphocytes. *The Journal of Experimental Medicine* 173:647-658.

Bennett, S.R.M., F.R. Carbone, F. Karamalis, J. Miller, and W.R. Heath. 1997. Induction of a CD8+ cytotoxic T lymphocyte response by cross-priming requires cognate CD4+ T cell help. *The Journal of Experimental Medicine* 186:65-70.

Benz, C., K. Heinzel, and C.C. Bleul. 2004. Homing of immature thymocytes to the subcapsular microenvironment within the thymus is not an absolute requirement for T cell development. *European journal of immunology* 34:3652-3663.

Bivona, T.G., I. Pérez De Castro, I.M. Ahearn, T.M. Grana, V.K. Chiu, P.J. Lockyer, P.J. Cullen, A. Pellicer, A.D. Cox, and M.R. Philips. 2003. Phospholipase Cγ activates Ras on the Golgi apparatus by means of RasGRP1. *Nature* 424:694-698.

Blackburn, C.C., and N.R. Manley. 2004. Developing a new paradigm for thymus organogenesis. *Nature Reviews Immunology* 4:278-289.

Bonizzi, G., and M. Karin. 2004. The two NFKB activation pathways and their role in innate and adaptive immunity. *Trends Immunol* 25:280-288.

Bootman, M.D. 2012. Calcium signaling. *Cold Spring Harbor perspectives in biology* 4:a011171.

Bousso, P., N.R. Bhakta, R.S. Lewis, and E. Robey. 2002. Dynamics of Thymocyte-Stromal Cell Interactions Visualized by Two-Photon Microscopy. *Science* 296:18761880.

Brekelmans, P., P. van Soest, P.J. Leenen, and W. van Ewijk. 1994. Inhibition of proliferation and differentiation during early T cell development by anti‐transferrin receptor antibody. *European Journal of Immunology* 24:2896-2902.

Bruno, L., H.J. Fehling, and H. von Boehmer. 1996. The αβ T cell receptor can replace the γδ receptor in the development of γδ lineage cells. *Immunity* 5:343-352.

Bruno, L., B. Rocha, A. Rolink, H. von Boehmer, and H.R. Rodewald. 1995. Intra- and extra-thymic expression of the pre-T cell receptor α gene. *Eur J Immunol* 25:1877-1882.

Bruyns, E., A. Marie-Cardine, H. Kirchgessner, K. Sagolla, A. Shevchenko, M. Mann, F. Autschbach, A. Bensussan, S. Meuer, and B. Schraven. 1998. T cell receptor (TCR) interacting molecule (TRIM), a novel disulfide-linked dimer associated with the TCR-CD3-zeta complex, recruits intracellular signaling proteins to the plasma membrane. *The Journal of Experimental Medicine* 188:561-575.

Buer, J., I. Aifantis, J.P. DiSanto, H.J. Fehling, and H. von Boehmer. 1997. Role of Different T Cell Receptors in the Development of Pre–T Cells. *The Journal of Experimental Medicine* 185:1541-1548.

Cai, Y., X. Shen, C. Ding, C. Qi, K. Li, X. Li, V.R. Jala, H.-g.G. Zhang, T. Wang, J. Zheng, and J. Yan. 2011. Pivotal role of dermal IL-17-producing γδ T cells in skin inflammation. *Immunity* 35:596-610.

Campese, A.F., P. Grazioli, S. Colantoni, E. Anastasi, M. Mecarozzi, S. Checquolo, G. De Luca, D. Bellavia, L. Frati, A. Gulino, and I. Screpanti. 2009. Notch3 and pTalpha/pre-TCR sustain the in vivo function of naturally occurring regulatory T cells. *International immunology* 21:727-743.

Carding, S.R., and P.J. Egan. 2002. γδ T cells: functional plasticity and heterogeneity. *Nature Reviews Immunology* 2:336-345.

Casanova, J.L., P. Romero, and C. Widmann. 1991. T cell receptor genes in a series of class I major histocompatibility complex-restricted cytotoxic T lymphocyte clones specific for a Plasmodium berghei nonapeptide: implications for T cell allelic exclusion and antigen-specific repertoire. *Journal of Experimental Medicine* 174:1371-1383.

Chan, A.C., M. Dalton, R. Johnson, G.H. Kong, T. Wang, R. Thoma, and T. Kurosaki. 1995. Activation of ZAP-70 kinase activity by phosphorylation

of tyrosine 493 is required for lymphocyte antigen receptor function. *The EMBO journal* 14:2499-2508.

Chatila, T., L. Silverman, R. Miller, and R. Geha. 1989. Mechanisms of T cell activation by the calcium ionophore ionomycin. *Journal of immunology* 143:1283-1289.

Cheroutre, H., F. Lambolez, and D. Mucida. 2011. The light and dark sides of intestinal intraepithelial lymphocytes. *Nature Reviews Immunology* 11:445-456.

Chiu, V.K., T. Bivona, A. Hach, J.B. Sajous, J. Silletti, H. Wiener, R.L. Johnson, A.D. Cox, and M.R. Philips. 2002. Ras signalling on the endoplasmic reticulum and the Golgi. *Nature cell biology* 4:343-350.

Ciofani, M., T.M. Schmitt, A. Ciofani, A.M. Michie, N. Cuburu, A. Aublin, J.L. Maryanski, and J.C. Zuniga-Pflucker. 2004. Obligatory Role for Cooperative Signaling by Pre-TCR and Notch during Thymocyte Differentiation. *The Journal of Immunology* 172:5230-5239.

Ciofani, M., and J.C. Zuniga-Pflucker. 2010. Determining γδ versus αβ T cell development. *Nature Reviews Immunology* 10:657-663.

Coffey, F., S.-Y.Y. Lee, T.B. Buus, J.-P.H.P. Lauritsen, G.W. Wong, M.L. Joachims, L.F. Thompson, J.C. Zúñiga-Pflücker, D.J. Kappes, and D.L. Wiest. 2014. The TCR ligand-inducible expression of CD73 marks γδ lineage commitment and a metastable intermediate in effector specification. *The Journal of Experimental Medicine* 211:329-343.

Cooper, M.D., and M.N. Alder. 2006. The Evolution of Adaptive Immune Systems. *Cell* 124:815-822.

Crowley, M.P., Z. Reich, N. Mavaddat, J.D. Altman, and Y. Chien. 1997. The recognition of the nonclassical major histocompatibility complex (MHC) class I molecule, T10, by the γδ T cell, G8. *The Journal of Experimental Medicine* 185:1223-1230.

Cruz, D., B.C. Sydora, K. Hetzel, G. Yakoub, M. Kronenberg, and H. Cheroutre. 1998. An opposite pattern of selection of a single T cell antigen receptor in the thymus and among intraepithelial lymphocytes. *The Journal of Experimental Medicine* 188:255-265.

D'Oro, U., K. Sakaguchi, E. Appella, and J.D. Ashwell. 1996. Mutational analysis of Lck in CD45-negative T cells: dominant role of tyrosine 394 phosphorylation in kinase activity. *Molecular and cellular biology* 16:4996-5003.

Daft, J.G., T. Ptacek, R. Kumar, C. Morrow, and R.G. Lorenz. 2015. Cross-fostering immediately after birth induces a permanent microbiota shift that is shaped by the nursing mother. *Microbiome* 3:17.

Daniels, M.A., E. Teixeiro, J. Gill, B. Hausmann, D. Roubaty, K. Holmberg, G. Werlen, G.A. Hollander, N.R. Gascoigne, and E. Palmer. 2006. Thymic selection threshold defined by compartmentalization of Ras/MAPK signalling. *Nature* 444:724-729.

Davis, M.M., and P.J. Bjorkman. 1988. T-cell antigen receptor genes and T-cell recognition. *Nature* 334:395-402.

Davis, S.J., and P.A. van der Merwe. 2006. The kinetic-segregation model: TCR triggering and beyond. *Nature Immunology* 7:803-809.

Del Porto, P., L. Bruno, M.G. Mattei, H. von Boehmer, and C. Saint-Ruf. 1995. Cloning and comparative analysis of the human pre-T-cell receptor α-chain gene. *Proceedings of the National Academy of Sciences* 92:12105-12109.

Denning, T.L., S. Granger, D. Mucida, R. Graddy, G. Leclercq, W. Zhang, K. Honey, J.P. Rasmussen, H. Cheroutre, and A.Y. Rudensky. 2007. Mouse TCR + CD8 intraepithelial lymphocytes express genes that down-regulate their antigen reactivity and suppress immune responses. *The Journal of Immunology* 178:4230-4239.

Dorshkind, K., and E. Montecino-Rodriguez. 2009. The ageing immune system: is it ever too old to become young again? *Nature Reviews* 9:57-62.

Douglas, N.C., H. Jacobs, and A.L.M. Bothwell. 2001. Defining the specific physiological requirements for c-Myc in T cell development. *Nature immunology* 2:307-315.

Enslen, H., J. Raingeaud, and R.J. Davis. 1998. Selective activation of p38 mitogen-activated protein (MAP) kinase isoforms by the MAP kinase kinases MKK3 and MKK6. *The Journal of biological chemistry* 273:1741-1748.

Fehling, H.J., A. Krotkova, C. Saint-Ruf, and H. von Boehmer. 1995. Crucial role of the pre-T-cell receptor α gene in development of αβ but not γδ T cells. *Nature* 375:795-798.

Foss, D.L., E. Donskoy, and I. Goldschneider. 2001. The importation of hematogenous precursors by the thymus is a gated phenomenon in normal adult mice. *The Journal of Experimental Medicine* 193:365-374.

Gallo, E.M., M.M. Winslow, K. Cante-Barrett, A.N. Radermacher, L. Ho, L. McGinnis, B. Iritani, J.R. Neilson, and G.R. Crabtree. 2007. Calcineurin sets the bandwidth for discrimination of signals during thymocyte development. *Nature* 450:731-735.

Gangadharan, D., and H. Cheroutre. 2004. The CD8 isoform CD8αα is not a functional homologue of the TCR co-receptor CD8αβ. *Current opinion in immunology* 16:264-270.

Gao, Y., W. Yang, M. Pan, E. Scully, M. Girardi, L.H. Augenlicht, J. Craft, and Z. Yin. 2003. γδ T cells provide an early source of interferon gamma in tumor immunity. *The Journal of Experimental Medicine* 198:433-442.

Germain, R.N. 2002. T-cell development and the CD4-CD8 lineage decision. *Nature Reviews Immunology* 2:309-322.

Gerondakis, S., R. Grumont, R. Gugasyan, L. Wong, I. Isomura, W. Ho, and A. Banerjee. 2006. Unravelling the complexities of the NF-κB signalling pathway using mouse knockout and transgenic models. *Oncogene* 25:6781-6799.

Gibbons, D., N.C. Douglas, D.F. Barber, Q. Liu, R. Sullo, L. Geng, H.J. Fehling, H. von Boehmer, and A.C. Hayday. 2001. The Biological Activity of Natural and Mutant Ptα Alleles. *The Journal of Experimental Medicine* 194:695-704.

Girardi, M., D.E. Oppenheim, C.R. Steele, J.M. Lewis, E. Glusac, R. Filler, P. Hobby, B. Sutton, R.E. Tigelaar, and A.C. Hayday. 2001. Regulation of cutaneous malignancy by γδ T cells. *Science* 294:605-609.

Giudicelli, V., D. Chaume, and M.-P. Lefranc. 2005. IMGT/GENE-DB: a comprehensive database for human and mouse immunoglobulin and T cell receptor genes. *Nucleic acids research* 33:

Godfrey, D.I., J. Kennedy, T. Suda, and A. Zlotnik. 1993. Pillars article: a developmental pathway involving four phenotypically and functionally distinct subsets of CD3-CD4-CD8- triple-negative adult mouse thymocytes defined by CD44 and CD25 expression. *Journal of Immunology* 150:4244-4252.

Goff, R.-L.O., and N.D. Huntington. 2009. Characterization of the thymic IL-7 niche in vivo. *Proceedings of the National Academy of Sciences* 106:1512-1517.

Gounari, F., I. Aifantis, C. Martin, and H.J. Fehling. 2002. Tracing lymphopoiesis with the aid of a pTα-controlled reporter gene. *Nature immunology* 3:489-496.

Gray, E.E., F. Ramirez-Valle, Y. Xu, S. Wu, Z. Wu, K.E. Karjalainen, and J.G. Cyster. 2013. Deficiency in IL-17-committed Vγ4+ γδT cells in a spontaneous Sox13-mutant CD45.1+ congenic mouse substrain provides protection from dermatitis. *Nature Immunology* 14:584-592.

Groettrup, M., K. Ungewiss, O. Azogui, R. Palacios, M.J. Owen, A.C. Hayday, and H. von Boehmer. 1993. A novel disulfide-linked heterodimer on pre—T cells consists of the T cell receptor β chain and a 33 kd glycoprotein. *Cell* 75:283294.

Guy-Grand, D., O. Azogui, S. Celli, S. Darche, M.C. Nussenzweig, P. Kourilsky, and P. Vassalli. 2003. Extrathymic T Cell Lymphopoiesis Ontogeny and Contribution to Gut Intraepithelial Lymphocytes in Athymic and Euthymic Mice. *The Journal of Experimental Medicine* 197:333-341.

Haks, M.C., J.M. Lefebvre, J.P. Lauritsen, M. Carleton, M. Rhodes, T. Miyazaki, D.J. Kappes, and D.L. Wiest. 2005. Attenuation of γδTCR Signaling Efficiently Diverts Thymocytes to the αβ Lineage. *Immunity* 22:595-606.

Hamada, S., M. Umemura, T. Shiono, K. Tanaka, A. Yahagi, M.D. Begum, K. Oshiro, Y. Okamoto, H. Watanabe, K. Kawakami, C. Roark, W.K. Born, R. O'Brien, K. Ikuta, H. Ishikawa, S. Nakae, Y. Iwakura, T. Ohta, and G. Matsuzaki. 2008. IL-17A produced by gammadelta T cells plays a critical role in innate immunity against listeria monocytogenes infection in the liver. *Journal of Immunology* 181:3456-3463.

Harding, A., T. Tian, E. Westbury, E. Frische, and J.F. Hancock. 2005. Subcellular localization determines MAP kinase signal output. *Current biology : CB* 15:869-873.

Harriague, J., and G. Bismuth. 2002. Imaging antigen-induced PI3K activation in T cells. *Nature immunology* 3:1090-1096.

Hayes, S.M., L. Li, and P.E. Love. 2005. TCR Signal Strength Influences αβ/γδ Lineage Fate. *Immunity* 22:583-593.

Heintz, N. 2001. Bac to the future: The use of bac transgenic mice for neuroscience research. *Nature Reviews Neuroscience* 2:861-870.

Hemmings, B.A., and D.F. Restuccia. 2012. PI3K-PKB/Akt Pathway. *Cold Spring Harbor Perspectives in Biology* 4:a011189.

Herblot, S., A.M. Steff, P. Hugo, P.D. Aplan, and T. Hoang. 2000. SCL and LMO1 alter thymocyte differentiation: inhibition of E2A-HEB function and pre-T α chain expression. *Nature Immunology* 1:138-144.

Heusch, M., L. Lin, R. Geleziunas, and W.C. Greene. 1999. The generation of nfkb2 p52: mechanism and efficiency. *Oncogene* 18:6201-6208.

Hoffman, E.S., L. Passoni, T. Crompton, T.M. Leu, D.G. Schatz, A. Koff, M.J. Owen, and A.C. Hayday. 1996. Productive T-cell receptor β-chain gene rearrangement: coincident regulation of cell cycle and clonality during development in vivo. *Genes & development* 10:948-962.

Hogquist, K.A., T.A. Baldwin, and S.C. Jameson. 2005. Central tolerance: learning self-control in the thymus. *Nature Reviews Immunology* 5:772-782.

Holmes, R., and J.C. Zuniga-Pflucker. 2009. The OP9-DL1 System: Generation of T-Lymphocytes from Embryonic or Hematopoietic Stem Cells In Vitro. *Cold Spring Harb Protoc* 2009:5156.

Houlden, B.A., L.A. Matis, R.Q. Cron, S.M. Widacki, G.D. Brown, C. Pampeno, D. Meruelo, and J.A. Bluestone. 1989. A TCR γδ cell recognizing a novel TL-encoded gene product. *Cold Spring Harb Symp Quant Biol* 54 Pt 1:45-55.

Hsieh, C.S., S.E. Macatonia, C.S. Tripp, S.F. Wolf, and A. O'Garra. 1993. Development of TH1 CD4+ T cells through IL-12 produced by Listeria-induced macrophages. *Science* 260:547-549.

Huang, C., and O. Kanagawa. 2004. Impact of early expression of TCR chain on thymocyte development. *European journal of immunology* 34:1532-1541.

Irving, B.A., F.W. Alt, and N. Killeen. 1998. Thymocyte Development in the Absence of Pre-T Cell Receptor Extracellular Immunoglobulin Domains. *Science* 280:905908.

Ishikawa, E., Y. Miyake, H. Hara, T. Saito, and S. Yamasaki. 2010. Germ-line elimination of electric charge on pre–T-cell receptor (TCR) impairs autonomous signaling for β-selection and TCR repertoire formation. *Proceedings of the National Academy of Sciences* 107:19979-19984.

Ito, K., L. Van Kaer, M. Bonneville, S. Hsu, D.B. Murphy, and S. Tonegawa. 1990. Recognition of the product of a novel MHC TL region gene (27b) by a mouse γδ T cell receptor. *Cell* 62:549-561.

Itohara, S., P. Mombaerts, J. Lafaille, J. Iacomini, A. Nelson, A.R. Clarke, M.L. Hooper, A. Farr, and S. Tonegawa. 1993. T cell receptor δ gene mutant mice: Independent generation of αβ T cells and programmed rearrangements of γδ TCR genes. *Cell* 72:337-348.

Janas, M.L., G. Varano, K. Gudmundsson, M. Noda, T. Nagasawa, and M. Turner. 2010. Thymic development beyond β-selection requires phosphatidylinositol 3-kinase activation by CXCR4. *The Journal of Experimental Medicine* 207:247-261.

Jenkinson, E.J., G. Anderson, and J.J. Owen. 1992. Studies on T cell maturation on defined thymic stromal cell populations in vitro. *The Journal of Experimental Medicine* 176:845-853.

Jenkinson, E.J., and J.J. Owen. 1990. T-cell differentiation in thymus organ cultures. *Semin Immunol* 2:51-58.

Jensen, K.D., X. Su, S. Shin, L. Li, S. Youssef, S. Yamasaki, L. Steinman, T. Saito, R.M. Locksley, M.M. Davis, N. Baumgarth, and Y.H. Chien. 2008. Thymic Selection Determines γδ T Cell Effector Fate: Antigen-Naive Cells Make Interleukin-17 and Antigen-Experienced Cells Make Interferon γ. *Immunity* 29:90-100.

Jordan, M.S., A. Boesteanu, A.J. Reed, A.L. Petrone, A.E. Holenbeck, M.A. Lerman, A. Naji, and A.J. Caton. 2001. Thymic selection of CD4+CD25+

regulatory T cells induced by an agonist self-peptide. *Nature Immunology* 2:301-306.

Kang, J., A. Volkmann, and D.H. Raulet. 2001. Evidence That γδ versus αβ T Cell Fate Determination Is Initiated Independently of T Cell Receptor Signaling. *The Journal of Experimental Medicine* 193:689-698.

Kaye, J., M.L. Hsu, M.E. Sauron, S.C. Jameson, N.R. Gascoigne, and S.M. Hedrick. 1989. Selective development of CD4+ T cells in transgenic mice expressing a class II MHC-restricted antigen receptor. *Nature* 341:746-749.

Kikly, K., and G. Dennert 1992. Evidence for extrathymic development of TNK cells. NK1+ CD3+ cells responsible for acute marrow graft rejection are present in thymus-deficient mice. *Journal of immunology* 149:403-412.

Klatzmann, D., F. Barré-Sinoussi, M.T. Nugeyre, C. Danquet, E. Vilmer, C. Griscelli, F. Brun-Veziret, C. Rouzioux, J.C. Gluckman, and J.C. Chermann. 1984. Selective tropism of lymphadenopathy associated virus (LAV) for helper-inducer T lymphocytes. *Science* 225:59-63.

Koller, B.H., P. Marrack, J.W. Kappler, and O. Smithies. 1990. Normal development of mice deficient in beta 2M, MHC class I proteins, and CD8+ T cells. *Science* 248:1227-1230.

Kondo, M., I.L. Weissman, and K. Akashi. 1997. Identification of clonogenic common lymphoid progenitors in mouse bone marrow. *Cell* 91:661-672.

Kong, G., M. Dalton, and J.B. Wardenburg. 1996. Distinct tyrosine phosphorylation sites in Zap-70 mediate activation and negative regulation of antigen receptor function. *Molecular and cellular biology* 16:5026-5035.

Krangel, M.S., J. Carabana, I. Abbarategui, R. Schlimgen, and A. Hawwari. 2004. Enforcing order within a complex locus: current perspectives on the control of V(D)J recombination at the murine T‐cell receptor α/δ locus. *Immunological Reviews* 200:224-232.

Krecko, E.G., and S. Tonegawa. 1989. Different γδ T-cell receptors are expressed on thymocytes at different stages of development. *Proceedings of the National Academy of Sciences* 86:631-635.

Kreslavsky, T., A.I. Garbe, A. Krueger, and H. von Boehmer. 2008. T cell receptor–instructed αβ versus γδ lineage commitment revealed by single-cell analysis. *The Journal of Experimental Medicine* 205:1173-1186.

Kreslavsky, T., M. Gleimer, M. Miyazaki, Y. Choi, E. Gagnon, C. Murre, P. Sicinski, and H. von Boehmer. 2012. β-Selection-induced proliferation is required for αβ T cell differentiation. *Immunity* 37:840-853.

Kronenberg, M., and L. Gapin. 2002. The unconventional lifestyle of NKT cells. *Nature Reviews Immunology*

Kunisawa, J., Y. Kurashima, M. Higuchi, M. Gohda, I. Ishikawa, I. Ogahara, N. Kim, M. Shimizu, and H. Kiyono. 2007. Sphingosine 1-phosphate dependence in the regulation of lymphocyte trafficking to the gut epithelium. *The Journal of experimental medicine* 204:2335-2348.

Kupzig, S., S.A. Walker, and P.J. Cullen. 2005. The frequencies of calcium oscillations are optimized for efficient calcium-mediated activation of Ras and the ERK/MAPK cascade. *Proceedings of the National Academy of Sciences* 102:7577-7582.

Kurobe, H., C. Liu, T. Ueno, F. Saito, I. Ohigashi, N. Seach, R. Arakaki, Y. Hayashi, T. Kitagawa, M. Lipp, R.L. Boyd, and Y. Takahama. 2006. CCR7-dependent cortex-to-medulla migration of positively selected thymocytes is essential for establishing central tolerance. *Immunity* 24:165-177.

Lacomini, J., R.S. Johnson, K. Herrup, and S. Tonegawa. 1992. RAG-1-deficient mice have no mature B and T lymphocytes. *Cell*

Lacorazza, H.D., C. Tucek-Szabo, L.V. Vasović, K. Remus, and J. Nikolich-Zugich. 2001. Premature TCR αβ expression and signaling in early thymocytes impair thymocyte expansion and partially block their development. *Journal of Immunology* 166:3184-3193.

Lambolez, F., M. Kronenberg, and H. Cheroutre. 2007. Thymic differentiation of TCRαβ+ CD8αα+ IELs. *Immunological Reviews* 215:178-188.

Larrick, J.W., and P. Cresswell. 1979. Modulation of cell surface iron transferrin receptors by cellular density and state of activation. *Journal of supramolecular structure* 11:579-586.

Laurent, J., N. Bosco, P.N. Marche, and R. Ceredig. 2004. New insights into the proliferation and differentiation of early mouse thymocytes. *International immunology* 16:1069-1080.

Lauritsen, J.P., G.W. Wong, S.-Y.Y. Lee, J.M. Lefebvre, M. Ciofani, M. Rhodes, D.J. Kappes, J.C. Zúñiga-Pflücker, and D.L. Wiest. 2009. Marked induction of the helix-loop-helix protein Id3 promotes the gammadelta T cell fate and renders their functional maturation Notch independent. *Immunity* 31:565-575.

Leishman, A.J., L. Gapin, M. Capone, E. Palmer, H.R. MacDonald, M. Kronenberg, and H. Cheroutre. 2002. Precursors of Functional MHC Class I- or Class II-Restricted CD8αα+ T Cells Are Positively Selected in the Thymus by Agonist Self-Peptides. *Immunity* 16:355-364.

Letourneur, F., and R.D. Klausner. 1992. Activation of T cells by a tyrosine kinase activation domain in the cytoplasmic tail of CD3 epsilon. *Science*

Lin, J., and A. Weiss. 2001. Identification of the minimal tyrosine residues required for linker for activation of T cell function. *Journal of Biological Chemistry* 276:29588-29595.

Liu, C., F. Saito, Z. Liu, Y. Lei, S. Uehara, P. Love, M. Lipp, S. Kondo, N. Manley, and Y. Takahama. 2006. Coordination between CCR7- and CCR9-mediated chemokine signals in prevascular fetal thymus colonization. *Blood* 108:2531-2539.

Liu, C., T. Ueno, S. Kuse, F. Saito, T. Nitta, L. Piali, H. Nakano, T. Kakiuchi, M. Lipp, G.A. Hollander, and Y. Takahama. 2005. The role of CCL21 in recruitment of T-precursor cells to fetal thymi. *Blood* 105:31-39.

Lucas, J.A., A.T. Miller, L.O. Atherly, and L.J. Berg. 2003. The role of Tec family kinases in T cell development and function. *Immunological Reviews* 191:119-138.

Ma, Y., U. Pannicke, K. Schwarz, and M.R. Lieber. 2002. Hairpin opening and overhang processing by an Artemis/DNA-dependent protein kinase complex in nonhomologous end joining and V (D) J recombination. *Cell* 108:781-794.

Macián, F. 2005. NFAT proteins: key regulators of T-cell development and function. *Nature Reviews Immunology* 5:472-484.

Macián, F., C. López-Rodríguez, and A. Rao. 2001. Partners in transcription: NFAT and AP-1. *Oncogene* 20:2476-2489.

Mahtani-Patching, J., J.F. Neves, D.J. Pang, K.V. Stoenchev, A.M. Aguirre-Blanco, B. Silva-Santos, and D.J. Pennington. 2011. PreTCR and TCRγδ signal initiation in thymocyte progenitors does not require domains implicated in receptor oligomerization. *Science signaling* 4:ra47.

Mahtani-Patching, J.L. 2010. Investigating the roles of the alternative Isoforms of the preTCR α (pTα) chain in T cell development. *PhD Thesis* https://qmro.qmul.ac.uk/jspui/handle/123456789/541:

Maillard, I., L.L. Tu, and A. Sambandam. 2006. The requirement for Notch signaling at the β-selection checkpoint in vivo is absolute and independent of the pre–T cell receptor. *The Journal of Experimental Medicine*

Makino, Y., N. Yamagata, T. Sasho, Y. Adachi, R. Kanno, H. Koseki, M. Kanno, and M. Taniguchi. 1993. Extrathymic development of V α 14-positive T cells. *The Journal of Experimental Medicine* 177:1399-1408.

Mallory, M.J., S.J. Allon, J. Qiu, M.R. Gazzara, I. Tapescu, N.M. Martinez, X.D. Fu, and K.W. Lynch. 2015. Induced transcription and stability of CELF2 mRNA drives widespread alternative splicing during T-cell signaling. *Proc Natl Acad Sci U S A* 112:E2139-2148.

Mansilla-Soto, J., and P. Cortes. 2003. VDJ Recombination Artemis and Its In Vivo Role in Hairpin Opening. *The Journal of Experimental Medicine* 197:543-547.

Maraskovsky, E., L.A. O'Reilly, M. Teepe, L.M. Corcoran, J.J. Peschon, and A. Strasser. 1997. Bcl-2 can rescue T lymphocyte development in interleukin-7 receptor-deficient mice but not in mutant rag-1-/- mice. *Cell* 89:1011-1019.

Mariathasan, S., M.F. Bachmann, D. Bouchard, T. Ohteki, and P.S. Ohashi. 1998. Degree of TCR Internalization and Ca2+ Flux Correlates with Thymocyte Selection. *Journal of Immunology* 161:6030-6037.

Mariathasan, S., A. Zakarian, D. Bouchard, A.M. Michie, J.C. Zuniga-Pflucker, and P.S. Ohashi. 2001. Duration and strength of extracellular signal-

regulated kinase signals are altered during positive versus negative thymocyte selection. *Journal of Immunology* 167:4966-4973.

Matloubian, M., C.G. Lo, G. Cinamon, M.J. Lesneski, Y. Xu, V. Brinkmann, M.L. Allende, R.L. Proia, and J.G. Cyster. 2004. Lymphocyte egress from thymus and peripheral lymphoid organs is dependent on S1P receptor 1. *Nature* 427:355-360.

McCaughtry, T.M., T.A. Baldwin, M.S. Wilken, and K.A. Hogquist. 2008. Clonal deletion of thymocytes can occur in the cortex with no involvement of the medulla. *The Journal of Experimental Medicine* 205:2575-2584.

McDonald, B.D., J.J. Bunker, I.E. Ishizuka, B. Jabri, and A. Bendelac. 2014. Elevated T Cell Receptor Signaling Identifies a Thymic Precursor to the TCRαβ+CD4−CD8β− Intraepithelial Lymphocyte Lineage. *Immunity* 41:219-229.

Mege, D., V. Di Bartolo, V. Germain, L. Tuosto, F. Michel, and O. Acuto. 1996. Mutation of Tyrosines 492/493 in the Kinase Domain of ZAP-70 Affects Multiple T-cell Receptor Signaling Pathways. *Journal of Biological Chemistry* 271:32644-32652.

Melichar, H.J., K. Narayan, S.D. Der, Y. Hiraoka, N. Gardiol, G. Jeannet, W. Held, C.A. Chambers, and J. Kang. 2007. Regulation of γδ versus αβ T lymphocyte differentiation by the transcription factor SOX13. *Science* 315:230-233.

Michael, G. 2006. Immunosurveillance and Immunoregulation by γδ T Cells. *Journal of Investigative Dermatology* 126:25-31.

Michel, M.-L.L., D.J. Pang, S.F. Haque, A.J. Potocnik, D.J. Pennington, and A.C. Hayday. 2012. Interleukin 7 (IL-7) selectively promotes mouse and human IL-17-producing γδ cells. *Proceedings of the National Academy of Sciences* 109:17549-17554.

Miller, J.F. 1961. Immunological function of the thymus. *Lancet* 2:748-749.

Miller, J.F. 1994. The thymus then and now. *Immunology and Cell Biology* 72:361-366.

Min, L., R.E. Joseph, and D.B. Fulton. 2009. Itk tyrosine kinase substrate docking is mediated by a nonclassical SH2 domain surface of PLCγ1. *Proceedings of the National Academy of Sciences* 106:21143-21148.

Minden, A., A. Lin, T. Smeal, and B. Derijard. 1994. c-Jun N-terminal phosphorylation correlates with activation of the JNK subgroup but not the ERK subgroup of mitogen-activated protein kinases. *Molecular and Cellular Biology*

Mingueneau, M., T. Kreslavsky, D. Gray, T. Heng, R. Cruse, J. Ericson, S. Bendall, M.H. Spitzer, G.P. Nolan, and K. Kobayashi. 2013. The transcriptional landscape of [α][beta] T cell differentiation. *Nature immunology* 14:619-632.

Misslitz, A., O. Pabst, G. Hintzen, L. Ohl, E. Kremmer, H.T. Petrie, and R. Förster. 2004. Thymic T cell development and progenitor localization depend on CCR7. *The Journal of Experimental Medicine* 200:481-491.

Miyazaki, T. 1997. Two distinct steps during thymocyte maturation from CD4-CD8- to CD4+CD8+ distinguished in the early growth response (Egr)-1 transgenic mice with a recombinase-activating gene-deficient background. *The Journal of Experimental Medicine* 186:877-885.

Molina, T.J., K. Kishihara, D.P. Siderovski, W. van Ewijk, A. Narendran, E. Timms, A. Wakeham, C.J. Paige, K.U. Hartmann, A. Veillette, and et al. 1992. Profound block in thymocyte development in mice lacking p56lck. *Nature* 357:161-164.

Mombaerts, P., A.R. Clarke, M.A. Rudnicki, J. Iacomini, S. Itohara, J.J. Lafaille, L. Wang, Y. Ichikawa, R. Jaenisch, M.L. Hooper, and et al. 1992. Mutations in T-cell antigen receptor genes α and β block thymocyte development at different stages. *Nature* 360:225-231.

Moran, A.E., K.L. Holzapfel, Y. Xing, N.R. Cunningham, J.S. Maltzman, J. Punt, and K.A. Hogquist. 2011. T cell receptor signal strength in Treg and iNKT cell development demonstrated by a novel fluorescent reporter mouse. *The Journal of Experimental Medicine* 208:1279-1289.

Mosmann, T.R., H. Cherwinski, and M.W. Bond. 1986. Two types of murine helper T cell clone. I. Definition according to profiles of lymphokine activities and secreted proteins. *The Journal of Immunology*

Murphy, K.M., A.B. Heimberger, and D.Y. Loh. 1990. Induction by antigen of intrathymic apoptosis of CD4+CD8+TCRlo thymocytes in vivo. *Science* 250:1720-1723.

Mysorekar, I.U., R.G. Lorenz, and J.I. Gordon. 2002. A gnotobiotic transgenic mouse model for studying interactions between small intestinal enterocytes and intraepithelial lymphocytes. *The Journal of biological chemistry* 277:37811-37819.

Neilson, J.R. 2004. Calcineurin B1 is essential for positive but not negative selection during thymocyte development. *Immunity* 20:255-266.

Nika, K., C. Soldani, M. Salek, W. Paster, A. Gray, R. Etzensperger, L. Fugger, P. Polzella, V. Cerundolo, O. Dushek, T. Hofer, A. Viola, and O. Acuto. 2010. Constitutively Active Lck Kinase in T Cells Drives Antigen Receptor Signal Transduction. *Immunity* 32:766-777.

O'Donnell, K.A., D. Yu, K.I. Zeller, and J. Kim. 2006. Activation of transferrin receptor 1 by c-Myc enhances cellular proliferation and tumorigenesis. *Molecular and cellular biology* 26:2373-2386.

O'Shea, C.C., A.P. Thornell, I.R. Rosewell, B. Hayes, and M.J. Owen. 1997. Exit of the Pre-TCR from the ER/cis-Golgi Is Necessary for Signaling Differentiation, Proliferation, and Allelic Exclusion in Immature Thymocytes. *Immunity* 7:591-599.

Oeckinghaus, A., M.S. Hayden, and S. Ghosh. 2011. Crosstalk in NF-[kappa]B signaling pathways. *Nature Immunology* 12:695-708.

Oettinger, M., D. Schatz, C. Gorka, and D. Baltimore. 1990. RAG-1 and RAG-2, adjacent genes that synergistically activate V(D)J recombination. *Science* 248:1517-1523.

Oh-Hora, M., N. Komatsu, M. Pishyareh, S. Feske, S. Hori, M. Taniguchi, A. Rao, and H. Takayanagi. 2013. Agonist-Selected T Cell Development Requires Strong T Cell Receptor Signaling and Store-Operated Calcium Entry. *Immunity* 38:881-895.

Okkenhaug, K., A. Bilancio, G. Farjot, H. Priddle, S. Sancho, E. Peskett, W. Pearce, S.E. Meek, A. Salpekar, M.D. Waterfield, A.J. Smith, and B. Vanhaesebroeck. 2002. Impaired B and T Cell Antigen Receptor Signaling in p110δ PI 3-Kinase Mutant Mice. *Science* 297:1031-1034.

Okkenhaug, K., and B. Vanhaesebroeck. 2003. PI3K in lymphocyte development, differentiation and activation. *Nature Reviews Immunology* 3:317-330.

Osborne, B.A. 2000. Transcriptional control of T cell development. *Current opinion in immunology* 12:301-306.

Pages, F., M. Ragueneau, R. Rottapel, A. Truneh, and J. Nunes. 1994. Binding of phosphatidyl-inositol-3-OH kinase to CD28 is required for T-cell signalling. *Nature*

Palmer, E. 2003. Negative selection — clearing out the bad apples from the T-cell repertoire. *Nature Reviews Immunology* 3:383-391.

Pang, S.S., R. Berry, Z. Chen, L. Kjer-Nielsen, M.A. Perugini, G.F. King, C. Wang, S.H. Chew, N.L. La Gruta, N.K. Williams, T. Beddoe, T. Tiganis, N.P. Cowieson, D.I. Godfrey, A.W. Purcell, M.C. Wilce, J. McCluskey, and J. Rossjohn. 2010. The structural basis for autonomous dimerization of the pre-T-cell antigen receptor. *Nature* 467:844-848.

Panigada, M., S. Porcellini, E. Barbier, S. Hoeflinger, P.A. Cazenave, H. Gu, H. Band, H. von Boehmer, and F. Grassi. 2002. Constitutive Endocytosis and Degradation of the pre-T Cell Receptor. *The Journal of Experimental Medicine* 195:1585-1597.

Panwala, C.M., J.C. Jones, and J.L. Viney. 1998. A novel model of inflammatory bowel disease: mice deficient for the multiple drug resistance gene, mdr1a, spontaneously develop colitis. *Journal of immunology (Baltimore, Md. : 1950)* 161:5733-5744.

Pardoll, D.M., B.J. Fowlkes, J.A. Bluestone, and A. Kruisbeek. 1987. Differential expression of two distinct T-cell receptors during thymocyte development. *Nature* 326:79-81.

Paul, S., and B.C. Schaefer. 2013. A new look at T cell receptor signaling to NF-κB. *Trends in immunology*

Paz, P.E., S. Wang, H. Clarke, X. Lu, D. Stokoe, and A. Abo. 2001. Mapping the Zap-70 phosphorylation sites on LAT (linker for activation of T cells) required for recruitment and activation of signalling proteins in T cells. *Biochemical Journal* 356:461.

Perez de Castro, I., T.G. Bivona, M.R. Philips, and A. Pellicer. 2004. Ras activation in Jurkat T cells following low-grade stimulation of the T-cell receptor is specific to N-Ras and occurs only on the Golgi apparatus. *Molecular and cellular biology* 24:3485-3496.

Peschon, J.J., P.J. Morissey, K.H. Grabstein, F.J. Ramsdell, E. Maraskovsky, B.C. Gliniak, L.S. Park, S.F. Ziegler, D.E. Williams, C.B. Ware, J.D. Meyer, and B.L. Davison. 1994. Early lymphocyte expansion is severely impaired in interleukin 7 receptor-deficient mice. *The Journal of Experimental Medicine* 180:1955-1960.

Petrie, H.T. 2003. Cell migration and the control of post-natal T-cell lymphopoiesis in the thymus. *Nature Reviews Immunology* 3:859-866.

Pham, C.T.N., D.M. MacIvor, and B.A. Hug. 1996. Long-range disruption of gene expression by a selectable marker cassette. *Proceedings of the …*

Pircher, H., K. Bürki, R. Lang, H. Hengartner, and R.M. Zinkernagel. 1989. Tolerance induction in double specific T-cell receptor transgenic mice varies with antigen. *Nature* 342:559-561.

Plotkin, J., S.E. Prockop, A. Lepique, and H.T. Petrie. 2003. Critical role for CXCR4 signaling in progenitor localization and T cell differentiation in the postnatal thymus. *Journal of Immunology* 171:4521-4527.

Pomerantz, J.L., E.M. Denny, and D. Baltimore. 2002. CARD11 mediates factor-specific activation of NF-kappaB by the T cell receptor complex. *The EMBO journal* 21:5184-5194.

Porritt, H.E., L.L. Rumfelt, S. Tabrizifard, T.M. Schmitt, J.C. Zuniga-Pflucker, and H.T. Petrie. 2004. Heterogeneity among DN1 Prothymocytes Reveals Multiple Progenitors with Different Capacities to Generate T Cell and Non-T Cell Lineages. *Immunity* 20:735-745.

Poussier, P., T. Ning, D. Banerjee, and M. Julius. 2002. A unique subset of self-specific intraintestinal T cells maintains gut integrity. *The Journal of Experimental Medicine* 195:1491-1497.

Prasad, K.V., Y.C. Cai, and M. Raab. 1994. T-cell antigen CD28 interacts with the lipid kinase phosphatidylinositol 3-kinase by a cytoplasmic Tyr (P)-Met-Xaa-Met motif. *Proceedings of the National Academy of Sciences*

Prinz, I., A. Sansoni, A. Kissenpfennig, L. Ardouin, M. Malissen, and B. Malissen. 2006. Visualization of the earliest steps of γδ T cell development in the adult thymus. *Nature Immunology* 7:995-1003.

Prinz, I., B. Silva-Santos, and D.J. Pennington. 2013. Functional development of γδ T cells. *European journal of immunology* 43:1988-1994.

Prockop, S.E., S. Palencia, C.M. Ryan, K. Gordon, D. Gray, and H.T. Petrie. 2002. Stromal cells provide the matrix for migration of early lymphoid progenitors through the thymic cortex. *Journal of Immunology* 169:4354-4361.

Radtke, F., A. Wilson, G. Stark, M. Bauer, J. Vanmeerwijk, H. Macdonald, and M. Aguet. 2000. Deficient T Cell Fate Specification in Mice with an Induced Inactivation of Notch1. *Immunity* 10:547-558.

Ramadani, F., D.J. Bolland, F. Garcon, J.L. Emery, B. Vanhaesebroeck, A.E. Corcoran, and K. Okkenhaug. 2010. The PI3K Isoforms p110α and p110δ Are Essential for Pre–B Cell Receptor Signaling and B Cell Development. *Sci Signal* 3:ra60.

Ramiro, A.R., M.N. Navarro, and A. Carreira. 2001. Differential developmental regulation and functional effects on pre-TCR surface expression of human pTαa and pTαb spliced isoforms. *The Journal of Immunology*

Ramsey, C. 2002. Aire deficient mice develop multiple features of APECED phenotype and show altered immune response. *Human Molecular Genetics* 11:397-409.

Reinhardt, A., S. Ravens, H. Fleige, J.D. Haas, L. Oberdorfer, M. Lyszkiewicz, R. Forster, and I. Prinz. 2014. CCR7-mediated migration in the thymus controls γδ T-cell development. *European Journal of Immunology* 44:1320-1329.

Reizis, B., and P. Leder. 1999. Expression of the Mouse Pre-T Cell Receptor α Gene Is Controlled by an Upstream Region Containing a Transcriptional Enhancer. *The Journal of Experimental Medicine* 189:1669-1678.

Reizis, B., and P. Leder. 2001. The Upstream Enhancer Is Necessary and Sufficient for the Expression of the Pre-T Cell Receptor α Gene in Immature T Lymphocytes. *The Journal of Experimental Medicine* 194:979-990.

Reizis, B., and P. Leder. 2002. Direct induction of T lymphocyte-specific gene expression by the mammalian Notch signaling pathway. *Genes & development* 16:295-300.

Remy, G., A.M. Risco, F.A. Iñesta-Vaquera, B. González-Terán, G. Sabio, R.J. Davis, and A. Cuenda. 2010. Differential activation of p38MAPK isoforms by MKK6 and MKK3. *Cellular signalling* 22:660-667.

Reth, M. 1989. Antigen receptor tail clue. *Nature*

Reynolds, L.F., L.A. Smyth, T. Norton, N. Freshney, J. Downward, D. Kioussis, and V.L. Tybulewicz. 2002. Vav1 transduces T cell receptor signals to the activation of phospholipase C-gamma1 via phosphoinositide 3-kinase-dependent and -independent pathways. *The Journal of Experimental Medicine* 195:1103-1114.

Ribot, J.C., A. deBarros, D.J. Pang, J.F. Neves, V. Peperzak, S.J. Roberts, M. Girardi, J. Borst, A.C. Hayday, D.J. Pennington, and B. Silva-Santos. 2009. CD27 is a thymic determinant of the balance between interferon-γ- and interleukin 17–producing γδ T cell subsets. *Nature Immunology* 10:427-436.

Ridge, J.P., D.F. Rosa, and P. Matzinger. 1998. A conditioned dendritic cell can be a temporal bridge between a CD4+; T-helper and a T-killer cell. *Nature* 393:474-478.

Rincón, M., A. Whitmarsh, D.D. Yang, L. Weiss, B. Dérijard, P. Jayaraj, R.J. Davis, and R.A. Flavell. 1998. The JNK pathway regulates the In vivo deletion of immature CD4(+)CD8(+) thymocytes. *The Journal of Experimental Medicine* 188:1817-1830.

Roller, A., A. Perino, P. Dapavo, and E. Soro. 2012. Blockade of phosphatidylinositol 3-kinase (PI3K) δ or PI3Kγ reduces IL-17 and ameliorates imiquimod-induced psoriasis-like dermatitis. *The Journal of Immunology* 189:4612-4620.

Sabapathy, K. 2001. C-Jun Nh2-Terminal Kinase (Jnk)1 and Jnk2 Have Similar and Stage-Dependent Roles in Regulating T Cell Apoptosis and Proliferation. *The Journal of Experimental Medicine* 193:317-328.

Sabapathy, K., Y. Hu, T. Kallunki, M. Schreiber, J.P. David, W. Jochum, E.F. Wagner, and M. Karin. 1999. JNK2 is required for efficient T-cell activation and apoptosis but not for normal lymphocyte development. *Current biology : CB* 9:116-125.

Sabapathy, K., T. Kallunki, J. David, I. Graef, M. Karin, and E. Wagner. 2001. c-Jun NH2-terminal kinase (JNK)1 and JNK2 have similar and stage-dependent roles in regulating T cell apoptosis and proliferation. *The Journal of experimental medicine* 193:317-328.

Saint-Ruf, C., O. Lechner, J. Feinberg, and H. von Boehmer. 1998. Genomic structure of the human pre‐T cell receptor α chain and expression of two mRNA isoforms. *European Journal of Immunology* 28:3824-3831.

Saint-Ruf, C., M. Panigada, O. Azogui, P. Debey, and H. von Boehmer. 2000. Different initiation of pre-TCR and γδTCR signalling. *Nature*

Saint-Ruf, C., K. Ungewiss, M. Groettrup, L. Bruno, H.J. Fehling, and H. von Boehmer. 1994. Analysis and expression of a cloned pre-T cell receptor gene. Science. 1994. 266: 1208-1212. *Journal of Immunology* 182:5165-5169.

Sakaguchi, N., T. Takahashi, H. Hata, T. Nomura, T. Tagami, S. Yamazaki, T. Sakihama, T. Matsutani, I. Negishi, S. Nakatsuru, and S. Sakaguchi. 2003. Altered thymic T-cell selection due to a mutation of the ZAP-70 gene causes autoimmune arthritis in mice. *Nature* 426:454-460.

Sakaguchi, S., N. Sakaguchi, M. Asano, M. Itoh, and M. Toda. 1995. immunologic self-tolerance maintained by activated T cells expressing IL-2 receptor α-chains (CD25). Breakdown of a single mechanism of self-tolerance causes various autoimmune diseases. *Journal of Immunology* 186:3808-3821.

Schild, H., N. Mavaddat, C. Litzenberger, E.W. Ehrich, M.M. Davis, J.A. Bluestone, L. Matis, R.K. Draper, and Y.H. Chien. 1994. The nature of major histocompatibility complex recognition by γδ T cells. *Cell* 76:29-37.

Schlissel, M.S., S.D. Durum, and K. Muegge. 2000. The interleukin 7 receptor is required for T cell receptor γ locus accessibility to the V (D) J recombinase. *The Journal of Experimental Medicine*

Schwab, S.R., J.P. Pereira, M. Matloubian, Y. Xu, Y. Huang, and J.G. Cyster. 2005. Lymphocyte sequestration through S1P lyase inhibition and disruption of S1P gradients. *Science* 309:1735-1739.

Sharan, S.K., L.C. Thomason, S.G. Kuznetsov, and D.L. Court. 2009. Recombineering: a homologous recombination-based method of genetic engineering. *Nature Protocols* 4:206-223.

Shim, E.K., S.H. Jung, and J.R. Lee. 2011. Role of two adaptor molecules SLP-76 and LAT in the PI3K signaling pathway in activated T cells. *Journal of Immunology* 186:2926-2935.

Shimizu, C., H. Kawamoto, and M. Yamashita. 2001. Progression of T cell lineage restriction in the earliest subpopulation of murine adult thymus visualized by the expression of lck proximal promoter activity. *International immunology*

Shires, J., E. Theodoridis, and A.C. Hayday. 2001. Biological insights into TCRγδ+ and TCRαβ+ intraepithelial lymphocytes provided by serial analysis of gene expression (SAGE). *Immunity* 15:419-434.

Sicinska, E., I. Aifantis, L.L. Cam, W. Swat, and C. Borowski. 2003. Requirement for cyclin D3 in lymphocyte development and T cell leukemias. *Cancer cell*

Simon, V., and D.D. Ho. 2003. HIV-1 dynamics in vivo: implications for therapy. *Nat Rev Microbiol* 1:181-190.

Sinclair, C., I. Bains, A.J. Yates, and B. Seddon. 2013. Asymmetric thymocyte death underlies the CD4:CD8 T-cell ratio in the adaptive immune system. *Proceedings of the National Academy of Sciences of the United States of America* 110:14.

Smelty, P., C. Marchal, R. Renard, L. Sinzelle, N. Pollet, D. Dunon, T. Jaffredo, J.Y. Sire, and J.S. Fellah. 2010. Identification of the pre–T-cell receptor α chain in nonmammalian vertebrates challenges the structure–function of the molecule. *Proceedings of the National Academy of Sciences* 107:19991-19996.

Snodgrass, H.R., Z. Dembic, M. Steinmetz, and H. von Boehmer. 1985. Expression of T-cell antigen receptor genes during fetal development in the thymus. *Nature* 315:232-233.

Sommer, K., B. Guo, J.L. Pomerantz, and A.D. Bandaranayake. 2005. Phosphorylation of the CARMA1 linker controls NF-κB activation. *Immunity*

Sommers, C.L., R.K. Menon, A. Grinberg, W. Zhang, L.E. Samelson, and P.E. Love. 2001. Knock-in Mutation of the Distal Four Tyrosines of Linker for Activation of T Cells Blocks Murine T Cell Development. *The Journal of Experimental Medicine* 194:135-142.

Spiegel, S., and S. Milstien. 2011. The outs and the ins of sphingosine-1-phosphate in immunity. *Nature Reviews Immunology* 11:403-415.

Starr, T.K., and K.A. Hogquist. 2005. A requirement for sustained ERK signaling during thymocyte positive selection in vivo. *Proceedings of the National Academy of Sciences*

Stefanová, I., J.R. Dorfman, and R.N. Germain. 2002. Self-recognition promotes the foreign antigen sensitivity of naive T lymphocytes. *Nature*

Straus, D.B., and A. Weiss. 1993. The CD3 chains of the T cell antigen receptor associate with the ZAP-70 tyrosine kinase and are tyrosine phosphorylated after receptor stimulation. *The Journal of Experimental Medicine*

Street, S.E., Y. Hayakawa, Y. Zhan, A.M. Lew, D. MacGregor, A.M. Jamieson, A. Diefenbach, H. Yagita, D.I. Godfrey, and M.J. Smyth. 2004. Innate immune surveillance of spontaneous B cell lymphomas by natural killer cells and gammadelta T cells. *The Journal of Experimental Medicine* 199:879-884.

Sudo, T., S. Nishikawa, and N. Ohno. 1993. Expression and function of the interleukin 7 receptor in murine lymphocytes. *Proceedings of the …*

Sugawara, T., T. Moriguchi, E. Nishida, and Y. Takahama. 1998. Differential Roles of ERK and p38 MAP Kinase Pathways in Positive and Negative Selection of T Lymphocytes. *Immunity* 9:565-574.

Sumaria, N., B. Roediger, L.G. Ng, J. Qin, R. Pinto, L.L. Cavanagh, E. Shklovskaya, B. Fazekas de St Groth, J.A. Triccas, and W. Weninger. 2011. Cutaneous immunosurveillance by self-renewing dermal γδ T cells. *The Journal of Experimental Medicine* 208:505-518.

Sun, S.C. 2010. Non-canonical NF-κB signaling pathway. *Cell Research* 21:71-85.

Takahama, Y. 2006. Journey through the thymus: stromal guides for T-cell development and selection. *Nature Reviews Immunology* 6:127-135.

Tan, Y.X., B.N. Manz, T.S. Freedman, C. Zhang, K.M. Shokat, and A. Weiss. 2014. Inhibition of the kinase Csk in thymocytes reveals a requirement for actin remodeling in the initiation of full TCR signaling. *Nature immunology* 15:186-194.

Tarakhovsky, A., S.B. Kanner, J. Hombach, J.A. Ledbetter, W. Muller, N. Killeen, and K. Rajewsky. 1995. A role for CD5 in TCR-mediated signal transduction and thymocyte selection. *Science* 269:535-537.

Tournier, C., A.J. Whitmarsh, J. Cavanagh, T. Barrett, and R.J. Davis. 1997. Mitogen-activated protein kinase kinase 7 is an activator of the c-Jun NH2-terminal kinase. *Proceedings of the National Academy of Sciences of the United States of America* 94:7337-7342.

Trampont, P.C., A.C. Tosello-Trampont, Y. Shen, A.K. Duley, A.E. Sutherland, T.P. Bender, D.R. Littman, and K.S. Ravichandran. 2009. CXCR4 acts as a costimulator during thymic [beta]-selection. *Nature Immunology* 11:162-170.

Tremblay, M., S. Herblot, E. Lecuyer, and T. Hoang. 2003. Regulation of pTα Gene Expression by a Dosage of E2A, HEB, and SCL. *Journal of Biological Chemistry* 278:12680-12687.

Trigueros, C., K. Hozumi, B. Silva-Santos, L. Bruno, A.C. Hayday, M.J. Owen, and D.J. Pennington. 2003. Pre-TCR signaling regulates IL-7 receptor α expression promoting thymocyte survival at the transition from the double-negative to double-positive stage. *European journal of immunology* 33:1968-1977.

Trop, S., M. Rhodes, D.L. Wiest, P. Hugo, and J.C. Zúñiga-Pflücker. 2000. Competitive displacement of pT α by TCR-α during TCR assembly prevents surface coexpression of pre-TCR and αβ TCR. *Journal of Immunology* 165:5566-5572.

Turchinovich, G., and A.C. Hayday. 2011. Skint-1 Identifies a Common Molecular Mechanism for the Development of Interferon-γ-Secreting versus Interleukin-17-Secreting γδ T Cells. *Immunity* 35:59-68.

Ueno, T., F. Saito, D.H. Gray, S. Kuse, K. Hieshima, H. Nakano, T. Kakiuchi, M. Lipp, R.L. Boyd, and Y. Takahama. 2004. CCR7 signals are essential for

cortex-medulla migration of developing thymocytes. *The Journal of Experimental Medicine* 200:493-505.

van Oers, N.S.C., B. Lowin-Kropf, D. Finlay, K. Connolly, and A. Weiss. 1996. αβ T Cell Development Is Abolished in Mice Lacking Both Lck and Fyn Protein Tyrosine Kinases. *Immunity* 5:429-436.

Villartay, D.J.P., A. Fischer, and A. Durandy. 2003. The mechanisms of immune diversification and their disorders. *Nature Reviews Immunology*

Wang, D., Y. You, S.M. Case, L.M. McAllister-Lucas, L. Wang, P.S. DiStefano, G. Nuñez, J. Bertin, and X. Lin. 2002. A requirement for CARMA1 in TCR-induced NF-kappa B activation. *Nature immunology* 3:830-835.

Wang, H., T.A. Kadlecek, B.B. Au-Yeung, H.E. Goodfellow, L.Y. Hsu, T.S. Freedman, and A. Weiss. 2010. ZAP-70: An Essential Kinase in T-cell Signaling. *Cold Spring Harbor Perspectives in Biology* 2:a002279.

Wang, H.Y., X. Xu, J.H. Ding, J.R. Bermingham, and X.D. Fu. 2001. SC35 plays a role in T cell development and alternative splicing of CD45. *Molecular cell*

Wange, R.L., S.N. Malek, and S. Desiderio. 1993. Tandem SH2 domains of ZAP-70 bind to T cell antigen receptor zeta and CD3 epsilon from activated Jurkat T cells. *Journal of Biological Chemistry*

Wencker, M., G. Turchinovich, R. Di Marco Barros, L. Deban, A. Jandke, A. Cope, and A.C. Hayday. 2014. Innate-like T cells straddle innate and adaptive immunity by altering antigen-receptor responsiveness. *Nature Immunology* 15:80-87.

Werlen, G., B. Hausmann, and E. Palmer. 2000. A motif in the alphabeta T-cell receptor controls positive selection by modulating ERK activity. *Nature* 406:422-426.

Williams, A., C.A. Peh, and T. Elliott. 2002. The cell biology of MHC class I antigen presentation. *Tissue Antigens* 59:3-17.

Wilson, A., and H.R. MacDonald. 1995. Expression of genes encoding the pre-TCR and CD3 complex during thymus development. *Int Immunol* 7:1659-1664.

Wood, C., and S. Tonegawa. 1983. Diversity and joining segments of mouse immunoglobulin heavy chain genes are closely linked and in the same

orientation: implications for the joining mechanism. *Proceedings of the National Academy of Sciences* 80:3030-3034.

Yamagata, T., D. Mathis, and C. Benoist. 2004. Self-reactivity in thymic double-positive cells commits cells to a CD8αα lineage with characteristics of innate immune cells. *Nature immunology* 5:597-605.

Yamasaki, S., E. Ishikawa, M. Sakuma, K. Ogata, K. Sakata-Sogawa, M. Hiroshima, D.L. Wiest, M. Tokunaga, and T. Saito. 2006. Mechanistic basis of pre–T cell receptor–mediated autonomous signaling critical for thymocyte development. *Nature Immunology* 7:67-75.

Yamasaki, S., and T. Saito. 2007. Molecular basis for pre-TCR-mediated autonomous signaling. *Trends in Immunology* 28:3943.

Yamashita, I., T. Nagata, T. Tada, and T. Nakayama. 1993. CD69 cell surface expression identifies developing thymocytes which audition for T cell antigen receptor-mediated positive selection. *International Immunology* 5:1139-1150.

Yates, A.J. 2014. Theories and quantification of thymic selection. *Frontiers in immunology* 5:13.

Yui, M.A. 2010. Fine-Scale Staging of T Cell Lineage Commitment in Adult Mouse Thymus. *J Immunol* 185:284-293.

Zarin, P., G.W. Wong, M. Mohtashami, D.L. Wiest, and J.C. Zúñiga-Pflücker. 2014. Enforcement of γδ-lineage commitment by the pre-T-cell receptor in precursors with weak γδ-TCR signals. *Proceedings of the National Academy of Sciences of the United States of America* 111:5658-5663.

Zhang, S.L., Y. Yu, J. Roos, J.A. Kozak, and T.J. Deerinck. 2005. STIM1 is a Ca2+ sensor that activates CRAC channels and migrates from the Ca2+ store to the plasma membrane. *Nature*

Zhang, W., J. Sloan-Lancaster, J. Kitchen, and R.P. Trible. 1998. LAT: the ZAP-70 tyrosine kinase substrate that links T cell receptor to cellular activation. *Cell*

Zhang, W., C.L. Sommers, D.N. Burshtyn, C.C. Stebbins, J.B. DeJarnette, R.P. Trible, A. Grinberg, H.C. Tsay, H.M. Jacobs, C.M. Kessler, E.O. Long, P.E. Love, and L.E. Samelson. 1999. Essential Role of LAT in T Cell Development. *Immunity* 10:323-332.

Zhang, W., R.P. Trible, M. Zhu, S.K. Liu, C.J. McGlade, and L.E. Samelson. 2000. The association of Grb2, Gads and phospholipase C-γ1 with phosphorylated LAT tyrosine residues: the effect of tyrosine mutations on T cell antigen receptor-mediated signaling. *Journal of Biological Chemistry* 275:23355-23361.